MIMICKING VIRUS REMOVAL AND TRANSPORT IN AQUIFER MEDIA USING SURFACE-MODIFIED SILICA NANOPARTICLES

A thesis submitted in partial fulfilment

of the requirements for the Degree of

Doctor of Philosophy in Microbiology

in the

University of Canterbury

by

Kata Farkas

University of Canterbury
Christchurch, New Zealand

2014

Acknowledgements

I first wish to thank my supervisors, Dr Arvind Varsani, Dr Liping Pang and Dr Wendy Williamson for their inspiration, encouragement, help and patience throughout the practical and written aspects of this thesis. This work could not have been carried out without their support.

My thanks go to all the staff at Environmental Science and Research Ltd. I would especially like to thank Shirley Jones and Darren Saunders for their assistance in the HPLC assays and to Chris Graham, Beth Robson, Susan Lin and Bronwyn Dumbleton for assisting with all the laboratory work.

Many thanks for the staff and students at the School of Biological Sciences at the University of Canterbury, in particular to Anisha Dayaram, Simona Kraberger, Daisy Stainton, Delphine Marjoshi, Maketalena Male and Matt Walters. I also wish to thank Glen Jackson and Rayleen Fredericks for their endless support. The efforts of all the collaborators at the University of Otago, University of Victoria, University of Cape Town and Bennett Scientific Services have also been invaluable.

I appreciate the scholarship and financial support to the project provided by the Royal Society of New Zealand in the form of a Marsden Fund.

Finally, I would like to thank my husband Roland, my sister Ildikó, my parents and friends, whose love, support and encouragement made this work possible.

Abstract

Contamination of drinking water sources, such as groundwater, by pathogens (protozoa, bacteria and viruses) is of major concern globally. Due to their small size, mobility and high infectivity, enteric viruses have been a focus of groundwater research. However, the behaviour of enteric viruses in aquifer media is still poorly understood, which is partially attributable to the lack of reliable surrogates for these viruses.

In the study reported in this thesis, a new type of surrogate was characterised and validated for its use in studying virus fate and transport in groundwater. The surrogates developed were composed of 70 nm carboxylated silica nanoparticles, labelled with dsDNA tags for sensitive detection, and coated with selected proteins to mimic the physico-chemical characteristics (size, charge, density) of two enteric viruses, human rotavirus and adenovirus, frequently found in faecal-contaminated groundwater. The selected enteric viruses and a commonly used virus surrogate, the MS2 bacteriophage, were purified and characterised in terms of size, surface charge, hydrophobicity and aggregation. For validation, the characteristics, the adsorption, degradation and transport of the surface-modified nanoparticles and the viruses were investigated in laboratory studies and compared.

The characterisation of the viruses and particles revealed that the modified silica nanoparticles resemble the size and negative surface charge of the rotavirus and adenovirus. In general, the nanoparticles were found to be less hydrophobic than the enteric viruses, thus presumably less interactive with hydrophobic media. In contrast, the MS2 bacteriophage was smaller in size than the enteric viruses studied and considerably more hydrophobic implying stronger interactions with hydrophobic media. The surface-modified nanoparticles were found to be more stable and remained more monodispersed over time than the purified enteric viruses.

In laboratory studies using simulated groundwater, the DNA-labelled nanoparticles were more stable over time than the rotavirus, the adenovirus or a plasmid DNA on its own. Interestingly, the study revealed that rotavirus was more persistent than the adenovirus over

time in terms of degradation and aggregation, however, day light considerably enhanced rotavirus degradation.

The adsorption studies revealed strong interactions between the enteric viruses and natural aquifer media (gravel and sand), whereas most of the surface-modified nanoparticles adsorbed weakly to these media. Only the casein-coated nanoparticles adsorbed strongly to the sand. The MS2 adsorbed to the gravel strongly, but weakly to the sand implying different interactions. The studies on virus and nanoparticle adsorption to hydrophobic-coated and non-modified Ottawa sand supported the results of characterisation.

Column studies investigating the transport of the viruses and the nanoparticles in gravel and sand showed that even though gravel had high adsorption capacity in the adsorption tests, all viruses and nanoparticles travelled though the gravel columns with little retention, probably due to insufficient interaction time. This highlights the vulnerability of gravel aquifers to virus contamination. Experiments using sand columns showed great differences in the transport of the particles. Results suggested that the recovery of the DNA-labelled nanoparticles was similar to the recovery of the adenovirus, however, their transport pattern was different. The glycoprotein-, the protein A- and the AMBP-coated nanoparticles mimicked the transport pattern and low recovery of the rotavirus. In contrast, the streptavidin- and casein-coated nanoparticles were not recovered, emphasising the great importance of surface structure in particle transport.

The results of this study demonstrated the usefulness of protein-coated silica nanoparticles as virus surrogates in groundwater studies. Surface-modified nanoparticles are able to mimic the surface characteristics of viruses. The glycoprotein-, protein A- and AMBP-coated particles were found to be suitable surrogates for rotavirus, whereas the DNA-labelled nanoparticles resembled adenovirus behaviour in hydrophilic media. Using particles with different material, size and protein-coating other pathogens can be modelled as well. Furthermore, these particles are expected to be safe to humans and the environment, thus can be used in a great variety of experiments in environmental research.

Preface

This thesis is submitted as partial fulfilment for the Doctor of Philosophy (PhD) degree at the University of Canterbury, Christchurch, New Zealand (UC). The work was carried out over the period of March 2011 to February 2014, which corresponds to the time of my enrolment for PhD in Microbiology at the School of Biological Sciences at the University of Canterbury.

Sections of Chapter 2 (rotavirus culture, purification and characterisation) have been published: Farkas, K., Pang, L., Lin, S., Williamson, W., Easingwood, R., Fredericks, R., Jaffer, M. A. & Varsani, A. (2013)**.** A Gel Filtration-Based Method for the Purification of Infectious Rotavirus Particles for Environmental Research Applications. *Food and Environmental Virology (5)*, 231-235. Figure 2.12 and Table 2.5 and 2.7 were adapted from this paper.

The rotavirus and adenovirus tissue cultures were prepared by Susan Lin of Environmental Science and Research Ltd., New Zealand (ESR), and the MS2 bacteriophage was propagated by Erin McGill (ESR). The DNA markers used for labelling were designed by Dr Arvind Varsani (UC). Dr Grant Bennett (Bennett Scientific Services) accomplished the DNA-labelling and protein-coating of the silica nanoparticles. The batch and column experiments involving MS2 plaque assays, and some of the adsorption tests for surrogates were accomplished with the help of Delphine Marjoshi (UC). Maketalena Male (UC) was involved in the washing and coating of the Ottawa sand, and in the adsorption tests for the surrogates. The Public Health Laboratory of ESR performed the test for bacteria growth. Hill Laboratoties, New Zealand performed the chemical analysis of solutions. Rayleen Fredericks (UC) contributed to the method development for rotavirus purification, and to the size and surface charge analyses of the viruses. Dr Urszula Nowostawska and Mike Brown of University of Otago, New Zealand (UO) delivered some of the size and surface charge measurements of the surrogates and the aquifer media. The electron microscopy images were provided by Mohamed A. Jaffer of University of Cape Town, South Africa (UCT), Dr Arvind Varsani (UC and UCT) and Richard Easingwood (UO).

I performed all of the experiments discussed in Chapter 2 – 6, apart from the specific help I received, as highlighted above. I wrote the majority of the published manuscript.

Dr Liping Pang (ESR), Dr Wendy Williamson (ESR and UC) and Dr Arvind Varsani (UC) assisted in the planning and editing of the thesis in their role as supervisors.

Table of Contents

List of Tables

List of Figures

Abbreviations

×g	times gravity
°C	degree Celsius
µg	microgram
µL	microlitre
µm	micrometre
µmol	micromole
Å	angstrom
AMBP	recombinant human α_1-microglobulin/bikunin precursor
AMBP-DNA-SiNP	AMBP-coated, DNA-labelled nanoparticles
ATCC	American Type Culture Collection
bp	base pair(s)
BTC	concentration breakthrough curve
C_0	initial/injection concentration
Cas-DNA-SiNP	casein-coated, DNA-labelled nanoparticles
cDNA	complementary deoxyribonucleic acid
cm	centimetre
d	diameter
DNA	deoxyribonucleic acid
DNA-SiNP	DNA-labelled silica nanoparticles
DNA-StrNP	DNA-labelled silica nanoparticles, precoated with streptavidin
DOC	dissolved organic carbon
DOM	dissolved organic matter
ds	double-stranded
EDC	1-ethyl-3-(3-dimethylaminopropyl)carbodiimide)
EDTA	ethylene-diamine-tetraacetic acid
ELISA	enzyme-linked immunosorbent assay
ESR	Institute of Environmental Science and Research Limited

EU	European Union
FBS MEM	minimal growth medium with foetal bovine serum
fg	femtogram
gc	genome copy/copies
Gly-DNA-SiNP	glycoprotein-coated, DNA-labelled nanoparticles
H%	percentage of hydrophobicity
HPLC	high-performance liquid chromatography
hr	hour(s)
HV	hydrophobicity value
ICC-PCR	integrated cell culture polymerase chain reaction
IPTG	isopropyl β-D-1-thiogalactopyranoside
IS	injection solution
kDa	kilodalton
L	litre
LB	Luria Broth
M	molar
MATH	microbial adhesion to hydrocarbons
mAU	milliabsorbance units
MEM	minimal essential medium
MES	2-(N-morpholino)ethanesulfonic acid
mg	milligram
min	minute(s)
mL	millilitre
mM	millimolar
mV	millivolt
ng	nanogram
nm	nanometre
nM	nanomolar
NSP	non-structural protein
nt	nucleotide(s)
OD	optical density
PBS	phosphate buffered saline

PC2	physical containment 2
PCR	polymerase chain reaction
PdI	polydispersity index
PES	polyethersulfone
pfu	plaque forming unit(s)
pg	picogram
pI	isoelectric point
PrA-DNA-SiNP	protein A-coated, DNA-labelled nanoparticles
PV	pore volume
PVDF	polyvinylidene fluoride
Q	flow rate
qPCR	quantitative polymerase chain reaction
qRT-PCR	quantitative reverse transcriptase polymerase chain reaction
RNA	ribonucleic acid
RT-PCR	reverse transcriptase polymerase chain reaction
rpm	rotation(s) per minute
s	second(s)
SD	standard deviation
SEC	size exclusion chromatography
SiNP	silica nanoparticle
ss	single-stranded
Str-DNA-SiNP	streptavidin-coated, DNA-labelled nanoparticles
StrNP	streptavidin-coated silica nanoparticles
TBE	Tris-borate-EDTA
TEM	transmission electron microscope
Tm	melting temperature
USEPA	United States Environmental Protection Agency
UV	ultraviolet
VP	viral protein
ZP	zeta potential

Chapter 1.
Introduction

The goal of the investigations carried out was to mimic virus fate and transport in groundwater by developing customised surrogates that mirror the physical and chemical characteristics of the enteric viruses. It is based on the hypothesis that if the surrogate is more similar to an enteric virus, it can approximate the attenuation of the pathogenic virus in porous media. The following review introduces the different mechanisms that influence virus transport through aquifer systems, discussing the properties of aquifer media and groundwater likely to retain or exclude human-relevant viruses.

1.1 Health concerns of virus contamination of groundwater

Safe and clean drinking water is a major priority for people globally. Groundwater composes 97% of global freshwater, and it is the main source for drinking water in many regions of the world (Howard *et al.*, 2006). In New Zealand, 50% of the population depends partially or completely on groundwater as a drinking water source (as of 19 March 2013 from the national Water Information for New Zealand database), and this high degree is also typical in other countries. According to the United States Environmental Protection Agency (USEPA) 40% of people in the USA use groundwater-derived drinking water through public water systems and an additional 15% have private wells (USEPA, 2012). Based on the data from the European Commission 75% of European Union (EU) citizens use drinking water derived from groundwater. In some countries (e.g. Denmark), groundwater is the only drinking water source (European Commission, 2008).

Contaminated groundwater commonly leads to waterborne outbreaks (Howard *et al.*, 2006). In the USA, 68% of all waterborne illnesses were associated with groundwater contamination (Craun *et al.*, 2002). Pathogens derived from human faeces can find their way into drinking water by contaminated surface or groundwater. While lakes and other surface water reservoirs are relatively simple to monitor and sample, subsurface water is hard to access, and hence

cannot be monitored or sampled as easily. Thus, groundwater contamination would only be realised well after the event and may only become evident due to higher disease incidence or outbreaks.

Pathogens present in contaminated groundwater include bacteria, protozoa and viruses. Viruses are simple biological entities comprising of nucleic acid genomes, which are either DNA or RNA, single- or double-stranded, encapsidated by a protein capsid. Some viruses, such as Ebola, influenza, hepatitis B and D viruses are enveloped viruses with an outer layer consisting lipoproteins and glycoproteins. In general, enveloped viruses are not as stable in the environment as the non-enveloped ones (Rzeżutka & Cook, 2004). The size of viruses varies between 18 nm (Tobacco mosaic virus) and 350 nm (Chlorella viruses and poxviruses) in diameter, although the size of some newly found viruses is 750 nm – 1 μm in diameter (Claverie & Abergel, 2010; Philippe *et al.*, 2013; Zaitlin, 2011).

Viruses are obligate intercellular pathogens, meaning they can only replicate in a host. Many of the viruses found in groundwater will have originated from infections of plants and bacteria (bacteriophages) and will not represent a risk to human health in their own right. Of the human-relevant viruses found in groundwater, the most harmful to human health are the enteric viruses, which are transmitted via the faecal-oral route. Enteric viruses can retain their infectious status in groundwater, and, due to their small size (20 – 100 nm diameter) these viruses move more easily in the subsurface area than bacteria (0.2 – 2 μm) or protozoan cysts (5 μm) (Jin & Flury, 2001). Viruses are also more difficult to remove and/or inactivate than bacteria by most common water purification and treatment methods such as filtration and disinfection with chemical agents (Rao & Melnick, 1986). Furthermore, most enteric viruses are highly infectious, and for some viruses, such as rotaviruses and the Norwalk virus, even one intact virus particle can result in infection and illness (Teunis *et al.*, 2008; Ward *et al.*, 1986). All these factors imply high risk of drinking water contamination and groundwater-borne enteric virus outbreaks.

Over 100 species of human pathogenic viruses can be found in sewage and polluted water (Gerba *et al.*, 1975; Rao & Melnick, 1986). The most common enteric viruses contaminating groundwater are enteroviruses, coxsackieviruses, echoviruses, polioviruses, noroviruses, rotaviruses, enteric adenoviruses and hepatitis A and E viruses. The largest reported outbreak caused by virus contaminated drinking water was in New Delhi in December 1955 – January 1956, where more than 29,000 cases were registered with hepatitis E virus (Purcell, 1996; Rao

& Melnick, 1986). Some enteric virus infections, such as those of coxsackievirus and echovirus, are asymptomatic in the majority of cases (Melnick, 1997). Other viruses, e.g. rotavirus, cause severe illness and even death, especially in infants. It is worth mentioning that in the case of highly infectious viruses it is hard to determine whether the source of an outbreak was contaminated water or it is a result of a previous person-to-person mediated transmission (Frost *et al.*, 2002), thus the number of waterborne outbreaks may be under- or overestimated.

Enteric viruses are excreted in faeces in very high numbers. Stool samples of patients infected with rotavirus can contain up to 10^{11} virus particles per mL (Desselberger, 2000). The usual concentration of viruses in sewage effluent is up to 10^4 plaque-forming unit (pfu) per litre (Matthess & Pehdeger, 1981). In some countries, such as the USA, Australia and New Zealand, the number of pathogens must be reduced to no more than 1 pfu per 4 gram, if the sewage is used for land applications (Horswell *et al.*, 2010). Based on the dose-response relationship of rotavirus, Regli *et al.* (1991) suggested that drinking water should contain fewer than 2.2×10^{-7} viruses per litre to ensure people are unlikely to be exposed to an unacceptable risk of waterborne viral infections. The Drinking-water Standards for New Zealand 2005 (revised in 2008) do not include a maximum acceptable value for viruses. However, when viruses are specifically sought, they should not be detected [Draft guidelines for drinking-water quality management for New Zealand (Ministry of Health 2005)].

Enteric viruses usually infiltrate the groundwater through irrigated agricultural fields, sewage treatment plants and septic tanks, land runoff, overwhelmed landfills and recharge of contaminated surface waters (Figure 1.1). Heavy rainfalls have a major impact on groundwater quality, as these events can lead to floods and land runoff enabling rapid contamination of groundwater. Fong *et al.* (2007) highlighted that groundwater in a region of Ohio (USA) experiencing a large waterborne outbreak, had been contaminated with pathogenic bacteria and adenovirus as a result of heavy rainfalls washing wastewater into the groundwater.

A study by Jean *et al.* (2006) revealed a direct connection between enteric virus-related outbreaks and groundwater contamination while examining groundwater and stool samples from patients during a gastro-enteritis outbreak in Taiwan in 1998. In most cases of waterborne disease outbreaks, both groundwater contamination and a failure of the water treatment system occurred simultaneously (Wallender *et al.*, 2013). For example, in 1998, a

pump failure at the water treatment plant in Switzerland caused a spill of sewage into the groundwater leading to a gastroenteritis outbreak, which were microscopically identified as small round structured viruses (SRSV) from stools of six patients (Maurer & Stürchler, 2000). Furthermore, in France, in 2000, groundwater was contaminated by agricultural overflow coupled with a failure in the drinking water chlorination system. During that outbreak, rotaviruses and noroviruses together with campylobacter were identified in the drinking water and in stool samples of hospitalised patients (Gallay *et al.*, 2006).

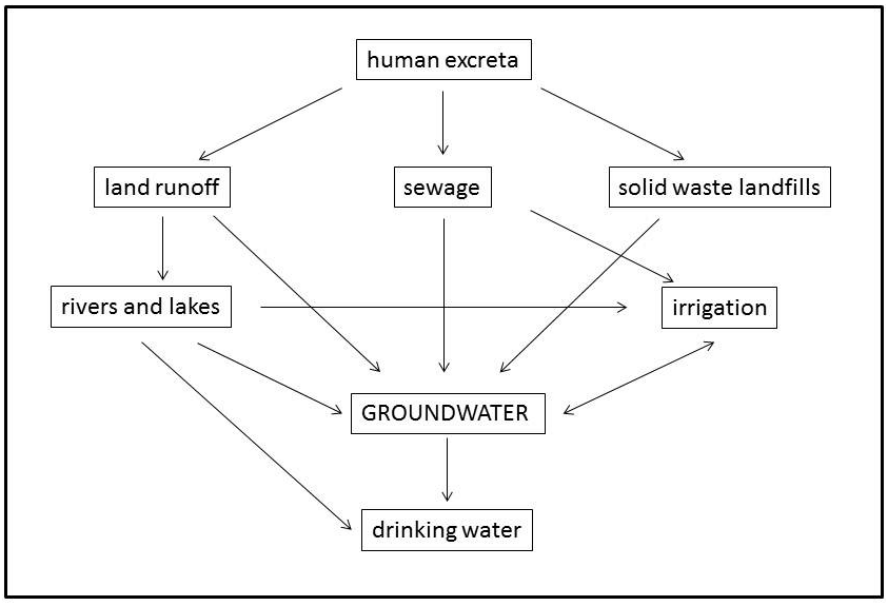

Figure 1.1 Routes of enteric virus transmission. Based on Rao and Melnick (1986).

Groundwater-borne enteric viruses often cause outbreaks in private and public settings which have their own water and wastewater treatment systems. Sewage overflow from septic tanks or cesspools was responsible for 43% of all reported outbreaks in the USA between 1971 and 1979 (Craun, 1984). Even with the improvement in quality of water treatment systems worldwide, recent studies still demonstrate connection between these systems and outbreaks. In South Carolina (USA), in 2006 a hepatitis A virus outbreak occurred due to a leakage of the septic tank from a farm (Tallon *et al.*, 2008). In South Korea, five consecutive gastroenteritis outbreaks were reported within a school in 2011 and it was later established that the catering services used norovirus-contaminated groundwater as a drinking water source (Lee *et al.*, 2012). In Wisconsin (USA), six people were hospitalised during a norovirus outbreak in 2007 as a result of a leakage from a restaurant's septic system (Borchardt *et al.*, 2011).

These above examples illustrate that human enteric viruses in groundwater can remain infectious for extended periods of time and are able to reach drinking water plants, which makes them a major risk to public health. In order to avoid large outbreaks of waterborne diseases, the understanding of movement and attenuation of these pathogens in drinking water sources is an important factor in environmental science.

1.2 Attenuation and transport of viruses in groundwater

The determination of the time and exact place of pathogen-contamination in groundwater is challenging. In order to protect subsurface drinking water sources, identifying the adequate setback distance between any possible source of contamination such as agricultural fields, sewage treatment plants, septic tanks, etc., and the production wells needs to be investigated. Therefore, accurate information on fate and transport of pathogens is required (Pang *et al.*, 2005).

Several factors are known to influence the behaviour of pathogens in subsurface water (Table 1.1). The main factors impacting the fate of viruses are the type of viruses and the aquifer media, however, there are other altering factors, which impact virus behaviour such as temperature, pH and ionic strength, presence of organic matter and living organisms, moisture content and hydraulic conditions (Jin & Flury, 2001). These factors have variable influence on the persistence and transport of viruses in groundwater. In New Zealand, data on the physical and chemical properties of the groundwater is collected by the National Groundwater Monitoring Program, which was established in 1990, and currently monitors more than 100 sites across 15 region of New Zealand (Daughney & Reeves, 2006). Although viruses in groundwater are not monitored in New Zealand, the information obtained on groundwater chemistry is useful towards understanding the conditions of virus transport in the subsurface environment.

Viruses are known to be removed from groundwater via attachment to solid particles (adsorption) or loss of infectivity (inactivation) (Schijven & Hassanizadeh, 2000). These mechanisms cause the retention of viruses during their transport.

Table 1.1 Factors influencing virus behaviour (inactivation and adsorption) in groundwater. Based on Jin and Flury (2001).

Factor	Influence on virus persistence in groundwater	Influence on virus adsorption to solids
Virus type	The inactivation rate of viruses is different.	The adsorption of viruses primarily depends on their surface characteristics.
Aquifer media	Attachment to solid particles generally decreases inactivation, however, some materials favour persistence.	Minerals found in aquifer have different adsorption capacity.
Temperature	High temperature may enhance virus inactivation.	High temperature may enhance virus adsorption.
pH	Most enteric viruses persist over a pH range of 3 – 9, especially at near-neutral pH.	Low pH typically favours adsorption, whereas high pH promotes desorption.
Microbial activity	The presence of microbes increases inactivation caused by extracellular enzymes produced by the microbes.	Unknown.
Ionic strength / conductivity	High ionic strength may promote virus aggregation, which may or may not result in loss of infectivity.	High ionic strength and conductivity favours adsorption, especially if multivalent cations are presented.
Organic matter	Attachment to solid particles generally decreases inactivation, however, some material favours persistence.	Dissolved organic matter competes for binding sites, thus inhibits adsorption of viruses. Solid organic matter may provide binding sites for the viruses.

1.2.1 Virus inactivation in groundwater

Viruses can lose their ability to infect host organisms in groundwater over time due to the degradation of capsid proteins or the nucleic acid. However, Alvarez *et al.* (2000) suggested that the inactivation of viruses could be reversible in groundwater. Their findings support the idea that during inactivation intermediate particles result, which have intact genome but lack some of the capsid proteins responsible for adsorption to the host cell resulting in low infectivity. Under optimised conditions these proteins reattach to the virus particle and the virus become infectious again (Schijven *et al.*, 2006).

The adsorption of viruses to solids (e.g. aquifer media, soil particles or organic matter) may result in inactivation of the viruses due to disintegration of the viral particles. Field and laboratory experiments have shown that attached viruses can go through inactivation when iron-oxide is presented on the surface of sand particles resulting in virus decay (Ryan *et al.*,

2002; Zerda & Gerba, 1984). However, in some cases the adsorption has no effect on the antigens present on the surface of the virus responsible for attachment to the host cell, thus the adsorbed virus particles may be infectious. In fact, the adsorbed virus particles are often prevented from inactivation by the surface they attached to (Schijven & Hassanizadeh, 2000). For example, Chrysikopoulos and Aravantinou (2012) observed that the viruses inactivated slower in the presence of quartz sand than without aquifer media, probably because the sand offered protection against inactivation.

Some viruses are known to aggregate in groundwater. Aggregation of viral particles usually decreases the infectivity rate (Gassilloud & Gantzer, 2005), however, it also protects viruses from physical damage, such as UV radiation, and helps the persistence of viruses within these aggregates (van der Wielen *et al.*, 2006).

Several factors have impact on the aggregation of the virus particles. Aggregation is more likely in concentrated virus stocks, where the virus particles have more chance to interact (Sinclair *et al.*, 2012). The pH of groundwater and the presence and concentration of different ions has a major effect on the aggregation of viruses. The study of Floyd and Sharp (1977) showed that polioviruses and reoviruses were not likely to form aggregates in alkaline solution, whereas acidic pH caused aggregation of both virus types. High ionic strength and the conductivity of groundwater increase the aggregation of viruses. Both variables are defined by the concentration of dissolved inorganic anions (negatively charged ions such as chloride, nitrate, sulphate, and phosphate ions) and cations (positively charged ions such as sodium, magnesium, calcium, iron, and aluminium ions). Floyd and Sharp (1977) observed that the viruses remained stable in low pH solution containing magnesium or sodium ions of low concentration. However, magnesium ion concentration higher than 0.25 mM promoted aggregation at all pHs studied. Other studies also showed that high concentrations of calcium (10 – 50 mM) and magnesium ions (10 – 50 mM) both promoted the aggregation of rotavirus and adenovirus at neutral pH via complementation of the ions and the capsid proteins of the virus particles. In contrast, the presence of sodium ion in solution did not promote the aggregation of the viral particles, possibly due to steric effects of capsid proteins (Gutierrez *et al.*, 2010; Wong *et al.*, 2012).

The main factors influencing virus persistence in groundwater (summarised in Table 1.1) are the virus type, temperature, groundwater chemistry and the presence of microorganisms (De Roda Husman *et al.*, 2009; Gordon & Toze, 2003; Jin & Flury, 2001; Nasser & Oman, 1999).

The inactivation rate of different viruses is likely to vary in the same groundwater. Some enteric viruses (coxsackievirus B1, poliovirus 3, human astrovirus and rhesus rotavirus) can remain infectious in groundwater for up to six months, while adenovirus type 2 may remain infectious in groundwater for up to one year (Charles *et al.*, 2009; Espinosa *et al.*, 2008). According to studies available in the literature, adenoviruses have been shown to be the most persistence enteric viruses in groundwater.

Gordon and Toze (2003) revealed that the presence of microorganisms in the groundwater has a major impact on the persistence of selected enteroviruses (poliovirus and coxsackievirus). There was an approximately three order of magnitude loss in concentration of the viruses within a month when microorganisms were present, while no significant loss of concentration was observed when the groundwater was filtered to eliminate these microbes. The study revealed that anaerobic conditions or large amount of nutrients (e.g. peptone and glucose) reduce the effect of microorganisms on viral persistence. The authors suggested that the lack of oxygen had negative effect on proliferation of the aerobe bacteria, and the nutrients added were more readily consumable for the microbes than the viruses.

Numerous studies showed that the majority of virus inactivation due to microbial presence is caused by proteolytic enzymes (produced by the microbes), which degrade the capsid proteins of the viral particles (Deng & Cliver, 1995; Flynn *et al.*, 2012; Hari Prasad *et al.*, 2012). The effect of these enzymes on virus decay depends on virus type. Nasser *et al.* (2002) observed that the extracellular enzymes produced by *Pseudomonas aeruginosa* in groundwater inactivated coxsackievirus and hepatitis B virus, whereas poliovirus remained infectious.

Temperature has also been proven to have a major effect on virus persistence and movement behaviour in groundwater in many studies (Gordon & Toze, 2003; Nasser & Oman, 1999; Nasser *et al.*, 1993; Ogorzaly *et al.*, 2010; Rigotto *et al.*, 2011; Sobsey *et al.*, 1986). All findings support the notion that viruses lose infectivity more rapidly at higher temperature (14 – 30°C), whereas they remain stable at lower temperature (4°C). A reason for that is the elevated temperature of the groundwater favours degradation of the viral capsid. Furthermore, higher temperature intensifies the effects of other factors, for instance most microorganisms are more active at higher temperature (John & Rose, 2005).

High pH is also known to increase the inactivation of viruses, however, it is only significant at pH higher than 10, which is not typical in groundwater. Consequently, the increase of pH in

sewage treatment systems is primarily to reduce viral activity, thus reduce the probability of groundwater contamination (Charles *et al.*, 2008).

Jansons *et al.* (1989) observed direct association between poliovirus persistence and the concentration of dissolved oxygen in groundwater. The results suggested that the elevated dissolved oxygen concentration may help virus inactivation. The dissolved oxygen may support the growth of microorganisms or the oxidation of the capsid proteins, however, the oxidative effect of dissolved oxygen has not been confirmed as yet.

1.2.2 Adsorption of viruses to aquifer media

The major mechanism for virus removal from groundwater is the attachment to solid particles. The attachment can be irreversible, meaning that there is no detachment from the surface, or the attachment can be reversible. In the latter case viruses detach from surface if conditions (such as pH, temperature or conductivity) change or if the adsorption reaches a kinetic equilibrium.

The attachment mainly depends on virus characteristics, mineral content of the media and groundwater conditions (John & Rose, 2005) (Table 1.1). Different virus strains may have different interactions with solids. For example, Meschke and Sobsey (1998) found that in tertiary treated wastewater poliovirus and Norwalk virus adsorbed at higher degree to different types of media (poliovirus adsorbed more strongly than Norwalk virus) compared with MS2 bacteriophage, which attached at lower degree.

The other main factor influencing virus attachment in groundwater is the type of aquifer media. Mineral particles with particular physical and chemical properties are able to adsorb high number of bioparticles (viruses, bacteria and protozoa). The number of bioparticles adsorbed defines the disinfection capacity of the media. Moore *et al.* (1981) explored the adsorption of poliovirus in 34 different types of soils and minerals. They observed that soils in general were weaker adsorbents than minerals. Among soil types, the soil that had very high concentration of organic matter (200 mg/g) and Genesee silt loam were the weakest to adsorb viruses, as the organic matter may have saturated the virus binding sites. Among types of minerals, montmorillonite, glauconite and bituminous shale were weak adsorbents of viruses, whereas magnetite and hematite were effective adsorbents possibly due to their iron content. Clay is known to adsorb bioparticles, such as viruses, permanently (Gülser *et al.*, 2008).

Meschke and Sobsey (1998) found that clay adsorbs many types of viruses strongly, while coarse sand and organic soil has weak adsorption capacity. The haematite and lime content also increases the adsorption capacity of the soil through the calcium hydroxide attaching to the virus causing flocculation (Bae & Schwab, 2008; Hansen *et al.*, 2007). Soils and minerals containing metal oxides have a great virus adsorption potential (Chu *et al.*, 2003; Pecson *et al.*, 2012). The roughness of mineral particles also has an effect on the adsorption by increasing the physical area available for attachment. Flynn *et al.* (2004) demonstrated that a sand washed repeatedly adsorbed fewer viruses than the fresh one because the surface of the sand particles became smoother as a result of washing.

The main interactions between viruses and solid particles are electrostatic, hydrophobic and covalent-ionic interactions and van der Waals forces. The role of electrostatic interaction in virus adsorption to aquifer media has been well studied. The electrostatic interaction potential is based on the difference between the surface charge of the viruses and solids. Some amino acids (glutamic acid, aspartic acid, histidine and tyrosine) of a viral capsid have carboxyl or amino groups available giving the capsid electrical charge (Gerba, 1984). Negatively charged viruses are more likely to adsorb (either irreversibly or reversibly) when the surface of minerals is coated with aluminium-oxide making the surface more positively charged (Zerda & Gerba, 1984; Zhuang & Jin, 2003). The surface charge of the viruses and the minerals is pH-dependent. The isoelectric point (pI) is the pH of the solution where the surface of the particles has zero net charge. At a certain pH, a virus can be strongly bound to the aquifer material due to difference in the isoelectric points, and when the pH changes the virus can be easily removed from the material (Loveland *et al.*, 1996). Furthermore, an investigation of Redman *et al.* (1997) showed that the adsorption of Norwalk virus is highly pH-dependent and suggested the different electrostatic interactions as reason.

Guan *et al.* (2003) studied virus adsorption at different pHs between 4.6 and 8.3 in order to determine the "critical pH", where virus behaviour changes entirely. They found that the critical pH depends on the isoelectric point of both the viruses and the porous media. The critical pH was observed approximately 0.5 pH unit below the highest isoelectric point of the viruses and the porous media. If the pH of the water was below that point, the virus had opposite charge to at least one component of the media and it was removed in a high rate. Above the critical pH, the charge of the virus and the media was similar, thus the adsorption of the virus was not likely. Other studies indicated that the virus behaviour changed 2.5 – 3.5

pH units above the isoelectric point of the mineral surface (Loveland *et al.*, 1996). Above this pH the virus attachment was reversible and below that pH the attachment was irreversible, suggesting major changes in the surface charges of particles.

At the near-neutral pH of the groundwater, most viruses are negatively charged due to their low isoelectric point (usually below 6), however, it can be higher, like in case of polioviruses, which have isoelectric point of 7. For this reason, it is hard to predict how poliovirus would behave when the pH conditions in groundwater change (Redman *et al.*, 1997).

Hydrophobic interactions also appear to play a major role in adsorption of viruses to solid material (Chattopadhyay & Puls, 1999). The hydrophobic interaction takes place when the particles aggregate and exclude water molecules. Certain amino acids (e.g. methionine, leucine and valine) in the coat proteins of the virus capsid are known to be hydrophobic as well as some solid matter found in aquifers (Chattopadhyay & Puls, 1999; Shimizu *et al.*, 1998). Viruses with hydrophobic surface tend to adsorb to hydrophobic surfaces, and hydrophilic viruses attach to hydrophilic material (Chattopadhyay *et al.*, 2002). Bales *et al.* (1993) noted that the attachment of poliovirus and MS2 bacteriophage to silica was increased when the silica was coated with hydrophobic material implying that these viruses are rather hydrophobic. Wait and Sobsey (1983) also suggested that hydrophobic interactions took place between enteric viruses (poliovirus, echovirus and rotavirus) and highly organic estuarine sediments. Hydrophobic interactions are usually reversible, and release have been showed to be enhanced by decreasing the ionic strength of the solution or giving beef extract, which is also hydrophobic, thus compete for the binding sites with the viruses (Bales *et al.*, 1993; Van Voorthuizen *et al.*, 2001).

The presence of dissolved organic matter (DOM) in groundwater has a major effect on the adsorption of viruses. DOM of groundwater usually derives from wastewater and soil. The most common DOM in groundwater are humic and fulvic acids, which are the products of enzymatic digestion of numerous organic substances in soil. Humic acids and fulvic acids, like some enteric viruses, are both hydrophobic and negatively charged in groundwater, thus they are strong competitors for hydrophobic and positively charged binding sites of solid surfaces (Gerba, 1984). A study by Weaver *et al.* (2013) revealed that the virus recovery from silica sand increased from 5% to 100% in the presence of dissolved organic carbon (DOC). Wall *et al.* (2008) also noted that virus removal decreased in pumice sand columns when DOC was added, further verifying the competition between DOC and the virus particles.

DOM can also wash viruses from the solid surfaces (Jin *et al.*, 2000a) by forcing the detachment of viruses. On the other hand, solid and DOM bonded to the media can increase the rate of virus adsorption by providing additional binding sites (Schijven & Hassanizadeh, 2000).

Surfactants can also be present in groundwater as a result of contamination by treated wastewater. Like humic and fulvic acids, surfactants are hydrophobic, hence they compete for binding sites with hydrophobic viruses (Dizer *et al.*, 1984).

High ionic strength and the conductivity of groundwater increase the attachment rate of viruses (Zhuang & Jin, 2003). The effect of the ions in solution is similar to the effect described for virus aggregation. The presence of multivalent cations predominantly favours the virus adsorption (Tong *et al.*, 2012; Wong *et al.*, 2012; Zhuang & Jin, 2003). Sadeghi *et al.* (2013) demonstrated that calcium ions increased virus attachment to soil particles, which was reversible when calcium was removed from solution. On the other hand, Ryan *et al.* (1999) suggested that phosphate anions may hinder the attachment of PRD1 bacteriophage to positively charged surfaces.

According to these findings, heavy rainfall is a potential risk factor favouring groundwater contamination. This is because the storm-water dilutes the groundwater resulting in low ionic strength and also washes organic matter into the groundwater, which promotes the detachment of adsorbed viruses. Both effects could result in elevated virus concentrations and migration of the viruses in groundwater (Quanrud *et al.*, 2003).

1.2.3 Virus transport in groundwater

Virus particles are able to travel long distances in groundwater without the loss of infectivity. For example, enteroviruses were shown to travel 18 m deep and more than 180 m horizontally in groundwater (Schaub & Sorber, 1977), and the MS2 and ΦX174 bacteriophages reached the depth of 38 m in groundwater under the site of contamination (DeBorde *et al.*, 1998). Borchardt *et al.* (2007) noted that enteric viruses were able to reach and go through a deep confined bedrock aquifer 61 m below ground surface, although the infectivity status of the virus after this passage was not confirmed. The study of DeBorde *et al.* (1998) demonstrated the fast transport of viruses; the MS2 and ΦX174 bacteriophages travelled with velocity of up to 3 m per day. Infectious MS2 virus particles were found to reach the depth of 1 m in 9 hr

through weathered granitic bedrock (Frazier *et al.*, 2002). Furthermore, in some cases viruses are able to flow with velocity of a few hundred meters per day (Rossi *et al.*, 1994; Woessner *et al.*, 2001). Due to adsorption to aquifer media and virus decay, the virus concentration changes during transport. Blanford *et al.* (2005) showed that the concentration of enteric viruses decreased by 9 – 12 orders of magnitude during the first 1 – 4 m of transport, then it remained relatively stable for another 13 m.

In general, small particles are able to move in solution due to diffusion, dispersion and advection. Diffusion is a phenomenon when particles move from areas of high concentration to areas of low concentration. This is a passive movement of particles in solution and is inversely proportional to particle size. Diffusion alone does not have a great impact on the transport of particles in groundwater, where the water is moving as well. In groundwater, the movement of particles is rather described by dispersion and advection. Dispersion is caused by diffusion and hydrodynamic mixing, whereas during advective transport particles drift along with the water flow (Sen, 2011).

Viruses generally reach the groundwater from the surface (septic tanks, wastewater plants, agricultural site, etc.). Scandura and Sobsey (1997) seeded a model enterovirus in a septic wastewater system and observed that the virus entered the groundwater in one day and was detectable for up to two months. Viruses first enter the vadose or unsaturated zone (Anders & Chrysikopoulos, 2009) where virus removal is significant due to the presence of oxygen, organic matter and microbial activity (Sen & Khilar, 2006). In this zone the water flow is usually vertical and viruses are transported to the lower saturated zone (Figure 1.2). Here viruses remain viable for longer because of the low oxygen level and the low sorption capacity of the matrix. The direction of water flow in this zone is mostly horizontal.

Under saturated conditions only the solid-water interface affects the virus adsorption. Under unsaturated conditions the air-water and air-solid interfaces have a key effect on virus behaviour (Figure 1.3). The presence of air has been shown to enhance retention of viral viability and adsorption in many studies (Anders & Chrysikopoulos, 2009; Jin *et al.*, 2000a; Thompson & Yates, 1999). In a laboratory study by Lance and Gerba (1984) poliovirus travelled 40 cm under unsaturated conditions and 160 cm when air was not present. Furthermore, Powelson and Gerba (1994) noted that the removal of viruses was three times higher under unsaturated as opposed to saturated conditions in the same soil medium.

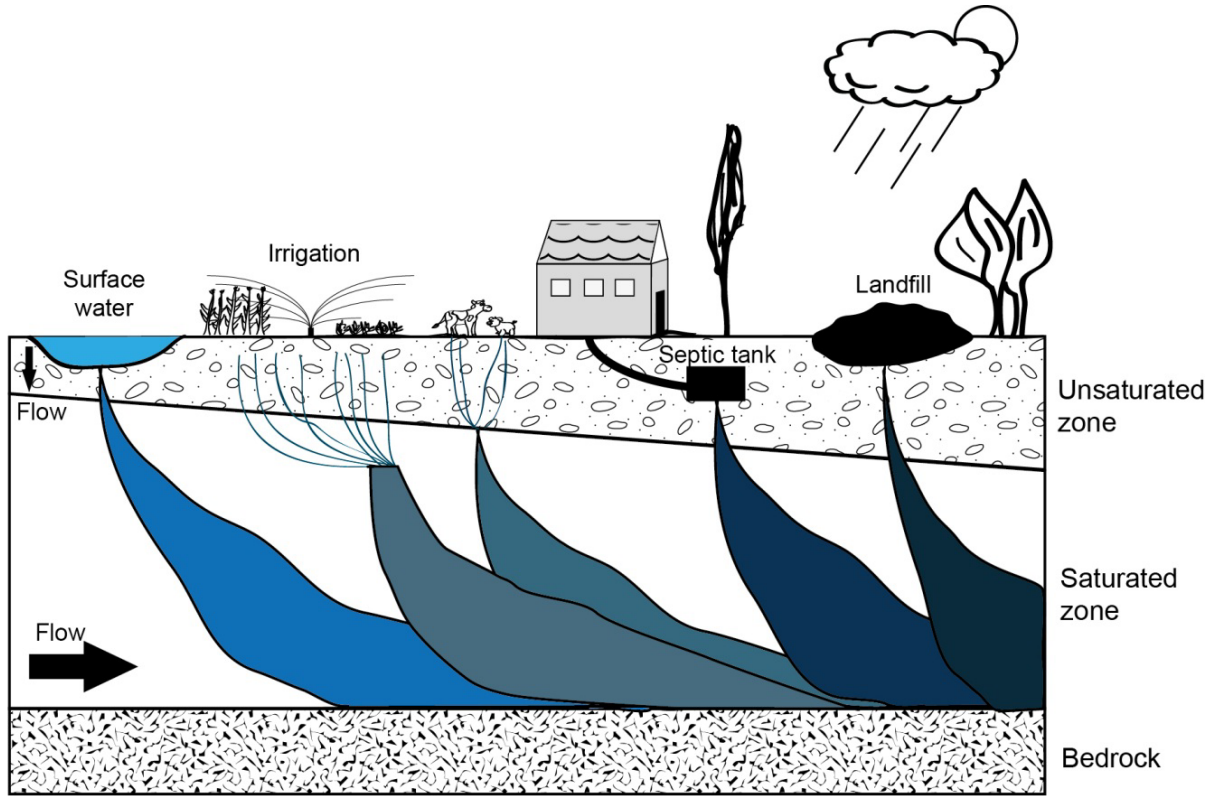

Figure 1.2 Sources and pattern of migration of viruses in the subsurface area. Based on Sen (2011).

Studies of Thompson and Yates (1999) and Lazouskaya and Jin (2008) both suggested that hydrophobic effects are crucial in colloid adsorption at the air-water interface, however, surface charges, contact angle and surface tension also affect the adsorption. Torkzaban *et al.* (2006) demonstrated that the attachment to air-water interface is mainly reversible. The presence of air has been shown to enhance both the adsorption and the inactivation of some viruses (Jin *et al.*, 2000a; Powelson *et al.*, 1990).

Flow rate of the groundwater has a major effect on virus transport. Fractured media allows for higher flow rate than porous media due to the size differences between porous and fractured void. In general, viruses travel with similar velocity as the flow rate of the groundwater (DeBorde *et al.*, 1999). The increased flow rate of the groundwater results in elevated virus velocity and decreased adsorption (Walshe *et al.*, 2010). Thus at high flow rate viruses will travel for long distances. The velocity of pathogens can exceed the average flow rate of the groundwater due to microscopic pathways, where the water flow is elevated (Taylor *et al.*, 2004). Low groundwater flow rate results in reduced dissolved oxygen level in the water, thus favours persistence of viruses (Sidhu & Toze, 2012).

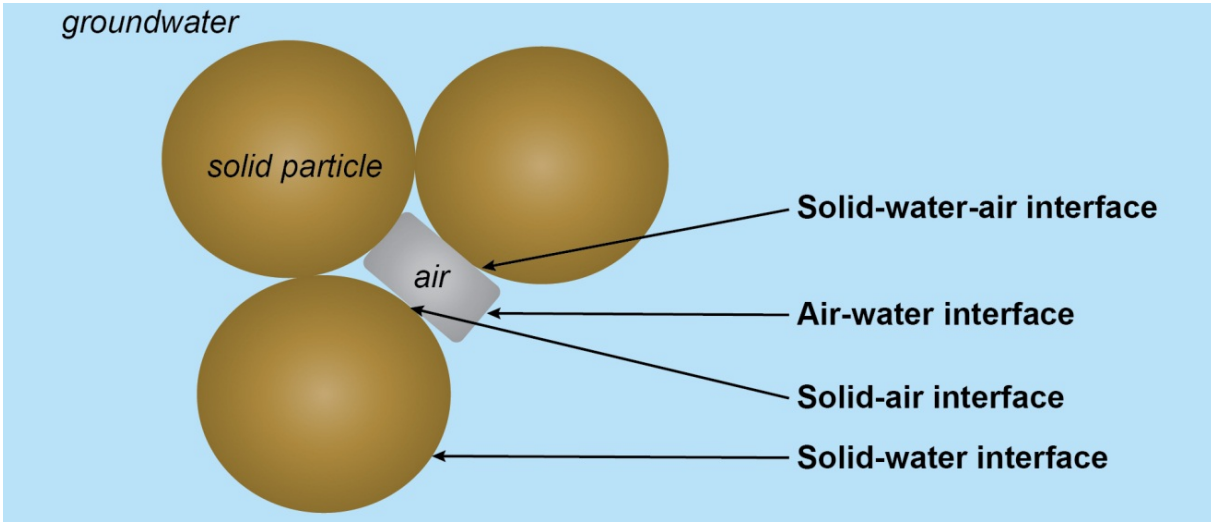

Figure 1.3 The main interfaces presented in groundwater.

The retention capacity of aquifers is dependent on the mineral content. Some minerals are permeable to colloidal particles while others retain viruses in a high rate. The hydraulic conductivity, porosity and sorption capacity appear to be the most important parameters of minerals in virus transport (Barth & Hill, 2005).

The size of mineral particles also affects the transport of viruses (Schijven & Hassanizadeh, 2000). In general coarse-size media facilitate the migration of small particles compared to fine-sized media (Quanrud *et al.*, 2003). Although Syngouna and Chrysikopoulos (2012) found no significant difference in migration of viruses in sand with particles smaller than 1.7 mm. The heterogeneity of the aquifer media affects virus transport as well. The different minerals and pore sizes force viruses to be transported through preferential pathways and to avoid some area of the groundwater body (Corapcioglu *et al.*, 2006).

The two major mechanisms limiting virus transport in aquifer are adsorption and exclusion/filtration. The adsorption of viruses to aquifer media has already been discussed (Section 1.2.2). During transport both reversible and irreversible attachment occurs (Woessner *et al.*, 2001). Under conditions that enhance attachment (e.g. low pH, high ionic strength and adsorption capacity of the minerals), virus transport will be retarded. When the adsorption of viruses is low, they can travel for long distances. In column studies, a decrease in pH or increased ionic strength resulted in retarded transport of viruses due to increased adsorption (Sadeghi *et al.*, 2011; Walshe *et al.*, 2010). Woessner *et al.* (2001) demonstrated correlation between the attachment of viruses during transport in groundwater and their isoelectric points,

which has a major effect on virus adsorption. Pieper *et al.* (1997) compared virus migration in sewage-contaminated and uncontaminated soil, and observed that three times more viruses travelled through the first meter of the contaminated zone than the uncontaminated zone, suggesting that virus adsorption was decreased, possibly due to high concentration of DOM competing for adsorption sites. The presence of anions, such as phosphate, sulphate or bicarbonate enhances virus transport, while the presence of bivalent cations (magnesium or calcium ions) retains viruses due to their effect on adsorption (Pieper *et al.*, 1997; Sadeghi *et al.*, 2013; Zhuang & Jin, 2003).

Virus particles are excluded from porous media due to their size and charge (Jin & Flury, 2001). Two possible mechanisms can be considered to be responsible for size exclusion. Size exclusion takes place when viruses do not penetrate the aquifer media because their size is larger than the pore size between the mineral particles. The other mechanism based on the phenomenon that the flow conditions in a pore are different near the soil/aquifer particles and in the middle of the pore: the water flows at higher velocities in the middle, therefore, large colloids are excluded from the slow flow regions near surfaces due to steric effects and thus experience a higher average flow velocity (DiMarzio & Guttman, 1970). Both mechanisms result in the fast transport of viruses compared to soluble tracers, which has been demonstrated in field studies (Corapcioglu *et al.*, 2006; Rossi *et al.*, 1994; Sinton *et al.*, 2000). In addition to steric exclusion, the negatively charged viruses may be repulsed by the negatively charged soil and mineral particles, therefore, the viruses are forced to travel in the high flow regions (i.e., anion exclusion) (Scheibe & Wood, 2003), however the relevance of this phenomenon in virus transport has not been properly investigated. Exclusion may be enhanced when the virus particles aggregate or travel attached to other colloids. In the latter case, viruses attach to the surface of colloids (e.g. DOM) in the wastewater or in the soil and then travel in a bonded form (Jin *et al.*, 2000b). The transport velocity and pattern of the linked particles may differ from the transport of the free colloids/viruses. For instance, Walshe *et al.* (2010) and (Sinton *et al.*, 2012) showed that the travel time and the recovery decreased when the virus particles were attached to kaolin.

Viruses are one of the largest health risks for drinking water. Therefore, it is crucial to understand how viruses reach drinking water wells and how long they are able to persist in an infective state under different conditions which may apply in groundwater. The main mechanisms and influencing factors on virus movement in groundwater have been relatively

well described and understood. However, it is still challenging to quantitatively predict the retention and transport of viruses in aquifer media.

1.3 Existing pathogenic virus surrogates and their limitations

Numerous studies have been performed in laboratory environments to understand the fate and transport of viruses in groundwater. In some cases the results obtained from these experiments do not support field observations. Pathogenic viruses cannot be introduced into natural aquifers for further observations as they are hazardous to public health. Furthermore, some viruses are hard to maintain *in vitro,* and due to their infectious nature, they need special environment and equipment to study. Therefore, there is a need for surrogates for enteric viruses to understand likely viral dynamics in different environments including groundwater.

A definition, suggested by Sinclair *et al.* (2012), for the term surrogate is "an organism, particle, or substance used to study the fate of a pathogen in a specific environment". The first surrogates used in groundwater studies were faecal coliform bacteria as indicators of faecal contamination. However, recent studies suggest that these organisms do not necessarily mimic viral contamination since their size, survival and transport patterns in groundwater differ from viruses (Lance & Gerba, 1984; Leclerc *et al.*, 2000). The most recently used enteric virus surrogates include bacteriophages, animal viruses and microspheres, which are discussed in detail below.

1.3.1 Bacteriophages

The most commonly used surrogates for human enteric viruses in groundwater studies are bacteriophages. Bacteriophages are bacteria-infecting viruses, and are present naturally in ecosystems and in human faecal matter. Bacteriophages of coliform bacteria are frequently used as surrogates for pathogenic viruses in groundwater research. Many species are involved in this group; their physical-chemical properties, such as size, shape and isoelectric point, show large variation.

The features that make bacteriophages good surrogates for pathogenic viruses were summarised by Schijven and Hassanizadeh (2000) and Jin and Flury (2001). In brief, bacteriophages are not pathogenic to human and, as they are viruses, they are unable to reproduce in groundwater due to the low number or the lack of host cells. They can be

prepared in large quantities suitable for field experiments and can be easily detected and quantified. Bacteriophages can be stained with fluorescent dyes without changing their behaviour in groundwater. Fluorescent-labelled bacteriophages are more easily detected by optical methods (e.g. fluorometer) compared with the traditional culturing technique (Gitis *et al.*, 2002). The stained bacteriophages can also be easily distinguished from the natural environmental strains.

The most important feature of an ideal model for enteric viruses is that they have similar or less sorption, inactivation and retention profiles as those of enteric viruses; this makes bacteriophages conservative estimators of pathogenic viruses that may be present. Some of the bacteriophages have similar characteristics to enteric viruses in terms of size, shape and isoelectric point, hence they have been used as surrogates. The most commonly used bacteriophages in groundwater research are MS2, PRD1 and ΦX174 (Collins *et al.*, 2006; Schijven & Hassanizadeh, 2000). The main characteristics of these bacteriophages and some enteric viruses are summarised in Table 1.2.

1.3.1.1 MS2 bacteriophage

The MS2 bacteriophage (Enterobacteria phage MS2) infects the *Escherichia coli* bacterium. MS2 is an F-specific bacteriophage, which means that it infects the host cell through the F-pilus, which is formed by some bacteria during their life cycle. MS2 has icosahedral capsid and is approximately 27 nm in diameter. Its isoelectric point is at pH 3.5 – 3.9 (Table 1.2). MS2 is the most widely used model virus in groundwater research. It has less adsorption and retention properties than enteric viruses in many type of soils, therefore, it can be considered as a worst case virus. For instance, a batch study revealed that MS2 had no adsorption to a soil, which adsorbed a high rate of hepatitis A virus and poliovirus (Blanc & Nasser, 1996). The transport of MS2 was also studied in three different sandy soils, and no significant removal was observed in the pH range of 5.7 – 8.0, which is the typical pH of groundwater (Kinoshita *et al.*, 1993). MS2 has been found to have greater recovery compared to Norwalk virus in laboratory studies when quartz sand was used as aquifer media (Redman *et al.*, 1997). Moreover, MS2 has been shown to have higher recovery than poliovirus in a column packed with silica with potential influence by electrostatic interactions (Bales *et al.*, 1993). On the other hand, the same study revealed that MS2 tends to attach to hydrophobic surfaces. MS2

has also been found to be sensitive to changes in ionic strength (Cao *et al.*, 2007; Chu *et al.*, 2000; Zhuang & Jin, 2003).

Table 1.2 Characteristics of enteric viruses and bacteriophages. *Reference for the size and genome for viruses: Tidona and Darai (2011). "ds": double-stranded, "ss": single-stranded. N/A: information not available.

Virus	Approximate size*	Genome*	pI	References for pI
Adenovirus (*Adenoviridae*)	80 nm	dsDNA	3.5 – 4.0 (type 2) 4.5 (type 5)	Wong *et al.* (2012) Trilisky and Lenhoff (2007)
Rotavirus (*Reoviridae*)	75 nm	dsRNA	4.5	Gutierrez *et al.* (2009)
Coxsackievirus (*Picornaviridae*)	28 – 30 nm	ssRNA	4.75 and 6.75	Butler *et al.* (1985)
Echovirus (*Picornaviridae*)	28 – 30 nm	ssRNA	5.0 – 6.4	Butler *et al.* (1985)
Poliovirus (*Picornaviridae*)	28 – 30 nm	ssRNA	6.6-7.1 and 4.5 (type 1)	Butler *et al.* (1985) Mandel *et al.* (1971)
Hepatitis A (*Picornaviridae*)	28 – 30 nm	ssRNA	2.8	Nasser *et al.* (1992)
Hepatitis E (*Hepeviridae*)	27 – 34 nm	ssRNA	N/A	-
Norovirus (*Caliciviridae*)	27 – 32 nm	ssRNA	5.2 – 6.9	Goodridge *et al.* (2004)
MS2 (*Leviviridae*)	27 nm	ssRNA	3.5 – 3.9	Langlet *et al.* (2008) Penrod *et al.* (1995)
PRD1 (*Tectiviridae*)	64 nm	dsDNA	< 4	Loveland *et al.* (1996) Ryan *et al.* (1999)
ΦX174 (*Microviridae*)	30 nm	ssDNA	6.6 – 6.8	Horká *et al.* (2007)

The major disadvantage of MS2 is that it inactivates faster than most enteric viruses, especially at temperature higher than 10°C. Collins *et al.* (2006) used four different solutions (groundwater, UV-treated groundwater, phosphate buffered saline and Ringer-solution) at 12°C to study the inactivation of MS2 bacteriophage and poliovirus in a 77-day experiment. They noted that the concentration of MS2 dropped by approximately 50% during the course of the experiment, while the decrease of poliovirus concentration was less than that (20 – 50%). Gitis *et al.* (2011) also observed the inactivation of MS2 at 4°C was not significant, but when temperature was increased to room temperature the inactivation rate increased

dramatically (0.001 vs. 0.15 ln/day). Ogorzaly *et al.* (2010) compared the inactivation rates of MS2 and human adenovirus type 2 viruses in groundwater in a 4-month experiment, and demonstrated that adenovirus was more stable in groundwater at both 20°C and 4°C.

1.3.1.2 PRD1 bacteriophage

PRD1 is a somatic coliphage that infects *E. coli* by attaching to its cell wall (rather than the F-pilus as MS2 does). PRD1 has icosahedral capsid like MS2, but is larger in size, approximately 60 nm (Table 1.2), which makes it a promising candidate for modelling larger enteric viruses such as rotavirus and adenovirus. The isoelectric point of PRD1 has not been properly determined. Surface charge measurements under different conditions indicated that is between pH 3 – 4 (Loveland *et al.*, 1996), however, extrapolation suggest that it may be below 3 (Ryan *et al.*, 1999). PRD1 adsorbs to soil at a higher rate than MS2, probably because it is more hydrophobic than MS2 (Kinoshita *et al.*, 1993), which has been noted in many studies; e.g. Bales *et al.* (1991) and Lytle and Routson (1995).

Woessner *et al.* (2001) observed that PRD1 behaves more conservatively than the other two model viruses (MS2 and ΦX174) and poliovirus in both sand and gravel aquifers. PRD1 seems to be more stable and less sensitive to temperature changes than MS2 (Harvey & Ryan, 2004). A study of Yahya *et al.* (1993) showed in a 80-day groundwater experiments that MS2 and PRD1 are both stable at 7°C, but between 10°C and 23°C MS2 inactivated 7 – 10 times faster than PRD1. Charles *et al.* (2008) studied the inactivation of MS2 and PRD1 in sewage and effluent and also found that increased temperature elevated the inactivation of MS2 but had little effect on PDR1.

It is worth mentioning that the PRD1 bacteriophage is not available at the American Type Culture Selection (ATCC), the most widely used commercial source of microorganisms and viruses. Thus PRD1 is hard to obtain, and the genetic similarity of the PRD1 used in different studies and the effect of genetic differences on experimental outcomes are questionable.

1.3.1.3 ΦX174 bacteriophage

ΦX174 is a somatic coliphage with icosahedral capsid 30 nm in diameter and isoelectric point 6.6 – 6.8, which is close to the pH of groundwater. Hence even minor changes in the pH of the groundwater entirely change its attachment behaviour. Its size and isoelectric point is

similar to poliovirus, thus it was thought to be an ideal model for poliovirus. However, early studies showed that there is a difference in their transport. Funderburg *et al.* (1981) studied the transport of poliovirus, reovirus and ΦX174 bacteriophage in eight different agricultural soils. They discovered that the retention of poliovirus and reovirus was mainly affected by the soil characteristics, whereas the retention of ΦX174 was rather time dependent. ΦX174 was retained at a high degree (90%), suggesting that ΦX174 is not a suitable model virus in the examined soils.

ΦX174 is presumably more inert than MS2 since it has little surface charge in groundwater and the electrostatic interactions have little relevance (Lytle & Routson, 1995). ΦX174 is not sensitive to the effect of surfactants and organic matter (which MS2 and PRD1 are) due to its low hydrophobicity (Chattopadhyay *et al.*, 2002). MS2 had a lower recovery than ΦX174 in sand column experiments when high ionic strength solution was used or the media was coated with aluminium-oxide to increase its positive charge (Zhuang & Jin, 2003). ΦX174 was found to be less sensitive to the presence of organic matter and more persistent to ambient temperature than MS2 (Chrysikopoulos & Aravantinou, 2012). Jin *et al.* (2000a) demonstrated that ΦX174 was reversibly adsorbed when injected to highly unsaturated quartz sand, whereas MS2 was irreversibly inactivated under similar conditions.

1.3.1.4 Other bacteriophages

T-phages are also broadly used to study virus transport in groundwater. They are coliphages as well, but their shape differs from MS2, PRD1 and ΦX174. T-phage have icosahedral head that varies in size between 80 – 100 nm and a tail (50 – 200 nm), which allows the attachment to the host cell. Several studies attempted to investigate the usefulness of T-phages as virus surrogates in groundwater. For example, T7 phage was successfully used as tracers to study the filtration capability of epikarst (Flynn & Sinreich, 2010). T2 phage has been shown to be more stable than ΦX174 over time and less sensitive to surfactants (Chattopadhyay *et al.*, 2002). T4 phage was recovered at a high rate (86%) from fractured chalk, compared with MS2 (65%) or ΦX174 (64%) probably due to its larger size (Weisbrod *et al.*, 2013).

A bacteriophage infecting *Bacteroides fragilis 40* was also found to have similar inactivation rates as poliovirus and rotavirus (Jofre *et al.*, 1986). Furthermore, it was found to be as resistant to chlorination as poliovirus and rotavirus (Tartera *et al.*, 1988). These findings

suggest that it would be a good surrogate for enteric viruses in long-term environmental studies.

1.3.2 Other viral surrogates

Some enteric viruses hardly or cannot be tissue cultured, thus the confirmation of infectious virus particles in samples is challenging. Therefore, the potential of closely related animal viruses as surrogates for human viruses has been investigated. This is based on the general observation that viruses belonging to the same genus have similar morphological and genome characteristics, hence their fate and transport in the environment should be similar as well.

A simian rotavirus strain SA-11 appears to be a good surrogate for human rotavirus. SA-11 can be maintained in laboratory, has similar characteristics to human rotavirus and both SA-11 and human rotavirus adsorb to membrane filters at low pH and detached at high pH. The adsorption of SA-11 to aluminium hydroxide and sludge flocks is also similar to the human rotavirus (Farrah *et al.*, 1978). Hence, it has been used in many groundwater studies (Dizer *et al.*, 1984; Espinosa *et al.*, 2008; Goyal & Gerba, 1979; Herbold-Paschke *et al.*, 1991) along with porcine rotavirus, which has also been used to investigate the aggregation and adsorption of rotaviruses (Gutierrez *et al.*, 2009; Gutierrez *et al.*, 2010).

Feline calicivirus has been suggested as a potential surrogate for human norovirus because of its similar surface and genome characteristics. Studies showed it was a suitable model for testing the efficacy of disinfectants (Doultree *et al.*, 1999), virus inactivation under high pressure (Grove *et al.*, 2008) and the inactivation of foodborne viruses (Straube *et al.*, 2011). Bae and Schwab (2008) compared the fate and behaviour of human norovirus to feline calicivirus, murine norovirus, poliovirus and a MS2 bacteriophage. They noted that feline calicivirus inactivated easily in surface and groundwater samples, thus it was not suitable to mimic the behaviour of norovirus in the environment. The study suggested that murine norovirus was the most promising surrogate for human norovirus.

Obviously neither of these potential surrogates can be used in field studies as they are a potential hazard to the animals, however, they can be used in laboratory experiments without any health concerns.

1.3.3. Microspheres

Microspheres have also been used for studying virus transport. The advantage of these surrogates is their easy and inexpensive detection. They are also biologically and chemically inert and available in various sizes, thus suitable to study the effect of size on pathogen transport (Close *et al.*, 2006).

Bales *et al.* (1997) observed that 100 nm polystyrene beads were less retarded in porous media than PRD1 and M-1 phage. (M-1 phage was isolated from a sewage tank, and has similar characteristics as T-phage.) Weisbrod *et al.* (2013) compared the transport of 20 nm and 200 nm fluorescent latex beads with MS2, ΦX174 and T4 bacteriophages, and observed that the 20 nm beads had slightly less recovery than MS2 and ΦX174 despite the size similarities. The authors suggested the reason was the lower density or the aggregation of the beads. The large beads (200 nm) were recovered entirely while the T4 phage, which has similar size, was slightly retained, probably due to its shape. These finding also support the idea that the size and diffusion capability of particles determine their retention. Contradictory, Mondal and Sleep (2013) found that 20 nm polystyrene microspheres had three times greater retention in dolomite fractures than the MS2 bacteriophage with similar size. Furthermore, they found that the transport of the 200 nm beads was more similar to the transport of the MS2 and PRD1 bacteriophages implying that surface characteristics also influence particle behaviour. They also observed that the microspheres were more sensitive to changes in the ionic strength of the solution than the bacteriophages. Other studies also support the observation that ionic strength and ionic composition of a solution have major effects on the fate and transport of colloidal particles (McCarthy *et al.*, 2002; Saiers & Lenhart, 2003).

Pang *et al.* (2009) proposed mimicking attenuation and transport of viruses using nanoparticles coupled with proteins that had surface charge characteristics similar to the virus of interest. They demonstrated that when the 20 nm polystyrene particles were covalently coupled with casein, which had an isoelectric point similar to MS2, the modified beads displayed a surface charge similar to that of MS2. However, the resemblance of the attenuation and transport behaviour of the modified beads to MS2 was not validated.

In summary, according to the current knowledge of enteric virus transport it is generally suggested to use a range of virus models to understand the transport of these viruses under specific conditions (Charles *et al.*, 2008). MS2 bacteriophage is considered a suitable

surrogate for many types of enteric viruses in short-term experiments at temperatures lower than 10°C. PRD1 is suitable for long term experiments at ambient temperatures. ΦX174 is the better choice in environments that favour hydrophobic interactions. Bacteriophages composed of a head and a tail can be used in comparison with icosahedral bacteriophages with different sizes to ascertain whether the size and shape of the virus affect the transport under certain conditions. Animal viruses are useful in laboratory studies to mimic the human strains. Synthetic microspheres are available in various sizes, and their surface charge can be easily modified, thus they can be customised to mimic the behaviour of specific viruses.

1.4 Research approach and objectives

The aim of this research thesis was the validation of new surrogates to study the behaviour of rotavirus and adenovirus in groundwater. The viruses were chosen because they are frequently found in groundwater and are responsible for gastrointestinal outbreaks amongst children globally. To model the behaviour of these enteric viruses, DNA-labelled and protein-coated silica nanoparticles were developed. These new surrogates were designed based on the hypothesis that particles with similar physico-chemical characteristics to the enteric viruses would resemble their fate and transport in groundwater. In order to survey the usefulness of the new surrogates, the behaviour of the most commonly used surrogate (MS2 bacteriophage) was also investigated.

The specific research objectives were as follows:

1) **Purification and characterisation of the viruses (Chapter 2)**
   The rotavirus, adenovirus and the MS2 bacteriophage were purified from culture material prior to all measurements. For adenovirus purification a commercially available kit was used, whereas for rotavirus and MS2 a new size exclusion chromatography method was developed. Quantitative polymerase chain reaction (qPCR) based methods were also developed for the quantification of the viruses. For characterisation, the surface charge, size, hydrophobicity and the stability of rotavirus, adenovirus and MS2 bacteriophage were investigated.

2) **Characterisation of the surrogates (Chapter 3)**

   DNA-labelled and protein-coated silica nanoparticles with size similar to the rotavirus and adenovirus were characterised for their size, surface charge, hydrophobicity and aggregation over time. Results were compared with those of viruses. The stability of the DNA-labelling was validated by agarose gel electrophoresis and qPCR.

3) **Validation of the surrogates' usefulness in groundwater studies (Chapter 4 – 6)**

   Laboratory-scale batch studies investigated the adsorption and degradation tendencies of both viruses and surface-modified nanoparticles. Column studies were set up to have a better understanding of virus attenuation and movement in groundwater. Similar columns were used to test the mimicry of the surrogates.

In order to mimic the properties of groundwater in the laboratory studies, experiments were performed using 2 mM sodium chloride (NaCl) solution with pH of 7.0. This electrolyte mimics the neutral pH (6.5 – 7.5) and low ionic strength (1.5 – 3 mM) typical for groundwater (Gerba & Bitton, 1984). Unless stated otherwise, the experiments were set up at room temperature (20 – 23°C). Two aquifer material, fine sand and fine gravel were used in the experiments, which represent aquifers in the Canterbury region of New Zealand (Rosen, 2001). Pure silica sand (Ottawa sand) and hydrophobic sand were also used to determine the role of hydrophobic interactions in virus adsorption.

Chapter 2.
Virus purification and characterisation

2.1 Introduction

Enteric viruses are able to maintain their virulence for prolonged periods of time in the environment and are transmitted to hosts through water, sewage, soil, food or animals. As reviewed in Chapter 1, the virus persistence and transport in water is dependent on the type of viruses. Size, surface structure and other physico-chemical properties all influence the behaviour of viruses. With a better understanding on these features, the fate of pathogens in the environment can be predicted more accurately.

This study focuses on two enteric viruses, rotavirus and adenovirus, and the MS2 bacteriophage. The rotavirus and the adenovirus are extremely contagious and stable in water systems, therefore, they have been a focus of environmental research. Due to their ability to infect humans and animals, the risk involved in release of enteric viruses for environmental studies is unacceptable. Therefore, in many environmental studies bacteriophages (most commonly the MS2 bacteriophage) are used as surrogates for rotavirus and adenovirus.

2.1.1 Rotavirus

Rotavirus has been established as the main causative agent of gastroenteritis among infants and young children (Desselberger & Gray, 2009; Wadell, 1984). In the United States, 95% of children experience at least one rotavirus infection by the age of five years (Atkinson *et al.*, 2011). Each year worldwide, rotavirus is responsible for nearly 600,000 deaths, usually as a result of severe dehydration (Parashar *et al.*, 2009).

The *Rotavirus* genus (family *Reoviridae*) contains seven serogroups (A to G), based on specificities of their antigens. According to current knowledge, rotavirus A, B and C have been found in both humans and animals, whereas the other serotypes infect animals (mainly birds and mammals) only (Estes & Greenberg, 2013). Rotavirus A is known to be the

predominant cause of human gastroenteritis among infants, rotavirus B infects mainly adults (Hoshino & Kapikian, 2000; Jiang *et al.*, 2008), and rotavirus C mostly cause illness in adults and in 3 – 5 year-old children (Castello *et al.*, 2002; Nilsson *et al.*, 2000; Oishi *et al.*, 1993). The virus enters the host through the mouth and replicates in the villous epithelium in the small intestine less than 48 hours post infection (Atkinson *et al.*, 2011). The typical symptoms are diarrhoea, nausea and fever, which mostly resolve in one week, and the infection usually confers long-lasting immunity (Estes & Greenberg, 2013).

Rotaviruses are non-enveloped virus with icosahedral capsid. The size of these viruses is approximately 75 nm in diameter (Gutierrez *et al.*, 2010), and their buoyant density is 1.36 – 1.40 g/cm^3 (Vonderfecht *et al.*, 1984). The rotavirus genome consists of 11 segments (approximately 18,600 base pairs) of double-stranded RNA (dsRNA), with six genome segment coding six structural viral proteins (VP) and five segments coding six non-structural proteins (NSP; Figure 2.1) (Bruggemann, 1985; Estes & Greenberg, 2013).

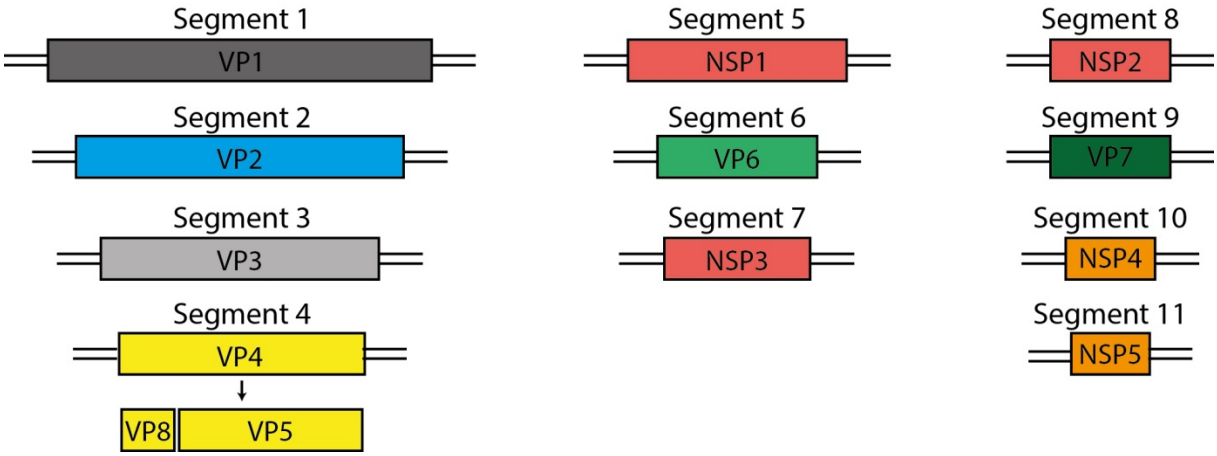

Figure 2.1 Segments of the rotavirus genome. The sizes of the segments are 660 – 3,300 nucleotides. Based on the illustration of the Swiss Institute of Bioinformatics at http://viralzone.expasy.org.

Structure of rotavirus capsid proteins has been well characterised using electron cryo-microscopy and X-ray crystallography (Chen, 2009; Lepault, 2001). Rotaviruses have a triple-layered capsid (Figure 2.2). The outer capsid of the mature infectious rotavirus is composed of VP7 and VP4. The icosahedral surface is comprised of assembled VP7 trimers surrounding channels. Dimers of the VP4 protein (formed by the connection of VP5 and VP8) compose spikes on the outer surface. The icosahedral intermediate layer of the capsid is formed by VP6 protein trimers. During infection, the outer capsid of the virion is removed following cell

entry, but the double-layered capsid stays intact during transcription (Venkataram Prasad & Estes, 1997). Underneath the VP6 layer is the core protein layer composed of VP2. This layer houses the genome surrounded by VP1 and VP3 proteins, which play a role in transcription and replication (Pesavento, 2006).

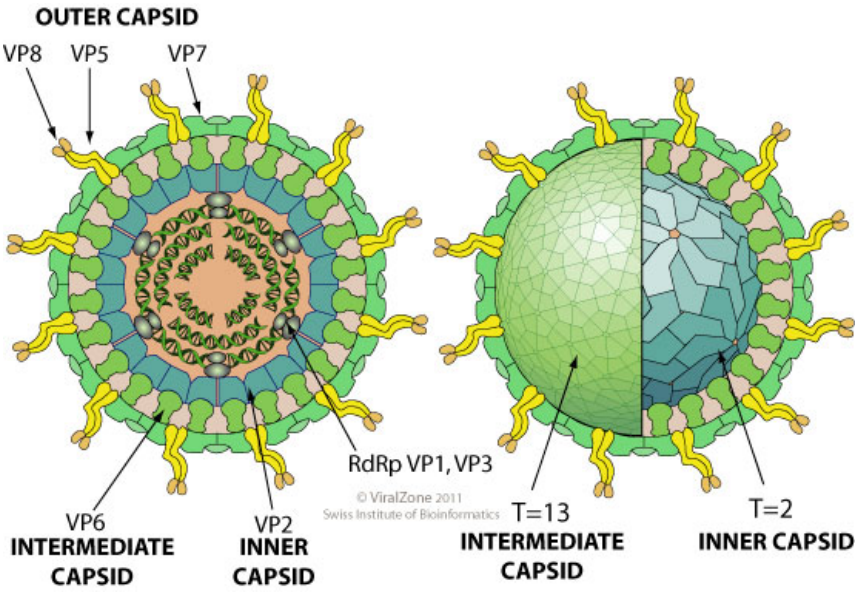

Figure 2.2 Structure of the rotavirus virion. Adapted from: http://viralzone.expasy.org.

2.1.2 Adenovirus

Up to 12% of gastroenteritis cases globally are related to adenovirus infection (Mena & Gerba, 2009). Due to the strong connection between contaminated drinking water and adenovirus outbreaks, the adenoviruses are amongst the pathogens included on the Drinking Water Candidate List (USEPA) since 1998 (http://water.epa.gov/scitech/drinkingwater/dws/ccl/ccl3.cfm). The list, updated in every five years, contains important yet unregulated contaminants of water systems that may require control.

According to the latest findings, 51 serotypes in six subgroups (A to F) of the *Adenovirus* genus (family *Adenoviridae*) cause various human infections such as gastroenteritis, respiratory and eye infections (Wold & Ison, 2013). However, diarrhoea can occur during most kinds of adenovirus infection, type 40 and type 41 adenoviruses (subgroup F) specifically responsible for gastro-intestinal illness (Mena & Gerba, 2009). Since 1986, adenovirus type 41 has been predominant worldwide (Okitsu-Negishi *et al.*, 2004). The symptoms of the adenovirus-related gastroenteritis are very similar to the illness caused by

rotavirus infection and usually occurs in children younger than four years (Wold & Ison, 2013).

Adenoviruses, like rotaviruses, are non-enveloped viruses with a 80 nm icosahedral capsid (Mei *et al.*, 2011), and their buoyant density is 1.32 – 1.35 g/cm^3 (Sprinzl *et al.*, 2001). Adenovirus contains a 36,000 base pairs double-stranded DNA (dsDNA), encoding structural and non-structural proteins (Figure 2.3).

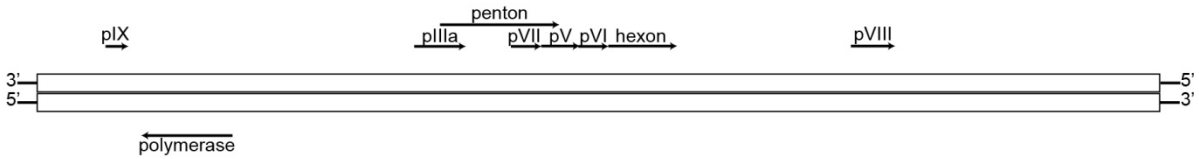

Figure 2.3 Adenovirus genome organisation. Based on the genome structure of the adenovirus type 2 and type 5, adapted from Berk (2013) .

The capsid of adenoviruses contains three major and three minor coat proteins. The major coat proteins are the hexon (polypeptide II) and the penton-complex formed from penton base (polypeptide III) and fibre (polypeptide IV; Figure 2.4). Nonetheless, subgroup F adenoviruses have unique surface characteristics as their capsid contains two distinct fibre proteins, a short and a long one, with molecular weight of 40 kDa and 60 kDa, respectively (Kidd *et al.*, 1993; Yeh *et al.*, 1994).

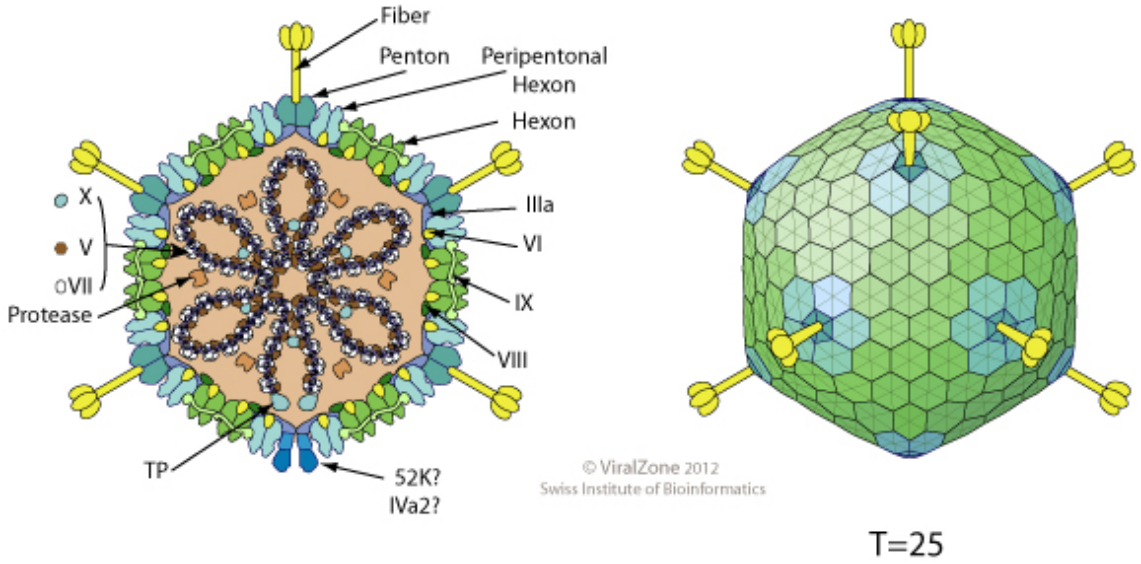

Figure 2.4 Structure of the adenovirus virion. Adapted from: http://viralzone.expasy.org.

The function of the minor coat proteins (polypeptide IIIa, VIII and IX) is still not clear due to the lack of high resolution structures (San Martin, 2012). It has been postulated that they may play role in virus assembly, viral structural stability and DNA packaging (Vellinga, 2005). The dsDNA binds covalently to terminal proteins (TP) and also interacts with polypeptide V, VII and X forming a chromatin-like structure, the core (Chatterjee *et al.*, 1986; Karen & Hearing, 2011; Samad *et al.*, 2007).

2.1.3 Bacteriophage MS2

The MS2 bacteriophage (family *Leviviridae*) is the most commonly used model virus in groundwater research. It infects *E. coli* (regularly found in human faeces and in the environment) via its F-pilus. An infection results in the lysis of the bacterial cell.

The MS2 capsid is composed of coat protein dimers, an assembly protein. The capsid houses the positive-sense single-strand RNA (ssRNA) genome, which contains only 3,569 nucleotides, encoding four genes (Figure 2.5) (Olsthoorn & Duin, 2011).

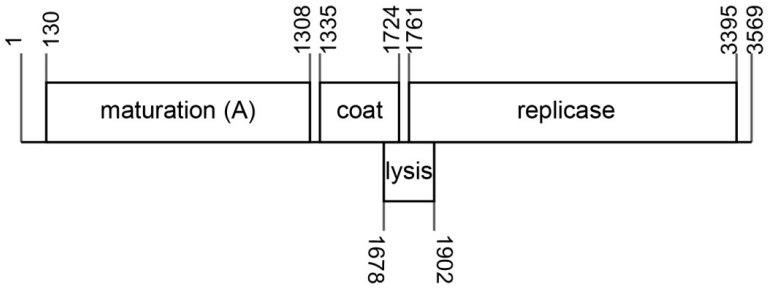

Figure 2.5 MS2 genome organisation. Based on Olsthoorn and Duin (2011).

The coat protein homo-dimers assemble to form the 26 nm icosahedral capsid (Figure 2.6). The capsid also contains a single copy of a maturation or assembly protein (A-protein) outside the capsid. The function of this protein is not fully known, however, research supports the idea that it is associated with RNA packaging and host recognition and attachment (Hendrix, 2013; Stockley *et al.*, 1994). The replicase catalyses the replication of the RNA. The lysis protein is synthesised during infection and triggers cell lysis when accumulated to an adequate level (Hendrix, 2013).

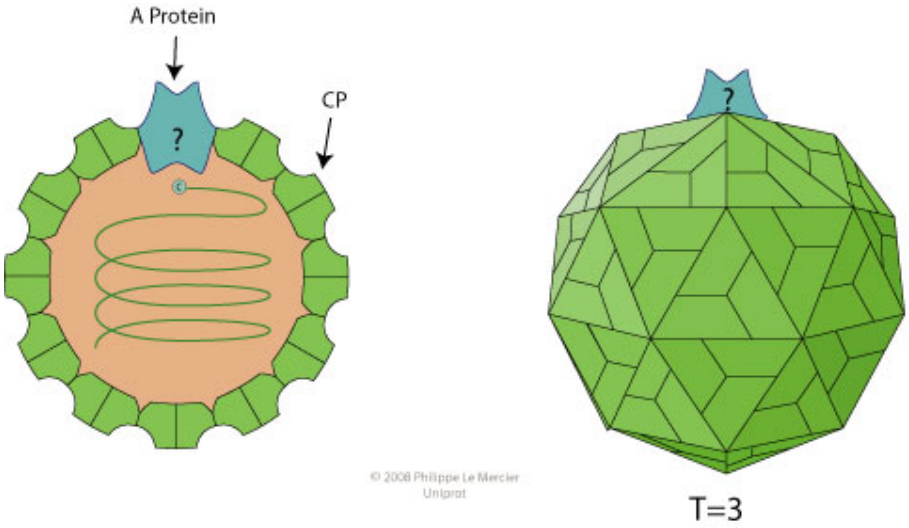

Figure 2.6 Structure of the MS2 virion. Adapted from: http://viralzone.expasy.org.

2.1.4 Virus purification

Viruses cannot replicate by themselves, therefore, they are cultured *in vitro* in suitable host cells or tissues. Virus cultures used in research are usually resourced from ATCC, which provides standard reference microorganisms and cell lines. The commercially available virus cultures have commonly been used in environmental studies. However, these are usually used in a semi-crude state, and as a result typically contain cell debris and non-encapsidated nucleic acids. These impurities may affect the outcome of experiments, and the virus characteristics (e.g. virus size, surface charge and concentration) cannot be accurately determined. Hence in order to obtain representative and reproducible data, virus stocks used for these studies need to be purified prior to their application in environmental research.

The most widely used method for virus purification is ultracentrifugation, which separates particles based on their density using caesium-chloride, iodixanol or colloidal silica gradients. However, ultracentrifugation-based methods require expensive equipment and prolonged centrifugation times (Table 2.1).

Chromatography-based methods have been used for virus purification as well. These methods include ion-exchange and size-exclusion chromatography (SEC) (Yang *et al.*, 2012). Ion-exchange chromatography allows the separation of particles based on their charge, whereas SEC (also known as gel filtration) purification is based on their size. The SEC, using columns with cross-linked dextran gel, works well as a polishing step following gradient ultracentrifugation, although if used alone, recovery can be low due to matrix interference

(Kalbfuss *et al.*, 2007). The chromatography methods are easier to perform than centrifugation-based methods, but a single chromatography run using columns with dextran gel still takes at least four hours (Yang *et al.*, 2012).

Table 2.1 Details of the most commonly used ultracentrifugation-based virus purification methods.

Virus	Gradient	Centrifugation conditions	Reference
Rotavirus	caesium-chloride	100,000×g, 1.5 hr, 4°C; 110,000×g, 18 hr, 10°C	(Arnold *et al.*, 2009)
	colloidal silica	82,500×g, 1 hr, 4°C; 100,000×g, 25 min, 4°C; 100,000×g, 1 hr, 4°C	(Villegas *et al.*, 2002)
Adenovirus	caesium-chloride	217,290×g, 1 hr, 10°C; 217,290×g, 16 hr, 10°C	(Peng *et al.*, 2006)
	iodixanol	217,290×g, 1 hr, 10°C	(Peng *et al.*, 2006)
	iodixanol	180,000×g, 3 hr, 4°C	(Dormond *et al.*, 2010)
MS2	caesium-chloride	60,000×g, 5 hr, 4°C; 260,000×g, 19 hr, 15°C	(Dika *et al.*, 2013)

2.1.5 Virus detection and quantification

The main methods of detecting viruses in environmental samples involve cell or tissue culturing, electron microscopy and the detection of the genome or surface antigens.

The most widely used methods for virus detection and quantification involve initial cell or tissue culturing. In the case of bacteriophages, the phages are inoculated on an agar plate with bacteria, and after one day of incubation the replicating viruses lyse cells forming clear spots (plaques). One plaque can be equated to one bacteriophage colony derived from a single infection, therefore, the number of plaques gives information on the initial number of virus particles (Adams, 1959). A similar method can be applied for animal and human viruses as well, using a suitable host tissue instead of bacteria (Dulbecco, 1952; Mocé-Llivina *et al.*, 2004). However, these viruses replicate more slowly than bacteriophages, thus an enteric virus assay can take weeks (Storch, 2000). For more sensitive quantification and for viruses that do not lyse the cell membranes during the infection, focus-forming assay is commonly used. This method utilises fluorescent antibodies sensitive to specific viral antigens to detect clusters (foci) of the infected cells by fluorescent microscopy (Payne *et al.*, 2006). For a few

viruses, the cytopathic effect (the damage on the host tissue) can be observed under light microscope. Nonetheless, some viruses (e.g. human noroviruses) cannot be maintained *in vitro*, hence culturing-based methods are not suitable for their detection.

By electron microscopy, intact and degraded viruses can be directly visualised using different stains. However, this method cannot distinguish whether the intact particles are infectious or non-infectious. The detection limit of electron microscopy is 10^5 – 10^6 virus particle/mL (Roingeard, 2008), therefore, concentration and purification of the environmental samples are often required for successful detection.

The genome of the viruses is commonly detected by polymerase chain reaction (PCR). During the PCR short DNA sequences (primers) bind to specific regions of the target DNA. A polymerase enzyme is used to extend these primers using thermal cycling (Figure 2.7) resulting in exponential amplification up to a level that can be detected by suitable staining of the nucleic acid.

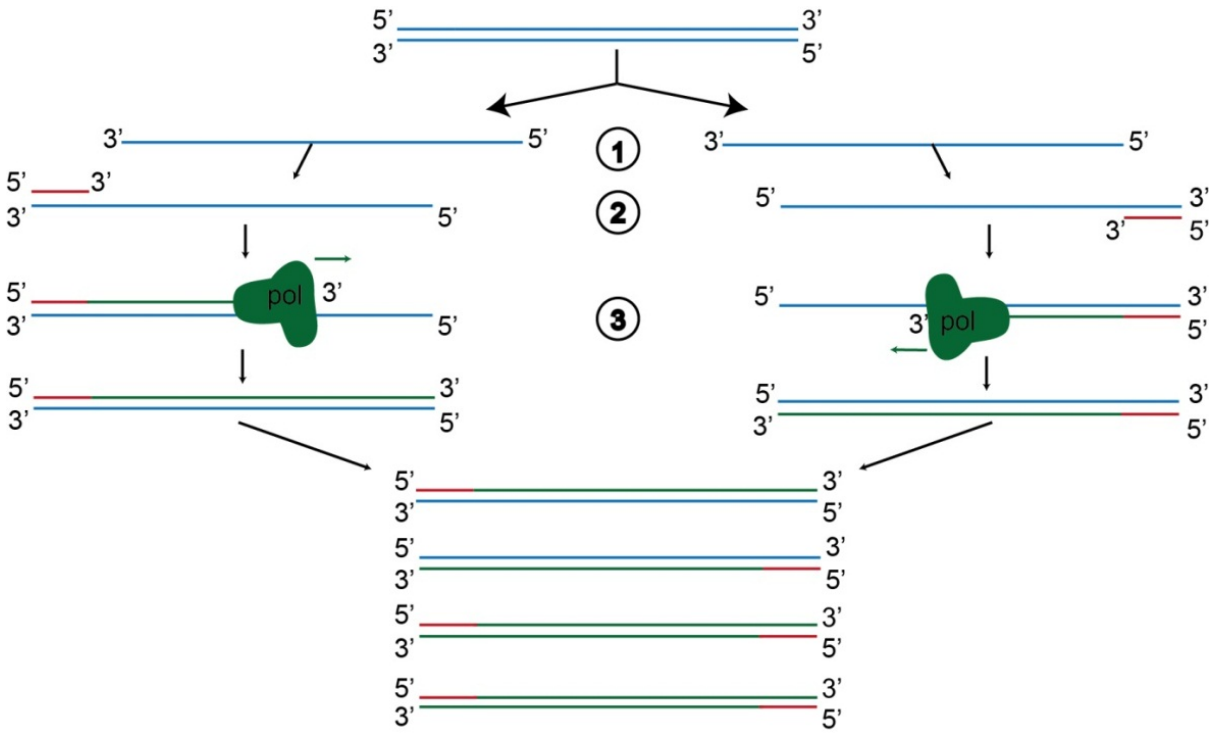

Figure 2.7 The steps of a PCR cycle. 1: denaturation of the dsDNA, 2: annealing of the primers to the ssDNA, 3: elongation: synthesis of the complementary DNA strand by DNA polymerase (pol) enzyme. Usually 20 – 45 cycles are sufficient for detection.

For the detection of RNA viruses, a reverse transcriptase PCR (RT-PCR) can be used. During the RT-PCR a target sequence of the virus RNA is first transcribed to complementary DNA (cDNA) by reverse transcriptase. After that, a DNA polymerase is used to generate copies of the target sequence using the cDNA as a template. The reverse transcription and the PCR reaction can be performed separately or in one step. In the single-step reaction the two mechanisms take place in one tube, thus it is more sensitive, reduces the risk of cross-contamination, and requires less time (Pang *et al.*, 2004b).

The original number of DNA or RNA copies in a sample can be quantified by real-time or quantitative PCR (qPCR) and RT-PCR (qRT-PCR). There are two commonly used qPCR methods for nucleic acid quantification. One is based on the addition of a specific probe to the reaction mix. The probe is an oligonucleotide sequence complementary to the inner region of the target sequence, labelled with a fluorescent reporter and a quencher. The probe binds to the target sequence, and when the polymerase enzyme reaches the probe it degrades the quencher, which allows the reporter to fluoresce. The other method uses a fluorescent dye (e.g. Sybr Green) that emits fluorescence when interacting with the amplified dsDNA. In that case the amplification is followed by a melting cycle to determine the melting temperature (Tm) of the amplified DNA. The Tm of a DNA fragment is unique, and even one nucleotide change alters it significantly. In both types of qPCR the intensity of the emitted fluorescence increases during the qPCR run as more copies of the template DNA are generated, and thus correlates with the concentration of the DNA. Hence, the nucleic acid concentration can be determined by a standard curve of samples with known concentration. The fluorescence is detected by a fluorometer after each cycle, thus the amplification can be followed real-time.

The PCR-based techniques enable fast and affordable detection with high sensitivity: as few as one copy of viral DNA or RNA can be amplified. On the other hand, PCR does not provide information on the presence of intact and infectious virus particles.

Most recently, integrated cell culture and PCR-based methods (ICC-PCR and ICC-RT-PCR) have been used for the detection and quantification of viruses. The virus replicates in cell/tissue culture and the increase of the viral DNA/RNA is determined by standard or quantitative PCR/RT-PCR. This technique is more sensitive than plaque assays (Fongaro *et al.*, 2013; Li *et al.*, 2010), thus the time of culturing can be reduced from weeks to days, and it is suitable for viruses that are difficult to culture *in vitro* in high concentrations (Greening *et al.*, 2002; Ogorzaly *et al.*, 2013; Rodríguez *et al.*, 2009).

The antigens presented on the surface of the viral capsids can be detected by their affinity to specific antibodies. The most commonly used antigen detection method in environmental studies is the enzyme-linked immunosorbent assay (ELISA) (Fu *et al.*, 1989; Gülser *et al.*, 2008; Park *et al.*, 2010). In ELISA, the viral antigen is linked to an antibody and the binding is visualised by staining (Figure 2.8). Using commercially available ELISA kits, the assay can be performed in one hour. The results of an ELISA gave good correlation with the results of tissue culturing, for example when virus degradation in wastewater and in groundwater was tested (Nasser *et al.*, 1995).

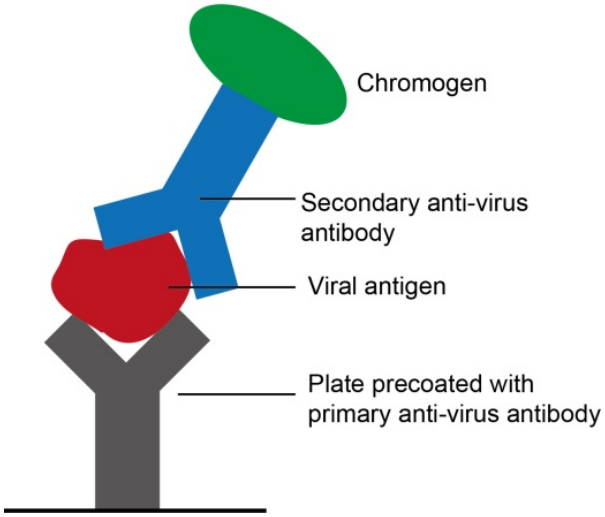

Figure 2.8 Schematic illustration of the ELISA. The virus antigen is immobilised to the solid surface by binding to the primary antibody. Then a secondary antibody is added and the binding is visualised by a chromogen.

An aim of this study was to purify and characterise viruses cultured using standard methods. For purification, simple, fast and affordable methods were employed that are suitable for purification of the large quantities of viruses derived from culturing. For rotavirus and MS2 bacteriophage a new SEC method was developed and validated. For adenovirus a commercially available purification kit was used. The concentration of the purified stocks was determined by qPCR and single-step qRT-PCR. The methods used allow for the measurement of virus concentration as genome copy (gc) per reaction by targeting genes with a single copy per virion. As the PCR-based methods only give information about the nucleic acid content of the samples, the viral integrity and infectivity was also analysed. For further validation, the virus particles of the samples were visualised by transmission electron microscope (TEM). The viruses were then characterised in terms of their size, concentration, surface charge, hydrophobicity and aggregation.

2.2 Methods and materials

2.2.1 Virus culture and purification

Viruses and cell stocks were obtained from the ATCC. The rotavirus and the adenovirus were cultured by Dr Susan Lin, and the MS2 bacteriophage was cultured by Erin Mcgill at the Institute of Environmental Science and Research Ltd. (ESR), New Zealand.

2.2.1.1 Rotavirus

Rotavirus cultivation and concentration

Rotavirus VR-2018 strain was cultured in MA-104 foetal monkey kidney cells and grown in minimal growth medium supplemented with 10% heat-inactivated foetal bovine serum (10% FBS MEM) containing 1% (w/v) penicillin – streptomycin. Prior to inoculation, the viruses in the sample were activated by incubating with 10 µg/mL trypsin at 37°C for 1 hr. Additionally, the MA-104 cell monolayer was washed three times with MEM and the third wash was left on the monolayer for 30 – 60 min at 37°C in a CO_2 incubator. After adding the virus/trypsin inoculum, the cells were incubated at 37°C for 2 hr with gentle rocking every 15 min to allow virus adsorption. Thereafter, cells were incubated with fresh medium containing trypsin with a final concentration of 1 µg/mL, and incubated at 37°C for seven days.

Rotaviruses were harvested by three cycles of freezing-thawing (–20°C/37°C), followed by sonication in an ultrasonic bath for 2 min and centrifuged for 15 min at 1,000×g to pellet out the cellular debris. The supernatant was stored at –80°C.

Prior to purification the rotavirus supernatant was concentrated by ultracentrifugation. An aliquot of 100 mL of the rotavirus supernatant was filtered through a 0.45 µm syringe filters and centrifuged at 100,000×g (Ti70 rotor, Beckman Coulter) at 4°C for 4 hr. The resulting pellet was resuspended in 1 mL of purification buffer (10 mM Tris pH 7.4, 140 mM NaCl, 10 mM $CaCl_2$).

Rotavirus purification

The rotavirus concentrate was purified by a SEC method. The concentrated rotavirus stock (1 mL) was injected into a TSKgel® G5000PWXL-CP (TOSOH Bioscience, USA), 10 µm, 1000Å column (with a TSKgel® Size Exclusion G2500PWxl guard column) set up on an AKTA Explorer10 (Amersham Pharmacia Biotech, Sweden). The base material of this column was poly-methacrylate $[(C_4H_6O_2)_n]$. The void volume of the column was determined by injecting 500 µL of 1M NaCl solution in a separate run. Runs were conducted at a constant flow rate of 0.4 mL/min using the purification buffer (10 mM Tris pH 7.4, 140 mM NaCl, 10 mM $CaCl_2$) with a UV detector set at 215 nm and 280 nm wavelengths. Fractions (0.5 mL/tube) were collected for 1 hr after injection using an autofraction collector Frac-900 (Amersham Pharmacia Biotech, Sweden). The fractions were stored at –80°C for up to six months.

Rotavirus quantification

A single-step qRT-PCR method was used for the detection and quantification of rotavirus. The primers selected for the qRT-PCR amplify an 87 base pair (bp) portion of the NSP3 gene (one gene/genome). This sequence was amplified and ligated into a pCR 2.1 TOPO vector (Life Technologies, USA) and used as a positive control (Figure 2.9). The plasmid containing the target sequence was provided by ESR, New Zealand. Dilution series of plasmids with the target sequences incorporated were used for method validation and for generating standard curves to determine the rotavirus gc concentrations of the samples.

Dilution series of the unpurified stock and the fractions from SEC were analysed by qRT-PCR. The dilutions were made with nuclease-free, sterile, double-distilled water. The viral RNA was extracted from 20 µL of samples by incubation at 97°C for 15 min. The qRT-PCR was carried out using KAPA SYBR FAST 1-step qRT-PCR kit (Kapa Biosystems, USA) in a Roche Light Cycler 480 Real-Time PCR System (Roche Diagnostics GmbH, Germany). The extracted RNA/plasmid DNA (4 µL) was added to KAPA SYBR FAST qPCR Master Mix with 200 nM of the forward and the reverse primers (Table 2.2) and 400 nM KAPA RT Mix. The total volume of the reaction mix was 20 µL. Reverse transcription to generate a cDNA was conducted at 42°C for 15 min followed by denaturation at 95°C for 5 min. Then, the following amplification protocol was used: 40 cycles of 95°C for 10 s, 60°C for 20 s and

72°C for 1 s. Amplifications were followed by one cycle of melting curve analysis at 95°C for 5 s; annealing 60°C for 1 min. Dissociation was carried out from 65°C to 97°C with a temperature ramp of 0.11°C/s. Analysis indicated a melting peak (Tm) at 77.3°C ± 0.2°C.

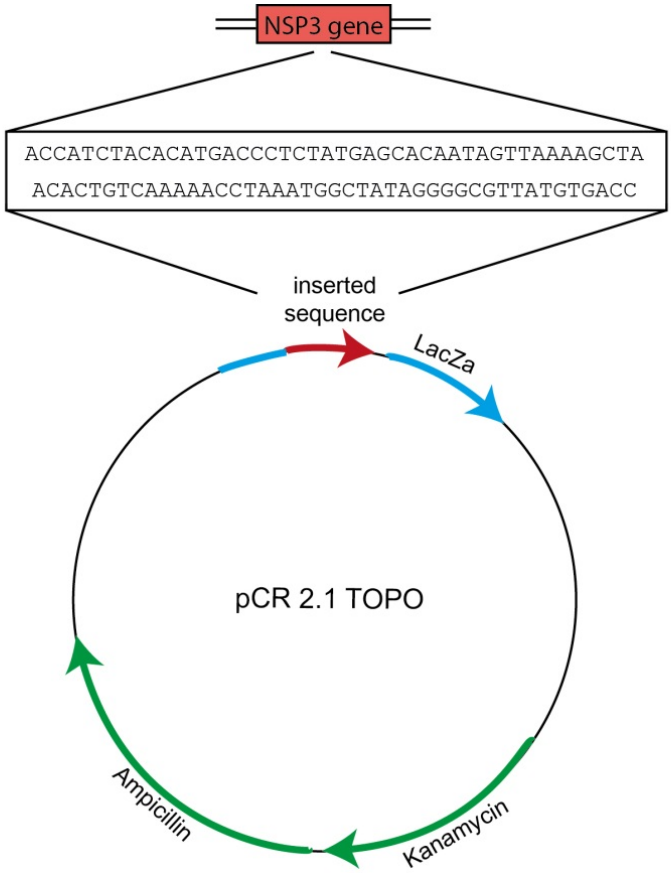

Figure 2.9 The TOPO pCR 2.1 plasmid holding the 87 bp sequence of the rotavirus NSP3 gene.

Table 2.2 Information on primers and target sequences of the qRT-PCR reactions used for quantification of rotavirus. [NVP3 stands for non-virion protein 3, synonym for non-structural protein 3 (NSP3).]

Primer name and position	Primer sequence	Reference	Length of product	Detection limit	Tm of the product
Forward - NVP3F (963-982)	5′-ACCATCTACA CATGACCCTC-3	Pang *et al.* (2004b)	87 bp	3 gc/µL	77.3 ± 0.2°C
Reverse - NVP3R (1049-1034)	5′-GGTCACATAA CGCCCC-3′				

Rotavirus integrity and infectivity

The virus integrity was determined by testing whether the samples contained non-encapsidated RNA fragments. For this propose, 100 µL of the unpurified rotavirus samples and fractions derived from SEC were filtered through Vivaspin 100 kDa filter units (Sartorius Stedim Biotech GmbH, Germany) at 13,000×g for 10 min. Filters were equilibrated by filtering through 500 µL of the purification buffer prior to rotavirus filtration. The unpurified virus and Fraction 1 were analysed in duplicates. Virus particles were recovered from the top of the filters using PBS pH 7.4 buffer with the final volume of 100 µL. The recovered samples and the flow through were all analysed by the single-step qRT-PCR method described above.

In order to determine whether the fractions from the purification contained infectious rotavirus particles, an ICC-qRT-PCR method was used by combining the culturing and the single-step qRT-PCR method described above. Samples of all fractions were cultured by Susan Lin. The culturing was performed in duplicates, and the incubation period was seven days. The crude extract of rotavirus was used as positive control; with the uninoculated growth medium as the negative control. The total RNA content of samples from day 0 and day 7 (200 µL each) were extracted using TRIzol reagent (Life Technologies, USA) according to manufacturer's instructions. RNA was resuspended in 50 µL of nuclease-free, sterile, double-distilled water. RNA was quantified by qRT-PCR.

Rotavirus antigen detection

The presence of the VP6 protein in dilution series of the unpurified rotavirus and the fractions from SEC were detected by Rotavirus ELISA Kit (Cortez Diagnostics, USA) according to the manufacturer's instructions. The 10 – 100 times dilutions were made with the washing buffer of the ELISA kit. For quality control, the positive control (containing high concentration of the VP6 protein) and the negative control (washing buffer) provided by the manufacturer were used. Results were recorded using a microplate reader (Synergy HT, BioTek Instruments, Inc., USA) at the wavelength of 450 nm. The samples with absorbance reading above the 0.15 optical density (OD) were considered as positive.

Rotavirus transmission electron microscopy

The transmission electron microscopy of the unpurified rotavirus and the fractions from SEC was outsourced to the University of Cape Town, South Africa. The samples were investigated by conventional negative staining. The virus samples (10 µL each) were applied to the carbon-coated grids and stained by 10 µL of 3% uranyl acetate. Samples were scanned using a Leo 912 (operating at 120 kV) TEM (Carl Zeiss AG, Germany) for intact virus particles.

2.2.1.2 Adenovirus

Adenovirus culture

Adenovirus type 41, VR-930 strain stocks were cultured in human embryonic cells (HEK) 293 cells. Briefly, cells were grown in 10% FBS MEM to confluence (2 – 3 days). Prior to virus inoculation, cells were washed twice with phosphate buffered saline (PBS; pH 7.2) and the virus inoculum was diluted in 2% FBS MEM and added to the cells to give a multiplicity of infection of approximately 0.01. The virus and cells were then incubated at 37^{o}C, 5% CO_2 for 90 min and the cells were supplemented with 2% FBS MEM and incubated at 37^{o}C, 5% CO_2 for nine days or until 90% cytopathic effect was evident. Adenovirus was harvested by the same freezing-thawing method as rotavirus described in Section 2.2.1.1. The resulting supernatant was stored at –80°C.

Adenovirus purification

The adenovirus supernatant derived from tissue culture was filtered through 0.45 µm filter and purified using ViraBind™ Adenovirus purification kit (Cell Biolabs, Inc., USA) according to manufacturer's instructions. The purification filter was pre-rinsed with 5 mL of the wash buffer and then 15 mL of the filtered adenovirus suspension was passed through the filter using gravity flow. To improve recovery, the flow through was filtered again through the same filter under the same conditions. The filter was washed three times with 10 mL of washing buffer. The viruses were recovered from the filter by passing through 3 mL of the elution buffer (25 mM Tris, pH 7.5, 2.5 mM Mg_2Cl, 1 M NaCl). The purified virus stock was stored at –80°C for up to nine months.

Adenovirus quantification

A qPCR method targeting a 132 bp region of the hexon protein gene (one gene/genome) was used for detection and quantification of adenovirus. The target sequence was amplified and ligated into yT&A vector (Yeastern Biotech Co., Taiwan) according to the manufacturer's instructions, resulted in a circular plasmid DNA incorporating the target sequence (Figure 2.10).

In order to produce large quantities of the plasmid, it was transformed into competent *E.coli* cells (DH5α), which readily incorporate foreign plasmid DNA. First, 5 µL of the ligation reaction was mixed with 50 µL of the DH5α cells. Then the mixture was incubated in ice for 10 min, and then heat shocked at 37°C for 90 s and chilled in ice for 2 min. Then 200 µL of standard Luria Broth (LB) bacterial culture medium was added, and the mixture was incubated at 37°C for 30 min. The mixture was plated into LB-agar plate containing isopropyl β-D-1-thiogalactopyranoside (IPTG), X-Gal and ampicillin and incubated at 37°C overnight. The ampicillin only allows the cells containing the plasmid with the resistance gene to grow.

The bacterial cells containing the plasmid incorporating the insert were assessed by blue-white selection. During the ligation the target sequence is ligated into the *LacZ* operon (Figure 2.10), which contains the β-galactosidase gene. The enzyme translated from that gene is responsible for the digestion of galactose. When the plasmids transformed into the bacterial cells have intact *LacZ* operon (the target sequence was not ligated), the β-galactosidase gene is induced by the IPTG, the β-galactosidase enzyme is translated and it digest the X-gal, which is a galactose linked to indole. The oxidised indole then forms a bright blue pigment, which turns the bacterial colony blue (blue colonies are not required). The cells containing the plasmids with the insert sequence have truncated β-galactosidase genes, therefore, the colonies are white.

A white colony was transferred into LB solution and incubated at 37°C overnight. The plasmids were purified by DNA-spin Plasmid DNA Purification Kit (iNtRON Biotechnology, South Korea) according to the manufacturer's instructions. The plasmid DNA was eluted in 50 µL nuclease-free water. The final DNA concentration was approximately 150 ng/µL, detected by Nanodrop-1000 (Thermo Fisher Scientific Inc., USA). For further validation the inserted DNA was sequenced by primer walking at Macrogen Inc. (Korea) The sequencing confirmed that the inserted sequence was the target sequence.

The yT&A plasmid holding the target sequence (Figure 2.10) was used as a positive control in the qPCR for adenovirus quantification, and its dilution series were used for method validation and for generating standard curves to determine the gc concentration in the samples.

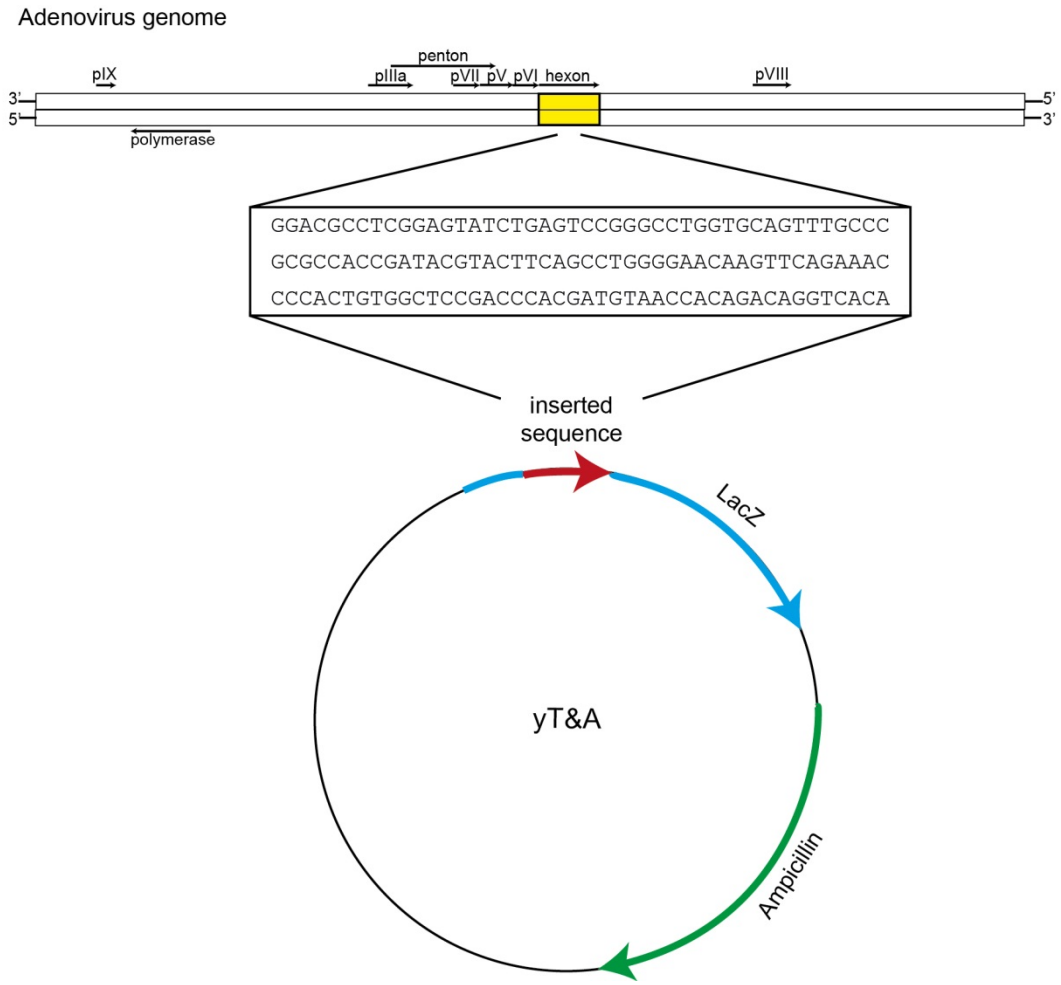

Figure 2.10 The yT&A plasmid holding the 132 bp sequence of the adenovirus hexon gene.

Dilution series of both unpurified and purified viruses were analysed by qPCR. The dilutions were made with nuclease-free sterile, double-distilled water. The viral DNA was extracted from 20 µL of samples by incubating at 97°C for 15 min. The qPCR was carried out using KAPA SYBR FAST qPCR kit (Kapa Biosystems, USA) in a Roche Light Cycler 480 Real-Time PCR System (Roche Diagnostics GmbH, Germany). The 10 µL qPCR reaction mix contained KAPA SYBR FAST qPCR 1×Master mix with 50 nM of the forward and the reverse primers (Table 2.3) and 1 µL of the sample/plasmid DNA. Amplification was carried out using the following thermal cycling conditions: 95°C for 5 min, then 45 cycles of 95°C for 10 s, 60°C for 20 s and 72°C for 5 s. Amplifications were followed by one cycle of

melting curve analysis with the same conditions as described in section 2.2.1.1 for rotavirus. Analysis indicated a melting peak (Tm) at 85.3°C ± 0.2°C.

Table 2.3 Information on primers and target sequences of the qPCR reactions used for quantification of adenovirus.

Primer name and position	Primer sequence	Reference	Length of product	Detection limit	Tm of the product
Forward - JHKXF (18891–19910)	5'-GGACGCCTCG GAGTACTGA-3'	Ko *et al.* (2005)	132 bp	1 gc/µL	85.3 ± 0.2°C
Reverse - JHKXR (19025–19007)	5'-CGCTGTGACC TGTCTGTGG-3'				

Adenovirus integrity and infectivity

To assess capsid integrity, enzymatic treatment using DNase enzyme was performed on both unpurified and purified samples. During the treatment the DNase enzyme degrades non-encapsidated viral DNA, thus the following qPCR reaction only detects the DNA encapsidated in intact virions.

The unpurified and purified virus samples (original and ten times diluted with nuclease-free, sterile, double-distilled water) were analysed with a DNase assay. The virus samples (50 µL) were incubated with 1 unit of RNase-free DNase I (Thermo Scientific Inc., USA) in the presence of the reaction buffer (with $MgCl_2$) at 37°C for 15 min. Viral DNA was extracted from the not treated (50 µL) and DNase-treated samples with High Pure Viral Nucleic Acid Kit (Roche Diagnostics GmbH, Germany) according to the manufacturer's instructions. Viral DNA was eluted in 50 µL nuclease-free, sterile, double-distilled water.

Adenovirus antigen detection

The hexon protein of the adenovirus capsid was detected in the unpurified and purified viral stocks by the Adenovirus ELISA Kit (Cortez Diagnostics, USA) according to the manufacturer's instructions. The virus stocks were diluted 10 – 10,000 times with the washing buffer of the ELISA kit. For quality control, the positive control (containing high concentration of the hexon protein) and the negative control (washing buffer) provided by the manufacturer were used. Results were recorded using a microplate reader (Synergy HT,

BioTek Instruments, Inc., USA) at the wavelength of 450 nm. The samples with absorbance reading above the 0.15 optical density (OD) were considered as positive.

Adenovirus transmission electron microscopy

The transmission electron microscopy of the purified adenovirus was outsourced to the University of Otago, New Zealand. The samples were investigated by conventional negative staining. Due to health and safety concerns, the adenovirus samples were treated with UV for 30 minutes before staining. The virus samples (10 µL each) were applied to the carbon-coated grids and stained by 10 µL of 3% uranyl acetate. Samples were scanned using a CM100 BioTWIN TEM (Philips, Netherlands) for intact virus particles.

2.2.1.3 MS2 bacteriophage

MS2 culture and purification

MS2 15597-B1 strain was propagated in *Salmonella typhimurium* WG 49 strain. The agar overlay method (Adams, 1959) was used for propagation.

The same SEC purification was carried out for MS2 as that for rotavirus. The MS2 stock from propagation (1 mL) was injected in triplicates into the TSKgel® G5000PWXL-CP (TOSOH Bioscience, USA), 10 µm, 1000Å column (with a TSKgel® Size Exclusion G2500PWxl guard column) set up on an AKTA Explorer10 (Amersham Pharmacia Biotech, Sweden). Runs were conducted at a constant flow rate of 0.4 mL/min using the purification buffer (10 mM Tris pH 7.4, 140 mM NaCl, 10 mM $CaCl_2$) with a UV detector set at 215 nm and 280 nm wavelengths. Fractions (0.5 mL/tube) were collected for 1 hr after injection using an autofraction collector Frac-900 (Amersham Pharmacia Biotech, Sweden). Fractions were stored at –80°C for up to six months.

MS2 quantification and infectivity

A single-step qRT-PCR method was used for the detection and quantification of MS2. The reaction targeted a 65 nucleotide (nt) RNA sequence coding the lysis protein. The target

sequence was amplified and ligated into a pCR 2.1 TOPO vector (Life Technologies, USA) according to the manufacturer's instructions. The plasmid was transformed into *E.coli* DH5α cells, and the cells holding the plasmids with the insert sequence were selected by blue – white screening as described for adenovirus in section 2.2.1.2. A white colony was grown in LB solution at 37°C overnight, and the plasmid was purified by High Pure Plasmid Isolation Kit (Roche Diagnostics GmbH, Germany) and eluted in in 50 µL nuclease-free, sterile, double distilled water. The DNA concentration was approximately 350 ng/µL detected by Nanodrop-1000 (Thermo Fisher Scientific Inc., USA). For further validation, the inserted DNA was sequenced by primer walking at Macrogen Inc. (South Korea). The sequencing confirmed that the inserted sequence was the target sequence.

The plasmid (Figure 2.11) with the target sequence was used as a positive control and its dilution series were used for method validation and for generating standard curves to determine the gc concentration in the samples.

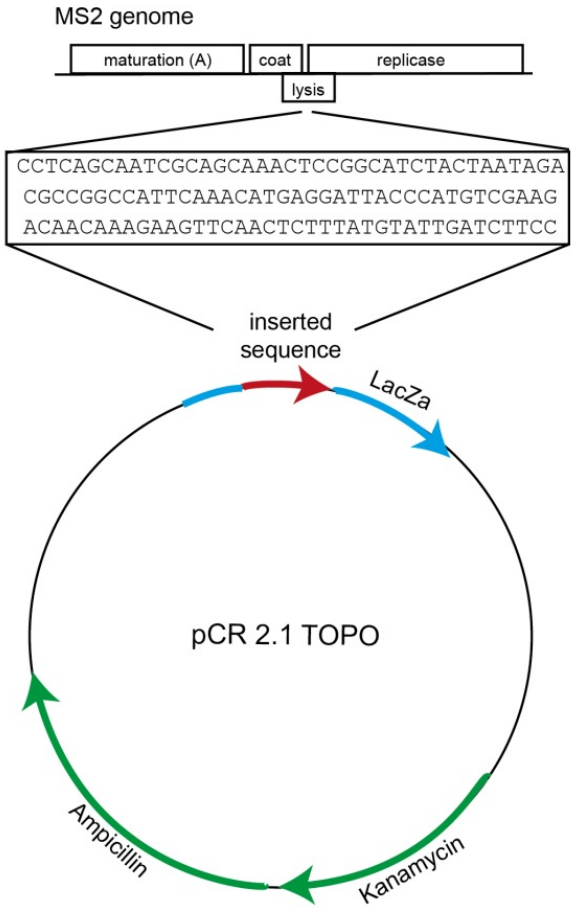

Figure 2.11 The TOPO pCR 2.1 plasmid holding the 115 bp sequence of the MS2 lysis protein gene.

For quantification, dilution series of virus samples derived from the unpurified stock and the fractions from SEC, viral RNA was extracted from 20 µL of samples by incubating at 97°C for 15 min. The dilutions were made with nuclease-free, sterile, double-distilled water. The qRT-PCR was carried out using KAPA SYBR FAST 1-step qRT-PCR kit (Kapa Biosystems, USA) in a Roche Light Cycler 480 Real-Time PCR System (Roche Diagnostics GmbH, Germany). The reaction was carried out in 20 µL final volume containing 1×KAPA Sybr FAST qPCR Master mix, 400 nM 1×KAPA RT mix with 200 nM of the forward and the reverse primers (Table 2.4) and 4 µL of the sample/plasmid DNA. Following a 15-min step of reverse transcription at 40°C and a 5-min step of denaturation at 95°C, the 45 cycles of amplification consisted 95°C for 10 s, 60°C for 30 s and 72°C for 1 s. Amplifications were followed by one cycle of melting curve analysis with the same conditions as described in section 2.2.1.1 for rotavirus. Analysis indicated a melting peak (Tm) at 81.9°C ± 0.2°C.

Table 2.4 Information on primers and target sequences of the qRT-PCR reactions used for quantification of MS2.

Primer name and position	Primer sequence	Reference	Length of product	Detection limit	Tm of the product
Forward - MS2F (3134-3150)	5'-CGGCTGCTCG CGGATA-3'	Agarwal *et al.* (2007) and Miyajima *et al.* (2013)	65 bp	2 gc/µL	81.9 ± 0.2°C
Reverse - MS2R (3198-3179)	5'-AACTTGCGTT CTCGAGCGAT-3'				

The concentration of infectious MS2 particles was quantified by a plaque assay infecting *E.coli* HS(pFamp)R strain (Debartolomeis & Cabelli, 1991). Samples were analysed by overlay pour plating of 1 mL volumes of serial dilutions according to the standard method (APHA *et al.*, 1998).

MS2 transmission electron microscopy

The transmission electron microscopy of the MS2 bacteriophage was outsourced to the University of Otago, New Zealand. Fraction 1 was analysed by negative staining. The virus sample (10 µL) was applied to the carbon-coated grids and stained by 10 µL of 3% uranyl acetate. The sample was scanned using an EM410 LS TEM (Philips, Netherlands) for intact virus particles.

2.2.2 Viral characterisation

2.2.2.1 Hydrophobicity of viruses

The hydrophobicity of the main capsid proteins of adenovirus, rotavirus and MS2 was determined using the Protein/Peptide Property Calculator (http://lifetein.com/peptide-analysis-tool.html). This tool calculates the hydrophobicity value (HV) by dividing the hydrophobicity of the amino acids composing the proteins (Appendix I) by the number of amino acids.

In order to test the hydrophobicity of the virus particles a modified Microbial Adhesion to Hydrocarbons (MATH) assay was used (Rosenberg, 2006). First, viruses were diluted with 2 mM NaCl pH 7 solution to 10^5 gc/µL concentration. Then, 0.5 mL of the stock was added to 0.5 mL of hexadecane (Sigma Aldrich, St. Louis, USA), in triplicates. The mixtures were shaken for 2 min, then incubated at room temperature for 4 min allowing the hydrophobic and water phases to separate. The water phase was removed and incubated at 97°C for 15 min to extract DNA/RNA. The RNA/DNA concentration (c) of the controls and the samples was determined by qRT-PCR and qPCR. Two tubes of control without the hexadecane were also tested. The percentage of hydrophobicity (H%) was determined by using the equation by Saini *et al.* (2011):

$$H\% = \frac{c_{control\ average} - c_{sample\ average}}{c_{control\ average}} * 100\%$$

2.2.2.2 Size and zeta potential of viruses

The size and zeta potential (ZP) of the viruses were determined by Zetasizer Nano ZS (Malvern Instruments, UK) using dynamic light scattering and laser Doppler microelectrophoresis, respectively. Viruses were diluted in 2 mM NaCl pH 7 solution to 10^9 gc/mL. Prior to the measurements, samples were filtered through 0.22 µm polyethersulfone (PES; Merck KGaA, Germany) (single-filtered samples) followed by 0.1 µm polyvinylidene fluoride filters (PVDF; Merck KGaA, Germany) (double-filtered samples). The hydrodynamic diameter and ZP of the viruses were measured in a background electrolyte of 2 mM NaCl at pH 7. All measurements were carried out in triplicates.

2.2.2.3 Aggregation test

The purified rotavirus and adenovirus samples were diluted in 2 mM NaCl pH 7 solution to 10^9 gc/mL. Both samples were filtered through the 0.22 µm PES filters (single-filtered). These samples were divided in two, and one set was filtered through the 0.1 µm PVDF filters (double-filtered). The hydrodynamic diameter and ZP of the samples were measured using Zetasizer right after preparation, then regularly for three months. The samples were hand-mixed before each measurement (set up in triplicates). Between measurements the samples were stored at room temperature. Two sets of the double-filtered adenovirus samples were stored at 4°C.

The purified MS2 was diluted with the same electrolyte to a final concentration of 10^9 gc/mL. The sample was double-filtered with the 0.22 and 0.1 um filters, and the size and ZP was analysed using Zetasizer regularly for three months. The MS2 sample was stored at 4°C between measurements (set up in triplicates).

2.3 Results and discussion

2.3.1 Viral purification

2.3.1.1 Rotavirus

Prior to the purification, the rotavirus stock was concentrated with ultracentrifugation. The ultracentrifugation step can easily be replaced with e.g. filtration, if equipment is not available. The concentrated rotavirus was purified by SEC using a poly-methacrylate column. The void volume of the column was 8.84 mL as determined by injecting 1 M NaCl solution (Figure 2.12A). When rotavirus was injected, seven peaks were distinguished at 7, 8.5, 10.5 12, 13.5, 15.5 and 17 mL at 215 nm and at 280 nm. At 280 nm, the first peak was the highest, suggesting high protein content (Figure 2.12A). To check for reproducibility, the purification was run in triplicates. The shape of each chromatogram was highly similar (Figure 2.12B) and the differences in the areas of the corresponding peaks were probably due to dissimilarities in concentrations of the injected concentrated virus stocks. All fractions were collected and analysed together with the original stock from culturing.

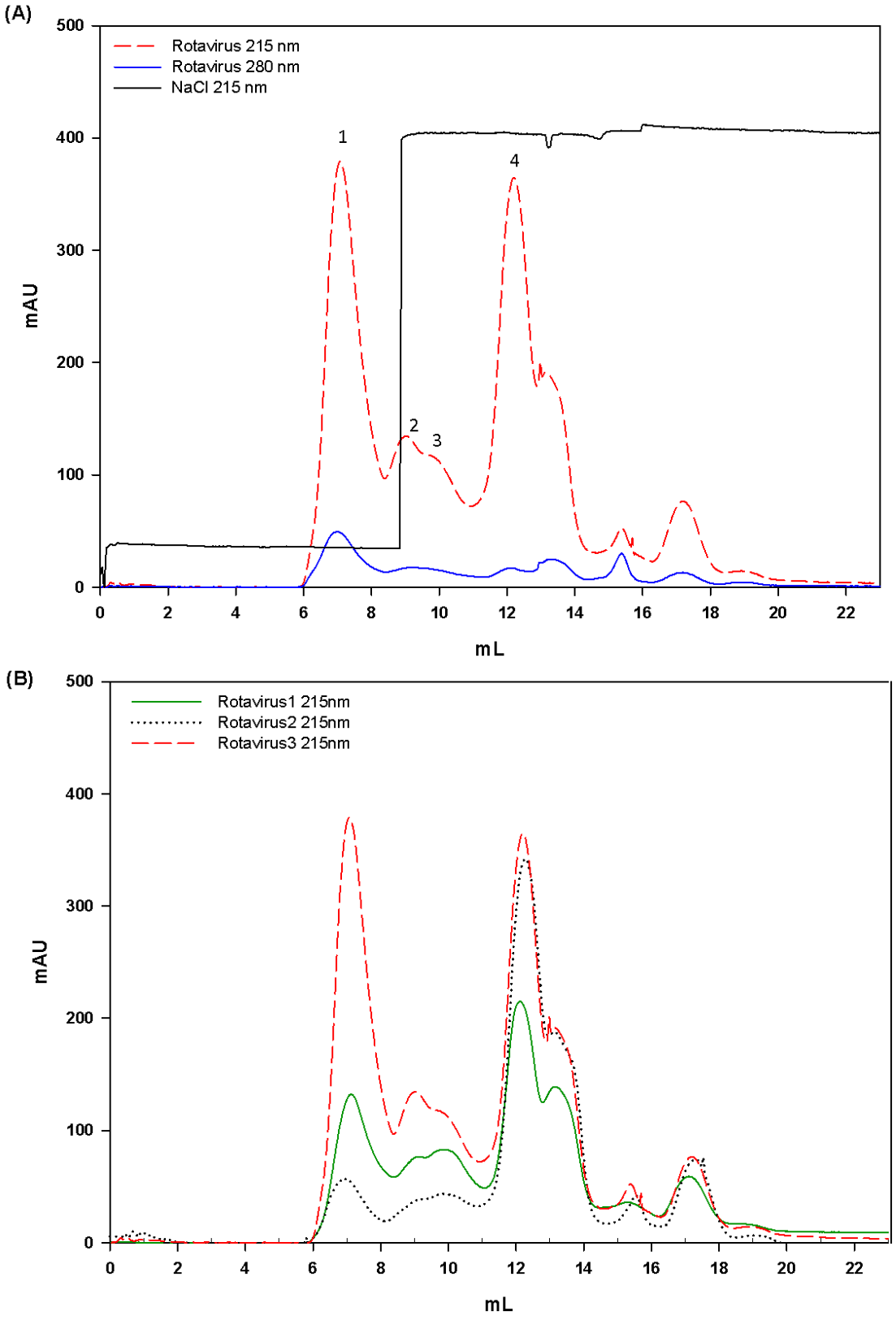

Figure 2.12 Chromatograms of the rotavirus purification. (A) Estimation of the void volume of the column, and identification of the main peaks of rotavirus. (B) Reproducibility of purification of rotavirus. The peaks observed at 215 nm in three separated runs.

The rotavirus RNA concentration of the unpurified rotavirus and the fractions from SEC was determined by single-step qRT-PCR. The detection limit of the method was 3 gc/µL. The qRT-PCR revealed a high concentration of rotavirus RNA in samples from the fractions corresponding to the first four peaks (Table 2.5). The gc concentration of the samples collected after the fourth peak contained little or no rotavirus RNA (data not shown), therefore, these samples were not further examined. Fraction 1 (corresponds to peak 1) had the highest rotavirus RNA concentration (2.8×10^8 gc/µL), which was one order of magnitude higher than the concentration found in Fractions 2, 3 and 4 (corresponds to peak 2, 3 and 4). Fraction 1 had 7×10^{11} gc while fractions 2, 3 and 4 contained 4.4×10^{10}, 1.5×10^{10} and 9.5×10^9 gc of rotaviruses, respectively. Overall, 7.7×10^{11} gc of rotaviruses was detected from the SEC purification procedure compared to 1×10^{12} gc of the concentrated crude extract injected, suggesting that 2.3×10^{11} rotavirus gc, presumably non-encapsidated RNA, was not recovered.

Table 2.5 Rotavirus genome copy (gc) concentrations and numbers of unpurified, concentrated rotavirus samples, and fractions derived from purification. Fraction 1 contained the majority of the rotavirus RNA. 23% of the RNA injected was not recovered.

Sample	Volume of sample (mL)	RNA concentration (gc/µL)	Number and degree of gc in sample
Concentrated virus culture by ultracentrifugation before SEC	1	1.0×10^9	1.0×10^{12} (100%)
Fraction 1	2.5	2.8×10^8	7.0×10^{11} (70%)
Fraction 2	2	2.2×10^7	4.4×10^{10} (4.4%)
Fraction 3	1	1.5×10^7	1.5×10^{10} (1.5%)
Fraction 4	0.5	1.9×10^7	9.5×10^9 (1.0%)
Total from peaks			**7.7×10^{11} (77%)**
Not recovered			**2.3×10^{11} (23%)**

In order to determine the number of the intact rotavirus particles and the non-encapsidated RNA, all the samples were filtered through 100 kDa filters, and then analysed by qRT-PCR. In the case of the unpurified stock, 32% of the total RNA content was filtered through the filters, suggesting this proportion was non-encapsidated RNA (Table 2.6, flow through of the stock solution from culturing). No RNA was detected in the flow through of Fraction 1. In both samples only ~80% of the total RNA content could be recovered, suggesting that 20% of the rotavirus was fixed in the filter. In Fraction 2, 3 and 4 most of the RNA was detected in

the flow through. The total recovery of the RNA content for these fractions was only 30 – 60%, which also indicated low number of intact particles. These findings correlate with the calculations for the concentration of all fractions and unpurified stock (Table 2.5), suggesting that Fraction 1 contained intact virus particles and little or no free viral RNA, whereas the majority of the RNA detected in Fractions 2 – 4 was non-encapsidated RNA.

Table 2.6 Rotavirus genome copy (gc) concentrations of the rotavirus stock solution from culturing and the fractions derived from purification, filtered through 100 kDa filter.

	Not filtered	**Filtered-recovered**		**Flow through**		**Total**
	gc/µL	**gc/µL**	**% of not filtered**	**gc/µL**	**% of not filtered**	**% recovered**
Stock solution from culturing	2.3×10^5	7.9×10^4	34.9%	7.4×10^4	32.8%	67.7%
	2.4×10^5	1.2×10^5	50.4%	7.8×10^4	32.1%	82.5%
Fraction 1	5.0×10^4	4.1×10^4	81.5%	0.0	0.0%	81.5%
	5.0×10^4	4.2×10^4	84.3%	0.0	0.0%	84.3%
Fraction 2	4.2×10^5	1.8×10^3	0.4%	2.5×10^5	60.3%	60.7%
Fraction 3	7.9×10^4	3.6×10^3	4.5%	2.1×10^4	26.8%	31.3%
Fraction 4	2.8×10^4	3.1×10^2	1.1%	1.8×10^4	65.0%	66.1%

The infectivity of the rotaviruses in the fractions derived from SEC was studied by ICC-qRT-PCR. The results indicated the presence of infectious particles, but the quantification was not reliable, as the duplicates showed large differences in their RNA content (Table 2.7). Nonetheless, an increase in gc from day 0 (T_0) to day 7 (T_7) was detected in all samples except the negative controls, confirming the purified virions were infectious.

Table 2.7 The qRT-PCR results for the rotavirus infectivity assay samples. T_0 represents the average initial gc concentration and T_7 is the average gc concentration detected after 7 days of incubation, where SD is the standard deviation.

Sample	**T_0 (gc/µL)**	**SD**	**T_7 (gc/µL)**	**SD**
Negative control	0	0	0	0
Positive control	2.0×10^5	3.5×10^4	4.7×10^5	6.1×10^5
Fraction 1	2.3×10^4	1.6×10^3	1.8×10^5	1.4×10^5
Fraction 2	3.5×10^2	3.2×10^2	1.6×10^4	1.4×10^4
Fraction 3	1.7×10^2	6.0×10^1	3.1×10^3	9.6×10^2
Fraction 4	8.5×10^1	6.3×10^1	8.7×10^3	9.1×10^3

The presence of the VP6 antigen in the unpurified stock and the fractions from SEC were tested by an ELISA. ELISA is a simple specific and cost effective technique and frequently used for the laboratory diagnosis of rotavirus infections (Kelkar *et al.*, 2004). It gave good correlation with the detection of rotavirus particles in stool samples by TEM (Cheung *et al.*, 1982), RT-PCR (Phillips *et al.*, 2009) and qRT-PCR (Adlhoch *et al.*, 2011). However, it does not give information on the integrity of the virus particles.

Table 2.8 Results of the ELISA assay detecting the VP6 protein of the rotavirus capsid from the virus stock from culturing and the fractions from purification. Samples with optical density (OD) ≥ 0.15 were considered as positive (+).

Sample		**OD at 450 nm**	**Approximate number of gc in the sample (100 µL)**
Negative control		0.085 (–)	-
Positive control		3.535 (+)	-
Stock solution from culturing	**Undiluted**	0.236 (+)	1.0×10^{7}
	1:10 diluted	0.094 (–)	1.0×10^{6}
Fraction 1	**1:10 diluted**	0.275 (+)	2.8×10^{9}
	1:100 diluted	0.081 (–)	2.8×10^{8}
Fraction 2	**Undiluted**	0.185 (+)	2.2×10^{9}
	1:10 diluted	0.084 (–)	2.2×10^{8}
Fraction 3	**Undiluted**	0.395 (+)	1.5×10^{9}
	1:10 diluted	0.128 (–)	1.5×10^{8}
	1:100 diluted	0.099 (–)	1.5×107
Fraction 4	**Undiluted**	0.117 (–)	1.9×10^{9}
	1:10 diluted	0.083 (–)	1.9×10^{8}

The unpurified stock and the ten times diluted Fraction 1 samples and the undiluted Fraction 2 and 3 were considered as positive (OD ≥ 0.15 at 450 nm; Table 2.8), and any further dilutions were negative, suggesting that the detection limit of the ELISA was relatively high (corresponds to 10^9 gc). However, the OD of the undiluted Fraction 4 and the ten times diluted Fraction 3 samples was above the OD of the negative control, but below 0.15, therefore, these samples may also contained the target protein in low concentrations. The unpurified rotavirus samples analysed here had similar OD to Fraction 1 samples, although the gc concentration of the unpurified stock was lower than the Fraction 1 samples, suggesting that the unpurified stock contained large amount of VP6 proteins, which were not

incorporated into capsid or formed empty capsids with no RNA. Despite the poor sensitivity of the ELISA assay, the results indicated that both the unpurified and purified stocks contained the intact VP6 antigen, supporting the qRT-PCR and the infectivity assays results.

The unpurified rotavirus stock and Fraction 1, 2 and 3 from SEC were analysed by TEM. The volume of fraction 4 was too low for electron microscopy. The TEM images of the unpurified stock indicated the presence of cell debris and other impurities not related to the rotavirus (Appendix II; Figure II.1). In that fraction some dark-centred virus particles (which is the typical appearance of the rotavirus capsomers containing no nucleic acid) were observed, supporting the ELISA results. Fraction 1 contained the majority of intact rotavirus particles (Appendix II; Figure II.2). The size of the viruses was 70 – 75 nm. This size correlated with the size of the porcine rotavirus (70 nm) described previously (Gutierrez *et al.*, 2009; Gutierrez *et al.*, 2010). The intact particles showed no structural damage, as the VP4 proteins were expressed on the surface of the particles. The TEM images of Fraction 1 showed significantly less impurities than the unpurified stock. In that fraction, some dark-centred virus particles and capsid fragments were observed which may have been a result of virus decay during the sample transport. Fraction 2 contained high amounts of impurities and dark-centred rotavirus particles (Appendix II; Figure II.3 and Figure II.4), which explains the high VP6 content detected by ELISA. Hardly any intact virus particles were observed, supporting the results of the viral integrity assay. The particles in Fraction 3 were similar to the particles in Fraction 2, however, remarkably fewer particles were detected.

2.3.1.2 Adenovirus

The ViraBind™ Adenovirus purification kit is widely used for producing high yield of purified recombinant adenovirus (Bian *et al.*, 2005; Chen *et al.*, 2011; Sabbatini *et al.*, 2010). The purification procedure takes only 30 minutes, and, according to the manufacturer, provides high recovery (90%) with similar purity to CsCl gradient. This method provided purified and five times concentrated adenovirus stocks.

The DNA content of the original and purified adenovirus was analysed by qPCR and compared (Table 2.9). The method was highly sensitive giving a detection limit of 1 gc/µL. The DNA concentration of the purified adenovirus was 20 times higher (8.9×10^7 gc/µL) than the concentration of the original stock (4.5×10^6 gc/µL). According to these results, more

adenovirus DNA was observed in the purified stock than in the original: 6.7×10^{10} gc was recovered from the 15 mL of the unpurified adenovirus stock. After purification (which involved a five times concentration), 2.7×10^{11} gc were detected in 3 mL. Results may suggest that the impurities in the unpurified sample may have inhibited the qPCR reaction. The purification process successfully eliminated the inhibitors and resulted in higher concentrations. However, the dilutions of the unpurified sample with water should have reduced the concentration of the inhibitors, thus much higher concentrations would have been observed in the diluted samples.

Viruses and nucleic acids are known to attach to plastic surfaces (Butot *et al.*, 2007; Gassilloud & Gantzer, 2005). The attachment of the adenovirus and its DNA to the inner wall of the polypropylene tubes used for storage was probably enhanced in the unpurified stock and depressed in the purified stock. The increased attachment to the tube wall could be responsible for the low gc concentration detected in the unpurified adenovirus samples.

Table 2.9 The genome copy (gc) concentrations and numbers of the virus stock from culturing and purified adenovirus samples.

Sample	Volume of sample	DNA concentration (gc/µL)	Number of copies in sample
Stock solution from culturing	15 mL	4.5×10^{6}	6.7×10^{10}
Purified stock	3 mL	8.9×10^{7}	2.7×10^{11}

The viral integrity test revealed that DNase had little effect on the original stock derived from culturing, however, when the diluted sample was analysed, DNase caused 1 $\log_{10}$ loss in DNA concentration (Table 2.10). Results suggest that the high concentration of organic material in the undiluted sample possibly inhibited the DNase activity. The dilution decreased the concentration of the inhibitors and let the DNase digest the non-encapsidated DNA. No meaningful difference was observed in the concentration of the DNase treated and not treated purified samples, implying that those samples contained no or few non-encapsidated viral DNA.

The infectivity of the adenovirus stock was not tested by a culturing method. Based on data available in the literature, adenoviruses purified with the kit used in this study yields high titre of infectious virus particles. The integrity of the virus particles were confirmed by the

enzymatic (DNase) assay. According to Fongaro *et al.* (2013) the enzymatic test slightly overestimates the number of infectious particles, however, the difference they observed was not significant. The higher number of intact particles detected could be due to degradation of the viral capsid proteins, which caused loss in infectivity. The adenovirus particles also tend to aggregate in high ionic strength solution (Wong *et al.*, 2012). When aggregated virus particles are present, the DNase test gives a more accurate estimation of the number of the intact and infectious virus particles, while the infectivity test would underestimate the number of them, because one aggregated virion mass acts as one infectious unit.

Table 2.10 The effect of DNase treatment on the adenovirus stock from culturing and purified adenovirus samples.

Sample		**No treatment gc/µL**	**DNase gc/µL**	**C/Co**	**Loss%**	**Average loss%**
Stock solution from culturing	**Undiluted**	1.9×10^{6} 1.5×10^{6}	1.7×10^{6} 1.8×10^{6}	0.9 1.2	7.6% 0%	3.8%
	1:10 diluted	2.7×10^{5} 2.7×10^{5}	1.4×10^{4} 2.5×10^{4}	0.1 0.1	95.0% 90.8%	92.9%
Purified stock	**Undiluted**	5.7×10^{7} 5.0×10^{7}	5.5×10^{7} 5.4×10^{7}	1.0 1.0	3.7% 0%	1.8%
	1:10 diluted	7.0×10^{6} 6.6×10^{6}	5.9×10^{6} 7.4×10^{6}	0.8 1.1	15.6% 0%	2.4%

The presence of the hexon capsid protein was tested by ELISA assay in both unpurified and purified adenovirus stocks (Table 2.11). The ELISA assay has been used as an initial screening for adenovirus infection in stool (Li *et al.*, 2005) and in tissue-cultured samples (Player & Westmoreland, 1989).

Both the unpurified and purified stocks were positive. The results for the dilution series of the purified stock showed good correlation with the DNA concentration, and even the 1,000 times diluted samples were positive. No correlation was found in the OD of the undiluted and ten times diluted samples of the unpurified stock, which may indicate the presence of not assembled hexon proteins or empty capsids often found in crude virus extracts.

Table 2.11 Results of the ELISA assay detecting the hexon protein of the adenovirus capsid from the virus stock from culturing and the purified virus samples. Samples with OD ≥ 0.15 were considered as positive (+).

Sample		**OD at 450 nm**	**Approximate number of gc in 100 µL**
Negative control		0.046 (–)	-
Positive control		3.174 (+)	-
Stock solution from culturing	**Undiluted**	3.174 (+)	2×10^8
	1:10 diluted	3.672 (+)	2×10^7
	1:100 diluted	2.991 (+)	2×10^6
Purified	**1:10 diluted**	2.033 (+)	1×10^8
	1:100 diluted	0.632 (+)	2×10^7
	1:1,000 diluted	0.155 (+)	2×10^6
	1:10,000 diluted	0.094 (–)	2×10^5

The purified adenovirus was examined by TEM. The images showed high number of intact virus particles (Appendix II.2). Their average size was 68 nm in diameter. The size measured was similar to previous findings (Wong *et al.*, 2012), where the measured size of adenovirus type 2 by TEM was approximately 70 nm. The purified stock contained little impurity.

2.3.1.3 MS2 bacteriophage

After propagation, the MS2 bacteriophage was purified using the same SEC method and conditions as described for rotavirus. The unpurified MS2 stock contained infectious virions at a high concentration, therefore, no concentration step was needed prior to purification. The chromatograms of the experiments are shown in Figure 2.13. Four peaks were observed on wavelength 215 nm and 280 nm at 8, 11.5, 13 and 17 mL (the insert of Figure 2.13 shows the peak at 8 mL). The purification was carried out in triplicate and the results were highly reproducible. All four fractions were collected for further analysis.

The MS2 concentration of the unpurified MS2 stock and the four fractions from SEC was determined by single-step qRT-PCR and plaque assay (Table 2.12). The detection limit was 1 pfu/mL for the plaque assay and 2 gc/µL for the qRT-PCR. Majority of MS2 RNA was recovered from Fraction 1. Fraction 2, 3 and 4 contained 9.8×10^8 in 1 mL 3.7×10^8 in 1.5 mL and 9.1×10^7 gc in 1.5 mL, respectively, which were 2 – 3 orders of magnitude lower than in

Fraction 1 (1.0×10^{11} gc in 1.5 mL). The number of RNA copies recovered from all fractions was 1.5 times higher than the number of gc of the original samples injected to the SEC column. The same phenomenon was observed during the quantification of the unpurified and purified adenovirus, discussed in Section 2.3.1.2. The low gc number observed in the unpurified MS2 stock could be attributed to the attachment of the viruses and viral nucleic acids to the wall of the tubes used for storage, or impurities of the original stock inhibiting the enzymes involved in the qRT-PCR reaction. Therefore, the gc number observed in the unpurified stock did not reflect the actual concentration of the sample.

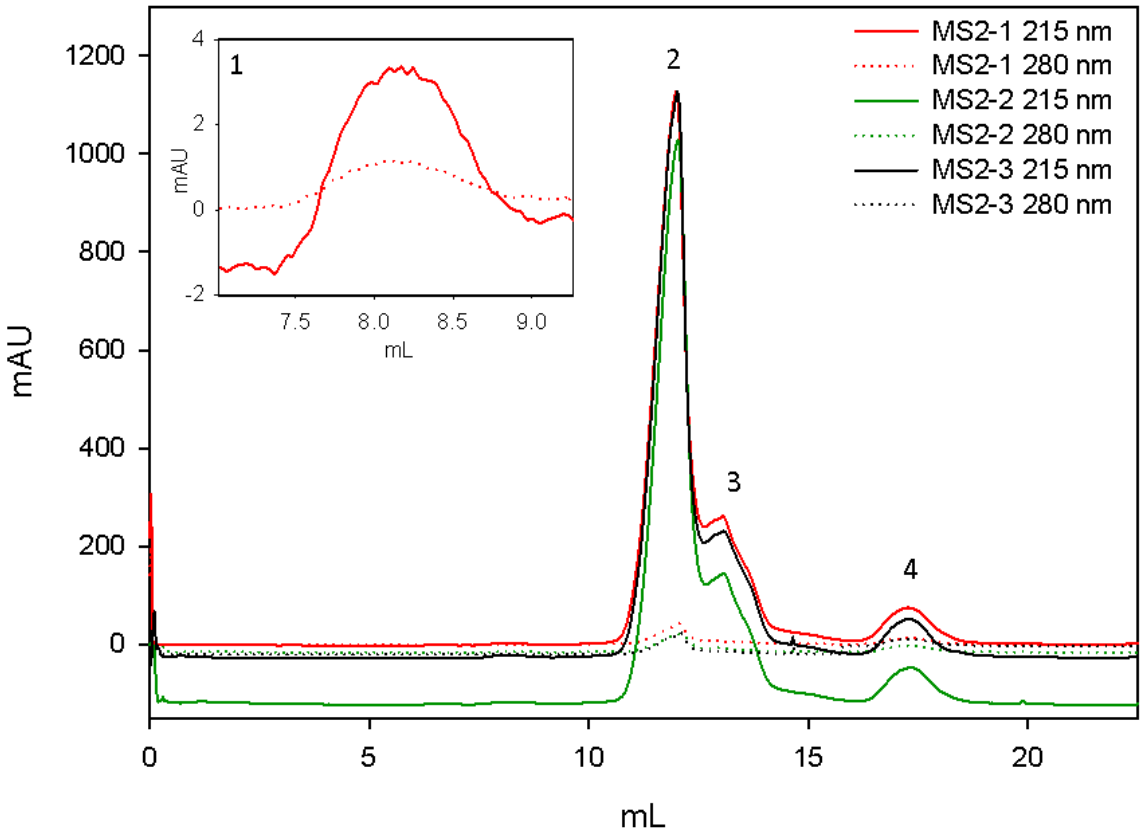

Figure 2.13 Chromatograms of three runs of MS2 purification, showing the peaks observed at 215 nm (solid lines) and 280 nm (dots). Run 1: red lines, run 2: green lines, run 3: black lines.

Based on the plaque assay, Fraction 1 contained most of the infectious MS2 particles. The number of plaques for all fractions (8.2×10^{9}) was lower than the number of plaques observed in the solution injected into the SEC column (2.1×10^{10}) implying some loss of particles during purification. However, MS2 particles are likely to aggregate in solution containing calcium ion (Mylon *et al.*, 2010), a component of the buffer used for MS2 purification, which would therefore result in underestimation of particle number by the plaque counting method.

Fraction 2, 3 and 4 contained 2 – 3 orders of magnitude less infectious MS2 particles than Fraction 1, verifying that the majority of the infectious MS2 particles were recovered in Fraction 1.

Table 2.12 The genome copy (gc) and plaque forming unit (pfu) concentration of the MS2 stock from culturing and the fractions derived from purification.

Sample	Volume of the sample (mL)	Number of gc in sample (qRT-PCR)	Number of pfu in sample (plaque assay)
Stock solution from culturing	1	6.8×10^{10}	2.1×10^{10}
Fraction 1	1.5	1.0×10^{11}	8.2×10^{9}
Fraction 2	1	9.8×10^{8}	3.3×10^{7}
Fraction 3	1.5	3.7×10^{8}	2.5×10^{7}
Fraction 4	1.5	9.1×10^{7}	4.1×10^{6}
Total from Fractions		**1.0×10^{11}**	**8.2×10^{9}**

The plaque assay yielded similar results as the qRT-PCR, however, all observed plaque concentrations were 3 – 30 times lower than the corresponding results of the qRT-PCR (Figure 2.14), which corresponds with previous findings. Gentilomi *et al.* (2008) used Sybr Green-based single-step qRT-PCR and plaque assay for the detection and quantification of MS2 bacteriophage in wastewater samples, and found that the qRT-PCR defined viral count 2 – 60 times higher than the plaque assay. The results of rotavirus integrity suggest that the SEC method successfully eliminates the uncapsidated viral RNA, thus the gc number detected by qRT-PCR in the purified stock (Fraction 1) reflects the number of intact particles. Overall, the two methods used for quantification correlated well; the difference in particle numbers of the purified MS2 (Fraction 1) detected by qRT-PCR and plaque assay was probably due to aggregation of viral particles.

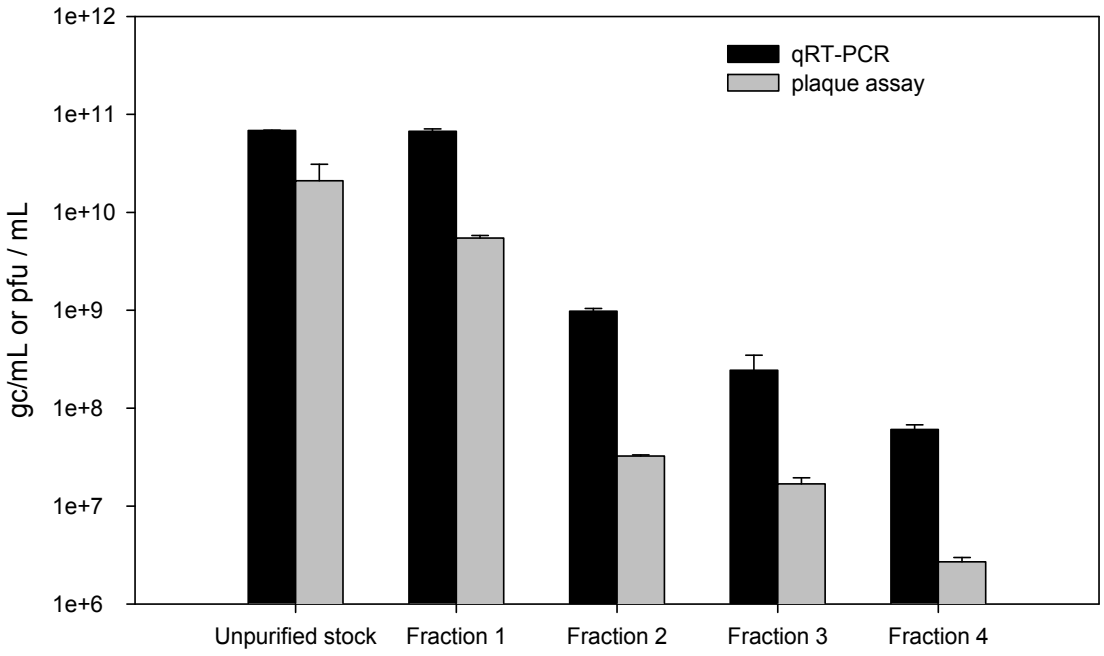

Figure 2.14 MS2 concentration of the virus stock from culturing stock and the fraction derived from purification determined by qRT-PCR (black bars) and plaque assay (grey bars). Error bars represent the standard deviations of the replicate assays.

A sample of Fraction 1 was analysed by TEM. The sample contained large number of intact MS2 particles, with size of 25 – 30 nm in diameter (Appendix II.3), similar to the finding of Gutierrez *et al.* (2009) who measured the size of the MS2 by TEM (25 nm) and Zetasizer (29 – 34 nm).

2.3.2 Viral characterisation

2.3.2.1 Hydrophobicity of the viruses

The theoretical hydrophobicity values (HVs) calculated for the capsid proteins of the three viruses showed little difference (Table 2.13). The capsid protein of the MS2 was fairly hydrophobic (HV = 23.24). The hexon protein of the adenovirus capsid was more hydrophilic than the outermost proteins of the capsid (short and long fibre proteins), which HVs were closer to the HV of the MS2 capsid protein (HV = 21.62 and 23.10, respectively). The VP6 and VP7 proteins of the rotavirus capsid were more hydrophobic than the proteins of the MS2 and the adenovirus, while the outmost protein of the rotavirus capsid (VP4) was less hydrophobic (HV = 20.21).

Table 2.13 Theoretical hydrophobicity of the main capsid proteins of MS2 adenovirus and rotavirus. HV: the hydrophobicity of amino acid at pH 6.8 divided by the number of amino acids. (See the hydrophobicity scores of amino acids: Appendix I.) *outmost protein of the capsid.

virus	Capsid protein	HV at pH 6.8
Rotavirus	VP6	24.26
	VP4*	20.21
	VP7	26.42
Adenovirus	hexon monomer	16.21
	short fibre protein	21.62
	long fibre protein*	23.10
MS2	MS2 coat protein*	23.24

The hydrophobicity of the purified viruses was determined by a modified MATH assay. For that propose, the Fraction 1 from SEC of the rotavirus and the MS2 was used. The MATH assay is commonly used to determine the hydrophobicity of bacteria (Rosenberg, 2006). The classical assay involves spectrophotometric absorbance measurements, which would not have been suitable for virus detection. Therefore, in this study qPCR and qRT-PCR was used to determine the concentration of the viruses. As the purified viruses were tested, the number of non-encapsidated viral nucleic acids were insignificant, thus the q(RT-)PCR detected intact viruses.

Results of the modified MATH test used to determine the hydrophobicity of the purified viruses are shown in Table 2.14. Among selected viruses the MS2 bacteriophage were found to be the most hydrophobic (H% = 98.26%). Nearly 2 $\log_{10}$ less MS2 was detected in the water phase after introducing the hexadecane to the solution. The adenovirus was also hydrophobic (H% = 88.93%): 1 $\log_{10}$ reduction was observed. In case of the rotavirus, little reduction was detected (H% = 42.49%).

The results supports previous finding, where MS2 was more readily adsorbed to silica when the silica was coated with hydrophobic material (Bales *et al.*, 1991; Bales *et al.*, 1993). Van Voorthuizen *et al.* (2001) also observed that MS2 was more retained by hydrophobic than hydrophilic membranes suggesting that hydrophobic interactions were superior to other interactions. Studies of Aronino *et al.* (2009) and Han *et al.* (2006) also showed higher removal when MS2 was injected to column filled with hydrophobic material. Rotavirus was

also demonstrated to bind to glass slides coated with a hydrophobic material (N-alkylated polyethylenimine) at high rate (Larson *et al.*, 2011), indicating that different hydrophobic materials may have different impact on virus adsorption. No data was found in literature about the hydrophobicity of adenovirus.

The test results showed some correlation with the calculated HVs of the outermost proteins of the capsids. The MS2 capsid protein and the adenovirus long fibre protein had high HVs, whereas the rotavirus VP4 had the lowest HV. However, very little difference was observed in the theoretical HVs of the proteins, while the results of the MATH test suggested fundamental differences in the hydrophobicity of the viruses. Hence, the hydrophobicity of the viral capsid is not only depends on the amino acid content; and the secondary/tertiary protein structure and protein interactions have an important role as well.

Table 2.14 Results of hydrophobicity assay on rotavirus, adenovirus and MS2 bacteriophage.

	Rotavirus	**Adenovirus**	**MS2**
Control 1 (gc/µL)	9.27×10^4	2.46×10^5	9.56×10^6
Control 2 (gc/µL)	9.36×10^4	1.29×10^5	7.64×10^6
Average (gc/µL)	9.32×10^4	1.88×10^5	8.60×10^6
Sample 1 (gc/µL)	6.69×10^4	1.67×10^4	3.89×10^4
Sample 2 (gc/µL)	5.37×10^4	2.27×10^4	1.43×10^5
Sample 3 (gc/µL)	4.02×10^4	2.29×10^4	2.66×10^5
Average (gc/µL)	5.36×10^4	2.08×10^4	1.49×10^5
H%	**42.49%**	**88.93%**	**98.26%**

2.3.2.2 Size and zeta potential of the viruses

Results of the size and ZP measurements are summarised in Table 2.15. The size of the unpurified rotavirus was measured as 123.9 nm with a ZP of –24.5 mV. The purification seems to have had little effect on the characteristics measured by the Zetasizer. The average size slightly decreased (106.6 nm) and the ZP was –19.6 mV and more consistent (SD = 1.1 mV). In order to disperse and/or eliminate the aggregated particles, the purified samples (fraction 1 from SEC) were filtered through 0.22 µm (single-filtered) and then 0.1 µm filters (double-filtered). After single-filtration the average size was measured as 115.2 nm and the ZP became –28.7 mV. Both measurements showed high deviation suggesting variation

between the analysed samples. After double-filtration, the size was measured as 78.5 nm, which is similar to the size measured by TEM. The ZP was determined as –24.4 mV. Using the double-filtration the polydispersity index (PdI), which indicates the width of the cumulative analysis of the size, was close to 0.2 indicating monodisperse particle solution.

Table 2.15 Size and zeta potential (ZP) of viruses. n: number of samples, n.m.: not measured, *Measurement data did not meet quality criteria (due to polydispersity or low sample concentration).

Sample		TEM Diameter (nm)	Zetasizer n	Diameter (nm)	PdI	ZP (mV)
Rotavirus						
Unpurified	**not filtered**	70 – 75	2	123.9 (±5.8)	0.26 (±0.05)	–24.5 (±17.9)
Purified	**not filtered**		2	106.6 (±3.2)	0.26 (±0.03)	–19.6 (±1.1)
Purified	**single-filtered**		2	115.2 (±10.2)	0.31 (±0.03)	–28.7 (±10.5)
Purified	**double-filtered**		6	78.5 (±9.0)	0.38 (±0.16)	–24.4 (±3.8)
Adenovirus						
Unpurified	**not filtered**	68	1	123.9*	0.48	–31.3
Purified	**not filtered**		4	146.9 (±84.8)	0.41 (±0.08)	–27.5 (± 0.5)
Purified	**single-filtered**		1	94.9	0.37	n.m.
Purified	**double-filtered**		3	73.7 (±1.3)	0.35 (±0.04)	–20.8(±1.8)
MS2						
Unpurified	**not filtered**	25 – 30	2	983.3 (±376.6)	0.77 (±0.23)	–32.0 (±0.8)
Purified	**double-filtered**		3	57.8 (±2.5)	0.48 (±0.12)	–23.5 (±1.9)

The size and ZP of porcine rotavirus was measured previously by others (Gutierrez *et al.*, 2009; Gutierrez *et al.*, 2010; Gutierrez & Nguyen, 2012). In those studies, the 0.05 – 0.2 µm fraction (separated by membrane filtration) of the extract derived from virus culture was characterised, thus most of the aggregated virus particles were eliminated. The observed hydrodynamic diameter varied between 113 – 127 nm in low ionic strength solutions at pH 5.9, which was similar to the results for the single-filtered, SEC-purified rotavirus of this study. The observed ZP of this sample also similar to previous findings (–22.8 mV) (Gutierrez *et al.*, 2009). Gutierrez and Nguyen (2012) found little variation in the sizes of rotavirus samples separated by membrane filtration (117 nm) and purified by the standard caesium-

chloride ultrafiltration (111 nm). These findings suggest that the aggregation of rotavirus particles cannot be entirely eliminated by filtering through 0.2 μm filter or by caesium-chloride ultrafiltration.

The average size of the unpurified stock of the adenovirus (123.9 nm) was similar to the 120 nm (in 1mM NaCl, pH 7) reported elsewhere (Wong *et al.*, 2012). The high PdI value (0.48) indicated heterogeneity in size, which could be the result of aggregation or the presence of impurities due to culturing. The ZP (–31.3 mV) slightly differed from previous findings (–25 mV) also suggesting the presence of impurities.

After purification, the average size of the adenovirus was measured as 146.9 nm, however, the high deviation (±84.8 nm) and the high PdI value (0.41) both suggested aggregation. The ZP of this sample was –27.5 mV, similar to previous findings (Wong *et al.*, 2012). In order to eliminate the aggregated particles, single- and double-filtration was used. The size was measured after each filtration. The filtration process adequately lowered the average size (~74 nm) and the PdI value (0.35). The size of the double-filtered adenovirus was similar to the size determined by TEM. The ZP of the double-filtered adenovirus sample was –20.8 mV.

The concentration of the filtered samples was determined by qPCR. No loss in concentration was found in the sample filtered through 0.22 μm filter, but one order of magnitude reduction was observed in the double-filtered sample. The differences in the ZP of the non-filtered and filtered rotavirus and adenovirus samples either could be an analytical error attributed to low particle concentration, or a results of an actual difference in the surface charge of the aggregated and singular virus particles, however, no data were found in literature to support this hypothesis.

The average size and ZP was determined for the unpurified and purified MS2 stocks (Fraction 1 from SEC) as well. Without purification, the average particles size of the MS2-containing samples was 983 nm and the ZP was –32 mV. The size measured probably indicated the presence of large amount of impurities or clumping of the bacteriophage particles. The purified stock was double-filtered prior to measurement. The purification and the following filtration to the size of MS2 was measured as 57.8 nm, however, this size was still larger than measured previously using Zetasizer. Gutierrez *et al.* (2009) characterised MS2 particles with concentration of 10^{10} pfu/mL in aqueous solutions with different ionic strength, and found that the average size was 29 – 34 nm. The difference between the size measured here and

what reported previously suggests that the MS2 particles were aggregated, and that was not eliminated by filtration. However, it is also possible that the concentration of the samples (10^9 gc/mL) was too low for accurate measurement. (The gc concentration was not affected by the filtration.) That study of Gutierrez *et al.* (2009) specified the ZP of MS2 in 1 mM NaCl pH 5.9 solution as –28 mV, which is similar to the ones measure in this study (–23.5 mV). The slight difference was probably due to charge differences of the strains or to the different solutions.

2.3.2.3 Aggregation of the viruses

The aggregation of the single-filtered and double-filtered rotaviruses (Fraction 1 from SEC) and adenoviruses (incubated at room temperature) was monitored over time, and the results are summarised in Table 2.16. The single-filtered viruses aggregated after six hours of storage. In contrast, the size and ZP of the double-filtered samples were more stable. The adenovirus and rotavirus were stable for two and eight weeks, respectively. However, slightly increased sizes were measured for adenovirus 6 hr after preparation, indicating aggregation is affecting the accuracy of the ZP measurements. When the aggregation of the virus particles started the ZP moved towards zero, even turned into positive, or, in case of the double-filtered rotavirus, it became more negative. According to the measurement file created by the Zetasizer software, the measurements of these samples did not meet the quality criteria sufficient for reliable measurement, which suggests that the sample concentration was too low or the samples were polydisperse. These findings indicate that the concentration decreased (due to virus degradation or aggregation) and the data did not reflect the charge of the viruses.

The aggregation of the double-filtered adenovirus incubated at 4°C was also followed. Interestingly, the results suggested that the adenovirus greatly aggregated in the first day of incubation (d = 263.2 ± 14.5 nm). As reviewed in Chapter 1 the virus adsorption to solid surfaces in enhanced at high temperature in water-based electrolytes, suggesting that the aggregation of viruses would be promoted by increased temperature as well. On the other hand, Charles *et al.* (2009) observed a rapid decrease in infectivity of adenovirus type 2 incubated in groundwater at 12°C, which was explained with aggregation (K. Charles, personal communication). Similar to the findings of my study, the aggregation occurred in days suggesting that aggregation of the adenovirus is enhanced at low temperature.

Table 2.16 Aggregation of (A) rotavirus and (B) adenovirus. n.m.: not measured, *Measurement data did not meet quality criteria (due to polydispersity or low sample concentration).

	A: Rotavirus				B: Adenovirus			
	Single-filtered		Double-filtered		Single-filtered		Double-filtered	
Day	Diameter (nm)	ZP (mV)	Diameter (nm)	ZP (mV)	Diameter (nm)	ZP (mV)	Diameter (nm)	ZP (mV)
0	108 (±7)	–36.1 (±4.0)	79 (±2)	–23.4 (±0.8)	95 (±1)	–16.4 (±0.1)	66 (±0.6)	–18.2
0.25	347 (±28)	-38.8	69	-30	264 (±1)	–17.5 (±0.4)	92 (±0.9)	n.m.
2	718 (±179)	–36 (±1.2)	65 (±3)	–28.3 (±1.2)	2399*	–8.1*	93 (±0.6)	–12.0*
5	1091*	–28.9 (±1.3)	84 (±3)	–29.8 (±0.5)	213 (±15)	–12.7*	93 (±0.4)	–11.8*
7	1629*	–1.16*	79 (±4)	–27.9 (±0.3)	17940*	9.4*	88 (±0.8)	–11.8*
14	1646*	15.5*	91 (±1)	-23.8	3207*	6.0*	88 (±1.7)	–12.3*
21	1799*	4.56*	87 (±6)	–21.8 (±0.4)	5769*	–4.3*	111 (±2.2)	–10.3*
28	1290*	10.36*	73	–19.6 (±0.1)	173800*	–8.1*	1058*	–12.7*
55	374*	16.4*	75 (±3)	–18.8 (±0.1)	3740*	6.7*	16105*	0.4*
83	11923*	13.4*	270*	–47.0*	5516*	–5.9*	7274*	8.4*

The initial size measured for the MS2 sample was 59 nm and ZP was –20.5 mV (Table 2.17). As the aggregation was not eliminated, the aggregation of the MS2 could not be accurately described. The size was stable for up to one week, and no significant change was observed in the surface charge for 1.5 months. The decreased charge may be the result of virus degradation.

Table 2.17 Aggregation of MS2. *Measurement data did not meet quality criteria (due to polydispersity or low sample concentration).

	MS2 - double-filtered	
Day	Diameter (nm)	ZP (mV)
0	59*	–21.2 (±1.2)
4	55*	–25 (±0.1)
6	59*	–24.1 (±1.1)
8	66 (±3)	–20.9 (±1.1)
19	119 (±11)	–21.9 (±0.4)
22	124 (±8)	–21.5 (±0.4)
47	309 (±13)	–21.4 (±0.4)
60	263.4 (±8.6)	–14.6 (±2.4)
85	129.2 (±4.6)	–19.2 (±1.2)

No long-term studies have been found in literature focusing on the aggregation of the adenovirus, rotavirus and MS2 bacteriophage. However, the effect of monovalent vs. divalent cations on adenovirus and rotavirus aggregation has been examined previously (Gutierrez *et al.*, 2010; Wong *et al.*, 2013). Similarly to my results, human adenovirus type 2 and porcine rotavirus created monodisperse solution in NaCl electrolytes at near-neutral pH, due to repulsive forces between the surface antigens of the viruses, while the aggregation was enhanced in the presence of $CaCl_2$ or $MgCl_2$.

2.4 Conclusions

The SEC method designed for rotavirus and MS2 purification and the use of ViraBind™ Adenovirus purification kit for the purification of adenovirus are all fast and affordable methods for virus purification. Results suggested that the Fraction 1 from SEC contained the majority of the intact and infectious virus particles, therefore, these fractions were used henceforth. The purified stocks contained intact and infectious virus particles in high concentration (10^{11} gc/mL). The purified adenovirus can be stored at –80°C for at least nine months without major loss of intact particles; and the purified rotavirus and MS2 stocks were stable for six months at –80°C.

The quantitative PCR-based methods allow for the rapid and accurate quantification of the nucleic acid content of virus samples. The single-step qRT-PCR method reduces the cross-contamination, which often occurs during the two-step RT-qPCR. When combined with nuclease treatment or filtration to eliminate free nucleic acids in solution, these methods can give a reliable estimation of the number of intact virus particles in a sample.

The size and surface characteristics of the viruses can be precisely determined by analysing the purified viruses with TEM, a modified MATH test, and Zetasizer measurements. The MS2 and the adenovirus were found to be hydrophobic, whereas rotavirus was hydrophilic. The size of the viruses determined by TEM corresponds to literature data for adenovirus and rotavirus, and was very similar to the hydrodynamic diameter measured by Zetasizer, when filtered through both 0.22 μm and 0.1 μm filters. These findings suggest that the aggregated particles can be eliminated from a sample by suitable filtration. No filters were available for the 25 – 30 nm MS2, therefore, the measurement of the hydrodynamic parameter was not accurate.

The results of the ZP measurements corresponded to the general observation that viruses, due to their low pI value, are negatively charged in water based electrolytes at near-neutral pH. The size and surface charge of adenovirus and rotavirus was relatively stable for 14 and 55 days, respectively. Together with aggregation of the virus particles, the observed ZP decreased. Most likely, the aggregation affected the accuracy of the measurement, and did not alter surface charge.

Chapter 3.
Virus surrogate characterisation

3.1 Introduction

3.1.1 Microspheres as pathogen surrogates

Microspheres have been used to study the behaviour of pathogens in groundwater. They were first used in a study by Champ and Schroeter (1988) to compare the transport of *E. coli*, conservative soluble tracers (bromide, nitrate, fluorescein and tritium) and neutral polystyrene beads of various size in fractured media. The results of their study showed that both the microspheres and the bacteria travelled faster than the soluble tracers, and suggested that the soluble tracers underestimated the health impact of a possible contamination. The microspheres gave a better interpretation on bacteria transport.

The most widely used microsphere surrogates in groundwater studies are the polystyrene microspheres. These particles are commercially available in various sizes, therefore, they may be suitable to mimic different pathogens. The microspheres are also available with positively, negatively charged and with neutral surface. The pathogens found in the environment are negatively charged, therefore mainly carboxylated particles are used in groundwater research. Nonetheless, the polystyrene microspheres are fundamentally hydrophobic, and may overestimate the retention of the pathogens in hydrophobic media.

Many studies have been carried out to demonstrate the usefulness of carboxylated microspheres as bacteria and protozoa surrogates, however, the results of the studies are often contradictory. For instance, field studies performed using neutral, positively (amidine-modified) and negatively charged (carboxyl-modified) microspheres showed that these particles, regardless of their charge, had greater removal than bacteria with similar size (Becker *et al.*, 2003; Harvey *et al.*, 1989; Harvey *et al.*, 2011; McCaulou *et al.*, 1995; Sinreich *et al.*, 2009). In contrast, in laboratory experiments with columns packed with glass beads and iron-oxyhydroxide coated glass beads, Becker *et al.* (2004) found that the positively and

negatively charged microspheres were not retained, even when the media used was positively charged.

Carboxylated polystyrene microspheres have been successfully used as surrogates for flagellates (Harvey *et al.*, 1995) and *Cryptosporidium* oocysts with similar size in field experiments (Metge *et al.*, 2007; Mohanram *et al.*, 2010). On the other hand, in laboratory experiments Harvey *et al.* (2008) demonstrated that the carboxylated microspheres (with ZP of –18.7 mV) can overestimate the retention of the *Cryptosporidium* oocysts (ZP = –3.6 mV), probably due to charge dissimilarities. The research on the usefulness of microspheres for mimicking viruses in groundwater is summarised in Chapter 1. The results of various laboratory and field experiments showed that these particles often overestimate the recovery of viruses.

The results of experiments on carboxylated microspheres discussed above showed that, despite the similar size, shape and charge to pathogens, these particles are not representative surrogates, probably as a result of their more negative charge and hydrophobicity. Therefore, to mimic pathogenic transport, further modification of microspheres in terms of surface charge and structure is essential.

Pang *et al.* (2012) have successfully modified the surface charge of the carboxylated microspheres by covalently binding proteins to the beads. The modified particles had similar surface charge, size, density and shape as the *Cryptosporidium* oocysts. In column experiments, the biotin- and glycoprotein-coated polystyrene microspheres showed similar recovery and travelling pattern as the oocysts through sand, whereas the recovery of the uncoated microspheres was one order of magnitude higher.

A similar surface modification as described for *Cryptosporidium* surrogates was used to produce surrogates for viruses using 20 nm carboxylated polystyrene beads coated with casein (Pang *et al.*, 2009). The size and surface charge of the surrogate was similar to MS2 bacteriophage, but no information is available on the transport behaviour of these surrogates due to the lack of sensitive method for quantification.

3.1.2 Detection and quantification of microspheres

In most cases fluorescent microspheres are used in groundwater studies for easy detection. Various methods are available for detection of fluorescent beads such as fluorescent microscopy, flow cytometry or spectrofluorometry. Fluorescent microscopy involves manual counting, hence it is time consuming. On the other hand, it is highly sensitive, which makes it suitable for environment studies. According to Chae *et al.* (2008), 350 particles per sample (25 – 40 particles per field) are sufficient for reproducible and accurate counting of 0.2 μm-sized microspheres. Flow cytometry and spectrofluorometry are both automatic counting methods and suitable when many samples are analysed. According to Becker *et al.* (1999) the detection limit of flow cytometry for 0.19 – 1μm size particles is 10^2 particles/mL, similar to the detection limit of microscopy, thus it is suitable for the analysis of environmental samples. In contrary, spectrofluorometry is only suitable for analysing samples with high particle concentration (10^3 particles/mL for protozoon-sized particles, 10^6 particles/mL for bacteria-sized particles, and 10^8 particles/mL for virus-sized particles) (Pang *et al.*, 2009; Pang *et al.*, 2012).

Alternatively radioactive labelling is also used for enabling easy detection of particles. Radiolabelled proteins and peptides are widely used in clinical diagnostics and therapeutics (Tolmachev & Stone-Elander, 2010). Radioactive tracers are often used to study metabolic processes (Ladrière *et al.*, 1999) and in medical imaging like positron emission tomography (PET) (Muehllehner & Karp, 2006). In the field of virus transport in groundwater, Ryan *et al*. (1999; 2002) demonstrated that PRD1 bacteriophage could be labelled with ^{32}P-phosphate, and these particles could be easily detected in both field and laboratory experiments. Nonetheless, the use of radioactive particles in environmental studies may be restricted. The radioactive labelling and detection also involves the use of special equipment that may not be available in many facilities.

DNA-labelling is a widely used technique in molecular biology. Short DNA sequences are usually immobilised to solid surfaces via protein interactions (Xu *et al.*, 2001) or covalent binding (Walsh *et al.*, 2001). Immobilised DNA is commonly used in medical research and protein engineering (Heller, 2002; Kallioniemi *et al.*, 1994; Kokoris *et al.*, 2000). Microarrays containing several hundred-thousand immobilised oligonucleotides have been used to screen environmental samples for pathogens (Ahmad *et al.*, 2009).

DNA-labelled particles have been shown to be useful tools in groundwater research. Yang *et al.* (1996) successfully coupled amino-modified oligomers (20 – 25 nucleotides) to silica microspheres (with size of 0.15 μm and 0.55 μm) via covalent bounding. In these experiments, the DNA-labelled particles were found to be stable over time under different physico-chemical conditions including various types of groundwater. The DNA tags bound to the surface of the silica particles were not affected by microbial activity. The detection of the DNA oligomers by hybridisation was showed to be more sensitive (0.1 pg) than autoradiography (used for radioactive substances) or fluorometry. However, DNA hybridisation cannot compete with the sensitivity of qPCR-based detection assays (detection limit < 1 fg).

The virus surrogates validated in this study are 70 nm carboxylated silica nanoparticles, labelled with a DNA marker and coated with selected proteins. Silica is a hydrophilic material, therefore, these particles are probably more conservative surrogates than polystyrene beads if hydrophobic matter is presented. The DNA-labelling allows sensitive and accurate detection by qPCR, while the protein coating mimics the surface charge of rotavirus and adenovirus and alters the surface characteristics on the nanoparticles. Presumably the protein-coating allows similar interactions as the capsid of a virion. Both the DNA and the proteins were bound to the nanoparticles covalently to assure they are stably immobilised. The physico-chemical properties of the carboxylated, the DNA-labelled and the protein-coated-DNA-labelled nanoparticles were investigated and compared to characteristics of the viruses used in the study.

3.2 Methods and materials

3.2.1 Surrogate synthesis

3.2.1.1 Silica nanoparticles

The silica nanoparticles were sourced from Micromod Partikeltechnologie GmbH (Germany). Two types of nanoparticles were used: carboxylated and streptavidin coated. The core properties of the nanoparticles, provided by the manufacturer, are summarised in Table 3.1. According to the manufacturer, the average size of the carboxylated particles was 70 nm, the streptavidin coated particles was 100 nm. Silica (silicon dioxide or SiO_2) is a physically and chemically inert material, and no data suggests that it is harmful for the environment. Silica

has no known adverse effects from ingestion, although long-term inhalation of the silica dust nanoparticles may cause the inflammation of the lungs (McCarthy *et al.*, 2012). Silica is the main component of many types of sand, especially coastal sand. Silica nanoparticles are hydrophilic, thus the particles are monodisperse in water (PdI < 0.2) and not likely to aggregate over time.

Table 3.1 Main features of the silica nanoparticles used in this study. Data is provided by Micromod Partikeltechnologie GmbH (Germany).

Particle	**Carboxylated silica nanoparticles (SiNPs)**	**Streptavidin-coated silica nanoparticles (StrNPs)**
Surface	-COOH	streptavidin
Size	70 nm	100 nm
Solid content	25 mg/ml	25 mg/ml
Polydispersity index (PdI)	< 0.2	< 0.2
pI	2.21 – 2.47	–
Shape	spherical	spherical
Density	2.0 g/cm^3	2.0 g/cm^3
Porosity	nonporous	nonporous
Particle/ml	7.0×10^{13}	2.4×10^{13}
Particle/mg	2.8×10^{12}	9.5×10^{11}
Density	1 µmol/g	–
Protein binding capacity	10 – 20 ng albumin (BSA) / mg particle	–

3.2.1.2 DNA markers and their detection

Five 198 bp DNA fragments were designed by Dr Arvind Varsani using a random sequence generator (http://www.faculty.ucr.edu/~mmaduro/random.htm). The 5' and 3' ends of these fragments contain four common domains for the purpose of PCR detection (Figure 3.1). The outer two domains are complementary to primers for the amplification of the DNA marker for particle labelling, whereas the two inner ones are complementary to the primers for general detection of the fragments (Figure 3.1). Specific primers for 198 bp long fragments of each sequence were also designed for individual detection. The 302 bp markers (with four common domains) contain two restriction sites to allow the cleaving of the DNA tag from the nanoparticles after labelling by digesting with restriction endonucleases (*Sty*I or *Bam*HI).

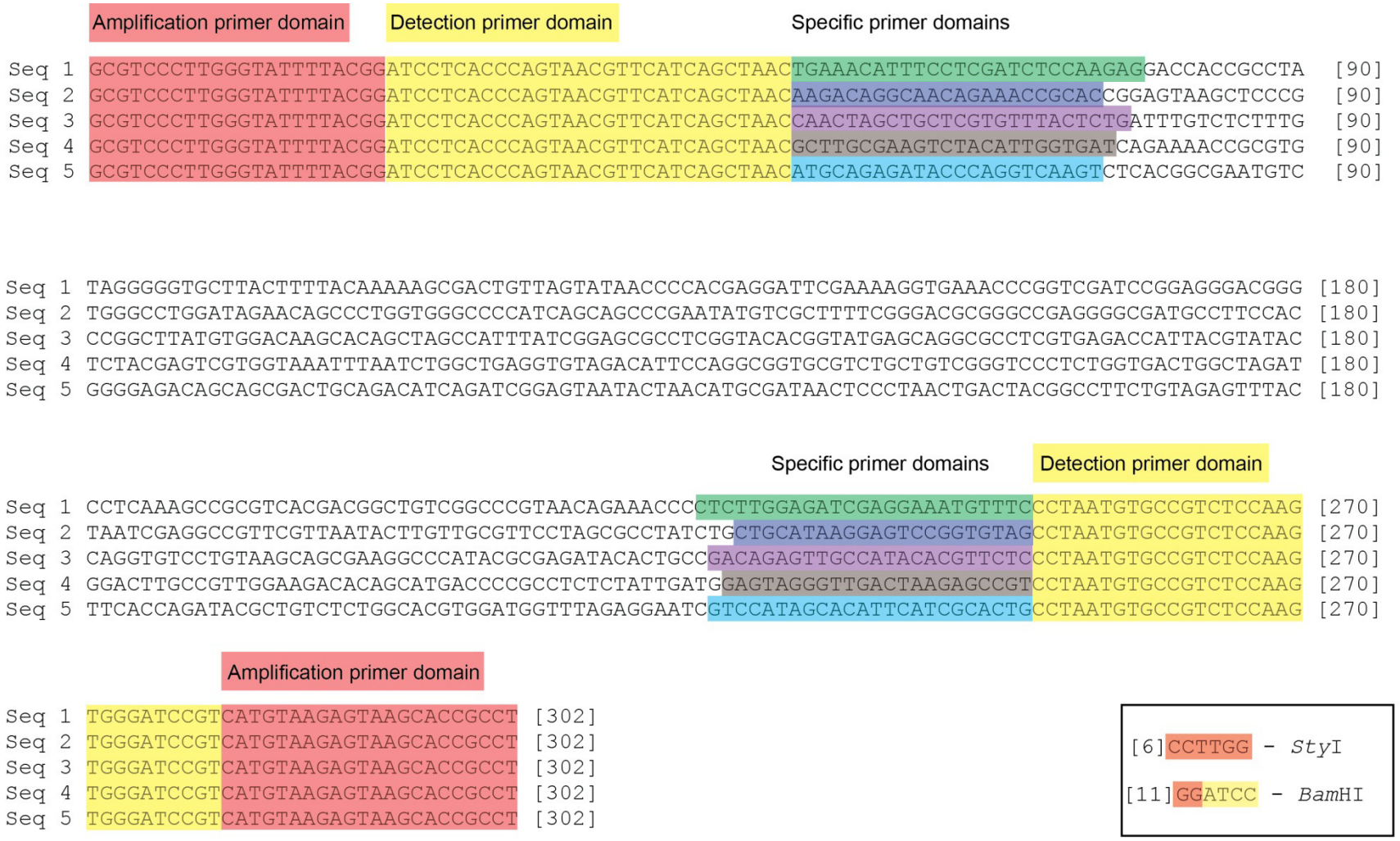

Figure 3.1 DNA sequences designed for labelling of the silica nanoparticles. Inserted figure shows the restriction sites of the *Sty*I and *BamH*I restriction endonucleases.

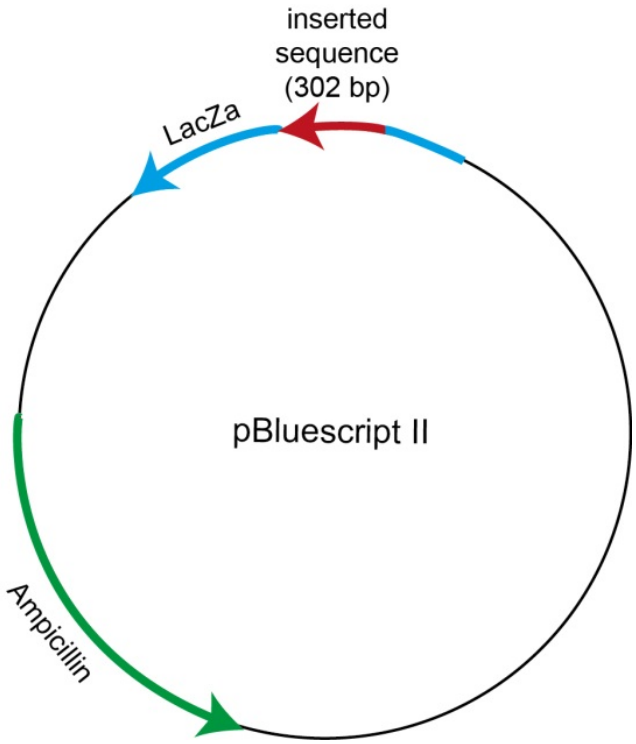

Figure 3.2 The pBlueScript plasmid holding the 302 bp DNA sequence used for particles-labelling.

The fragments were commercially synthesized and cloned in pBlueScript plasmid (Figure 3.2) at Epoch Life Sciences (USA). This plasmid was used as a template to amplify DNA for particle labelling and also used as a positive control for the qPCR to detect and quantify the DNA markers.

In order to detemine the detection limits of the qPCR reactions, the five DNA fragments (1 µL each) were amplified by qPCR from the plasmids using 100 nM of the detection and the internal primers pairs (Table 3.2) in a 10 µL reaction mix containing KAPA SYBR FAST qPCR Master mix (KAPA Biosystems, USA). Amplification was conducted at 95°C for 10 min, followed by 45 cycles of 95°C for 10 s, 60°C (65°C when sequence 1 primer pair was used) for 30 s and 72°C for 10 s in a Roche Light Cycler 480 Real-Time PCR System (Roche Diagnostics GmbH, Germany).

The amplification was followed by one cycle of melting curve analysis at 95°C for 5 s; annealing 60°C for 1 min. Dissociation was carried out from 65°C to 97°C with a temperature ramp of 0.11°C/s. Dilution series of the plasmid DNA (Figure 3.2) were used to generate standard curves and determine the detection limit of the qPCR (Table 3.2). Sequence 2 was

found to be optimal for detection (detection limit: 3 DNA copies/µL), thus this sequence was used for further work.

Table 3.2 Information on primers and target sequences of the (q)PCR reactions used for quantification of the plasmid/DNA marker. n.d.: not determined.

Primers for	Forward	Reverse	Length of the product	Detection limit	Tm
Amplification	5'-GCGTCCCTTGGGTATTTTACGG-3'	5'-AGGCGGTGCTTACTCTTACATGAC-3'	302 bp	n.d.	n.d.
General detection	5'-TCACCCAGTAACGTTCACAGCTAAC-3'	5'-CACTTGGAGACGGCACATTAGG-3'	256 bp	300 DNA copies/µL	84–87°C
Sequence 1	5'-TGAAACATTTCCTCGATCTCCAAGAG-3'	5'-GAAACATTTCCTCGATCTCCAAGAG-3'	198 bp	10^6 DNA copies/µL	86.9± 0.2°C
Sequence 2	5'-AAGACAGGCAACAGAAACCGCAC-3'	5'-CACTTGGAGACGGCACATTAGG-3'	198 bp	3 DNA copies/µL	85.9± 0.2°C
Sequence 3	5'-CAACTAGCTGCTCGTGTTTACTCTG-3'	5'-GAGAACGTGTATGGCAACTCTGTC-3'	198 bp	70 DNA copies/µL	84.5± 0.1°C
Sequence 4	5'-GCTTGCGAAGTCTACATTGGTGATC-3'	5'-ACGGCTCTTAGTCAACCCTACTC-3'	198 bp	12 DNA copies/µL	84.5± 0.3°C
Sequence 5	5'-ATGCAGAGATACCCAGGTCAAGTC-3'	5'-CAGTGCGATGAATGTGCTATGGAC-3'	198 bp	70 DNA copies/µL	82.8± 0.1°C

3.2.1.3 Proteins

Five proteins were selected for coating the nanoparticles (Table 3.3). All the five proteins have low pI value, thus they all are negatively charged at neutral pH similar to rotaviruses and adenoviruses. Two of them (casein and glycoprotein) have been used previously for coupling pathogen surrogates (Pang *et al.*, 2009; Pang *et al.*, 2012).

Caseins (α-, β- and κ-casein) are found naturally in mammalian milk at high concentrations. Caseins in general are considered as hydrophobic proteins, which makes them poorly solvable in water. The α-casein used in this study was purified from bovine milk. Its molecular weight is approximately 23 kDa and its isoelectric point is 4.42.

Glycoproteins are conjugated proteins: they have carbohydrate component. Glycoproteins are produced by many organisms from bacteria to humans. Some viral capsids (e.g. rotavirus) contain glycoproteins as well (Estes & Greenberg, 2013). In this study a human α_1-acid-

glycoprotein with molecular weight of 40 kDa and isoelectric point of 2.7 was used. The human α_1-acid-glycoprotein is soluble in water at concentration as high as 10 mg/mL.

Streptavidin is a protein produced by the bacterium *Streptomyces avidinii*. It has high affinity for biotin, thus it is commonly used tool used in molecular biology. The isoelectric point of the recombinant streptavidin (53 kDa) used in this study is 5, therefore may have little surface charge in groundwater.

Protein A is the cell wall component of the bacterium *Staphylococcus aureus.* It is used in molecular research, due to its binding capability to a specific type of antibody (immunoglobulin G) produced by mammalians. The protein A used in this study had a molecular weight of 47 kDa. Like streptavidin, it has a relatively high isoelectric point of 5.16.

The AMBP (α_1-microglobulin/bikunin precursor) is a human recombinant polypeptide produced in yeast. It is a small molecule with molecular weight of 20 kDa and its predicted pI is 4.5, similar to the α-casein.

Table 3.3 Characteristics of the proteins used for coating of the silica nanoparticles. N/A: information not available.

Protein	**α-Casein**	**α_1-Acid-Glycoprotein**	**Streptavidin**	**Protein-A**	**AMBP**
Origin source	Sigma-Aldrich, USA	Sigma-Aldrich, USA	Thermo Fisher Scientific, USA	Thermo Fisher Scientific, USA	Creative Biomart, USA
Molecular weight	23 kDa	40 kDa	53 kDa	47 kDa	20 kDa
pI	4.42 (measured)	2.7 (measured)	5 (theoretical)	5.16 (theoretical)	4.5 (theoretical)
Reference of pI	Pang *et al.* (2009)	Pang *et al.* (2012)	Thermo Fisher Scientific	Thermo Fisher Scientific	Creative Biomart
Solubility in water	unknown	10 mg/mL	≥ 20 mg/mL	≥ 15 mg/mL	Soluble
Reference of solubility	–	Sigma-Aldrich	Thermo Fisher Scientific	Thermo Fisher Scientific	Creative Biomart
Purity	> 70%	99%	≥ 17 units/mg	N/A	> 98%

3.2.1.4 Covalent coupling

The DNA-labelling and protein-coating of the nanoparticles were performed by Bennett Scientific Services (New Zealand). In order to produce large quantities of the DNA tag for labelling, a specific DNA sequence was amplified from the plasmid by PCR using the amplification primer pair (Table 3.2). The forward primer contained six carbon linker and an amine group (5AmMC6 modification, Integrated DNA Technologies, USA), thus the DNA could be linked to the carboxyl group of the nanoparticles.

A simplified two-step EDC protocol was used for coupling based on TechNote 205 of the Bangs Laboratories (2002) and instructions of Thermo Fisher Scientific Inc. (USA). During the procedure, the carboxylated nanoparticles were covalently coupled with the selected proteins and the DNA tag by a water soluble carbodiimide cross-linker, EDC (1-ethyl-3-(3-dimethylaminopropyl) carbodiimide hydrochloride). Prior to labelling/coupling the carboxylated silica nanoparticles were filtered through 0.1 µm PVDF filters (Merck KGaA, Germany), and the streptavidin-coated nanoparticles were vigorously shaken. The nanoparticles were then activated in 2-(N-morpholino) ethane sulfonic acid (MES) buffer containing EDC (Thermo Fisher Scientific Inc., USA) and N-hydroxysulfosuccinimide (Thermo Fisher Scientific Inc., USA). Following activation, particles were recovered by centrifugation and combined with the selected DNA tag (sequence 2) and proteins before being incubated overnight at room temperature. After incubation, particles were recovered by centrifugation and stored in sterile distilled water at 4°C. Each time 250 µL of the nanoparticles were labelled/coated. All surface-modified nanoparticles were stored at 4°C.

In order to determine the amount of DNA needed to be added for successful labelling, first different amounts of the amino-modified tag were added to the same amount of nanoparticles. No proteins were added to these mixtures. The amount of DNA varied between 1,600 and 14,400 ng (Table 3.4, Batch 1). To address the reproducibility, the DNA-labelling was repeated for an additional five samples (DNA-SiNP-1 to DNA-SiNP-5) by adding 4,800 ng DNA to each sample (Table 3.4, Batch 2).

Table 3.4 (Batch 3) summarises the information about the samples where proteins were also added for coupling. Sample SiNP was the negative control for which no DNA or protein was added through the process. Sample DNA-SiNP was only labelled with DNA and not coupled

Table 3.4 Construction of the DNA labelled and protein coated nanoparticles.

Sample name	Particle used	250 µL containing particles	Protein used	250 µL containing	
				Protein	DNA tag
Batch 1:					
SiNP+1600	sicastar -COOH	1.75×10^{13}	none	0 µg	1,600 ng
SiNP+3200	sicastar -COOH	1.75×10^{13}	none	0 µg	3,200 ng
SiNP+4800	sicastar -COOH	1.75×10^{13}	none	0 µg	4,800 ng
SiNP+6400	sicastar -COOH	1.75×10^{13}	none	0 µg	6,400 ng
SiNP+8000	sicastar -COOH	1.75×10^{13}	none	0 µg	8,000 ng
SiNP+9600	sicastar -COOH	1.75×10^{13}	none	0 µg	9,600 ng
SiNP+11200	sicastar -COOH	1.75×10^{13}	none	0 µg	11,200 ng
SiNP+12800	sicastar -COOH	1.75×10^{13}	none	0 µg	12,800 ng
SiNP+14400	sicastar -COOH	1.75×10^{13}	none	0 µg	14,400 ng
Batch 2:					
DNA-SiNP-1	sicastar -COOH	1.75×10^{13}	none	0 µg	4,800 ng
DNA-SiNP-2	sicastar -COOH	1.75×10^{13}	none	0 µg	4,800 ng
DNA-SiNP-3	sicastar -COOH	1.75×10^{13}	none	0 µg	4,800 ng
DNA-SiNP-4	sicastar -COOH	1.75×10^{13}	none	0 µg	4,800 ng
DNA-SiNP-5	sicastar -COOH	1.75×10^{13}	none	0 µg	4,800 ng
Batch 3:					
Gly-DNA-SiNP	sicastar -COOH	1.75×10^{13}	α1-Acid-Glycoprotein	75 µg	4,800 ng
Str-DNA-SiNP	sicastar -COOH	1.75×10^{13}	Streptavidin	125 µg	4,800 ng
PrA-DNA-SiNP	sicastar -COOH	1.75×10^{13}	Protein A	125 µg	4,800 ng
AMBP-DNA-SiNP	sicastar -COOH	1.75×10^{13}	AMBH	41.5 µg	4,800 ng
Cas(5)-DNA-SiNP	sicastar -COOH	1.75×10^{13}	α-Casein	5 µg	4,800 ng
Cas(50)-DNA-SiNP	sicastar -COOH	1.75×10^{13}	α-Casein	50 µg	4,800 ng
Cas(50)-DNA-SiNP'	sicastar -COOH	1.75×10^{13}	α-Casein	50 µg	4,800 ng
Cas(500)-DNA-SiNP	sicastar -COOH	1.75×10^{13}	α-Casein	500 µg	4,800 ng
Cas(2000)-DNA-SiNP	sicastar -COOH	1.75×10^{13}	α-Casein	2,000 µg	4,800 ng
DNA-StrNP	sicastar-streptavidin	6.00×10^{12}	none	0 µg	4,800 ng
DNA-SiNP	sicastar -COOH	1.75×10^{13}	none	0 µg	4,800 ng
SiNP	sicastar -COOH	1.75×10^{13}	none	0 µg	0 ng

with any protein. The streptavidin-coated nanoparticles (Micromod Partikeltechnologie GmbH, Table 3.1) were DNA-labelled only (DNA-StrNP).

The Gly-DNA-SiNPs were coated with glycoprotein, the Str-DNA-SiNPs with streptavidin, the PrA-DNA-SiNPs with protein A and the AMBP-DNA-SiNPs with AMPB. The Cas(5)-DNA-SiNP, Cas(50)-DNA-SiNP, Cas(500)-DNA-SiNP and Cas(2000)-DNA-SiNP were coated with different amount of casein. To address the reproducibility of the process, Cas(50)-DNA-SiNP and Cas(50)-DNA-SiNP' were both coated with the same amount of casein (50 µg).

3.2.2 Particle characterisation

3.2.2.1 Confirmation of the DNA attachment

To visualise if the DNA tag was successfully bound to the nanoparticles, agarose gel electrophoresis was used. This method separates DNA fragments based on their size allowing the negatively charged DNA molecules to migrate in the agarose matrix. The velocity of their transport depends on the size of the DNA.

The samples analysed by gel electrophoresis were the DNA-labelled and the protein coated silica nanoparticles (Table 3.4). The particles labelled with 4,800 ng of DNA (DNA-SiNP-1 to -5) were sampled and analysed frequently for 22 weeks and the protein-coated particles for one year. Between sampling, the nanoparticles were stored at 4°C, except sample DNA-SiNP-2, which was stored at room temperature.

The samples (18 – 24 µL) were loaded onto 2% agarose gel containing ethidium bromide (AppliChem GmbH, Germany) or Sybr Safe (Life Technologies, USA). These dyes are able to bind to the DNA, and, when bound, fluoresce when exposed to UV-light. For determination of the size of the DNA fragments, 100 bp DNA ladder (New England Biolabs, USA) was also loaded onto the gels. The run was performed at 100 V for 60 min when the nanoparticles were labelled with different amounts of DNA (Batch 1) were loaded. The other runs were performed at 80 V for 50 min. For visualisation the gels were UV radiated in a Gel Doc system (Bio-Rad, USA).

3.2.2.2 Quantification of the DNA-labelled and protein-coated nanoparticles

The DNA concentration of the nanoparticles was also determined by qPCR using the sequence 2 primer pair (Table 3.2) with the same conditions as described in Section 3.2.1.2. For accurate measurements, dilution series of the nanoparticles were analysed. All dilutions were made with nuclease-free, sterile, double-distilled water.

To assess whether the silica nanoparticles affected the accuracy of the qPCR, the DNA-labelled silica nanoparticles (DNA-SiNP+4800, 4,800 ng DNA used for labelling) were digested by *Bam*HI restriction endonuclease, in replicates. The DNA-SiNP was diluted to 5×10^4 DNA copies/µL with nuclease-free water and 17 µL of it was incubated with 15 units of *Bam*HI enzyme (Life Technologies, USA) in the presence of 1x Buffer K (Life Technologies, USA) at 30°C for 1 hr. The enzyme was inactivated by incubating the mixture at 65°C for 20 min. The samples were then centrifuged at 14,100xg for 20 min to pellet the nanoparticles. The supernatants, together with the non-treated nanoparticle solutions, were analysed by qPCR.

3.2.2.3 Hydrophobicity of the proteins and the nanoparticles

The theoretical hydrophobicity of the proteins used for particle-coating was determined using the Protein/Peptide Property Calculator (http://lifetein.com/peptide-analysis-tool.html). This tool calculates the hydrophobicity value (HV) by dividing the hydrophobicity of the amino acids of proteins (Appendix I) by the number of amino acids.

The hydrophobicity of the DNA-labelled and the protein-coated silica nanoparticles were tested using the modified MATH assay as described for viruses in Chapter 2. The particle solutions were diluted with 2 mM NaCl pH 7 to 10^5 DNA copies/µL concentration. Then, 0.5 mL of these solutions, in triplicates, were mixed with 0.5 mL hexadecane for 2 min and incubated at room temperature for 4 min allowing the separation of the water and hydrophobic phases. In order to determine the DNA concentration, 1 µL the water phase was directly analysed by qPCR.

3.2.2.4 Size and zeta potential of the proteins and the nanoparticles

To have a better understanding on the characteristics of the selected proteins in groundwater, their zeta potential (ZP) was measured by Zetasizer Nano ZS (Malvern Instruments, UK). Protein solutions with concentration of 0.1 mg/mL were made using 2 mM NaCl pH 7 solution. Samples were mixed vigorously and sonicated for 5 min before measurements, which were set up in triplicates. The ZP of the background (NaCl) solution was also measured.

The size and ZP of the carboxylated, the surface-modified (DNA-labelled and protein-coated) particles were measured by Zetasizer Nano ZS (Malvern Instruments, UK). For the Zetasizer measurements, samples were diluted to 10^{10} – 10^{11} DNA copies/mL concentration with 2 mM NaCl pH 7 solution. The carboxylated particles were sonicated for 10 min before each measurement. The surface-modified particles were only hand shaken. All measurements were set up in triplicates.

3.2.2.5 Aggregation of the nanoparticles

The stability of size and ZP of the nanoparticles over time was also followed by Zetasizer measurements. The surface-modified nanoparticles were measured 12, 221 and 365 days after preparation. The samples were hand-mixed before each measurement (set up in triplicates). Samples were stored at 4°C between measurements.

3.3 Results and discussion

3.3.1 Confirmation and stability of the DNA-binding

Figure 3.3 shows an image of the agarose gel electrophoresis of silica nanoparticles labelled with different amount of DNA. Results indicated that due to their size the DNA-labelled nanoparticles were not able to migrate in the agarose matrix with the velocity of the DNA tag itself. The unbound 302 bp DNA tag used for labelling was also present in the samples. In samples where a high amount of DNA was added for labelling (6,400 – 14,400 ng DNA/250 µL nanoparticles) more unbound DNA was present than in samples where less DNA had been used. The presence of the free DNA tag in the samples is probably the result of non-covalently bound DNA that detached from the surface of the silica nanoparticles by the

electric forces during the electrophoresis. Another explanation for the presence of unbound DNA is that these are fragments that they were not washed from the solution during the DNA-labelling process.

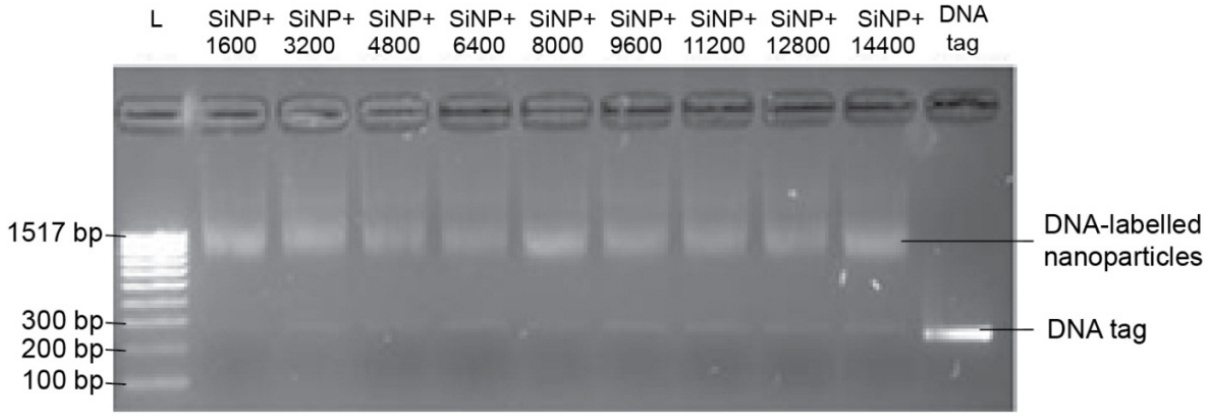

Figure 3.3 Results of the electrophoresis of silica nanoparticles labelled with different amounts of DNA (Batch 1). The numbers above the wells show the ng of DNA added to 250 µL of nanoparticles for labelling. "L" represents the 100 bp DNA ladder. Gel was dyed with 1 µg/mL Sybr Safe and the run was performed at 100 V for 60 min. 18 µL of each sample was loaded.

The stability of DNA labelling of the nanoparticles (without protein-coating) over time was also assessed using agarose gel electrophoresis (Figure 3.4). All samples were DNA-labelled silica nanoparticles where 4,800 ng DNA was used for labelling 250 µL nanoparticles.

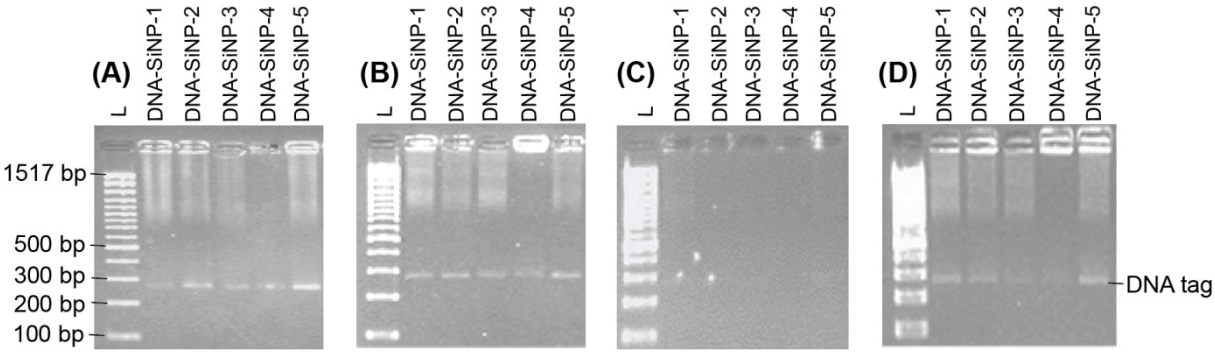

Figure 3.4 Stability of DNA-labelling of the nanoparticles (Batch 2). Gels were stained with 10 µg/mL ethidium bromide and the runs were performed at 80 V for 50 min. All samples contained silica nanoparticles labelled with the same amount of DNA (4,800ng/250µL). Samples were stored at 4°C between the runs, except the DNA-SiNP-2, stored at room temperature. "L" represents the 100 bp DNA ladder. Sample loaded: (A, B and C): 18 µL, (D): 24 µL. Runs performed: (A) one week, (B) 12 weeks, (C) 19 weeks and (D) 22 weeks after labelling.

With reducing the voltage from 100 V to 80 V and adjusting the duration of the run to 50 min the majority of the labelled particles were immobilised at the top of the gel, completely separated from the free DNA. The findings suggested that the DNA labelling was stable for 3 – 4 months. After 19 weeks, hardly any DNA was detected (Figure 3.4C), however, when the volume of samples loaded onto the gel was increased to 24 µL (Figure 3.4D), the same pattern was observed as at the beginning of the experiment. These results suggest that the DNA concentration of the samples slightly decreased and not entirely degraded in 19 weeks, which can be a result of the partial degradation of the DNA. No difference was observed between the sample stored at room temperature (DNA-SiNP-2) and those stored at 4°C.

The stability of DNA-labelled and protein-coated nanoparticles was also monitored (Figure 3.5). The pattern was very similar to the DNA-labelled particles, which were analysed under similar conditions (80 V for 50 min).

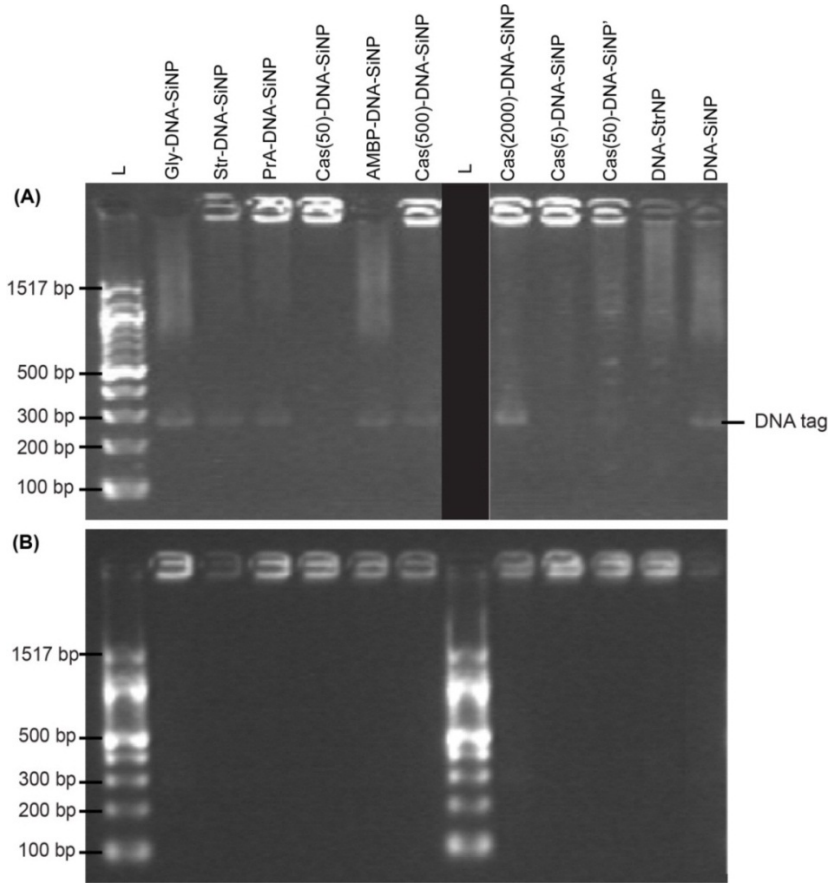

Figure 3.5 Stability of the DNA-labelled and protein-coated nanoparticles (Batch 3). Gels were stained with 10 µg/mL ethidium bromide and the runs were performed at 80 V for 50 min. "L" represents the 100 bp DNA ladder. 18 µL of samples were loaded. Runs performed: (A) seven weeks and (B) one year after coating.

The DNA-labelling of the protein-coated particles was more stable over time than the particles labelled only with DNA: the protein-coated and DNA-labelled particles were stable for at least one year, whereas the DNA-content of the only DNA-labelled ones started to degrade after 3 – 4 months. These observations suggested that the protein-coating protected the DNA from degradation.

3.3.2 Quantification of the surface-modified nanoparticles

The aim of the DNA labelling of the nanoparticles was to bind one DNA tag to one nanoparticle. In order to determine the amount of DNA sufficient for labelling, various amounts of DNA (1,600 – 14,400 ng/250 µL nanoparticles, Batch 1) were added to the activated nanoparticles. The concentration of the DNA in these samples was determined by qPCR using the internal primer pair for sequence 2. When 4,800 ng or more DNA was added to the 250 µL of nanoparticles solution, the DNA concentration was 1.6×10^{13} DNA copies/mL (Table 3.5). Considering some loss of the particles due to centrifugation and the filtration prior to coupling, these samples contained ~1 DNA tag/particle on average. Both the qPCR data and the results of the agarose gel electrophoresis (Figure 3.3) suggest that 4,800 ng of DNA added to nanoparticles was sufficient, therefore, this DNA amount was used for labelling nanoparticles henceforth.

Table 3.5 DNA concentration of the silica nanoparticles labelled with various amount of DNA (Batch 1), determined by qPCR. The concentration of the original nanoparticle solution was 7×10^{13} particle/mL, according to data from the manufacturer (Micromod Partikeltechnologie GmbH, Germany).

Sample name	DNA added to 250 µl of nanoparticles ng	DNA concentration determined by qPCR DNA copies/mL
SiNP+1600	1,600	5.0×10^{11}
SiNP+3200	3,200	3.0×10^{12}
SiNP+4800	4,800	1.6×10^{13}
SiNP+6400	6,400	1.8×10^{13}
SiNP+8000	8,000	9.1×10^{12}
SiNP+9600	9,600	1.5×10^{13}
SiNP+11200	11,200	8.6×10^{12}
SiNP+12800	12,800	1.2×10^{13}
SiNP+14400	14,400	2.2×10^{13}

To address the reproducibility of the DNA labelling, the labelling process used for sample SiNP+4800 was repeated five times (DNA-SiNP-1 to DNA-SiNP-5, Batch 2), and the DNA was quantified by qPCR. The qPCR results indicated that the DNA concentration was 1.2×10^{13} – 2.1×10^{13} DNA copies/mL, thus the DNA-labelling was determined to be reproducible (Table 3.6).

Table 3.6 Reproducibility of the DNA labelling of the nanoparticles. All samples were labelled with 4,800 ng DNA/250 µL nanoparticles (Batch 2). The concentration of the original nanoparticle solution was 7×10^{13} particle/mL, according to data from the manufacturer (Micromod Partikeltechnologie GmbH, Germany).

Sample name	DNA added to 250 µl of nanoparticles ng	DNA concentration DNA copies/mL
DNA-SiNP-1	4,800	1.2×10^{13}
DNA-SiNP-2	4,800	1.4×10^{13}
DNA-SiNP-3	4,800	2.1×10^{13}
DNA-SiNP-4	4,800	1.2×10^{13}
DNA-SiNP-5	4,800	1.4×10^{13}

One of the DNA-labelled particle samples was used to explore whether the binding to the silica nanoparticles affected the accuracy of the qPCR analysis. Therefore, the sample was digested by *Bam*HI restriction endonuclease, which cleaved the DNA tag from the nanoparticle. The qPCR on samples before and after the enzymatic treatment were similar (Table 3.7). Thus, the presence of silica nanoparticles had not affected the efficacy of the qPCR, and the DNA-labelled samples can be analysed by qPCR directly.

Table 3.7 DNA concentration of the not treated and the *Bam*HI endonuclease treated DNA-labelled nanoparticles.

Sample name	No treatment DNA copies/µL	***Bam*HI treatment DNA copies/µL**
DNA-SiNP+4800	8.66×10^{4}	7.60×10^{4}
DNA-SiNP+4800	4.72×10^{4}	4.90×10^{4}

The dilution series of the protein-coated samples (Batch 3) were also analysed by qPCR (Table 3.8). Samples in this batch contained the protein-coated-DNA-labelled samples, the only DNA-labelled particles and unmodified, carboxylated particles as a negative control. Sample DNA-StrNP contained streptavidin-coated nanoparticles (Micromod

Partikeltechnologie GmbH; Table 3.1), which were DNA-labelled only. The DNA concentration of the samples varied between 9.8×10^{12} and 3.4×10^{13} DNA copies/mL. The DNA concentration for most of the samples was in the same order of magnitude as observed for the DNA-SiNPs, suggesting that the proteins had no effect on the qPCR reaction. The negative control (SiNP) contained no DNA, thus the cross-contamination during the covalent coupling was negligible. Overall, the protein coating had little observable effect on the number of DNA-tags bound to the nanoparticles. Based on the qPCR results and the nanoparticles concentration it was estimated that the surface-modified nanoparticles had approximately one DNA tag/nanoparticle.

Table 3.8 Concentration of surface-modified nanoparticles (Batch 3) determined by qPCR. The concentration of the original nanoparticle solution was $7x10^{13}$ particles/mL, except for the DNA-StrNP ($2.4x10^{13}$ particles/mL), according to data from the manufacturer (Micromod Partikeltechnologie GmbH, Germany).

Sample name	DNA added to 250 µl of SiNPs	Protein added to 250 µl of SiNPs	DNA concentration
Gly-DNA-SiNP	4,800 ng	α1-Acid-Glycoprotein, 75 µg	2.4×10^{13} DNA copies/mL
Str-DNA-SiNP	4,800 ng	Streptavidin, 125 µg	3.4×10^{13} DNA copies/mL
PrA-DNA-SiNP	4,800 ng	Protein A, 125 µg	9.8×10^{12} DNA copies/mL
AMBP-DNA-SiNP	4,800 ng	AMBH, 41.5 µg	2.9×10^{13} DNA copies/mL
Cas(5)-DNA-SiNP	4,800 ng	αS1- Casein, 5 µg	1.2×10^{13} DNA copies/mL
Cas(50)-DNA-SiNP	4,800 ng	αS1- Casein, 50 µg	1.6×10^{13} DNA copies/mL
Cas(50)-DNA-SiNP'	4,800 ng	αS1- Casein, 50 µg	1.2×10^{13} DNA copies/mL
Cas(500)-DNA-SiNP	4,800 ng	αS1- Casein, 500 µg	1.8×10^{13} DNA copies/mL
Cas(2000)-DNA-SiNP	4,800 ng	αS1- Casein, 2,000 µg	3.0×10^{13} DNA copies/mL
DNA-StrNP	4,800 ng	none	1.1×10^{13} DNA copies/mL
DNA-SiNP	4,800 ng	none	1.7×10^{13} DNA copies/mL
SiNP	0 ng	none	–

In order to assess whether the DNA bound to the nanoparticles degraded over time, the DNA concentration of the samples was re-analysed by qPCR one year after preparation. The DNA concentration of all samples was similar after one year to the concentration observed 24 days after preparation (Table 3.9). The difference in concentrations for the same types of nanoparticles in some cases was probably due to sample variation, as the solutions (10,000 times diluted) analysed were freshly prepared before each qPCR.

In comparison, the concentration of the purified rotavirus and adenovirus characterised in Chapter 2 is 10^{11} gc/mL, which is two orders of magnitude lower than the concentration of the nanoparticles. The DNA-labelled-protein-coated nanoparticles were found to be stable in concentration for at least one year when stored at 4°C, whereas the DNA-labelled only nanoparticles showed slight DNA degradation 3 – 4 months after preparation. In contrast, the concentration of the virus stocks reduced by 1 $\log_{10}$ in 6 – 9 months, even when stored at –80°C.

Table 3.9 The DNA concentration of the surface-modified nanoparticles (Batch 3) 24 days and one year after labelling/coating.

Sample name **10,000 times diluted**	**Day 24** **DNA copies/µL**	**Day 365** **DNA copies/µL**
Gly-DNA-SiNP	1.50×10^{6}	2.09×10^{6}
Str-DNA-SiNP	1.21×10^{6}	9.89×10^{5}
PrA-DNA-SiNP	6.35×10^{5}	4.44×10^{5}
AMBP-DNA-SiNP	2.78×10^{5}	1.86×10^{5}
Cas(5)-DNA-SiNP	1.01×10^{6}	7.30×10^{5}
Cas(50)-DNA-SiNP	2.78×10^{5}	1.86×10^{5}
Cas(50)-DNA-SiNP'	3.23×10^{5}	3.79×10^{5}
Cas(500)-DNA-SiNP	2.08×10^{6}	2.40×10^{6}
Cas(2000)-DNA-SiNP	4.63×10^{5}	2.36×10^{5}
DNA-StrNP	5.17×10^{5}	4.35×10^{5}
DNA-SiNP	1.25×10^{6}	8.66×10^{5}

3.3.3 Hydrophobicity of the proteins and the nanoparticles

The theoretical hydrophobicity of the proteins based on their amino acid content was determined using the Protein/Peptide Property Calculator (http://lifetein.com/peptide-analysis-tool.html). The calculated hydrophobicity values (HVs) of proteins are summarised in Table 3.10. All proteins had low HV (< 22), especially protein A (4.52), thus all proteins were considered rather hydrophilic based on their amino acid content. Nonetheless, casein is poorly soluble in water, which imply that the interaction between the amino acids of the protein also affect the overall hydrophobicity.

Table 3.10 Hydrophobicity of the proteins. HV: the hydrophobicity of amino acid at pH 6.8 divided by the number of amino acids. (See the hydrophobicity scores of amino acids: Appendix I.)

Protein	HV at pH 6.8
α_1-Acid-Glycoprotein	21.51
Streptavidin	20.99
Protein A	4.52
α-Casein	19.44
AMBP	21.44

Results of the hydrophobicity assay (modified MATH test) for the nanoparticles are summarised in Table 3.11. Silica is a hydrophilic material, and the DNA labelling alone did not affect this characteristic of the nanoparticles. In contrast, the coating with some of the proteins made considerable changes in the hydrophobicity of the nanoparticles. As a result of the protein-coating, the streptavidin- and glycoprotein-coated particles were rather hydrophobic (H% > 50%), even though these proteins are soluble in water (Table 3.3). The AMBP-, protein A- and casein-coated particles remained more hydrophilic (H% < 50%). A possible explanation for the low hydrophobicity of the casein-coated nanoparticles is that some of the hydrophobic amino acids (e.g. methionine, valine and leucine) of the casein are incorporated in the covalent bond to the silica nanoparticles, therefore, casein-coated nanoparticles may not interact with a hydrophobic material. A similar phenomenon would explain the high hydrophobicity of the glycoprotein/ and protein A-coated nanoparticles.

As for the viruses, little correlation between the calculated HVs for the proteins and the H% of the protein-coated nanoparticles was observed. The calculated HV of the protein A was extremely low, while the protein A-coated nanoparticles were moderately hydrophilic. The AMBP and the glycoprotein had the highest HV, whereas the AMBP-coated nanoparticles were hydrophilic. These results further verify the importance of the secondary/tertiary structure of the proteins and the protein interactions in the overall hydrophobicity of a particle.

Table 3.11 Hydrophobicity of nanoparticles determined by modified MATH assay.

	DNA-SiNP	Gly-DNA-SiNP	Str-DNA-SiNP	PrA-DNA-SiNP	Cas(50)-DNA-SiNP	AMBP-DNA-SiNP
Control 1 (DNA copies/µL)	3.37×10^5	1.67×10^5	9.47×10^4	2.68×10^5	3.64×10^5	1.33×10^5
Control 2 (DNA copies/µL)	3.82×10^5	1.67×10^5	1.90×10^5	2.56×10^5	2.76×10^5	1.24×10^5
Average (DNA copies/µL)	3.59×10^5	1.67×10^5	1.42×10^5	2.62×10^5	3.20×10^5	1.29×10^5
Sample 1 (DNA copies/µL)	3.58×10^5	1.94×10^4	7.46×10^4	1.96×10^5	1.62×10^5	1.13×10^5
Sample 2 (DNA copies/µL)	5.12×10^5	3.98×10^4	8.67×10^4	1.90×10^5	2.02×10^5	9.71×10^5
Sample 3 (DNA copies/µL)	3.34×10^5	6.23×10^4	3.31×10^4	2.09×10^5	2.73×10^5	1.06×10^5
Average (DNA copies/µL)	4.02×10^5	4.05×10^4	6.48×10^4	1.98×10^5	2.12×10^5	1.06×10^5
H%	**0.00%**	**75.78%**	**54.45%**	**24.41%**	**33.64%**	**18.00%**

Based on the H% values (where high percentage indicates high hydrophobicity) determined by the modified MATH test for the nanoparticles and viruses (described in Chapter 2), the order of hydrophobicity is: MS2 (98.26%) > adenovirus (H% 88.93%) > Gly-DNA-SiNP (75.78%) > Str-DNA-SiNP (54.45%) > rotavirus (H% 42.49%) > Cas-DNA-SiNP (33.64%) > PrA-DNA-SiNP (24.41%) > AMBP-DNA-SiNP (18.00%) > DNA-SiNP (0%).

3.3.4 Size and zeta potential measurements

The results of ZP measurements of the proteins used for particle-coating and the 2 mM NaCl solution are summarised in Table 3.12. The NaCl solution had little negative charge and was considered as zero. Overall the proteins, like the viruses, were negatively charged in low ionic strength solution at neutral pH. The ZP of the proteins varied between –24.2 and –40.5 mV. It was expected that proteins with low pI value would be more negatively charged than the proteins with higher pI (~5) at pH 7, but no such correlation was observed.

The results of size and ZP determination of the nanoparticles are summarised in Table 3.13. The PdI of all size measurements were below 0.3, indicating that the solutions were monodisperse. The average of the measurements for 11 samples showed the average size of the unmodified silica nanoparticles was 68.5 nm. The results of both size and ZP values

(–36.5 mV) were very similar to the data provided by the manufacturer of the particles (66.9 nm and –39.3 mV).

Table 3.12 Zeta potential (ZP) and isoelectric point (pI) of proteins. *Theoretical value.

	pI	**ZP** **mV**
α1-Acid-Glycoprotein	2.7	–28.5 (±6.0)
Protein-A	*5.16	–34.8 (±4.6)
AMBP	*4.5	–27.7 (±0.5)
Streptavidin	*5	–24.2 (±1.2)
α-Casein	4.42	–40.5 (±4.4)
2 mM NaCl pH 7	–	–1.8 (±0.3)

Table 3.13 Size and zeta potential (ZP) of nanoparticles. N: number of samples measured. Measurements were performed at University of Otago. *Data is provided by Micromod Partikeltechnologie GmbH.

	N	**Size** **nm**	**PdI**	**ZP** **mV**
SiNP*	2	66.9 (±1.9)	< 0.2	–39.3 (±1.6)
StrNP*	1	100.0	< 0.2	–40.5
SiNP	11	68.5 (±4.9)	0.09 (±0.06)	–36.5 (±7.6)
DNA-SiNP	4	71.3 (±10.2)	0.16 (±0.06)	–40.9 (±3.5)
Gly-DNA-SiNP	1	68.1	0.17	–41.1
PrA-DNA-SiNP	1	89.6	0.21	–40.3
AMBP-DNA-SiNP	1	81.8	0.23	–41.3
Str-DNA-SiNP	1	88.4	0.18	–43.7
DNA-StrNP	1	173.5	0.20	–41.9
Cas(5)-DNA-SiNP	1	111.1	0.27	–40.2
Cas(50)-DNA-SiNP	1	122.1	0.25	–39.8
Cas(50)-DNA-SiNP'	1	74.6	0.21	–39.6
Cas(500)-DNA-SiNP	1	83.9	0.18	–38.2
Cas(2000)-DNA-SiNP	1	118.9	0.26	–40.1

Results of measurements on the DNA-labelled particles suggest that size was hardly affected by labelling. The measured size for most protein-coated nanoparticle samples was slightly larger. However, the larger size could be attributed to aggregation of the nanoparticles rather than changes in particle size due to protein-coating. Considerable difference in the size of the two types of streptavidin-coated particles was observed, suggesting that the particles coated with streptavidin before DNA-labelling (DNA-StrSiNP) tend to aggregate (d = 173.5 nm), while no considerable aggregation was found in samples that were DNA-labelled and streptavidin-coated in one step (Str-DNA-SiNP; d = 88.4 nm). The ZP of the unmodified, DNA-labelled and protein-coated nanoparticles were also similar (–36.5 mV to –43.7 mV), as the initial charges of the nanoparticles, the DNA and the proteins were not substantially different from each other.

The size and surface charge of the nanoparticles are similar to the size and charge of the rotavirus (78.5 nm, –24.4 mV) and adenovirus (73.7 nm, –20.8 mV) characterised in Chapter 2, however, the nanoparticles are slightly more negatively charged. Due to the aggregation of the virus particles, the virus samples were filtered before the Zetasizer measurement, which prolong the time of sample preparation and will result in virus loss. On the other hand, a vigorous shake usually created monodisperse nanoparticle solution.

3.3.5 Aggregation of the nanoparticles

The stability of the nanoparticles over time was monitored for one year. The size and the ZP of the nanoparticles were measured 12, 221 and 365 days after preparation (Table 3.14). Results suggested that the glycoprotein-, protein A- and AMBP-coated particles showed little aggregation. Their size and ZP showed little variation in one year. The streptavidin-coated particles, where the protein-coating and the DNA-labelling was performed in one step (Str-DNA-SiNP), were also stable over time. Contradictory, the nanoparticles where the streptavidin coating was performed prior to DNA-labelling (DNA-StrNP) showed some aggregation. The size of some of the casein coated particles was also elevated, however, the degree of aggregation reduced after one year. This phenomenon indicates that casein-coated particles readily form aggregates, but the aggregation can be reduced by a vigorous shake.

The size of the DNA-labelled nanoparticles was also stable over the one year (Table 3.14). Interestingly, these particles became less negatively charged after 221 days of incubation (ZP = –19 mV), and remained at that level. This phenomenon can be a result of DNA degradation

over time, which would correlate with the agarose gel electrophoresis results. However, the qPCR results for these samples indicated no meaningful decrease in concentration of the DNA-tag. These findings suggest that over time some proportion of the DNA marker, which was not covalently bound to the nanoparticles, probably detached from the surface of the nanoparticles. Thus, they were detected by qPCR, but altered the results of the gel electrophoresis and the ZP measurements.

Table 3.14 Aggregation of the surface-modified nanoparticles. n.m.: not measured.

Sample	Day 12		Day 221		Day 365	
	diameter (nm)	**ZP (mV)**	**diameter (nm)**	**ZP (mV)**	**diameter (nm)**	**ZP (mV)**
Gly-DNA-SiNP	68.1 (±2.9)	–41.1 (±1.0)	63.6 (±2.2)	–40.7 (±1.0)	66.4 (±1.0)	–39.5 (±1.1)
PrA-DNA-SiNP	89.6 (±1.6)	–40.3 (±0.2)	89.7 (±0.6)	–41.5 (±0.8)	83.8 (±0.7)	–41.4 (±1.6)
AMBP-DNA-SiNP	81.8 (±7.2)	–41.3 (±3.0)	68.5 (±0.2)	–39.0 (±0.6)	63.0 (±0.0)	–42.8 (±0.7)
Str-DNA-SiNP	88.4 (±0.4)	–43.7 (±0.6)	86.4 (±7.9)	–42.5 (±0.7)	91.8 (±1.6)	–39.8 (±0.5)
DNA-StrSiNP	173.5 (±3.5)	–41.9 (±0.8)	152.4 (±1.3)	–38.9 (±1.0)	143.2 (±0.3)	–39.3 (±0.3)
Cas(5)-DNA-SiNP	111.1 (±6.6)	–40.2 (±1.5)	n.m.	n.m.	65.8 (±1.2)	–37.6 (±0.6)
Cas(50)-DNA-SiNP	122.1 (±3.1)	–39.8 (±2.0)	63.9 (±0.5)	–41.7 (±1.4)	62.8 (±0.2)	–37.0 (±1.0)
Cas(50)-DNA-SiNP'	74.6 (±1.7)	–39.6 (±0.7)	n.m.	n.m.	76.5 (±0.1)	–36.0 (±0.7)
Cas(500)-DNA-SiNP	83.9 (±0.5)	–38.2 (±1.3)	n.m.	n.m.	88.7 (±0.3)	–37.4 (±0.9)
Cas(2000)-DNA-SiNP	118.9 (±1.8)	–40.1 (±1.0)	n.m.	n.m.	93.6 (±0.5)	–41.0 (±1.7)
DNA-SiNP	69.8 (±2.4)	–38.9 (±0.6)	63.4 (±0.8)	–18.9 (±1.5)	73.0 (±2.2)	–20.0 (±2.3)

Overall findings suggest that the silica nanoparticles are more stable over time than the rotavirus and the adenovirus. As described in Chapter 2 the rotavirus was stable in size and charge for two months, and the adenovirus started to aggregate after two weeks, when

samples were stored at room temperature. The adenovirus samples stored at 4°C (similarly to the nanoparticles) aggregated in one day.

3.4 Conclusions

The two-step EDC method used for particle labelling and coating is a suitable tool for producing high concentrations of DNA-labelled and protein-coated silica nanoparticles. The DNA and the selected proteins were immobilised on the surface of the nanoparticles via covalent bond, thus the DNA-labelling and protein-coating was stable over time. The proteins on the surface of the nanoparticles protected the DNA tag from degradation. The particles can be produced in high quantities and concentrations, and can be stored at 4°C. Unlike microbes and viruses, these nanoparticles have little health and safety concerns. The protein-coated nanoparticles were more stable over time at 4°C than the viruses stored at –80°C.

The size and the surface charge of the nanoparticles were slightly affected by the surface modifications. The DNA-labelling strengthened the surface charge, while the protein-coating altered the hydrophobicity of the silica nanoparticles. The modified silica nanoparticles mimic the size, shape, density and surface charge of the rotavirus and adenovirus. Most of the nanoparticles were less hydrophobic than the two enteric viruses. Therefore, the particles are presumably more inert in the groundwater than the viruses as they less readily interact with hydrophobic materials found in the groundwater. These findings suggest that the modified nanoparticles are promising candidates for virus surrogates in environmental studies.

Chapter 4.
Virus and DNA degradation in simulated groundwater

4.1 Introduction

Emerging from human and animal effluent, viruses are transported to surface water, soil and deep groundwater. Viruses can contaminate sediment invertebrates and, through irrigation using effluent, viruses contaminate the surfaces of crops for human and animal consumption. Enteric viruses have been shown to persist in the environment over time, especially in groundwater due to the low temperature, absence of light, fewer microbial populations, mostly near-neutral pH and low ionic strength (Bosch *et al.*, 1997; Callahan *et al.*, 1995; Espinosa *et al.*, 2008; Ogorzaly *et al.*, 2010; Straub *et al.*, 1993).

Adenoviruses are found to be remarkably persistence in groundwater (Charles *et al.*, 2009; Ogorzaly *et al.*, 2010). No long-term (> one year) studies have been reported on rotavirus inactivation in groundwater, however, some results suggest that it is almost as stable as adenovirus (Sidhu *et al.*, 2010). Adenoviruses, especially type 40 and 41, have been found to be extremely resistant to sunlight and UV irradiation (Hijnen *et al.*, 2006). Therefore, adenoviruses can persist in surface water, on plant surfaces and remain infectious during water treatment ultimately playing a significant role in both foodborne and waterborne diseases. A possible mechanism of the persistence is the aggregation of the virus particles. Rotavirus and adenovirus have been shown to form aggregates in 2 mM NaCl pH 7 solution over time (described in Chapter 2), and in the presence of bivalent cations (Gutierrez *et al.*, 2010; Wong *et al.*, 2013). Virus aggregation is likely to provide protection to the virus particles in the core of the aggregate.

Conversely, the aggregation also alters the results of the laboratory studies. During culturing-based quantification assays the aggregates, containing numerous particles, only form one plaque/focus/cytopathic unit, thus the number of infectious particles is often underestimated.

The genomes of the viruses degrade at lower rates than those of infectious particles (Charles *et al.*, 2009; Espinosa *et al.*, 2008; Ogorzaly *et al.*, 2010). Hence, amplification-based methods alone are not suitable for viral quantification of environmental samples, as these techniques are able to detect the RNA/DNA from both infectious and degraded virus particles. Integrated cell culturing and RT-qPCR methods (ICC-RT-qPCR) have been shown to be a reliable and sensitive option to determine the quantity of infectious virions (Fongaro *et al.*, 2013; Ko *et al.*, 2005; Li *et al.*, 2010). However, these methods still involve the tissue culturing of the viruses, which is an elaborate process, requiring special equipment, trained personnel and not suitable for viruses that cannot be cultured *in vitro*.

Viancelli *et al.* (2012) combined the qPCR with enzymatic (DNase) treatment for accurate detection of intact adenovirus particles. This method has been found to be suitable to assess the effects of high hydrostatic pressure (Kovač *et al.*, 2012) and chlorination (de Abreu Corrêa *et al.*, 2012) on adenovirus. The method showed good correlation with the results of ICC-RT-qPCR used for detecting adenoviruses in surface water samples (Fongaro *et al.*, 2013). The enzymatic technique can be a promising substitute for culture-based detection for viruses that are hard to maintain *in vitro*.

Due to the challenges with working with enteric viruses, bacteriophages have been widely used to study virus inactivation in groundwater. At temperatures higher than 10°C the F-specific bacteriophages (such as MS2) have been found to degrade at higher rates than enteric viruses (Ogorzaly *et al.*, 2010). This brings into question whether MS2 is suitable for predicting virus inactivation in the New Zealand setting, where the average temperature of groundwater is 13.4°C with 90% of measurements between 10.8 and 18.3°C (New Zealand Ministry for the Environment, 2013).

In this study, the persistence of the adenovirus and rotavirus was examined in simulated groundwater for 1.5 and one year, respectively. Due to the difficulties with culturing, the numbers of intact particles were monitored using DNase treatment or filtration followed by qPCR for adenovirus and qRT-PCR for rotavirus. The effect of light on persistence of the viruses was also studied. The presence of viral surface antigens was confirmed by enzyme-linked immunosorbent assay (ELISA) regularly. The DNA degradation of plasmid DNA and the proposed virus surrogate, (the DNA-labelled silica nanoparticles; DNA-SiNP) were followed under similar conditions as the viruses for two and 1.5 years, respectively, and compared with virus degradation.

4.2 Methods and materials

4.2.1 Experimental setup

The stability of plasmid DNA used to label the nanoparticles, the DNA-SiNP, the rotavirus and the adenovirus were examined. The viruses were purified prior to the experiments as described in Chapter 2.

In order to explore virus and DNA degradation in groundwater, three types of solutions were used. A 2 mM NaCl pH 7 solution, which has similar ionic strength and pH as the groundwater of Christchurch, New Zealand, and the solutions of two natural aquifer media, i.e. fine beach sand and fine gravel (see Appendix III for details). The solutions of the aquifer media were prepared by mixing with 2 mM NaCl pH 7 solution and agitating overnight. The solutions were separated from the solid material and filtered through 0.22 μm filters. Using this treatment the adsorption of the viruses and the DNA to the aquifer media was avoided, and the effects of the soluble content of the aquifer media on the DNA and virus degradation could be examined.

The three solutions were inoculated with the plasmid and the DNA-SiNP at four concentrations (C_0 = 10^8, 10^7, 10^6 and 10^5 DNA copies/mL) and with the viruses at two concentrations (C_0 = 10^8 and 10^7 gc/mL). In order to eliminate the unbound DNA from the DNA-SiNP stock, the DNA-SiNPs were pelleted by centrifugation at 13,000×g for 20 min and resuspended in 2 mM NaCl solution prior to sample preparation. Negative controls with solutions only (without plasmid, DNA-SiNP or virus) were also set up. The samples in the 2 mM NaCl solutions were divided into two: one set of the tubes was exposed to light, by storing the tubes wrapped in plastic bags on the bench of the laboratory. A set was stored in dark, together with the rest of the samples. All stocks were stored at room temperature. The degradation of the rotavirus was monitored for one year, the degradation of the adenovirus and the DNA-SiNP for 1.5 years and the plasmid degradation was examined for 2 years. Each sample set was sampled on day 0, then weekly for two months, fortnightly for another four months, and monthly for six months. After one year, the adenovirus, the DNA-SiNP and the plasmid stocks were sampled in every three months until the end of the experiment.

4.2.2 Detection and quantification

Each time 50 µL of the rota- and adenovirus-containing stocks were sampled. To detect intact virus particles only, the adenovirus samples were treated with DNase and analysed by the qPCR method described in Chapter 2. For the same reason the rotavirus samples were filtered through 100 kDa filter units and analysed by single-step qRT-PCR, as described in Chapter 2. Samples containing the plasmid DNA and the DNA-SiNP were analysed directly by the qPCR method with the internal primer pair, as described in Chapter 3, using a Rotor-Gene Q qPCR system (Qiagen, Netherlands).

The presence of intact virus antigens in the samples was detected by commercially available ELISA kits (Cortez Diagnostics, USA). The Rotavirus ELISA Kit detects the VP6 protein of the capsid, and the Adenovirus ELISA Kit is sensitive to the hexon protein. Aliquots of 50 – 100 µL of the samples with initial concentration (C_0) of 10^8 gc/mL were analysed as described in Chapter 2. Absorbance readings above 0.15 optical density (OD) at 450 nm were considered as positive.

After one year the negative controls of the rotavirus degradation study were tested for bacterial growth by the ESR Public Health Laboratory (New Zealand). The samples (1 mL each) were enriched in brain heart infusion at 25°C and 35°C for five days. The broths were then subcultured to blood and McConkey agar plates and incubated at 25°C and 35°C for two days.

4.2.3. Determination of degradation rates

Assuming degradation rate follows a first-order law it can be expressed as:

$$C_t = C_0 exp[-\lambda(t - t_0)]$$

where C_t is the concentration measured as gc/mL or DNA copies/mL at time t, C_0 is the initial concentration, λ is the first order degradation rate, t is time, t_0 is initial time and exp is exponential function.

The first order degradation rate (ln/day) for samples with C_0 of 10^8 10^7 gc/mL or DNA copies/mL was optimised using the Solver tool in Microsoft Excel. For all particles the results of the first year were used. The logarithmic degradation rates (log_{10}/day) were calculated by

dividing the rate by 2.303. The r^2 values for the exponential fit were also calculated using the Data Analysis tool in Microsoft Excel.

4.3 Results

4.3.1 Rotavirus degradation

Figure 4.1 summarises the rotavirus degradation over one year. The overall reduction was between 1 and 4 $\log_{10}$. The virus degradation in samples with different C_0 was similar. The samples stored in the 2 mM NaCl solution, in dark and the samples stored in the solutions of the two aquifer media reduced by 1 – 2 $\log_{10}$, whereas the samples exposed to light reached 3 – 4 $\log_{10}$ reduction, suggesting that the light enhanced the virus degradation.

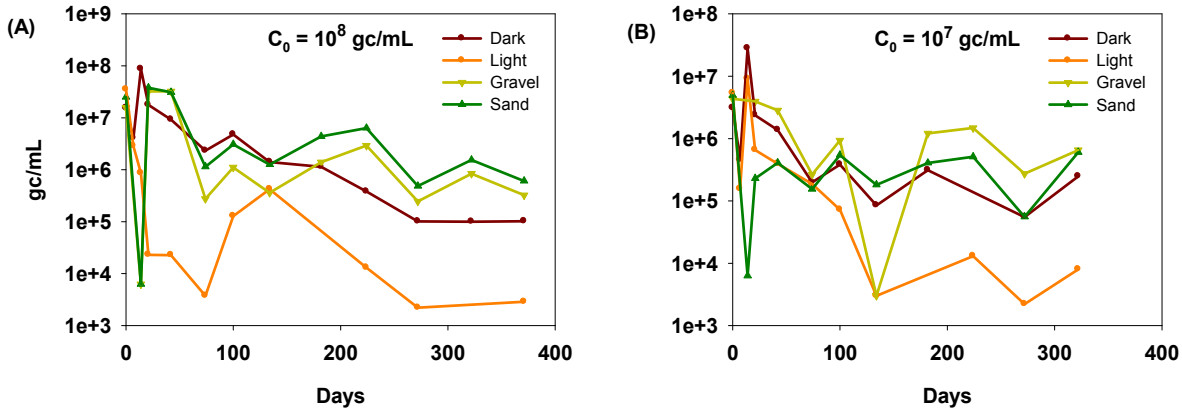

Figure 4.1 Rotavirus degradation of samples stored in 2 mM NaCl solution, in dark (brown lines), exposed to light (orange lines), in gravel solution (yellow lines) and in beach sand solution (green lines) with initial concentration (C_0) of (A) 10^8 gc/mL and (B) 10^7 gc/mL.

The degradation rates also indicated low reduction of concentration (Table 4.1). Elevated degradation rates were observed in the samples exposed to light (0.153 $\log_{10}$/day and 0.012 $\log_{10}$/day) and in the sample with C_0 of 10^7 gc/mL, incubated in the beach sand solution (0.060 $\log_{10}$/day). In contrast, the degradation rates of all the other samples were 0.003 – 0.006 $\log_{10}$/day.

Together with the virus-containing samples the negative controls were also analysed for rotavirus RNA to eliminate the possibility of cross-contamination. No RNA was detected in the negative controls over the 1-year experiment.

Table 4.1 Degradation rates of the rotavirus samples with two initial concentrations (C_0) based on the results of the 1-year experiment.

	$C_0 = 10^8$ gc/mL		$C_0 = 10^7$ gc/mL	
	Degradation rate log_{10}/day	**r^2**	**Degradation rate log_{10}/day**	**r^2**
2 mM NaCl, dark	0.003	0.839	0.003	0.639
2 mM NaCl, light	0.153	0.775	0.012	0.640
Gravel solution	0.004	0.818	0.006	0.579
Beach sand solution	0.004	0.423	0.060	0.898

The presence of the VP6 protein was verified by ELISA assay (Table 4.2) in the samples collected at the start of the experiment. Of all the samples collected through the experiment, only the sample incubated in the 2 mM NaCl solution for three months in dark was considered as positive. This sample had the highest gc concentration as well. Some other samples also showed elevated OD values compared to the negative control, but none of them reached the OD = 0.15, thus they were considered as negative. These findings suggest that the concentration of the samples was too low to detect by the ELISA assay.

Table 4.2 The OD values of the ELISA test for rotavirus samples. The sample volumes (50 – 100 µL) are shown in brackets. Samples with OD > 0.15 were considered as positive (+).

	Start (50 µL)	**3 months (50 µL)**	**6 months (50 µL)**	**9 months (50 µL)**	**12 months (100 µL)**
2 mM NaCl, dark	0.361 (+)	0.739 (+)	0.093 (–)	0.099 (–)	0.091 (–)
2 mM NaCl, light	-	0.095 (–)	0.092 (–)	0.093 (–)	0.099 (–)
Gravel solution	-	0.091 (–)	0.094 (–)	0.091 (–)	0.103 (–)
Beach sand solution	-	0.094 (–)	0.099 (–)	0.090 (–)	0.091 (–)

The negative controls were tested for bacteria growth after one year of incubation. Pure growth of a rod shaped bacteria was found in the beach sand solution but not in gravel solution and in the 2 mM NaCl solutions.

4.3.2 Adenovirus degradation

Figure 4.2 displays adenovirus degradation observed over 1.5 years, which showed similar trends as the rotavirus samples. An initial 5 – 10 times drop in virus concentration was observed in all samples during the first week of the experiment, presumably due to adsorption to the inner wall of the plastic tube used for storing the samples. After that the virus degradation was nearly exponential in all samples in both concentrations ($C_0 = 10^8$ and 10^7 gc/mL), resulting in 1 – 3 $\log_{10}$ reductions over 1.5 years. The virus stored in dark in 2 mM NaCl solution was the most stable, followed by the viruses incubated in the beach sand solution. Little difference in virus degradation in the gravel solution and in the samples exposed to light was observed in samples with $C_0 = 10^7$ gc/mL, whereas the degradation of the more concentrated samples incubated in gravel solution was more elevated. The last set of samples collected after 18 months had higher concentrations than the previously collected samples, probably due to evaporation of the solution.

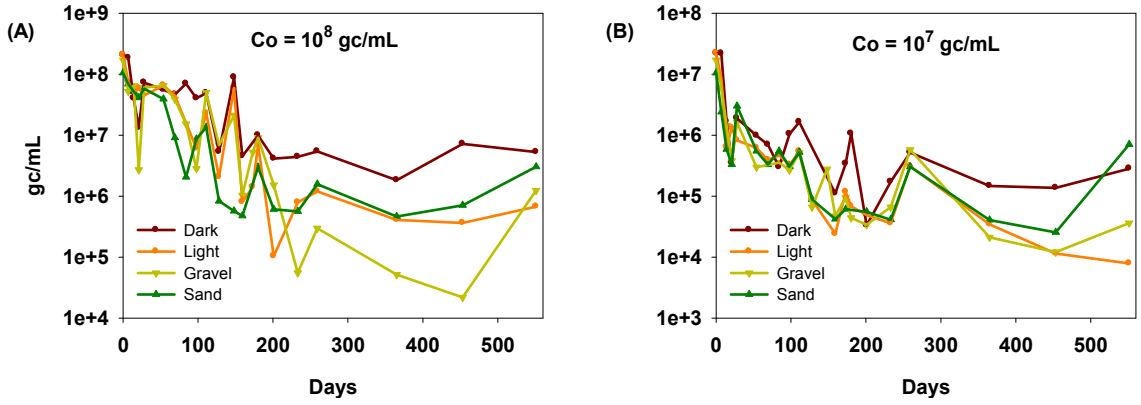

Figure 4.2 Adenovirus degradation of samples stored in 2 mM NaCl solution, in dark (brown lines), exposed to light (orange lines), in gravel solution (yellow lines) and in beach sand solution (green lines) with initial concentration (C_0) of (A) 10^8 gc/mL and (B) 10^7 gc/mL.

The degradation rates (shown in Table 4.3) based on the 1-year results suggest that the adenovirus degradation was more elevated in the diluted samples (degradation rates: 0.036 – 0.087 $\log_{10}$/day) than in the samples with C_0 of 10^8 gc/mL (degradation rates: 0.014 – 0.040 $\log_{10}$/day). Little difference was found in the degradation rates of the adenovirus samples incubated in different types of solutions.

Together with the virus-containing samples the negative controls were also analysed for virus DNA to eliminate the possibility of cross-contamination. No DNA was detected in the negative controls over the 1.5-year experiment.

The hexon protein of the adenovirus capsid was detected using ELISA (Table 4.4). The samples incubated in the 2 mM NaCl solutions were positive over 1.5 years, suggesting the presence of intact hexon proteins. The OD values decreased over time, which corroborates with the qPCR results. For the samples where the adenovirus was incubated in the gravel solution, only the sample (collected after six months of incubation) was positive. The DNA concentration of the samples incubated in gravel solution was the lowest, thus the negative ELISA readings could be attributed to the low concentration of the viruses. Of the samples incubated in the beach sand solution, only the last one was positive, where the volume of the sample was doubled. The OD of the samples collected after six and 15 months were below 0.15, but above the OD of the negative control.

Table 4.3 Degradation rates of the adenovirus with two initial concentrations (C_0) based on the first year results of the experiment.

	$C_0 = 10^8$ gc/mL		$C_0 = 10^7$ gc/mL	
	Degradation rate log_{10}/day	**r^2**	**Degradation rate log_{10}/day**	**r^2**
2 mM NaCl, dark	0.025	0.839	0.036	0.639
2 mM NaCl, light	0.038	0.775	0.067	0.640
Gravel solution	0.040	0.818	0.066	0.579
Beach sand solution	0.014	0.423	0.087	0.898

Table 4.4 The OD values of the ELISA test for adenovirus samples. The sample volumes (50 – 100µL) are shown in brackets. Samples with OD > 0.15 were considered as positive (+).

	Start (50 µL)	**6 months (50 µL)**	**12 months (50 µL)**	**15 months (50 µL)**	**18 months (100 µL)**
2 mM NaCl, dark	2.218 (+)	2.991 (+)	1.160 (+)	0.986 (+)	1.646 (+)
2 mM NaCl, light	-	2.407 (+)	0.673 (+)	0.638 (+)	0.815 (+)
Gravel solution	-	0.272 (+)	0.045 (–)	0.048 (–)	0.040 (–)
Beach sand solution	-	0.132 (–)	0.049 (–)	0.101 (–)	0.160(+)

4.3.3 Degradation of the plasmid DNA

Figure 4.3 summarises the degradation of the plasmid DNA over two years. In all samples where the plasmid was added to the solutions, the DNA concentration reduced by 1 $\log_{10}$ after a week, like in case of the adenovirus samples.

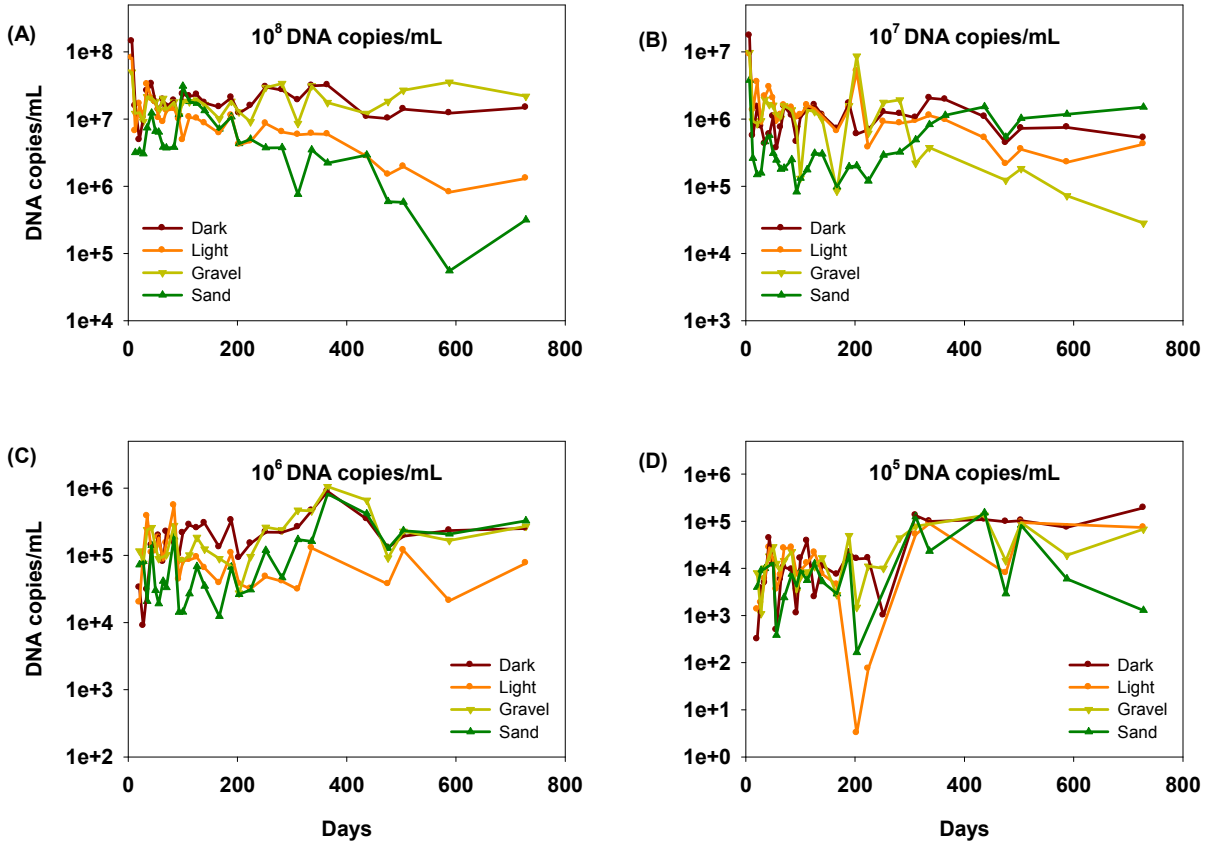

Figure 4.3 Degradation of the plasmid DNA samples stored in 2 mM NaCl solution, in dark (brown lines), exposed to light (orange lines), in gravel solution (yellow lines) and in beach sand solution (green lines) with initial concentration (C_0) of (A) 10^8 DNA copies/mL, (B) 10^7 DNA copies/mL, (C) 10^6 DNA copies/mL and (D) 10^5 DNA copies/mL.

After the initial drop in concentration, the most concentrated samples stored in the gravel solution and in the 2 mM NaCl solution, in dark showed little reduction over the 2-year experiment. The concentration of the samples with C_0 of 10^8 DNA copies/mL exposed to light and stored in the beach sand solution reduced by 1 $\log_{10}$ during the first year. After that the samples exposed to light remained stable in the second year, whereas the samples stored in the beach sand solution reduced by an additional 1 $\log_{10}$ during the second year. The

degradation rates in the first year of the experiment for the most concentrated samples varied between 0.032 – 0.055 log_{10}/day (Table 4.5).

The samples with C_0 of 10^7 DNA copies/mL showed similar reduction to the more concentrated samples. After the initial drop in concentration during the first week, less than 1 log_{10} reduction was observed in the samples incubated in 2 mM NaCl solution in dark and exposed to light. The degradation rates based on the first year results for these samples were 0.027 log_{10}/day and 0.019 log_{10}/day, respectively (Table 4.5). The sample incubated in gravel solution, was stable for one year (degradation rate: 0.034 log_{10}/day), however, great variation in the measured DNA concentration was observed. During the second year the DNA of the sample degraded by 1 log_{10} following an exponential decline. The DNA concentration in the beach sand solution remained stable for one year (degradation rate: 0.055 log_{10}/day), and then the concentration increased and reached the initial level, probably due to evaporation.

In the samples with low C_0 (10^6 and 10^5 DNA copies/mL) no degradation was observed for up to two years, instead, elevated concentrations were detected after one year. The observed elevated concentration was probably due to the evaporation of the eluent or detachment of the immobilised DNA from the wall of the tube.

Table 4.5 Degradation rates of the plasmid samples with high initial concentration (C_0) based on the first year results of the experiment.

	$C_0 = 10^8$ DNA copies/mL		**$C_0 = 10^7$ DNA copies/mL**	
	Degradation rate log_{10}/day	**r^2**	**Degradation rate log_{10}/day**	**r^2**
2 mM NaCl, dark	0.041	0.839	0.027	0.639
2 mM NaCl, light	0.032	0.775	0.019	0.640
Gravel solution	0.054	0.818	0.034	0.579
Beach sand solution	0.055	0.423	0.055	0.898

Together with the plasmid-containing samples the negative controls were also analysed for plasmid DNA to eliminate the possibility of cross-contamination. No DNA was detected in the negative controls over the 2-year experiment.

4.3.4 Degradation of the DNA-SiNP

Figure 4.4 summarises the DNA degradation of the DNA-SiNP examined over 1.5 years. An initial drop in DNA concentration was observed in some samples but this was less pronounced than for the adenovirus and plasmid samples. In the most concentrated samples ($C_0 = 10^8$ DNA copies/mL) incubated in the 2 mM NaCl solution (stored in dark and exposed to light), the DNA concentration showed no considerable reduction in 1.5 years. In contrast, the DNA concentration of the samples stored in the gravel and the beach sand solutions reduced by 2 $\log_{10}$ over the same period of time.

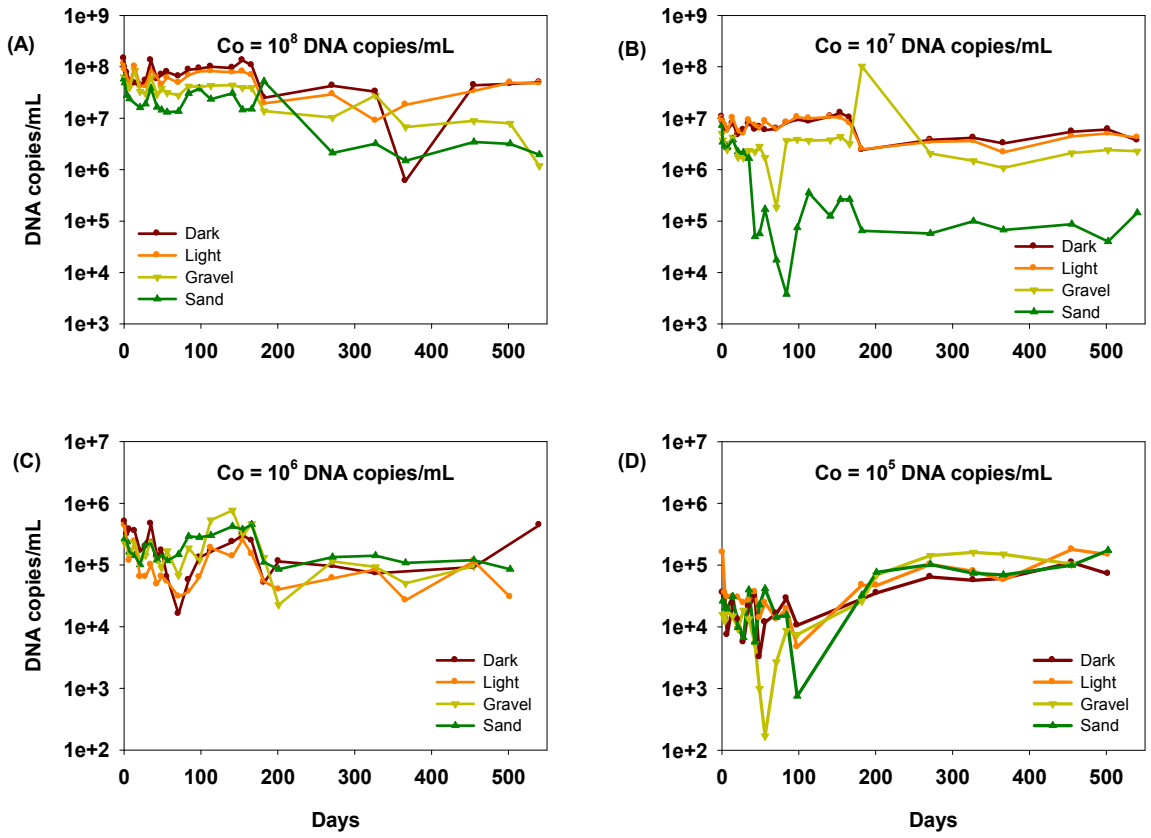

Figure 4.4 DNA degradation of the DNA-SiNP samples stored in 2 mM NaCl solution, in dark (brown lines), exposed to light (orange lines), in gravel solution (yellow lines) and in beach sand solution (green lines) with initial concentration (C_0) of: (A) 10^8 DNA copies/mL, (B) 10^7 DNA copies/mL, (C) 10^6 DNA copies/mL and (D) 10^5 DNA copies/mL.

The samples with C_0 of 10^7 and 10^6 DNA copies/mL reduced less than 1 $\log_{10}$. An exception was that the sample incubated in beach sand solution with C_0 of 10^7 DNA copies/mL showing a 2 $\log_{10}$ reduction after two months. Then little DNA loss was observed during the additional 16 months of the experiment. The most diluted samples ($C_0 = 10^5$ DNA copy/mL), similar to

the diluted plasmid DNA samples, showed elevated DNA concentrations after six months, most likely due to evaporation. The 1-year degradation rates (Table 4.6) of the samples with C_0 10^8 and 10^7 DNA copies/mL were as low as 0.001 – 0.006 $\log_{10}$/day, except the samples with C_0 of 10^7 DNA copies/mL, incubated in the beach sand solution (0.030 $\log_{10}$/day).

No DNA was found in the negative controls (tested together with the DNA-SiNP samples) over the 1.5-year experiment, suggesting no cross-contamination among the samples.

Table 4.6 Degradation rates of the DNA-SiNP samples with high initial concentration (C_0) based on the first year results of the experiment.

	$C_0 = 10^8$ DNA copies/mL		**$C_0 = 10^7$ DNA copies/mL**	
	Degradation rate $\log_{10}$/day	**r^2**	**Degradation rate $\log_{10}$/day**	**r^2**
2 mM NaCl, dark	0.003	0.839	0.002	0.639
2 mM NaCl, light	0.003	0.775	0.001	0.640
Gravel solution	0.003	0.818	0.003	0.579
Beach sand solution	0.006	0.423	0.030	0.898

4.3.5 Comparison of 1-year results

The DNA degradation of the DNA-SiNP and the degradation of the virus samples with corresponding initial concentrations were compared (Figure 4.5). The overall results showed that the DNA-SiNP was more stable over time than the viruses. Only one sample ($C_0 = 10^7$ copy DNA/mL, incubated in beach sand solution) reached similar reduction to the viruses. The degradation of the adenovirus and rotavirus samples was very similar. However, data suggested that the rotavirus was more stable over time than the adenovirus when incubated in in dark. On the other hand the reduction of rotavirus was affected by light. For the samples exposed to light in one year, rotavirus reduced by 3 – 4 $\log_{10}$, while adenovirus reduced by only 2 – 3 $\log_{10}$ similar to the adenovirus samples incubated in dark. The degradation of the plasmid and the DNA-SiNP was not affected by light.

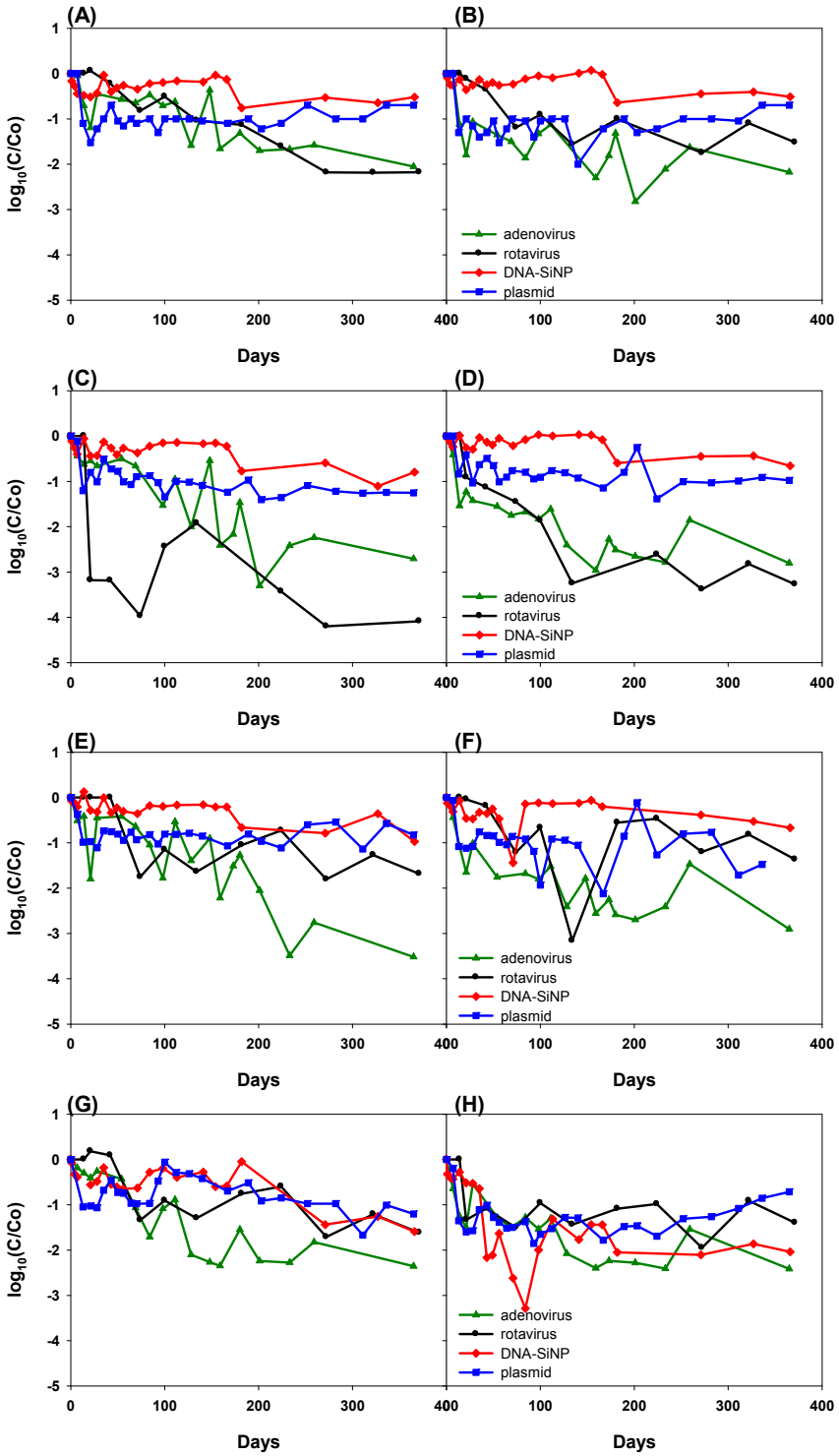

Figure 4.5 Comparison of 1-year results of the degradation of the rotavirus (black circle), adenovirus (green triangle), DNA-SiNP (red diamond) and the plasmid (blue square) in a one year experiment in 2 mM NaCl solution, incubated in dark (A and B), exposed to light (C and D), in gravel solution (E and F) and in beach sand solution (G and H). The left side graphs (A, C, E and G) show the degradation of samples with $C_0 = 10^8$ gc/mL or DNA copies/mL, and the right side graphs (B, D, F and H) show the degradation of samples with $C_0 = 10^7$ gc/mL or DNA copies/mL.

The degradation rates for the first year of the experiments were also compared (Figure 4.6). Data suggest that the plasmid degraded at a higher rate than the DNA content of the DNA-SiNP. The effect of light on the degradation of the rotavirus was also shown in the degradation rates. The degradation rates verified that the DNA-SiNP is more stable that the rotavirus, adenovirus and the plasmid DNA.

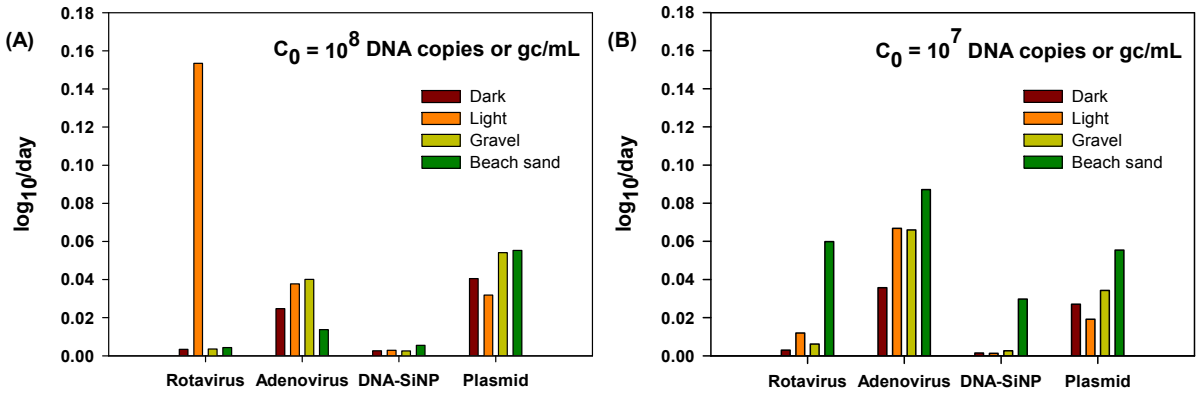

Figure 4.6 Comparison of the degradation rates (based on the first-year results) for samples stored in 2 mM NaCl solution, in dark (brown bars), exposed to light (orange bars), in gravel solution (yellow bars) and in beach sand solution (green bars) with initial concentration (C_0) of (A) 10^8 gc/mL or DNA copies/mL and (B) 10^7 gc/mL or DNA copies/mL.

4.4 Discussion

4.4.1 Virus degradation

4.4.1.1 Virus degradation in dark

Rotavirus persisted in all types of simulated groundwater incubated in dark. The 1 – 2 log_{10} reduction observed for these rotavirus samples over one year is similar to the results of previous studies measuring the loss of infectivity performed on various rotavirus strains. In filtered, thus microbe-free river water, rotavirus was stable for two months at 20°C (Raphael *et al.*, 1985) and no significant reduction was demonstrated in sterile groundwater for 200 days at 20°C (Sidhu *et al.*, 2010). These studies also highlighted that the presence of microbes enhance rotavirus inactivation. Hence, the elevated rotavirus degradation in the beach sand solution ($C_0 = 10^7$ gc/mL) was most likely due to microbial activity, as discussed in Chapter 1. The possibility of microbial contamination due to the long term storage at room temperature

and the regular sampling was addressed. Due to the infectious nature of the rotavirus, only the negative control solutions (without rotavirus) were cultured after one year of incubation. The results showed bacteria growth in the beach sand solution, therefore, it is possible that other samples were also contaminated. The chemical analysis of the gravel and beach sand solutions showed that these solutions, especially the beach sand solution, contained nutrient and ions at high concentrations, which may have enhanced microbial activity.

Previous study showed that the genome of rotavirus degraded about 1 $\log_{10}$ after seven months of incubation in groundwater at 10°C (Espinosa *et al.*, 2008). In that study the rotavirus RNA was quantified by qRT-PCR, but the free nucleic acid content was not eliminated before the analysis, therefore the genome quantification over-predicted the number of rotavirus particles. The same study revealed a rapid reduction (2 $\log_{10}$ in one month) in virus infectivity, which was most likely due to aggregation of the rotavirus particles. Thus these results probably underestimated the number of infectious virus particles.

The adenovirus degradation results showed that the adenovirus was also stable over time, however, it was slightly more amenable to degradation, especially in the gravel solution, relative to the rotavirus. The observed reductions correspond to previous findings. For example, Charles *et al.* (2009) found that adenovirus type 2 particles persisted in groundwater at 12°C for up to one year, and the adenovirus genome was detectable for 22 months. They observed a rapid 3 $\log_{10}$ reduction in infectivity during the first three weeks (most likely due to aggregation), retaining the same level for up to one year. These results correspond with the 3 $\log_{10}$ adenovirus degradation observed in the gravel solution. The adenovirus degradation of the samples incubated in dark in 2 mM NaCl solution or in beach sand solution shown in the current study corroborate with a previous results from the study by Ogorzaly *et al.* (2010) where a 2 $\log_{10}$ reduction in adenovirus type 2 infectivity was observed in groundwater at 20°C in one year.

By combining the genome quantification (qRT-PCR) with the elimination of the non-encapsidated RNA (filtration) and DNA (DNase treatment), the results of my study represents the number of intact virus particles in the samples, and the quantification was not affected by the aggregation of the viruses. The number of intact virus particles has been shown to correspond to the number of infectious viruses (Fongaro *et al.*, 2013), therefore, the results of my study indicated the potential viral infectivity.

4.4.2.2 The effect of light

The pattern of rotavirus degradation was different when the samples were exposed to light. In those samples, regardless of the initial concentration, rotavirus showed a rapid decrease over time resulting in 3 – 4 $\log_{10}$ reduction in one year. In contrast, adenovirus degradation was less affected by light. The results from previous studies also support that rotaviruses are more sensitive to sunlight, especially to UV-B irradiation, than adenoviruses. Romero *et al.* (2011) observed 1 $\log_{10}$ reduction of rotavirus samples exposed to sunlight for 0.2 hr in sodium buffer, whereas Silverman *et al.* (2013) found practically no reduction in the adenovirus type 2 spiked into coastal water samples exposed to sunlight over the similar period of time. The effects of UV radiation on rotavirus have been studied. The UV causes morphological damage in the rotavirus capsid, which lead to rotavirus degradation (Rodgers *et al.*, 1985), which was demonstrated in my study. UV radiation of rotavirus particles also results in permanent damage of the nucleic acid content mainly via the formation of uracil-dimers (Smirnov *et al.*, 1991). The presence of uracil-dimers would not necessarily affect the qRT-PCR, therefore, the effect of light on rotavirus RNA was not verified here.

Adenoviruses, especially type 40 and 41, have been found to be significantly UV resistant in the environment (Gerba *et al.*, 2002; Hijnen *et al.*, 2006; Thurston-Enriquez *et al.*, 2003). This is partly due to their dsDNA genome, which, unlike RNA viruses, uses the repair mechanisms of the host cell (Hijnen *et al.*, 2006). Previous research suggest that UV-C light results in extensive DNA damage, and sunlight may contribute to the structural damage on the capsid proteins resulting in poor attachment to the host cell (Bosshard *et al.*, 2013).

In the current study, due to health and safety reasons, the samples were stored in plastic tubes wrapped by a plastic bag indoors. Under these conditions not the full spectrum of sunlight reached the particles, thus the experiment probably underestimated the effects of sunlight in the environment.

4.4.2.3 Presence of virus antigens

In order to assess the possibility of structural damage in the viral capsids, viral antigens were tested using ELISA. The presence of the hexon protein was verified by an ELISA even after 1.5 years in all adenovirus samples except in the adenovirus incubated in the gravel solution. In that sample the hexon protein was only detected in the samples collected after six months.

The detected OD values suggested lower hexon protein concentration on the samples exposed to light than in the corresponding samples stored in dark, thus the light may affect the structure of the capsid proteins. For the rotavirus samples the ELISA was probably not sensitive enough for detection of the virus antigen, as only one sample, taken after three months of incubation, was positive. However, the antibodies used in this study are specific for intact adenoviral hexon protein and the rotavirus VP6, and give no information on the presence of the other capsid proteins responsible for binding to the host cell during infection. Therefore, it is possible that the positive results derived from the ELISA indicate non-infectious particles or disassembled capsid proteins. On the other hand, the assay is only sensitive for proteins without structural damage. As structural damage of the capsid proteins usually lead to loss of infectivity, the presence of intact proteins can be an indication of infectious viruses. Previous study also showed good correlation between ELISA-based and culturing results in an experiment on virus inactivation in wastewater and groundwater, concluding that the ELISA detected infectious viruses (Nasser *et al.*, 1995).

4.4.2 DNA degradation

In this study, it was demonstrated that the degradation of the plasmid DNA was similar to the degradation of the adenovirus. However, the plasmid degradation was similar in samples with different C_0, whereas the adenovirus degradation was enhanced in the less concentrated samples. The degradation of the plasmid was not affected by day light. In some samples (those stored in beach sand solution, one stored in gravel solution with $C_0 = 10^7$ copy DNA/mL) the DNA degradation was more rapid than in the rest of the samples probably due to microbial activity, as described for rotavirus.

The DNA-SiNP was more stable in the simulated groundwater than the adenovirus and the rotavirus. Interestingly, the DNA of the DNA-SiNP was more stable over time than the circular plasmid. The DNA concentration of the DNA-SiNP was less affected than the viruses in the NaCl solutions that were either incubated in dark or exposed to light. The soluble content of the two aquifer media had little effect on the DNA degradation. The DNA-SiNP degraded at similar rate to the viruses in only one sample (beach sand solution $C_0 = 10^7$ DNA copies/mL). In contrast, enhanced degradation was not observed in any other DNA-SiNP samples incubated in the beach sand solution. Thus the result of the beach sand solution at $C_0 = 10^7$ DNA copies/mL was probably due to nucleases produced by microbes contaminating the sample, similar to the corresponding rotavirus samples. The volume of the DNA-SiNP and

plasmid samples was too low for culturing at the end of the degradation experiment, therefore the presence of microbes in these samples could not be investigated.

Previous studies have also shown that the microbial activity is the major cause of the degradation of DNA in the environment. The enzymatic degradation of the extracellular nucleic acids produces inorganic orthophosphate, which is a crucial nutrient for living organisms. The microbes found in natural water can digest free nucleic acids in days (Romanowski *et al.*, 1992; Zhu, 2006). In contrast, in water samples where the microbes were eliminated, the DNA remained stable for weeks, and was still detectable after more prolonged times (Alvarez *et al.*, 1996; Matsui *et al.*, 2001; Zhu, 2006). These findings support the notion that the observed DNA loss in the current study can be attributed to microbial activity in the samples rather than DNA degradation caused by the physico-chemical properties of the solution.

The stability of the DNA-SiNP is due to the simple structure of the particle. Silica is also a physically and chemically inert material. The strong covalent bond between the nanoparticles and the DNA tag prevents detachment. The nucleic acids are also more stable in the environment than the intact virus particles (Charles *et al.*, 2009; Espinosa *et al.*, 2008). This observation is supported by the 2-year experiment set up for the plasmid DNA, which showed approximately 1 $\log_{10}$ reduction of DNA concentration over the two years of incubation.

4.4.3 Data variability

In nearly all the samples, the concentration of DNA and the adenovirus decreased rapidly by 5 – 10-fold in one week, which may have been a result of attachment to the inner wall of the tubes used to store the samples. (Excluding samples taken prior to the drop in concentration did not affect considerably the degradation rates – data not shown.) After one year of incubation, the adenovirus samples and most plasmid and DNA-SiNP samples with lower C_0 showed elevated concentrations. This was probably a result of water evaporation over time causing particles to concentrate in the solution. In addition, the detachment of particles from the tube wall may have also contributed the apparently high concentrations.

The results of the qPCR showed some variability especially for the virus samples, suggesting that the preparation of samples had an effect on the reaction. While the plasmid DNA and the DNA-SiNP samples were analysed directly, the virus samples were filtered or DNase-treated,

followed by a step of RNA/DNA extraction (by heat shock or enzymatic treatment of the virus particles). These additional steps could affect the efficiency of the quantification of the nucleic acid content of the samples. Furthermore, the two viruses were shown to have a tendency of aggregation at room temperature in the 2 mM NaCl solution, and the aggregation may influence various assays. However, in general, aggregation would have less (if any) impact on the results of the PCR-based methods than the results of culturing-based assays.

4.5 Conclusions

The DNA-SiNP showed higher stability over time in simulated groundwater than the rotavirus and the adenovirus. The quantification of the DNA-SiNP was faster, easier and more accurate than the viruses, as the samples were analysed directly by qPCR, whereas for the viruses various techniques were used before quantification. The DNA-SiNP was as stable in dark as the rotavirus, whereas the degradation of the plasmid DNA reflected the degradation of the adenovirus. The stability of the DNA-SiNP and the plasmid DNA was not affected by light. Its resistance to light can also extend the shelf-life of the DNA-SiNP.

The intact rotavirus and adenovirus particles are both stable over time showing less degradation in one year than expected. The exposure to light had no effect on the adenoviruses degradation, but had remarkable impact on rotaviruses. The techniques applied in this study detected the intact particles only, thus the results of the quantification show strong correlation with the inactivation of the viruses. The presence of undamaged adenovirus capsid proteins was detectable in most samples, however, the ELISA was less sensitive than the qPCR. Despite of the limitations of the methods used here, the results of virus degradation show good corroboration with reports in the literature where the infectivity of the viruses were tested. These findings suggest that the detected virus particles were intact and undamaged therefore highly likely infectious.

The techniques used in this study can be used in environmental studies to evaluate the number of intact virus particles without using culturing-based methods. Many samples can be processed without cross-contamination, giving the opportunity to study broad areas. The stability of the DNA-SiNP makes it a good surrogate in long-term studies to the most persistent viruses found in the environment.

Chapter 5.
Adsorption study of viruses and virus surrogates to porous media

5.1 Introduction

Adsorption plays a very important role in virus removal in aquifer media. As summarised in Chapter 1, there are many factors influencing virus adsorption, including the surface characteristics of the virus and the porous media, temperature, pH, ionic strength, and the composition of the groundwater.

The main interactions between viruses and porous media in the groundwater are electrostatic and hydrophobic interactions. The type of interactions between the porous media and the viruses depends on their surface characteristics, e.g. the structure of the capsid proteins (Jin & Flury, 2001). As demonstrated in Chapter 2 rotavirus, adenovirus and MS2 are all negatively charged (zeta potential was –24 to –28 mV) implying the possibility of electrostatic adsorption. On the other hand, the capsids of rotavirus and adenovirus contain several different proteins, thus the virus adsorption and behaviour may show high variation.

For instance, rotaviruses have been found to adsorb to various porous media – including clay, charcoal, haematite – and to marine sediment tightly (> 70% adsorption) with low (< 4%) desorption (Clark *et al.*, 1998; Gutierrez *et al.*, 2009; LaBelle & Gerba, 1979). Contradictory, compared to other enteric viruses, rotavirus adsorbed to sandy loam at a lower degree (~50%) (Goyal & Gerba, 1979). Rotavirus has been shown to adsorb onto glass slides coated with the hydrophobic polyethylenimine (Larson *et al.*, 2011). Nevertheless, the low hydrophobicity (42.5%, determined in Chapter 2) of the rotavirus suggests weak interactions with hydrophobic material.

Despite its common presence in contaminated groundwater and its impact on human health, few studies have been undertaken on the adsorption of adenovirus to aquifer media. Wong *et*

al. (2012) demonstrated that adenovirus type 2 adsorbed weakly to sand and that hydrophobic interactions had little effect on adenovirus adsorption. Nonetheless, according to the virus characterisation results summarised in Chapter 2, adenovirus was found to be rather hydrophobic. Hence, investigation on adenovirus behaviour in environment containing hydrophobic material is essential.

MS2, among other bacteriophages, is a widely used surrogate for enteric viruses in adsorption studies. It is often used for testing the efficacy of filtration systems used in water treatment (Tanneru *et al.*, 2013; Wang *et al.*, 2013) and for studying virus adsorption to porous media under various conditions (Cao *et al.*, 2010; Schaldach *et al.*, 2006; Zhang *et al.*, 2007). MS2 has been shown to adsorb to quartz sand, red soil, soil minerals and organic matter (Chrysikopoulos & Aravantinou, 2012; Davis *et al.*, 2006; Pham *et al.*, 2009; Syngouna & Chrysikopoulos, 2010; Zhang *et al.*, 2010). Previous research (Bales *et al.*, 1991; Bales *et al.*, 1993) and the results of the hydrophobicity test (described in Chapter 2) suggested that MS2 is hydrophobic, thus may overestimate enteric virus adsorption and removal in environment containing hydrophobic surfaces.

The surface-modified nanoparticles (characterised in Chapter 3) used in the current study comprised of the negatively charged and rather hydrophilic silica, DNA and proteins. The DNA, due to its sugar-phosphate backbone, is negatively charged at neutral pH as well. Free plasmid and extracellular DNA has been shown to adsorb onto soils, quartz, clay, humic acid and other organic matter often presented in groundwater (Crecchio & Stotzky, 1998; Nguyen & Chen, 2007; Nguyen & Elimelech, 2007; Romanowski *et al.*, 1992; Tang *et al.*, 2012; Wang *et al.*, 2009). The sequence and secondary structure of the DNA has little effect on the adsorption to porous media (Cleaves *et al.*, 2011). No hydrophobic interactions between DNA and solids have been documented, supporting the hydrophilic nature of the DNA-SiNPs (described in Chapter 3).

The proteins used to coat the nanoparticles are also negatively charged, and the coated particles were rather hydrophilic mainly due to the overall hydrophilic nature of the silica nanoparticles (see Chapter 3 for details). As only one type of protein was used at a time, the surface characteristics of the modified nanoparticles are more uniform than the viruses, thus their adsorption may be more predictable.

In this study, the adsorption of rotavirus, adenovirus, MS2 bacteriophage and several surface-modified silica nanoparticles to natural aquifer media (gravel and sand) was investigated. In order to assess the possible interactions, the adsorption of the viruses and nanoparticles to unmodified and organosilane-coated (hydrophobic) sand was compared.

5.2 Methods and materials

5.2.1 Porous media

Four types of porous media were used to study particle adsorption (Appendix III). The fine beach sand (d_{50} = 0.2 mm) and the fine gravel (d_{50} = 3 mm) are natural media, collected in New Brighton, Christchurch (New Zealand) and Canterbury plains (New Zealand), respectively. Prior to experiments, the media was sieved, washed and autoclaved as described in Appendix III. The commercially available Ottawa sand, mesh 20-30 (Fisher Scientific, UK) was acid washed and half of this was modified by organosilane, based on the method of Bales *et al.* (1991), which gave hydrophobic coating to the sand particles (see Appendix III for details).

5.2.2 Viruses and nanoparticles

In the batch experiments, the adsorption of the rotavirus, adenovirus, MS2 bacteriophage and several surface-modified silica nanoparticles, all of the latter were labelled with the 302 bp dsDNA tag, to porous media was tested (Table 5.1). The nanoparticles used were coated with glycoprotein, streptavidin, protein A, casein and AMBP, and the adsorption of the DNA-labelled nanoparticles without protein-coating was tested as well. In order to eliminate the unbound DNA from the nanoparticle stocks, the nanoparticles were pelleted by centrifugation at 13,000×g for 20 min and resuspended in 2 mM NaCl pH 7 solution before sample preparation. The viruses were purified prior to the experiments by the methods described in Chapter 2. In the experiment where the MS2 adsorption to beach sand was studied, unpurified MS2 (MS2-crude) was used.

Table 5.1 The viruses and nanoparticles used for the adsorption experiments. The detailed description on the virus purification and characteristics of the modified nanoparticles is in Chapter 2 and 3. +: adsorption was tested, –: adsorption was not tested. *The numbers in the brackets represent the amount of protein used for coating.

Name	Description	Gravel	Beach sand	Ottawa sand	Coated Ottawa sand
Rotavirus	Purified	+	+	+	+
Adenovirus	Purified	+	+	+	+
MS2-crude	Unpurified from culturing	–	+	–	–
Purified MS2	Purified	+	–	+	+
DNA-SiNP	DNA-labelled silica nanoparticles	+	+	+	+
Gly-DNA-SiNP	Glycoprotein-coated, DNA-labelled silica nanoparticles	+	+	+	+
Str-DNA-SiNP	Streptavidin-coated, DNA-labelled silica nanoparticles	+	+	+	+
PrA-DNA-SiNP	Protein A-coated, DNA-labelled silica nanoparticles	+	+	+	+
Cas(5)-DNA-SiNP*	casein-coated, DNA-labelled silica nanoparticles	+	+	–	–
Cas(50)-DNA-SiNP*	casein-coated, DNA-labelled silica nanoparticles	+	+	+	+
Cas(500)-DNA-SiNP*	casein-coated, DNA-labelled silica nanoparticles	+	+	–	–
Cas(2000)-DNA-SiNP*	casein-coated, DNA-labelled silica nanoparticles	+	+	–	–
AMBP-DNA-SiNP	AMBP-coated, DNA-labelled silica nanoparticles	+	+	–	–
DNA-StrNP	DNA-labelled silica nanoparticles pre-coated with streptavidin	+	+	–	–

5.2.3 Experimental setup

In the adsorption experiments, 2-mL plastic centrifuge tubes were packed under saturated conditions with the porous media and the stock solution containing adenovirus, rotavirus, purified MS2 or the surface-modified silica nanoparticles. Stock solutions were made by using 2 mM NaCl pH 7 solution containing approximately 10^8 gc/mL or DNA copies/mL viruses/nanoparticles. When the unpurified MS2 bacteriophage (MS2-crude) was tested, 15-mL centrifuge tubes were packed with MS2-crude stock solution with a final concentration of

10^5 pfu/mL. All tubes were sealed with parafilm before closing the cap to protect samples from air, and rotated at 2 rpm at room temperature. All experiments were set up in replicates (n = 2) except the one experiment, where the adsorption of the DNA-SiNP to beach sand was studied (n = 1). The stock solutions without gravel or sand material were used as a control, and incubated together with the samples.

5.2.4 Sampling and quantification

Separate tubes were sampled 0.5, 1, 2, 4 and 6 hr after preparation. Each time 50 µL of the rotavirus, adenovirus, the purified MS2 and the surface-modified silica nanoparticles, and 1 mL of the MS2-crude was collected. The purified MS2, adenovirus and rotavirus samples were incubated at 97°C for 15 min, and then quantified with qRT-PCR and qPCR, respectively, using the methods described in Chapter 2. The samples of the MS2-crude were analysed by a plaque assay as described in Chapter 2. The surface modified nanoparticles were analysed directly by the qPCR method described in Chapter 3.

5.2.5 Data analysis

In order to eliminate adsorption to the plastic tubes used during the adsorption experiment, the relative concentrations (C_{rel}) of the samples taken and the percentage adsorptions (Ads%) were calculated according to the following formulas:

$$C_{rel} = \frac{C_{sample\ 6} - C_{control\ 6}}{C_0}$$

$$Ads\% = \left(\frac{C_{control\ 6} - C_{sample\ 6}}{C_0}\right) * 100\%$$

where C_0 is the average concentration of the stock solutions, $C_{sample\ 6}$ is the average sample concentration after 6 hr and $C_{control\ 6}$ is the average concentration of the stocks after 6 hr incubation.

The kinetics of the adsorption were characterised by determining the adsorption/desorption rate coefficient ratio (adsorption/desorption ratio; k_a/k_d), using the approach of Schijven and Hassanizadeh (2000):

$$C_{rel} = \frac{k_d + k_a \exp[-(k_a + k_d)t]}{k_a + k_d}$$

where k_a is the adsorption rate coefficient, k_d is the desorption rate coefficient, t is the time when the sample was taken and exp is exponential function.

The relative concentration to the stock solution was calculated for all samples taken using the results of the qPCR, and the adsorption and desorption rates where optimised using the Solver tool in Microsoft Excel. The r^2 values for the exponential fit were also calculated using the Data Analysis tool in Microsoft Excel.

5.3 Results

Results of the tests are summarised in Figure 5.1, Figure 5.2 and Figure 5.3, which show the average relative concentrations of the viruses/nanoparticles during the 6-hour experiment. The percentage adsorptions (Table 5.2) were calculated using the concentrations of the samples taken at the beginning and at the end of the 6-hour experiment. The adsorption/desorption ratios (Table 5.2) were calculated using the concentrations of all samples taken through the experiment and give information on the strength of the adsorption. Therefore, if the adsorption/desorption ratio was high, the particles adsorbed strongly to the porous media with low desorption, whereas low ratios refer to weak adsorption and high rate of desorption. When the adsorption/desorption ratio was zero, no considerable adsorption took place during the 6-hour experiment and/or the desorption was fast. When the adsorption was irreversible the adsorption/desorption ratio could not be calculated ($k_d = 0$).

5.3.1 Adsorption to gravel

Results suggest that both rotavirus and adenovirus adsorbed to the gravel. The adsorption was 95.6% for rotavirus and 83.6% for adenovirus with most the adsorption complete within 30 min for rotavirus and within 2 hr for the adenovirus (Figure 5.1).

The adenovirus concentration of the stock solution (without gravel) was reduced by 10.5%, during the experiment, suggesting that this proportion of the adenoviruses attached to the inner wall of the plastic tubes. No attachment to the tube was observed for the rotavirus.

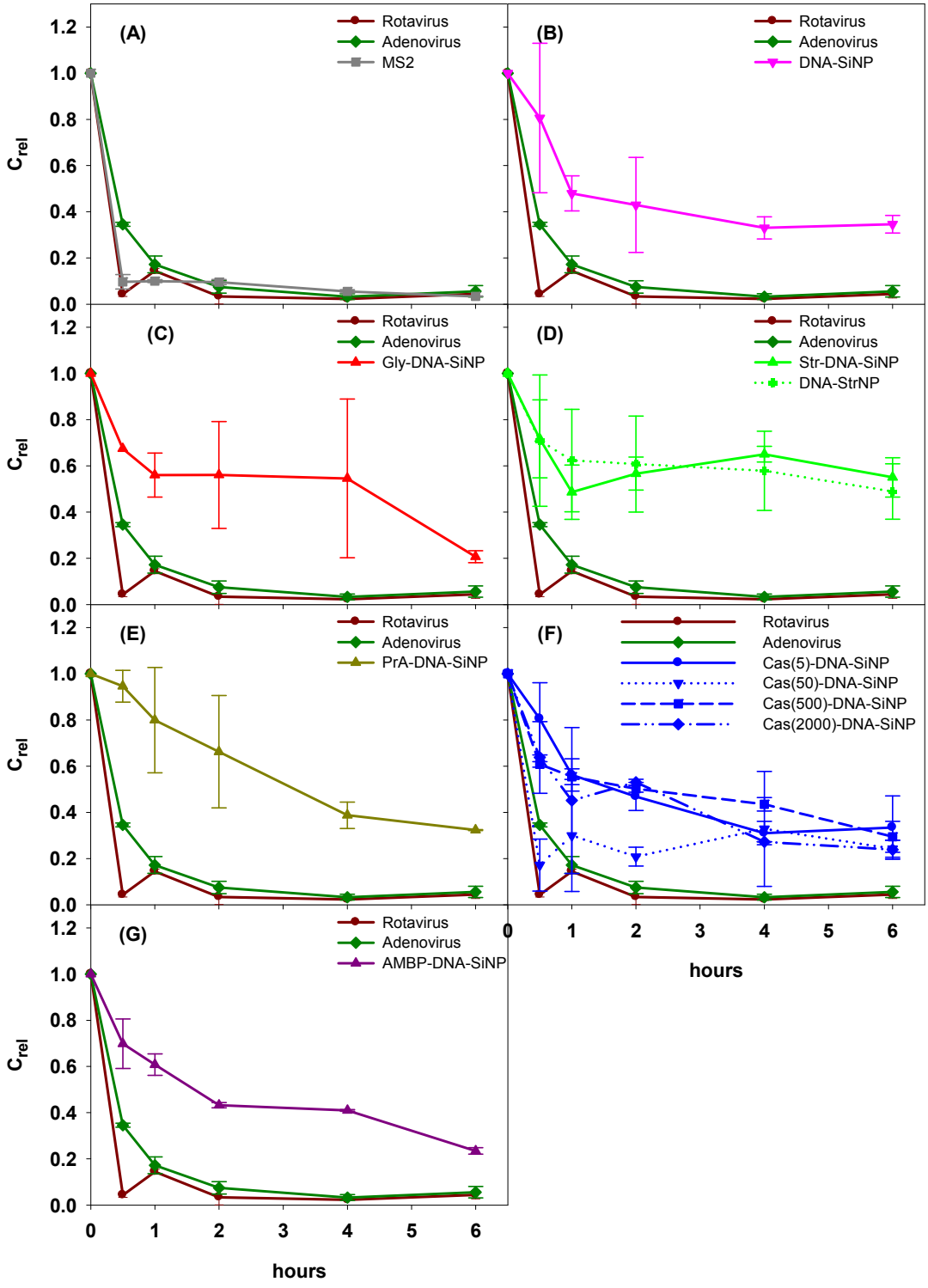

Figure 5.1 Virus/nanoparticle adsorption to fine gravel. Error bars represent the average deviation of the replicate experiments. Graphs shows the relative concentration of the enteric viruses compared to (A) MS2 bacteriophage, (B) DNA-labelled nanoparticle, (C) glycoprotein-coated nanoparticle, (D) streptavidin-coated nanoparticles, (E) protein A-coated nanoparticle, (F) casein-coated nanoparticles and (G) AMBP-coated nanoparticle.

Similar to rotavirus, a rapid and almost complete initial adsorption (96.5%) was observed for the MS2 bacteriophage with 30 min. After this time the concentration of the MS2 did not changed considerably. No adsorption of the MS2 to the wall of the tube was observed in the control experiment. All three viruses had high adsorption/desorption ratios (13.16 – 17.64) suggesting strong adsorption and little desorption.

In general, all the surface-modified nanoparticles adsorbed at a lesser degree and at a lower rate to gravel than the enteric viruses. The calculated adsorption varied between 46.9% and 76.2% (Table 5.2). The adsorption/desorption ratios varied between 0.80 and 10.62, indicating much weaker adsorption than what was observed for the viruses. In some cases (DNA-SiNP, Gly-DNA-SiNP, PrA-DNA-SiNP) the replicate experiments showed considerable variation (Figure 5.1), which could be due to the heterogeneous nature of the aquifer media.

The adsorption of the Str-DNA-SiNP (where the DNA-labelling and protein coating was carried out in one step) and the DNA-StrNP (where protein-coating was performed prior to DNA-labelling) was very similar: the calculated adsorption was 46.9% and 56.2%, respectively, and the shapes of the degradation curves were also similar (Figure 5.1D). Four samples of the casein-coated nanoparticles were tested. In each sample a different amount of the protein was used for coating. The adsorption of these nanoparticles was similar. In one case [Cas(50)-DNA-SiNP] a rapid decline in concentration was observed, whereas the other casein-coated nanoparticles were adsorbed more consistently (Figure 5.1F). The concentration of the control solutions for the protein A- and the AMBP-coated particles decreased by 9% and 8%, respectively during the experiments, suggesting that these proteins slightly enhanced the particle adsorption to plastic. The other surface-modified nanoparticles did not attach to the tube wall.

5.3.2 Adsorption to beach sand

The virus/nanoparticle adsorption to beach sand is summarised in Figure 5.2, and the percentage adsorption and the adsorption/desorption ratios are presented in Table 5.2. The rotavirus was adsorbed to the beach sand entirely in the first 30 min of the experiment and no desorption was noted.

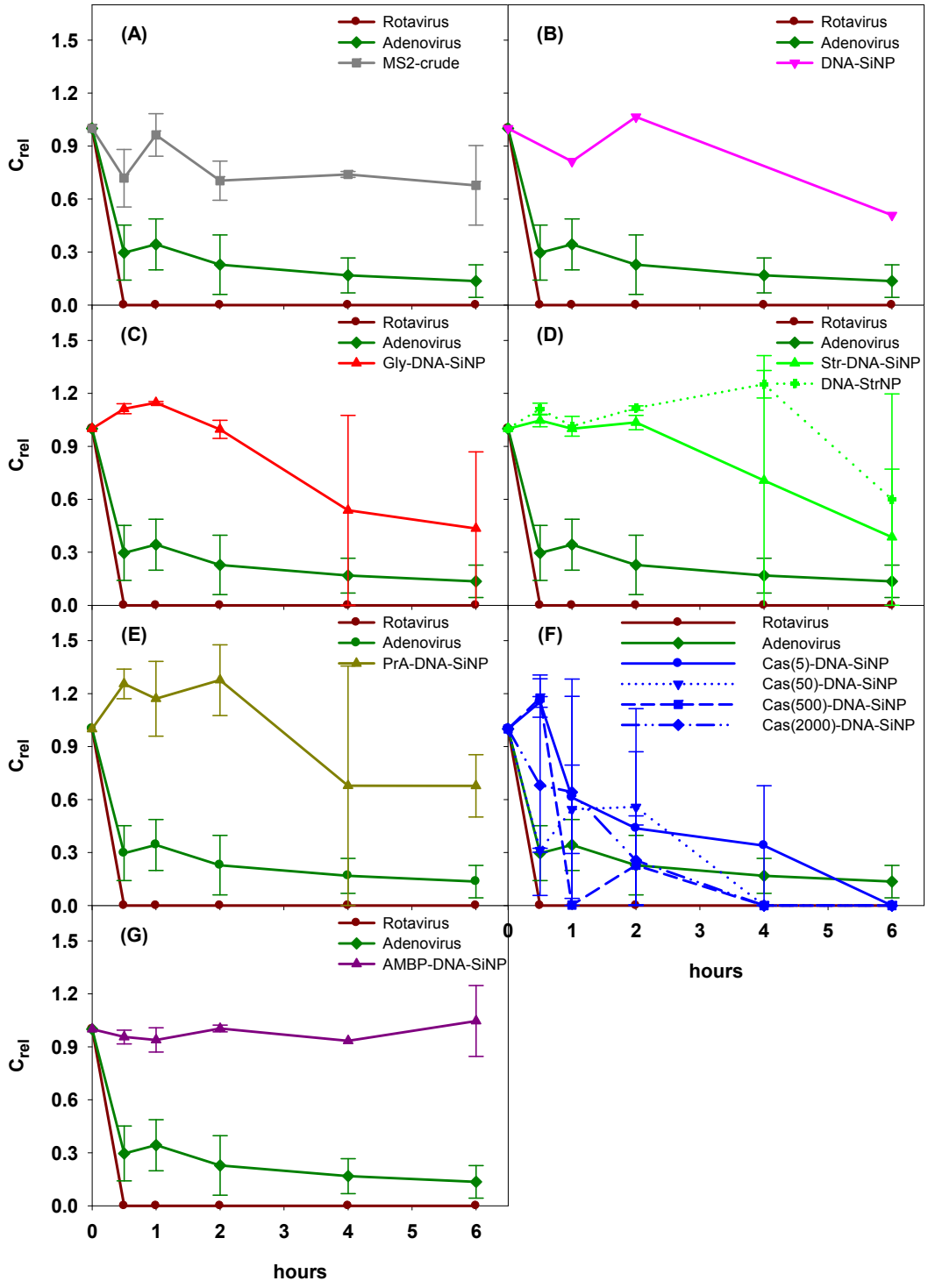

Figure 5.2 Virus/nanoparticle adsorption to beach sand. Error bars represent the average deviation of the replicate experiments. Graphs shows the relative concentration of the enteric viruses compared to (A) MS2 bacteriophage, unpurified, (B) DNA-labelled nanoparticle (one experiment), (C) glycoprotein-coated nanoparticle, (D) streptavidin-coated nanoparticles, (E) protein A-coated nanoparticle, (F) casein-coated nanoparticles and (G) AMBP-coated nanoparticle.

Table 5.2 The size, the zeta potential (ZP), the hydrophobicity based on MATH assay (H%), the percentage adsorption (Ads%) and adsorption/desorption ratios (k_a/k_d) together with the r^2 values (goodness-of-fit from fitting the kinetic adsorption-desorption model) of viruses and nanoparticles *Unpurified MS2 was used, analysed by plaque assay. N/A: data not available. –: no desorption ($k_d = 0$).

	ZP (mV)	H%	Gravel			Beach sand			Ottawa sand			Hydrophobic Ottawa sand		
			Ads%	k_a/k_d	r^2	Ads%	k_a/k_d	r^2	Ads%	k_a/k_d	r^2	Ads%	k_a/k_d	r^2
Rotavirus	–24	42	95.6	16.35	0.26	100	–	0.23	32.2	5.09	0.45	23.7	0.93	0.28
Adenovirus	–22	89	83.6	17.64	0.43	80.3	3.90	0.43	84.5	24.79	0.25	86.1	–	0.85
MS2	–24	98	96.5	13.16	0.29	29.4*	0.32*	0.31*	6.4	0.18	0.01	91.1	8.39	0.40
DNA-SiNP	–41	0	66.4	2.11	0.56	50.9	–	0.71	10.8	0	0.13	15.4	0.29	0.00
Gly-DNA-SiNP	–41	76	65.3	2.68	0.79	42.4	–	0.86	42.4	0	0.03	43.0	0.46	0.37
PrA-DNA-SiNP	–40	24	55.4	10.62	0.94	20.5	0	0.61	39.7	0.45	0.09	48.3	–	0.89
AMBP-DNA-SiNP	–41	18	66.3	2.24	0.78	0	0.23	0.06	0	0	0.00	19.5	0	0.55
Str-DNA-SiNP	–44	55	46.9	0.80	0.25	59.2	–	0.89	46.6	1.25	0.70	0	0	0.01
DNA-StrNP	–42	N/A	56.2	1.04	0.43	44.9	–	0.29	N/A	N/A	N/A	N/A	N/A	N/A
Cas(5)-DNA-SiNP	–40	N/A	68.9	2.33	0.72	100	–	0.79	N/A	N/A	N/A	N/A	N/A	N/A
Cas(50)-DNA-SiNP	–40	34	64.7	6.29	0.19	100	–	0.71	0.2	0.09	0.12	0	0.10	0.34
Cas(500)-DNA-SiNP	–38	N/A	68.2	1.46	0.65	100	–	0.47	N/A	N/A	N/A	N/A	N/A	N/A
Cas(2000)-DNA-SiNP	–40	N/A	76.2	2.33	0.69	100	–	0.79	N/A	N/A	N/A	N/A	N/A	N/A

The adsorption of the adenovirus to the beach sand was similar to gravel: 80.3% adsorption was observed. The majority of the adsorption occurred in the first 30 min of the experiment. The adsorption/desorption ratio for adenovirus was relatively high (3.90), indicating rather strong adsorption and little desorption.

The adsorption of the unpurified MS2 bacteriophage (using plaque assay for quantification) to the beach sand was also studied. The MS2 was found to adsorb to the beach sand at considerably lower degree (29.4%) than the rotavirus and adenovirus. The adsorption/desorption ratio (0.32) indicated weak adsorption and high desorption.

Considerable variation in the adsorption of the surface modified nanoparticles was observed. The AMBP- and the protein A-coated nanoparticles barely adsorbed to the beach sand: 0% and 20.5% adsorption, respectively was calculated, and consequently the adsorption/desorption ratios were close to zero. In contrast, the casein-coated nanoparticles, regardless the amount of the protein used for coating, were not recovered from the solution (100% adsorption, no desorption).

Approximately 50% of the DNA-labelled, the glycoprotein- and the streptavidin-coated nanoparticles adsorbed without desorption. No major difference in the adsorption of the Str-DNA-SiNP (59.2% adsorption, no desorption) and the DNA-StrNP (44.9% adsorption, no desorption) was observed. The replicates of the protein-coated nanoparticles showed some variation, which was probably a result of the heterogeneity of the beach sand.

5.3.3 Effect of hydrophobic media on particle adsorption

The adsorption of the viruses/nanoparticles to the unmodified and hydrophobic Ottawa sand is summarised in Figure 5.3. The rotavirus adsorbed to the unmodified and the hydrophobic sand at a low rate. Slightly less adsorption was observed to the hydrophobic sand (23.7%) than to the unmodified sand (32.2%; Table 5.2). The adsorption/desorption ratios showed low desorption from the Ottawa sand and high desorption from the hydrophobic sand. In contrast, the adsorption of the adenovirus to the two types of sand was high (84.5% and 86.1%). The adsorption/desorption ratios indicated little or no desorption (Table 5.2).

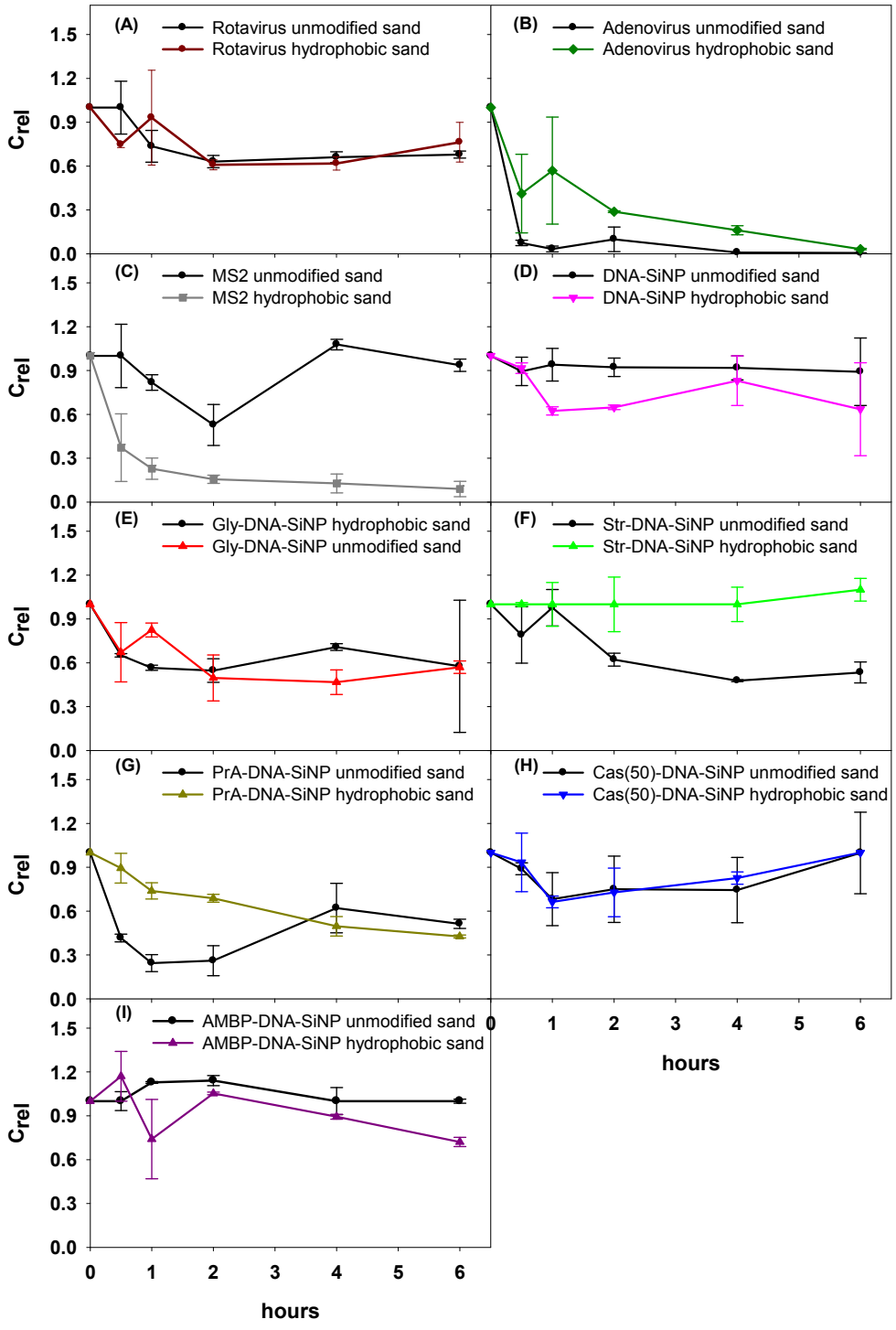

Figure 5.3 Comparison of virus/nanoparticle adsorption to unmodified and hydrophobic Ottawa sand. Error bars represent the average deviation of the replicate experiments. Graphs show the relative concentrations for (A) rotavirus, (B) adenovirus, (C) MS2 bacteriophage, (D) DNA-labelled nanoparticle, (E) glycoprotein-coated nanoparticle, (F) streptavidin-coated nanoparticle, (G) protein A-coated nanoparticle, (H) casein-coated nanoparticle and (I) AMBP-coated nanoparticle. The black lines show to adsorption to unmodified sand, the coloured lines show adsorption to the sand coated with hydrophobic material.

Almost an order of magnitude difference was observed in the adsorption of the MS2 bacteriophage to the two types of sand. Little adsorption was noted to the unmodified sand with adsorption of 6.4% (k_a/k_d = 0.18), while 91.1% of the MS2 strongly adsorbed to the hydrophobic sand without significant desorption (k_a/k_d = 8.39).

In general, the adsorption of the surface-modified nanoparticles to the unmodified and hydrophobic sand was similar. As the adsorption of the Str-DNA-SiNP and the DNA-StrNP had been found to be similar for both the gravel and beach sand, it was decided that only the Str-DNA-SiNP would be tested with the Ottawa sand. For the same reason, only one of the casein-coated nanoparticles [Cas(50)-DNA-SiNP] was tested.

The adsorption/desorption ratios were low for all the nanoparticles in both media (< 1.25). The DNA-SiNP adsorbed at a very low rate (10.8% and 15.4%) to the two types of sand. The low adsorption/desorption (0.00 – 0.29) ratios indicated reversible and weak adsorption to the unmodified and hydrophobic sand.

The adsorption of the glycoprotein-coated nanoparticles was similar to the unmodified and to the hydrophobic sand (43%, k_a/k_d close to zero). The percentage adsorptions of the protein A-coated nanoparticles were also very similar (39.7% and 48.3%) to the two types of sand. Nonetheless, the adsorption/desorption ratios indicated fast desorption from the unmodified and no desorption from the hydrophobic sand, suggesting that different interactions took place in the sands with different surface. Interestingly, the streptavidin-coated nanoparticles adsorbed to the unmodified Ottawa sand (46.6%), while no adsorption was observed to the hydrophobic sand. However, the adsorption/desorption ratios calculated for the unmodified sand indicated reversible adsorption.

Conversely, no adsorption of the AMBP-coated nanoparticles to the unmodified Ottawa sand was noted, whereas 19.5% adsorption was observed when the nanoparticles were incubated with the hydrophobic sand. The difference may not have been significant, as the adsorption/desorption ratios indicated no adsorption. The casein-coated nanoparticles were not adsorbed to the unmodified or the hydrophobic sand either.

5.4 Discussion

In this study, the adsorption of the rotavirus, adenovirus, MS2 bacteriophage and several surface-modified nanoparticles to porous media was investigated. In order to determine the concentration of the viruses/nanoparticles in the solution when incubated with porous media, in most cases qPCR and qRT-PCR was used. Meschke and Sobsey (1998) found that the adsorption determined by RT-PCR corresponded well with the results of culturing when the adsorption of poliovirus and MS2 to soils was tested, however, in some cases the RT-PCR gave false negative results, which was probably due to the presence of inhibitors to RT-PCR being present in the samples. The preliminary findings of current study suggest that the solution rotated with the porous media had no inhibiting effect on the q(RT)-PCR (described in Appendix III), hence the results discussed here reflect the adsorption of the viruses and nanoparticles.

The results of the replicate experiments for studying the adsorption of viruses/nanoparticles to gravel and beach sand showed high variation, especially for the adsorption of the protein-coated nanoparticles. Conversely, the experimental replicates for the unmodified and hydrophobic Ottawa sand were similar. A possible explanation for that is the heterogeneity of the gravel and beach sand. These media are derived from natural aquifers in Canterbury (New Zealand), and probably contain various minerals that have different effects on particle adsorption. On the other hand, the Ottawa sand is pure silica sand, and the adsorption of the viruses/nanoparticles to the uniform sand particles was more reproducible.

In this study, the percentage adsorption and the adsorption/desorption ratios for the 6-hour experiment were both calculated. In most cases the percentage adsorption gives a good indication of the kinetics of adsorption: high percentiles indicate strong and irreversible adsorption, whereas the low rates suggest equilibrium in the adsorption and desorption. However, for some nanoparticles the low percentage adsorption suggested weak interactions, but the desorption rate coefficient (k_d) was zero, thus the interactions between the porous media and the nanoparticle were strong. Contradictory, for some of the nanoparticles the percentage adsorption indicated some interactions with the unmodified Ottawa sand, however, the adsorption/desorption ratio (k_a/k_d) was zero implying no adsorption. In those cases, the concentration of the samples taken through the experiment showed some fluctuation, suggesting weak adsorption and fast desorption. Data suggest that for a better understanding

on the interactions between particles and aquifer media, both kinetics and equilibrium approaches are needed.

5.4.1 Adsorption of viruses to porous media

Rotavirus was found to adsorb strongly (95 – 100%) and irreversibly to the gravel and the beach sand. Rotavirus adsorbed almost completely to the beach sand in 30 min, and no virus particles were recovered during the experiment. Results suggested that both media have high adsorption capacity and may retard rotaviruses during their transport. Both media are negatively charged (Appendix III) like the viruses, therefore electrostatic interactions may have had no significant role in virus adsorption.

In contrast, the adsorption of rotavirus to the Ottawa sand was considerably lower (32.2%), however, once adsorbed, there was little desorption of rotavirus. Other researchers have also noted a relatively low degree of adsorption (53%) during the transport of the simian rotavirus in a column packed with quartz sand, which is an inert matrix like the silica (Herbold-Paschke *et al.*, 1991). The Ottawa sand is pure silica sand, therefore negatively charged, which may explain the low virus adsorption. The adsorption of the rotavirus was further reduced when the hydrophobic sand was used (23.7%). The stronger adsorption to the unmodified sand and the faster desorption from the hydrophobic sand confirms that the hydrophobic material occupied the binding sites that may have otherwise become occupied by rotavirus particles. This explanation is supported by previous findings in poliovirus adsorption. Research showed that poliovirus did not adsorb to soil with high concentration of organic matter as organic matter saturated the virus binding sites (Moore *et al.*, 1981). As described in Chapter 2, rotavirus is rather hydrophilic (Table 5.2), therefore, the low adsorption to hydrophobic sand was expected. To date no other batch studies have been carried out on the adsorption of rotavirus to sand and gravel.

The adenovirus adsorption to the Ottawa sands (unmodified and hydrophobic), beach sand and gravel was high (80.3 – 86.1%). In all media the virus particles attached to the sand/gravel in the first 0.5 – 2 hr, and then the virus concentration in the solution was stable, suggesting no further adsorption or desorption. Contradictory to this study, Wong *et al.* (2012) noted weak adsorption of adenovirus type 2 to Ottawa sand mesh 30 – 40 in monovalent cation solution. The different observations between the studies may be due to the different virus strains or the larger particle size of the sand used. As described in Chapter 2

the adenovirus type 41 is negatively charged (ZP of –22 mV) and, according to the results of the modified MATH test, rather hydrophobic (Table 5.2). The data of current study suggest that hydrophobic and other interactions occur during the adsorption of the adenovirus to porous media.

The adsorption of the MS2 bacteriophage showed differences from the adsorption of rotavirus and adenovirus despite their similar surface charge (ZP of –24 mV, Table 5.2). MS2 adsorbed to gravel irreversibly to a higher degree (96.5%) than any of the enteric viruses. Contradictory, MS2 weakly adsorbed to beach sand and unmodified Ottawa sand (29.4% and 6.4%, respectively) followed by fast desorption, which indicates different interactions occurring at the phage/gravel and phage/sand interfaces. Previous studies also demonstrated that the adsorption of enteric viruses and bacteriophages to the same porous media can be different (Goyal & Gerba, 1979; Schaldach *et al.*, 2006). The bacteriophage adsorption to sand was similar to previous findings where weak adsorption of the MS2 bacteriophage to sand and sandy soil during transport was found in monovalent cation solutions in the absence of organic matter (Attinti *et al.*, 2010; Cao *et al.*, 2010; Chu *et al.*, 2000; Davis *et al.*, 2006; Weaver *et al.*, 2013).

MS2 was hardly recovered from the hydrophobic Ottawa sand (i.e. high adsorption at 91.1%), which agrees with the results of the modified MATH test, showing great hydrophobicity (Table 5.2). Previous studies also found that MS2 readily adsorbs to hydrophobic surfaces (Bales *et al.*, 1991; Bales *et al.*, 1993; Han *et al.*, 2006).

5.4.2 Adsorption of surface-modified nanoparticles to porous media

In general, the replicate experiments for the surface-modified nanoparticles showed higher variations than what was observed for the viruses, especially in the gravel and beach sand experiments. This phenomenon may be the result of the heterogeneity of the aquifer media. The experiments with the surface-modified nanoparticles were performed later than those with the viruses, and in some cases not the same batch of media was used. The batch used for the surrogates may have been more heterogenic than the one used for the viruses. Nonetheless, the k_a/k_d values calculated for the surface-modified nanoparticles indicated weaker interaction with the porous media and more desorption than what was noted for the viruses. The kinetics of the adsorption/desorption may have caused the variations in sample concentrations in the replicate experiments.

The adsorption of the surface-modified nanoparticles to gravel was uniform, the percentage adsorption varied between 46.9% and 76.2% regardless of the coating. The percentage adsorptions were similar to the adenovirus adsorption, however, the adsorption/desorption ratios indicated weak interactions between the nanoparticles and the gravel, except for the protein A-coated nanoparticles, which strongly adsorbed.

The adsorption of the nanoparticles in beach sand showed large variation. The casein-coated nanoparticles strongly adsorbed to the beach sand mimicking the rotavirus adsorption, whereas the protein A- and AMBP-coated nanoparticles showed weak or no adsorption. The DNA-labelled only nanoparticles (without protein coating) together with the glycoprotein- and the streptavidin-coated nanoparticles showed 40 – 60% adsorption to beach sand, thus may be suitable surrogates for adenovirus in aquifers composed of this type of sand. In both the gravel and the beach sand experiments, the adsorption of the casein-coated nanoparticles, with different amounts of protein used for coating, adsorbed similarly, suggesting that the amount of protein used for coating did not alter the surface characteristics of the casein-coated nanoparticles. No difference was found in the adsorption of the streptavidin-coated nanoparticles (coated using different methods) to the gravel and the beach sand, further confirming that the steps of DNA-labelling and protein-coating can be done in either one step or separated. (For more details on the development and characterisation of the protein-coated nanoparticles see Chapter 3.)

In general, the nanoparticles weakly adsorbed to the unmodified and hydrophobic Ottawa sand. No notable difference was found in the adsorption of the DNA-labelled, glycoprotein-, protein A- and casein-coated nanoparticles to the unmodified and hydrophobic Ottawa sand. However, unlike the results presented here, casein has been shown by others to readily attach to hydrophobic surfaces (Fragneto *et al.*, 2000). Therefore, the casein-coating was probably not the main factor influencing the weak hydrophobicity of these nanoparticles. It is possible, that many of the hydrophobic amino acids (e.g. methionine, valine and leucine) are involved in binding to the silica nanoparticles, thus reducing the chance of hydrophobic interactions. The AMBP-coated nanoparticles showed some adsorption to the hydrophobic sand and no interactions with the unmodified sand. Nonetheless, the observed adsorption to the hydrophobic sand was weak, therefore, the incidence of hydrophobic interactions is ambiguous.

5.4.3 Hydrophobicity of the viruses and nanoparticles – usefulness of the MATH assay

The results of the modified MATH assay (described in Chapters 2 and 3; H% in Table 5.2) for viruses/nanoparticles are compared to the percentage adsorption of the viruses/nanoparticles to hydrophobic Ottawa sand in Figure 5.4 and Table 5.2. Overall, the adsorption rates derived from the different tests are similar for the viruses and the AMBP-coated nanoparticles.

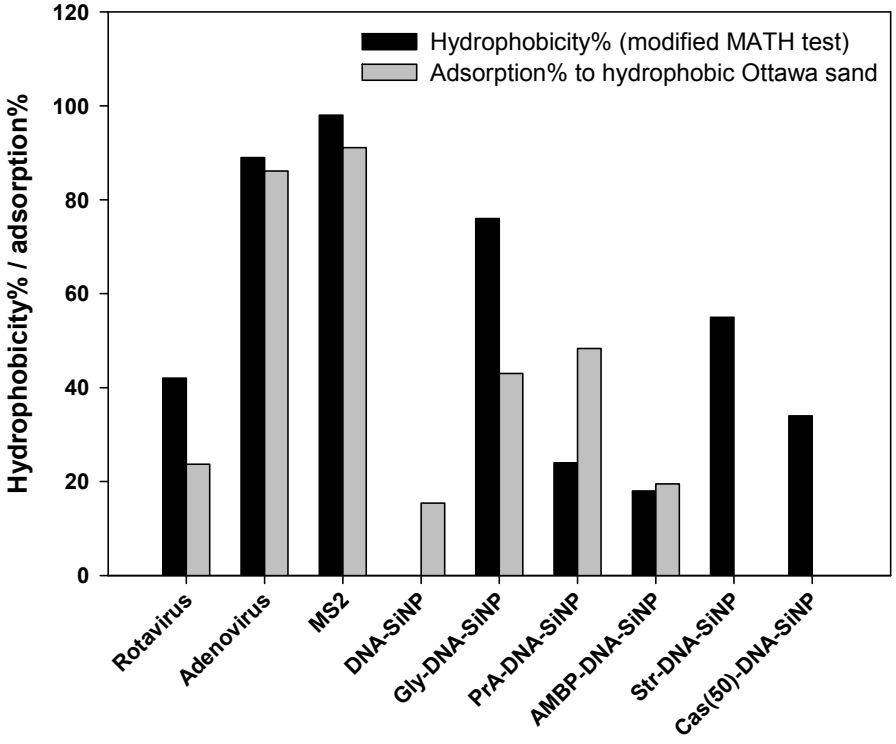

Figure 5.4 Comparison of the hydrophobicity% determined by modified Microbial Adhesion to Hydrocarbons (MATH) assay (black columns) and the adsorption% to hydrophobic Ottawa sand (grey columns). Missing bars indicate zero hydrophobicity or the lack of adsorption.

For the glycoprotein-, streptavidin- and casein-coated nanoparticles the MATH assay showed some hydrophobicity. However, this was not confirmed by the adsorption to hydrophobic sand. Dynamic conditions break aggregated particles and enhance the adsorption to and desorption from the porous media (Chrysikopoulos & Aravantinou, 2012), therefore, the slow rotation applied to the tubes during the assay may have favoured desorption from the hydrophobic surface. Contradictorily, this cannot be the complete explanation because the DNA-labelled and the protein A-coated nanoparticles adsorbed to the hydrophobic sand more readily than would have been expected based on the MATH assay results, by approximately 20% difference between the results of the two assays. However, taken together the results are

suggesting that the nanoparticles are rather hydrophilic. Furthermore, the uniformity of the hydrophobic-coating was not tested. Therefore, the sand particles may not have been uniformly covered by the organosilane, leaving some adsorption sites available for the nanoparticles. Overall, the MATH assay gave useful preliminary indication on hydrophobicity, and was valuable to indicate the possibility of hydrophobic interactions between viruses/nanoparticles and porous media.

5.5 Conclusions

The gravel and beach sand used in this study were derived from Canterbury, New Zealand and found in local aquifers. All viruses showed remarkable adsorption to these media, suggesting that sand and gravel aquifers are able to remove great proportions of enteric viruses, if there is sufficient length of interaction time. The adsorption of the surface-modified nanoparticles to the gravel was uniform, whereas the adsorption to the beach sand showed variation indicating that the surface characteristics had a major impact on the behaviour of the viruses.

The virus adsorption to hydrophobic sand reflected the results of the modified MATH assay. The rotavirus hardly adsorbed to the hydrophobic sand, thus the virus is hydrophilic, whereas the adenovirus and the MS2 bacteriophage strongly adsorbed as they are rather hydrophobic. The MATH assay and the adsorption tests both indicated that the DNA-labelled and protein-coated nanoparticles (except the glycoprotein-coated one) are hydrophilic. The deviations in the results of between the two methods may be due to the uneven coating of the sand.

The adsorption of the most widely used virus surrogate, the MS2 bacteriophage, only reflected the adsorption of the rotavirus in the gravel. Due to its hydrophobicity, the adsorption of the MS2 to the hydrophobic sand reflected the adsorption of the adenovirus.

Taking into account that a suitable surrogate should have a similar or less adsorption than the modelled pathogen, the overall findings suggest that the DNA-labelled, glycoprotein-, streptavidin-, protein A- and AMBP-coated nanoparticles may be useful tools for studying the adsorption of the rotavirus and adenovirus to porous media. The casein-coated nanoparticles may not be a viable option due to their stronger interactions and greater adsorption, than the

model viruses. Nevertheless, casein-coated nanoparticles can be useful if hydrophobic matter is presented.

Chapter 6.
Column transport study of viruses and virus surrogates in aquifer media

6.1 Introduction

Rotavirus and adenovirus both have been associated with waterborne outbreaks (Fong *et al.*, 2007; Gallay *et al.*, 2006; Hopkins *et al.*, 1984; Koroglu *et al.*, 2011; Kukkula *et al.*, 1997). Rotavirus has been frequently detected in sewage, groundwater and surface water (Bradbury *et al.*, 2013; He *et al.*, 2008; Park *et al.*, 2010). Despite its impact on human health and presence in drinking water sources, little is known about its transport in groundwater. However, a laboratory study showed that 47% of the injected simian rotavirus was recovered from a quartz sand column (Herbold-Paschke *et al.*, 1991) suggesting that rotavirus is transported in the subsurface water without significant reduction.

The transport of adenoviruses in the environment has been studied more thoroughly. Adenoviruses are known to be transported in groundwater and reach surface water and drinking water wells (Fong *et al.*, 2007; Futch *et al.*, 2010; Hunt *et al.*, 2010). Testing samples from sewage, groundwater and surface water, Bradbury *et al.* (2013) found that adenoviruses were the most frequently found enteric viruses in all environment, while rotavirus was only detected in sewage samples. The same study revealed that these viruses are able travel to confined aquifers in weeks.

The MS2 bacteriophage is the most commonly used surrogate to study the transport of enteric viruses in groundwater. Since the MS2 is harmless to humans and animals, it has been used in field-scale studies (Anders & Chrysikopoulos, 2005; Chendorain *et al.*, 1998; DeBorde *et al.*, 1998; Pang *et al.*, 2005; Ryan *et al.*, 2002; Sinton *et al.*, 1997; Sinton *et al.*, 2000; Woessner *et al.*, 2001). Using MS2 as a tracer, many laboratory-scale studies have investigated the effect of temperature (Gitis *et al.*, 2011), groundwater chemistry (Gitis *et al.*, 2011; Kinoshita *et al.*, 1993; Sadeghi *et al.*, 2011; Zhuang & Jin, 2003; 2008) and the presence of organic

matter (Cao *et al.*, 2007; Wall *et al.*, 2008; Walshe *et al.*, 2010; Weaver *et al.*, 2013) on virus transport. The transport of MS2 has been compared under different flow conditions (Keller *et al.*, 2004; Syngouna & Chrysikopoulos, 2012) and under saturated vs. unsaturated conditions (Anders & Chrysikopoulos, 2009; Gitis *et al.*, 2011; Han *et al.*, 2006; Jin *et al.*, 2000a; Keller & Sirivithayapakorn, 2004; Torkzaban *et al.*, 2006). Using MS2 together with other surrogates, the effect of virus size, pI and hydrophobicity on virus transport has been investigated (Dowd *et al.*, 1998; Kinoshita *et al.*, 1993; Mondal & Sleep, 2013; Weisbrod *et al.*, 2013). MS2 has been used to study virus transport in sewage (Bradford *et al.*, 2006; Charles *et al.*, 2004; Powelson & Gerba, 1994), irrigation (Enriquez *et al.*, 2003) and to test the efficacy of sand filters used in water treatment (Aronino *et al.*, 2009; Hijnen *et al.*, 2004).

The MS2 transport has been compared to the transport of enteric viruses in laboratory studies using the same experimental set up for the different viruses. MS2 was demonstrated to behave similarly to the same-sized Aichi virus (human pathogen) during their transport through 10 cm long columns packed with neutral, goethite- and aluminium oxide-coated sand (Attinti *et al.*, 2010). The MS2 successfully mimicked the transport of the coxsackievirus, but overestimated the recovery of the poliovirus (Schijven *et al.*, 2003). Other studied showed the MS2 had little or no retention in columns packed with quartz sand, whereas rotavirus and Norwalk virus were retained significantly (Herbold-Paschke *et al.*, 1991; Redman *et al.*, 1997).

Several laboratory and field experiments have been published on DNA transport in the subsurface environment. Results of those laboratory experiments suggest that in spite of the degradation of DNA in soil under saturated and unsaturated conditions, DNA was able be transported through the 10 – 60 cm long columns suggesting that DNA can reach the groundwater (Ceccherini *et al.*, 2007; Poté *et al.*, 2003; Poté *et al.*, 2007). Field-scale studies also suggested that DNA persists in both saturated groundwater and in the vadose zone and able to travel long distances (e.g. released at an agricultural field and reach a drinking water supply) like enteric viruses (Poté *et al.*, 2009; Sabir *et al.*, 1999; Sabir *et al.*, 2000).

The DNA tracers can be easily quantified by highly sensitive qPCR (Foppen *et al.*, 2011; Sabir *et al.*, 1999). As the DNA is negatively charged electrostatic interactions may occur between DNA and positively charged solid surfaces in the groundwater, and these interactions are influenced by solution chemistry (Rysz & Alvarez, 2006).

The usefulness of silica nanoparticles with size of 150 nm and 550 nm, labelled with short DNA sequences as tracers for groundwater studies has been investigated (Yang *et al.*, 1996). The particles were injected into a silica sand column, and showed significant retardation. The transport of the particles with different size showed deviation, suggesting that the DNA-labelled particles have potential as tracers for groundwater studies.

In this study, the transport of rotavirus, adenovirus, MS2 and surface modified (DNA-labelled and protein-coated) silica nanoparticles in porous media was investigated. The transport of the particles was studied in column experiments under saturated conditions using two natural aquifer media (fine gravel and fine sand). The flow rate and the composition of the electrolyte were carefully adjusted to mimic the conditions applied in a natural aquifer. The aim was to identify potential surrogates, which may mimic the transport behaviour of the adenovirus and rotavirus in groundwater.

6.2 Methods and materials

6.2.1 Aquifer media

The attenuation capacity of two natural aquifer media was investigated. The beach sand (fine sand, d_{50} = 0.19 mm) and the fine gravel (d_{50} = 3 mm) represents the most common natural aquifer media of Canterbury region, New Zealand. Prior to experiments, the media were sieved, washed and autoclaved as described in Appendix III.

6.2.2 Tracers and their quantification

6.2.2.1 Viruses and surrogates

The retention and transport of the rotavirus, the adenovirus and the MS2 bacteriophage were tested in column experiments. The virus stocks were purified as described in Chapter 2 prior to the experiments. The transport of the unpurified MS2 bacteriophage was also studied. For quantification qPCR (for adenovirus), qRT-PCR (for rotavirus and MS2) and plaque assay (for MS2) was used as described in Chapter 2. Several surface modified nanoparticles were tested in the column experiments. All nanoparticles were DNA-labelled as described in Chapter 3, thus the particles could be quantified by qPCR. In this study, the transport of the DNA-labelled nanoparticles and six protein-coated was examined (Table 6.1). In order to

eliminate the unbound DNA from the nanoparticle stocks, the nanoparticles were pelleted by centrifugation at 13,000×g for 20 min and resuspended in 2 mM NaCl pH 7 solution before sample preparation.

Table 6.1 The viruses and nanoparticles tested by column experiments. The detailed description on the virus purification and characteristics of the modified nanoparticles is in Chapter 2 and 3.

Name	Description
Rotavirus	Purified
Adenovirus	Purified
MS2	Purified
MS2-crude	Unpurified from culturing
DNA-SiNP	DNA-labelled silica nanoparticles (70 nm)
Gly-DNA-SiNP	Glycoprotein-coated, DNA-labelled silica nanoparticles (70 nm)
Str-DNA-SiNP	Streptavidin-coated, DNA-labelled silica nanoparticles (70 nm)
PrA-DNA-SiNP	Protein A-coated, DNA-labelled silica nanoparticles (70 nm)
Cas-DNA-SiNP	casein-coated (50 µg/250µL SiNP), DNA-labelled silica nanoparticles (70 nm)
AMBP-DNA-SiNP	AMBP-coated, DNA-labelled silica nanoparticles (70 nm)
DNA-StrSiNP	DNA-labelled silica nanoparticles pre-coated with streptavidin (100 nm)

6.2.2.2 Soluble tracer

A non-reactive solute tracer, bromide, in the form of potassium bromide (KBr; sourced from VWR International, USA) solution was used to test reproducibility of physical condition and to obtain water flow parameters. The KBr solution was injected together with the viruses/nanoparticles in each experiment.

The bromide concentration was determined by high-performance liquid chromatography (HPLC) using an LC 10A HPLC System (Shimadzu, Japan). The samples were filtered through 0.45 µm filters before analysis. An aliquot of 100 µL of each sample was injected into Hamilton PRP-X 100 column (Hamilton Co., USA) containing 10 µm particles with 100 Å pore size. The mobile phase contained 12% acetonitrile, 0.55 g/L NaCl and 0.60 g/L Na_2HPO_4 in water, and the flow rate was adjusted to 2 mL/min. Bromide was detected at the wavelength of 205 nm using a diode array detector (Shimadzu, Japan). Dilution series of the

KBr solution were used to generate a standard curves and determine the concentration of each sample. The detection limit of this method was 0.1 mg bromide/L.

6.2.3 Column setup

Figure 6.1 illustrates the setup of the column experiments. Prior to each experiment, glass columns (30 cm long × 3.5 cm inner diameter) were packed with the washed and sterilised beach sand or gravel under saturated conditions using the tap and fill method (Bales *et al.*, 1991). The bottom of each column contained a layer of 5 mm glass beads (Paul Marienfeld GmbH, Germany) to avoid the access of the gravel/sand particles to the tubing system. For the same reason, the columns packed with beach sand contained a 1 cm layer of gravel at the bottom and at the top. Based on the dry weight of the media and the water used, the porosity and bulk density of the columns were calculated (Appendix III). The packed columns were wrapped with tin foil to protect the media from light. A flow was introduced by a MilliGAT Pump (Global FIA Inc., USA) at the bottom of the column to maintain saturated conditions.

Prior to the experiments the columns were flushed with 2 – 3 pore volume (PV) of sterilised 2 mM NaCl pH 7 solution. To mimic the low ionic strength and near-neutral pH typical of Christchurch groundwater, this solution was used as a background electrolyte in all experiments.

Each type of virus/nanoparticle was injected in separate columns. In order to test the possible interactions between the viruses, in one beach sand column experiment the rotavirus and the adenovirus were injected together. In each experiment 20 mL of the injection solution (IS) containing the viruses/nanoparticles and the bromide was injected at the bottom of the column (Figure 6.1). Immediately before injection the ISs were filtered through 0.22 µm and 0.1 µm filters to generate monodisperse particle solution. In the case of two beach sand column experiments, where DNA-SiNP and Cas-DNA-SiNP was injected, the ISs were filtered through 0.22 µm filters only. According to Zetasizer measurements, the 0.22 µm filtration also created monodisperse nanoparticle solution (data not shown). The final concentration of the rotavirus and the adenovirus ISs was adjusted to ~ 10^8 gc/mL and the concentration of the silica nanoparticle ISs was 10^8 DNA copies/mL. The MS2 was injected in various concentrations between 10^3 and 10^7 pfu/mL. The bromide concentration of the ISs was adjusted to approximately 50 mg/L.

After the injection the columns were washed with the 2 mM NaCl pH 7 solution at a constant flow rate of 1.33–1.40 mL/min for 400 min (4.5 PV). Fractions of every 5 min (80 fractions altogether) were collected by an FC 204 Fraction Collector (Gilson Inc., USA). The weight of the tubes collecting the fractions was measured before and after the experiment to get the weight of the fractions. The pH of the ISs and every tenth fractions was measured. The media was discarded after each experiment. When sufficient amount of material was available, experiments were performed in replicates. In total, 19 gravel and 21 beach sand column experiments, were performed and analysed.

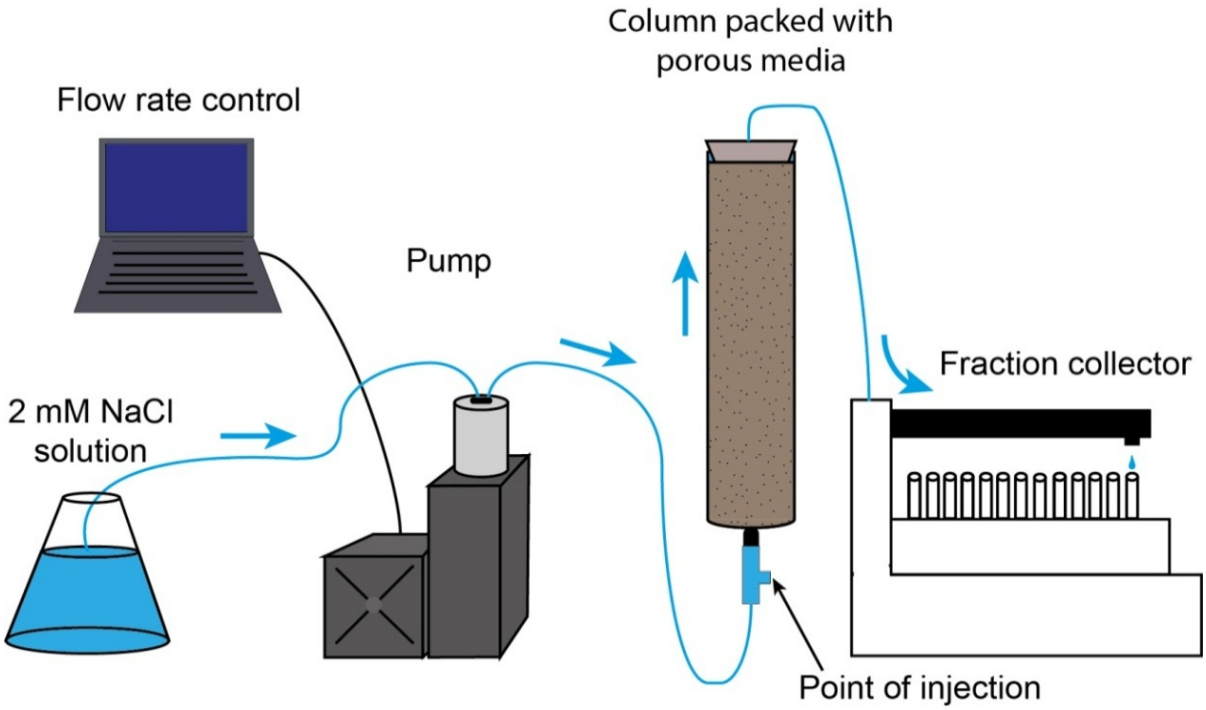

Figure 6.1 Schematic illustration of the column experiment used for particle-transport studies. The blue arrows show the water flow.

6.2.4 Data analysis

Based on the tracer concentrations in the IS (C_0) and the fractions collected (C), and the relative concentrations (C/C_0) were determined. The actual flow rate (Q) was calculated by dividing the volume of the fractions (equals to the weight of the fraction, as the density of water is 1 g/mL) by the sampling interval (5 min).

Breakthrough curves (BTC) showing the relative concentration versus time were generated and compared. The mass recovery percentile (Rec%) was calculated using the following formula:

$$Rec\% = \frac{\sum_{i=1}^{80} C_i * V_i}{C_0 * V_0} * 100\%$$

where C_i and V_i are the concentration and volume of each fraction, and C_0 and V_0 are the concentration and volume of the IS.

6.3 Results

6.3.1 Column experiments with gravel

Table 6.2 summarises the experimental conditions and the calculated recoveries of the gravel column experiments. The experiments were set up in replicates (n = 2) for all viruses and nanoparticles except for DNA-SiNP (n = 1). The flow rate of all experiments varied between 1.33 – 1.36 mL/min, based on the averages of the actual flow rates determined for the 80 fractions collected in each experiment. The pH of the fractions was 6.40 – 6.98 in all experiments. The rotavirus, adenovirus and nanoparticle concentration of all ISs was 1.15 – 3.51×10^8 gc/mL or DNA copies/mL. The MS2 was studied in two concentrations. The samples were analysed by plaque assay when low concentration of MS2 was injected (1.56 – 1.64×10^4 pfu/mL), and by qRT-PCR, when high IS concentration was applied (1.15 – 2.42×10^8 gc/mL). In one of the replicated experiments where high concentration of MS2 was injected the samples were analysed by both quantification methods. The measured bromide concentration of the ISs was 37.47 – 53.42 mg/L.

In the gravel column experiments all particles showed high recoveries (Rec% = 23.1 – 115.8). The transport of the viruses/nanoparticles was very similar to the transport of the soluble tracer (Figure 6.2). The replicate experiments showed high reproducibility (Figure 6.3). The variation observed in the recovery of the replicate experiments of rotavirus, PrA-DNA-SiNP and Cas-DNA-SiNP could be a result of the heterogeneity of the aquifer media.

The shape of the rotavirus BTCs (Figure 6.3) was similar to the MS2 bacteriophage and the nanoparticles, showing a similar transport pattern. In contrast, the adenovirus BTCs were

more dispersed and retarded than the BTCs of the other particles, which was probably due to the aggregation of the adenovirus particles during the experiment.

Table 6.2 Experiment conditions and test results of the gravel column experiments. Rec%: recovery percentile. *pfu/mL.

Experiment	run	Q mL/min	pH	Virus/surrogate		Bromide	
				C_0 gc or DNA copies/mL	Rec%	C_0 mg/L	Rec%
Rotavirus	1	1.35	6.68	3.38×10^8	23.1	48.99	76.7
	2	1.35	6.90	2.39×10^8	77.2	46.39	71.0
Adenovirus	1	1.33	6.58	$2.64v10^8$	72.6	52.93	89.4
	2	1.33	6.40	1.42×10^8	40.4	50.77	82.4
MS2 high IS concentration	1	1.34	6.77	1.15×10^8 (3.54×10^7*)	75.1 (87.6)	45.00	73.0
	2	1.36	6.94	2.42×10^8	114.3	43.13	98.3
MS2 low IS concentration	1	1.35	6.90	1.56×10^4*	97.3	37.87	103.1
	2	1.36	6.98	1.64×10^4*	75.0	37.47	105.4
DNA-SiNP	1	1.35	6.96	1.85×10^8	92.6	49.26	95.9
Gly-DNA-SiNP	1	1.34	6.89	2.81×10^8	88.8	40.38	91.5
	2	1.34	n.m.	3.51×10^8	92.9	49.92	89.6
Str-DNA-SiNP	1	1.36	6.88	1.62×10^8	115.8	46.97	94.6
	2	1.35	6.91	1.51×10^8	90.9	47.52	88.0
PrA-DNA-SiNP	1	1.35	6.88	1.26×10^8	112.5	53.42	85.8
	2	1.35	6.94	1.74×10^8	68.9	51.50	89.2
Cas-DNA-SiNP	1	1.35	6.85	3.34×10^8	57.5	42.11	94.5
	2	1.36	6.91	$1.19v10^8$	79.1	42.73	78.8
AMBP-DNA-SiNP	1	1.35	6.94	1.52×10^8	85.3	48.39	88.5
	2	1.35	6.98	1.41×10^8	88.2	47.29	93.1

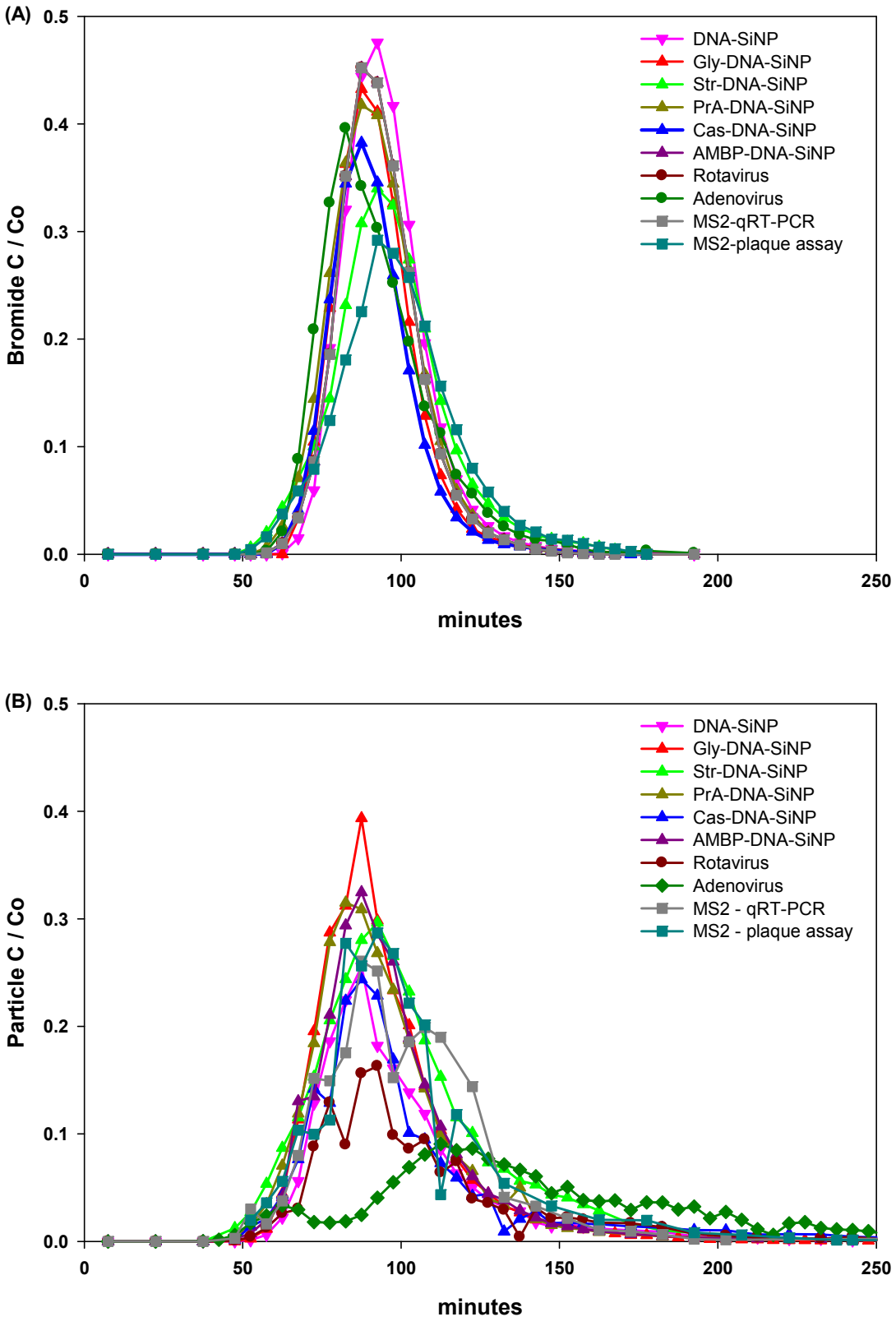

Figure 6.2 Comparison of (A) bromide and (B) particle breakthrough curves for the gravel column experiments. Where experiments were set up in replicates, the lines represent the average relative concentrations. Where there were no replicated experiments, lines represent the individual results.

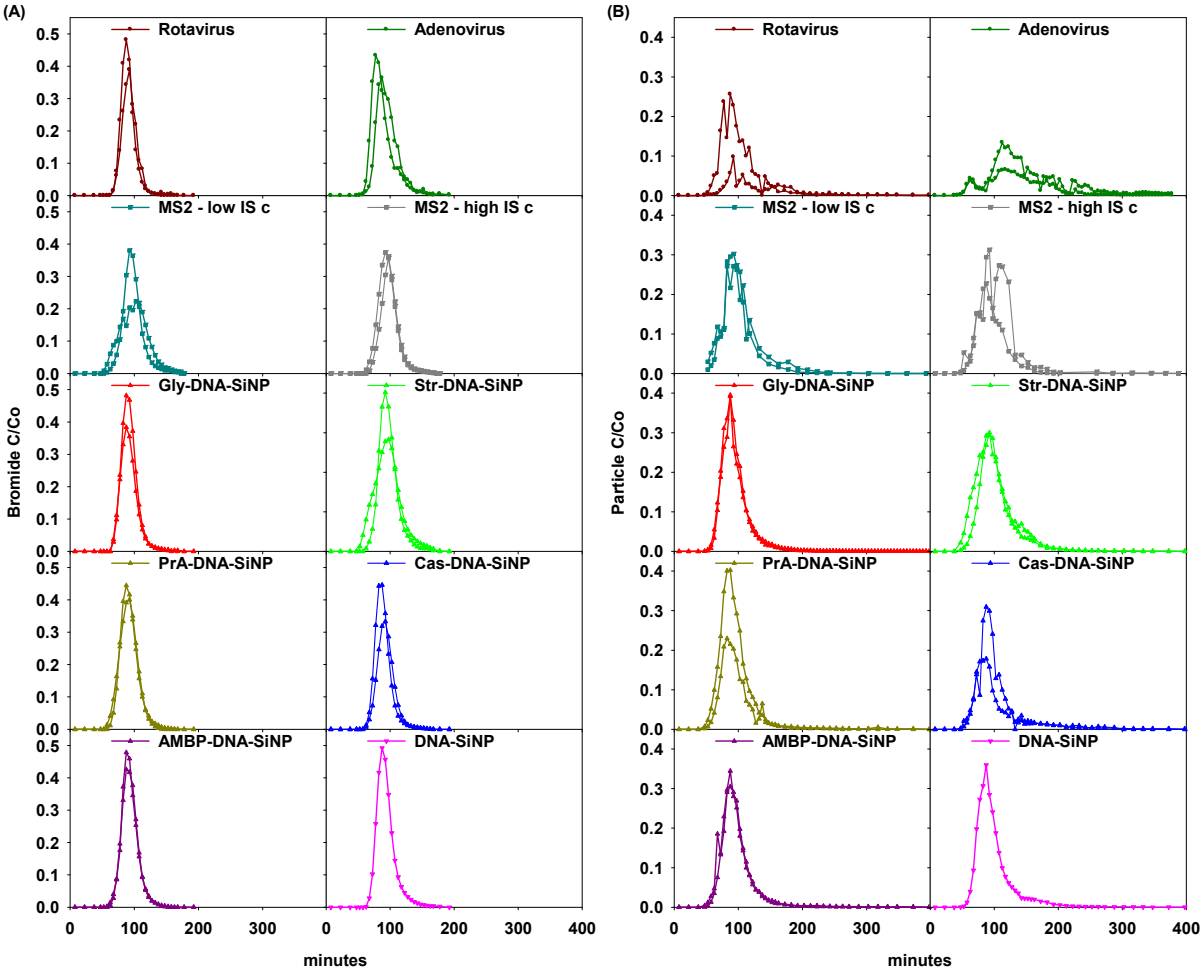

Figure 6.3 (A) Bromide and (B) particle breakthrough curves for the gravel column experiments. The lines represent the results of the individual experiments.

The MS2 bacteriophage was studied at low (1.6×10^4 pfu/mL) and high (3.5×10^7 pfu/mL, 1.2×10^8 gc/mL) IS concentration. The fractions derived from the low IS concentration experiments were analysed by plaque assay, and the fraction of the high IS concentration columns were quantified by qRT-PCR. To assess the differences between the two methods, samples from one of the high IS concentration columns were assayed by both methods. When the plaque assay was used the recovery was shown to be greater resulting in a sharper peak, compared to the results of the qRT-PCR (Figure 6.4).

No difference was observed in the recovery and the BTCs of the MS2 when injected at different concentrations (Figure 6.3). In one of the replicated experiments where the samples were analysed by qRT-PCR the BTC showed double peaks, which is typical when particles have different size populations and/or different attachment rates probably due to aggregation (Figure 6.3). The BTCs for the MS2 analysed by plaque assay showed single peaks.

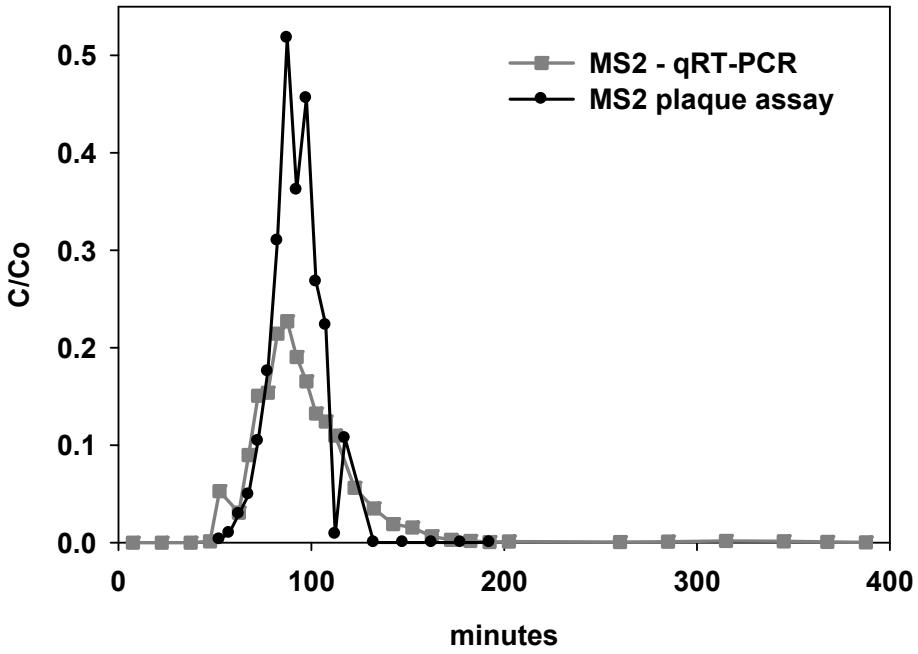

Figure 6.4 Comparison of the plaque assay and the qRT-PCR quantification using samples of one of the gravel columns where the MS2 bacteriophage was injected at high concentration (1.15×10^8 gc/mL / 3.54×10^7 pfu/mL).

6.3.2 Column experiments with beach sand

Table 6.3 summarises the information on the experimental conditions and results of the beach sand columns. The flow rate varied between 1.36 – 1.42 mL/min, and the pH of the 2 mM NaCl electrolyte was slightly increased during passing through the column to 7.19 – 8.06. A single experiment was set up to study the transport of the DNA-SiNP, the DNA-StrNP and the AMBP-DNA-SiNP, and the results of three experiments are available for the Gly-DNA-SiNP.

All particles were injected into separate columns except in one experiment where the rotavirus and the adenovirus were injected together (virus mix). The purified rotavirus and adenovirus was quantified by qRT-PCR and qPCR. The concentration of the IS containing these viruses varied between 1.20×10^7 – 2.46×10^8 gc/mL. Both the purified MS2 (C_0 = 7.50 – 8.85×10^3 pfu/mL) and the MS2-crude (C_0 = 8.10×10^5 – 1.80×10^6 pfu/mL) were analysed using plaque assay for quantification. The modified nanoparticles were injected with concentration of 8.99×10^7 – 2.37×10^8 DNA copies/mL.

Table 6.3 Experiment conditions and test results of the beach sand column experiments. Rec%: recovery percentile. *pfu/mL.

Experiment		run	Q mL/min	pH	Virus/surrogate		Bromide	
					C_0 gc or DNA copies/mL	Rec%	C_0 mg/L	Rec%
Virus mix	**Rotavirus**	1	1.37	7.73	1.20×10^{7}	14.6	47.02	84.6
	Adenovirus				2.46×10^{8}	91.0		
Rotavirus		1	1.37	7.22	3.45×10^{7}	3.3	32.01	73.0
		2	1.40	7.44	1.01×10^{8}	4.9	35.18	73.0
Adenovirus		1	1.38	7.51	1.77×10^{8}	63.5	48.82	83.9
		2	1.36	n.m.	2.05×10^{8}	50.9	44.28	93.5
MS2-crude – plaque assay		1	1.36	7.24	8.10×10^{5}*	108.9	54.52	87.3
		2	1.39	8.06	1.80×10^{6}*	87.3	54.17	83.8
Purified MS2 – plaque assay		1	1.38	7.64	7.50×10^{3}*	133.1	49.09	96.2
		2	1.40	7.53	8.25×10^{3}*	178.7	41.50	95.5
DNA-SiNP		1	1.39	7.15	1.35×10^{8}	35.3	49.55	83.7
Gly-DNA-SiNP		1	1.40	7.11	1.53×10^{8}	1.1	36.12	90.0
		2	1.42	7.30	2.37×10^{8}	12.5	35.16	87.4
		3	1.41	7.38	2.00×10^{8}	0.2	44.59	93.1
Str-DNA-SiNP		1	1.42	7.32	8.99×10^{7}	0.4	43.73	95.5
		2	1.41	7.33	1.31×10^{8}	0.1	41.25	106.0
DNA-StrNP		1	1.42	7.19	1.05×10^{8}	0.3	42.72	105.9
PrA-DNA-SiNP		1	1.41	7.25	1.20×10^{8}	9.1	46.36	91.6
		2	1.41	7.37	1.24×10^{8}	0.9	49.31	98.0
Cas-DNA-SiNP		1	1.39	7.22	1.44×10^{8}	0.2	47.97	89.2
		2	1.36	7.19	1.40×10^{8}	0.2	47.02	89.4
AMBP-DNA-SiNP		1	1.40	7.19	1.70×10^{8}	1.7	51.93	83.8

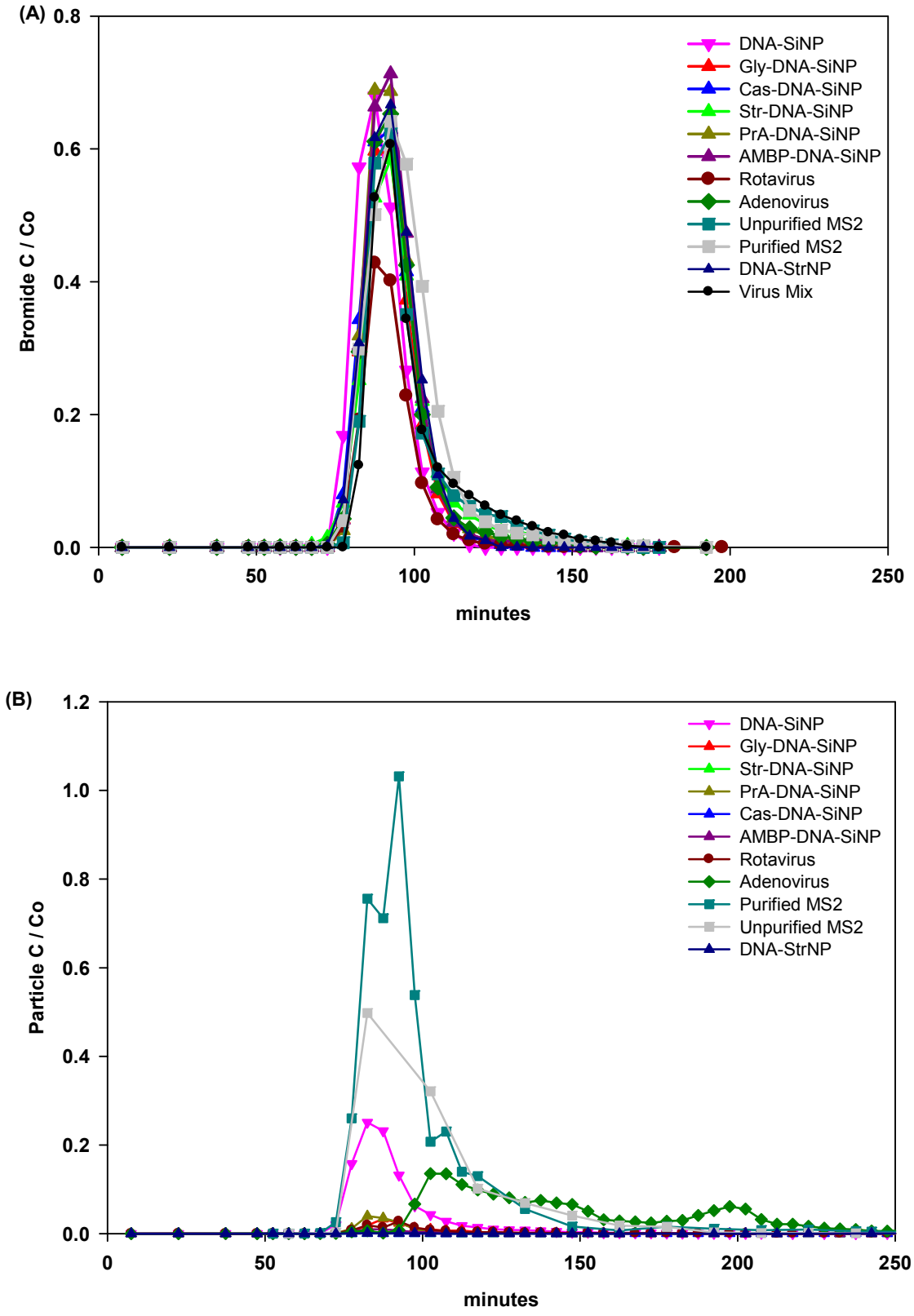

Figure 6.5 Comparison of (A) bromide and (B) particle breakthrough curves for the column experiments with beach sand. Where experiments were set up in replicates, the lines represent the average relative concentrations. Where there were no replicated experiments, lines represent the individual results.

Similar to the gravel column experiments, the bromide analysis showed high recoveries (73.0 – 106.0%) in every experiment. The bromide BTCs were similar in the replicated experiments and between the experiment where different particles were injected (Figure 6.5, Figure 6.6) suggesting that the physical conditions of the column experiments were very similar. However, in some bromide BTCs (e.g. adenovirus, PrA-DNA-SiNP and DNA-StrNP experiments) slight tailing was observed suggesting physical heterogeneity due to column packing. This phenomenon had no demonstrated effect on the bromide recoveries and presumably did not alter the particle transport considerably.

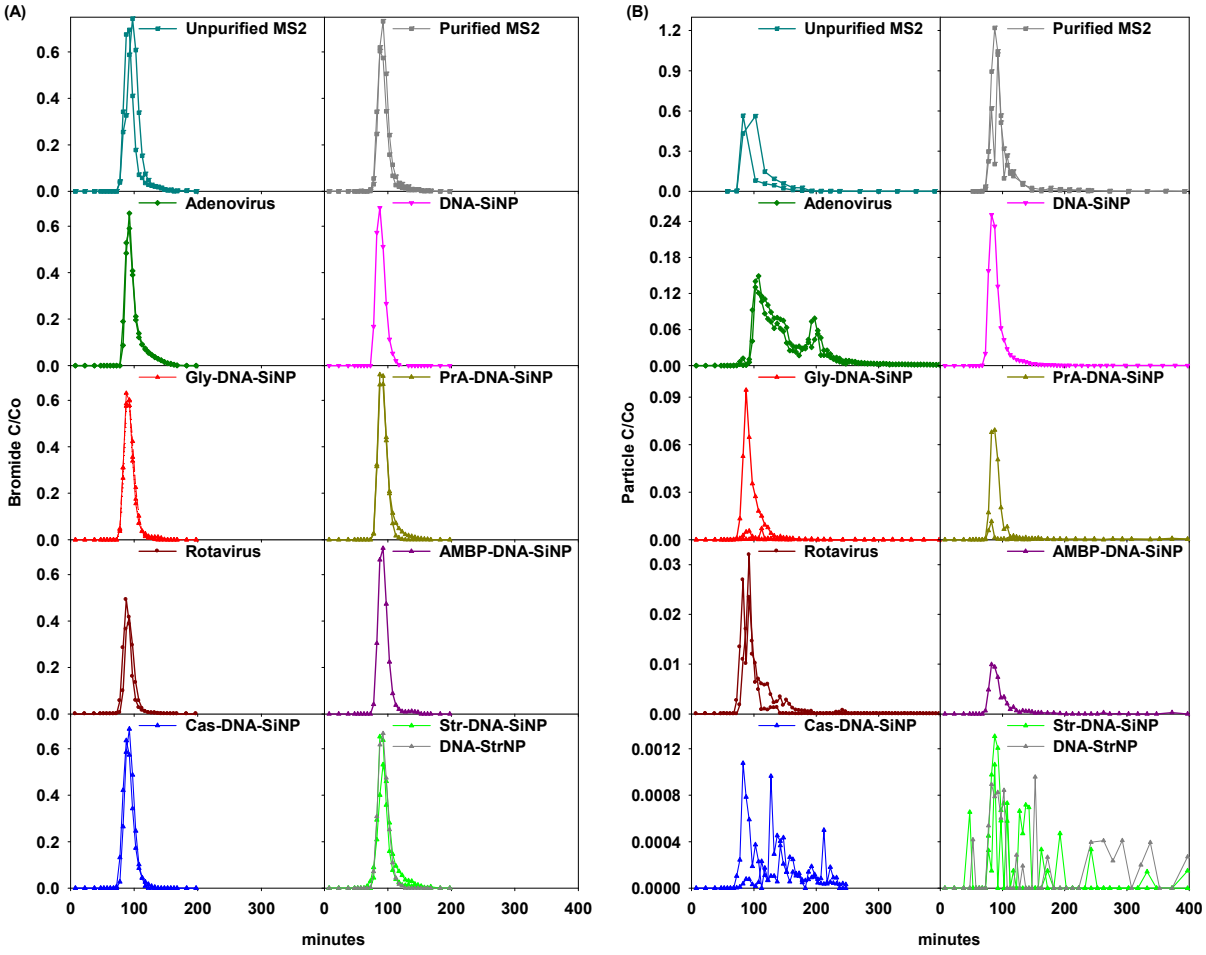

Figure 6.6 (A) Bromide and (B) particle breakthrough curves for the beach sand column experiments. The lines represent the results of the individual experiments.

The transport of both the unpurified and the purified MS2 bacteriophage was examined in replicate experiments. All experiments with MS2 showed high mass recovery (> 87 %) and the virus BTCs were similar to bromide BTCs (Figure 6.6), indicating that the MS2 was not retained during its transport in the beach sand media. The replicated experiments for the unpurified MS2 showed some variation: in one experiment the peak observed on the BTC was

wider than in the other. When the purified MS2 was injected the recovery exceeded 100% (133.1 – 178.7%).

Rotavirus, the adenovirus and the nanoparticles all showed greater retention than the MS2 bacteriophage during their transport through the beach sand columns. Adenovirus had relatively high recovery (50.9 – 63.5%), and the BTCs of the replicated experiments were similar as well. The adenovirus BTCs showed wide, multiple peaks, which could be an indication of virus aggregation. In contrast, the rotavirus showed a great retention with a recovery of 3.3 – 4.9% in the replicated experiments. The BTCs of rotavirus showed little variation.

When the two viruses were injected together (virus mix), their transport changed dramatically (Figure 6.7). The adenovirus recovered at a high degree (91.0%) and the multiple peaks (presented on the BTC of the experiments where the adenovirus was injected alone) merged into one wide plateau. Rotavirus also showed higher recovery (14.6%) when injected with adenovirus than when injected alone. The BTC appeared later than when the rotavirus was injected alone, indicating retardation of rotavirus in the virus mix experiment probably due to virus interaction.

The DNA-labelled nanoparticles showed similar recovery as adenovirus (35.3%). However, unlike adenovirus, the BTC of DNA-SiNP showed a single sharp peak with little retardation. Both the glycoprotein- and protein A-coated nanoparticles showed high variation in the recovery among the replicated experiments (0.2 – 12.5% for Gly-DNA-SiNP and 0.9 – 9.1% for the PrA-DNA-SiNP), however, the shapes of their BTCs were similar. The casein- and the streptavidin-coated nanoparticles showed little recovery (0.1 – 0.4%), and their BTCs did not show distinguished peaks. No difference was observed in the retention and transport of the streptavidin-coated nanoparticles where the DNA-labelling and protein-coating was performed in one step (Str-DNA-SiNP) and where pre-coated particles were DNA-labelled (DNA-StrNP).

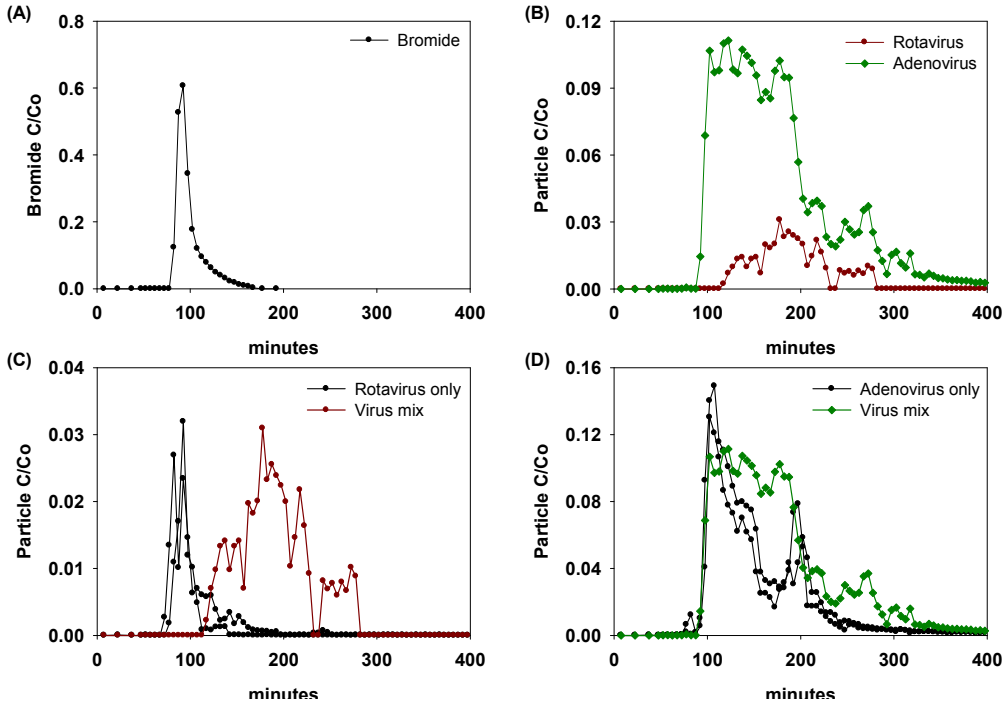

Figure 6.7 Breakthrough curves (BTCs) for the experiment where rotavirus and adenovirus was injected together (virus mix). (A) Bromide BTC, (B) BTCs for rotavirus (brown line) and adenovirus (green line), (C) rotavirus BTC (virus mix, brown line) compared to BTCs where rotavirus alone was injected (black lines), (D) adenovirus BTC (virus mix, green line) compared to BTCs where adenovirus alone was injected (black lines).

6.4 Discussion

6.4.1 Vulnerability of gravel

The retention and transport of rotavirus, adenovirus, MS2 bacteriophage and the surface-modified nanoparticles in gravel column experiments was tested. The results showed that the transport of all viruses/nanoparticles was very similar to the transport of the soluble tracer (bromide). In some cases, the recovery exceeded 100%. Studying the transport of artificial DNA tracers in field experiments, Foppen *et al.* (2011) also noted a 122% recovery, which was explained by analytical errors (J.W. Foppen, personal communication). As the recoveries exceeding 100% were not reproducible, they were most likely due to analytical errors as well.

In my study, the high recoveries of the viruses/nanoparticles suggest that despite the high adsorption capacity of the gravel (discussed in Chapter 5) the viruses are able to travel through gravel aquifers with little reduction when reaction time is insufficient. The high

recovery was probably due to the large particle size of the gravel (2 – 4 mm, d_{50} = 3 mm), hence with the resulting large pore sizes in the column allowing the penetration and transport of the particles (Sinton, 2001). The BTCs of the adenovirus (both experiments) and the MS2 bacteriophage (one experiment) showed multiple peaks, most likely indicating the presence of aggregated virus particles, which attachment and transport pattern differ from the individual virus particles. As discussed in Chapter 2, adenovirus and MS2 readily aggregate in 2 mM NaCl pH 7 solution. The rotavirus and the modified nanoparticles showed single-peak BTCs suggesting no aggregation during their transport through the gravel columns, which corresponds with the results of the rotavirus and nanoparticle aggregation tests (described in Chapter 2 and Chapter 3) showing monodispersed rotavirus is stable for two months, and the nanoparticles are stable for one year in 2 mM NaCl pH 7 solution.

The high recoveries observed for the MS2 bacteriophage in the gravel column experiments allowed the validation of the qRT-PCR method used for phage quantification. Therefore, the IS and the fractions derived from one gravel column experiments where the purified MS2 bacteriophage was injected and tested by qRT-PCR and the traditionally used plaque assay. The observed concentration of the IS suggested lower virus concentrations with the plaque assay than with the qRT-PCR. The differences can be due to particle aggregation, which affects the results of the plaque assay. The BTCs for the MS2 were similar, suggesting that the fractions of the peak contained non-aggregated MS2 particles. The higher peak and slightly greater recovery observed using the plaque assay further verified the presence of aggregates MS2 particles in the IS, which were disaggregated during the transport through the column.

In order to test whether the particle concentration of the IS affects the virus transport, the MS2 bacteriophage was injected in two concentrations (1.6×10^4 and 3.5×10^7 pfu/mL). The recovery and BTCs were similar in all MS2 experiments, suggesting that the injected particle concentration in that range has no effect on the retention and transport of the particles in the gravel aquifer media.

6.4.2 Transport through beach sand

The transport of the viruses and the potential surrogates showed large variation when injected into the beach sand columns. According to the calculated recoveries, four groups of particles (with complete, high, little and no recovery; Figure 6.8) can be distinguished.

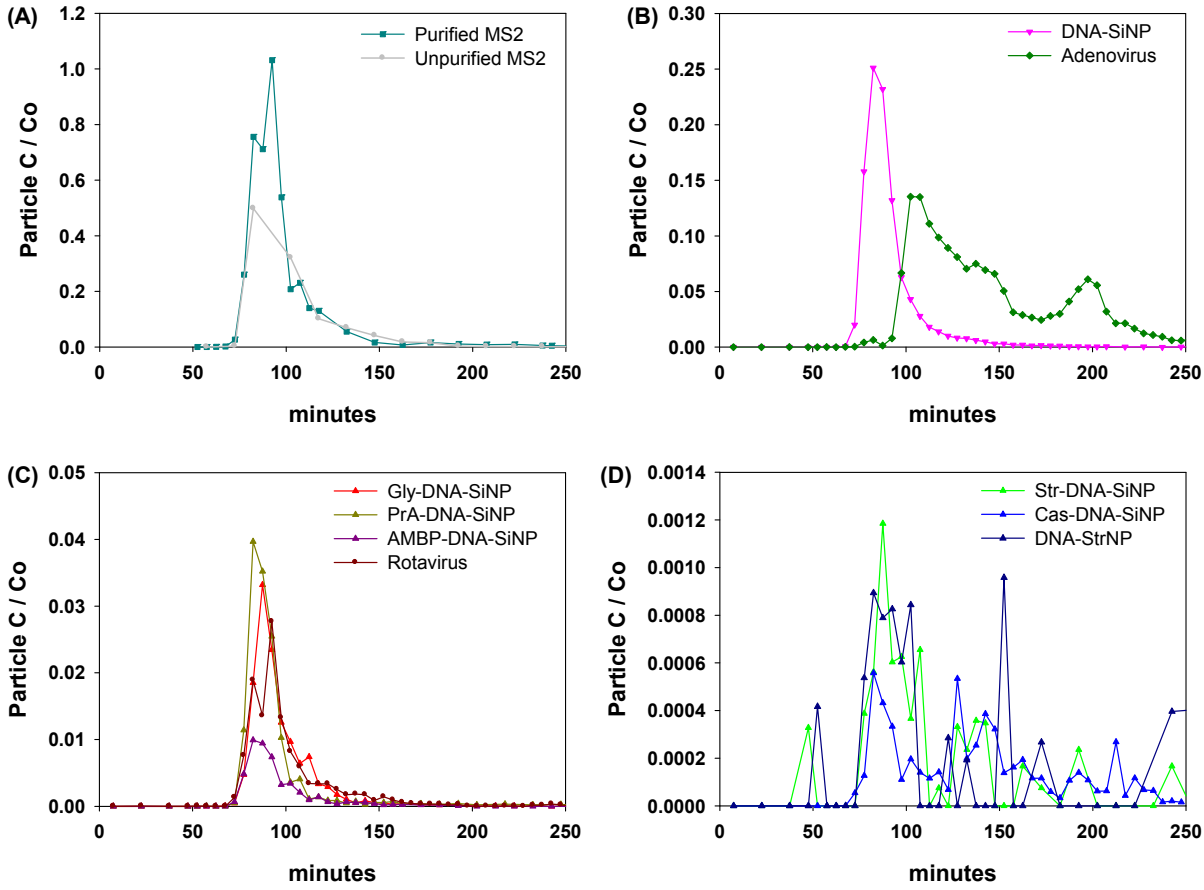

Figure 6.8 Breakthrough curves for the four groups of particles of the beach sand column experiments. (A) complete recovery, (B) high recovery, (C) little recovery, (D) no recovery. Where experiments were set up in replicates, the lines represent the average relative concentrations. Where there were no replicated experiments, lines represent the individual results.

The MS2 bacteriophage showed no retention in the beach sand (Figure 6.8A). Its transport was similar to the transport of the soluble tracer injected together with the MS2. The transport of both purified and unpurified MS2 was investigated. For bacteriophage quantification, the ISs and the fractions were analysed by plaque assay. When the purified MS2 was injected the recovery exceeded 100%. As described above, this phenomenon was most likely due to the aggregation of the MS2 particles in the IS, which would result in low plaque count. During their transport through the column the aggregates may disintegrate, and the plaque assay of the fractions better reflected the number of the virus particles.

The adenovirus and the DNA-SiNP were recovered at a high rate (50.9 – 63.5% and 35.3%, respectively; Figure 6.8B). The multiple peaks observed on the BTCs of the adenovirus were a result of aggregation during its transport through the beach sand columns. Particle aggregation was not observed during the transport of the DNA-SiNP. Thus, despite of the

similar recoveries the DNA-SiNP did not satisfactorily mimic the transport pattern of the adenovirus.

The rotavirus, the glycoprotein-, the protein A- and the AMBP coated nanoparticles were recovered at a low amounts (Figure 6.8C). The average recovery was between 1.7% and 5.0%. The rotavirus transport was similar in the replicate experiments. In contrast, the recovery observed in the replicate experiments for the glycoprotein- and protein-A-coated nanoparticles showed high variation, which could be a result of the heterogeneity of the beach sand or of the differences in the kinetics of the adsorption/desorption as discussed in Chapter 5. Despite of the differences in the replicated experiments, the overall findings suggest that the glycoprotein-, the protein A- and the AMBP coated nanoparticles represented the retention and transport of the rotavirus in the beach sand.

The streptavidin- and the casein-coated nanoparticles were practically not recovered from the beach sand columns (Rec% = 0.1 – 0.4; Figure 6.8D), thus failed to mimic the transport of the viruses. No difference in the transport of the streptavidin-coated particles labelled and coated in one (Str-DNA-SiNP) or two steps (DNA-StrNP) was observed, further verifying that the two labelling/coating methods resulted in particles with similar characteristics.

6.4.3 Effects of physico-chemical characteristics on particle transport

The viruses and the potential surrogates have been characterised in terms of their size, surface charge and hydrophobicity. The results are discussed in Chapter 2 and Chapter 3 and summarised in Table 6.4 together with the percentage recoveries derived from the gravel and beach sand column experiments.

In both aquifer media, the recovery of the MS2 bacteriophage was close to 100%, which was probably due to the small size of the phage (25 – 30 nm). The average size (measured by Zetasizer) of the other viruses and nanoparticles was larger: 70 – 90 nm, except for the DNA-StrNP. The observed large size (170 nm) of the DNA-StrNP was probably a result of the aggregation of the nanoparticles. The size measurements of the adenovirus and the MS2 bacteriophage also showed a tendency for aggregation, which was resulted in multiple peaks in the BTCs of the gravel and beach sand column experiments (Figure 6.3 and Figure 6.5). Only one column experiment was set up for the DNA-StrNP. The particles were hardly recovered, thus the aggregation of the particles during their transport was not indicated.

Table 6.4 The average size, zeta potential (ZP), hydrophobicity determined by modified MATH assay (H%) and recovery (Rec%) of the viruses and the potential surrogates. n.d.: not determined. *Particles tend to aggregate over time.

Particle	Size (nm)	ZP (mV)	H% (%)	Rec% $_{gravel}$ (%)	Rec% $_{beach\ sand}$ (%)
MS2	25 – 30*	–24	98	> 75	> 87
Rotavirus	79	–24	42	23 – 77	3 – 5
Adenovirus	74*	–22	89	40 – 73	51 – 63
DNA-SiNP	71	–41	0	93	35
Gly-DNA-SiNP	68	–41	76	89 – 91	0.2 – 13
Str-DNA-SiNP	88	–44	55	> 91	0.1 – 0.4
DNA-StrNP	170*	–42	n.d.	n.d.	0.3
PrA-DNA-SiNP	90	–40	24	> 69	0.9 – 9
Cas-DNA-SiNP	75	–40	34	57 – 79	0.2
AMBP-DNA-SiNP	82	–41	18	85 – 88	2

Particles with similar size had different recoveries in columns packed with beach sand, suggesting that other features also influence the transport. The ZP and the hydrophobicity of the viruses and the nanoparticles were also measured, but no direct correlation was found between these characteristics and the particle transport pattern in either aquifer media (Table 6.4). The size, ZP, hydrophobicity, shape and density of the protein-coated nanoparticles were all similar, suggesting the amino acid content and structure of the proteins used for coated had a major effect on the transport of the particles.

6.5 Conclusions

The results of the gravel column experiments suggest that the gravel aquifer is vulnerable to virus contamination, as all particles, including the enteric viruses, travelled through the columns with little retention. No remarkable difference in the transport of the different particles was observed.

The beach sand column experiments demonstrated that the MS2 bacteriophage, the most commonly used surrogate in groundwater studies, did not represent the behaviour of the adenovirus and rotavirus. The results show that the MS2 overestimated the recovery of the adenovirus and rotavirus by 1 and 2 orders of magnitude, respectively. That is, MS2 is a

highly conservative surrogate for adenovirus and rotavirus and may imply more treatment is required than the likely risk. The DNA-labelled nanoparticles recovered from the beach sand columns at similar rate as the adenovirus, however, the nanoparticles failed to mimic the transport pattern of the aggregated adenovirus. The streptavidin- and casein-coated nanoparticles were poorly recovered from the beach sand columns, therefore these particles are not suitable surrogates for either of the enteric viruses. The glycoprotein- the protein A- and the AMBP coated nanoparticles successfully mimicked the transport of the rotavirus. Despite the observed variations of the recoveries between some of the replicated experiments, these particles are promising surrogates for rotavirus.

The usefulness of the qPCR-based quantification in column studies was also demonstrated. The qPCR-based techniques reduce the time of virus quantification from days – weeks to hours. The q(RT)-PCR is also more sensitive and cost effective than the culturing-based assays. Using q(RT)-PCR the numbers of aggregated particles are determined accurately.

Chapter 7.
Conclusions and future research

7.1 Summary and conclusions

Safe and clean drinking water is vital worldwide. In order to attain and maintain the quality of drinking water, the protection of the water sources (surface water and groundwater) is essential. The presence of pathogens, e.g. enteric viruses in groundwater has been a primary focus point in public health research. Previous studies have used bacteriophages to investigate the fate and behaviour of viruses in groundwater. Although some bacteriophages are structurally similar to the enteric viruses, their physico-chemical characteristics can differ from the target pathogens. Due to these dissimilarities their adsorption, persistence and transport in the environment often differ as well.

The aim of this study was to examine the usefulness of DNA-labelled and protein-coated silica nanoparticles as surrogates for rotavirus and adenovirus, two important enteric viruses that are of health concern globally. The hypothesis is that particles with similar properties to the target viruses may have similar retention and transport behaviours in groundwater. In order to construct these surrogates, a better understanding of the characteristics of the rotavirus and adenovirus was needed. For reliable results, the viruses were first purified to eliminate any residual impurities derived from culturing, and then their size, surface charge, hydrophobicity and concentration was determined. Then the surrogates were designed, constructed and their characteristics also determined and compared to the viruses.

The surrogates were carboxylated silica nanoparticles with similar shape, size and density to the viruses, labelled with dsDNA for quantification. The surface of the surrogates was further modified by coating with carefully selected proteins with similar surface charge to the viruses. The proteins used for coating were the human α_1-acid-glycoprotein and AMBP (α_1-microglobulin/bikunin precursor), the bacterial streptavidin and protein-A, and the bovine α-casein. Finally, the adsorption, degradation and transport of the viruses and the six surrogates were examined in laboratory studies, and the results were compared. In order to have a better

understanding on the usefulness of these surrogates, the results of the characterisation and validation were compared to a commonly used virus surrogate, the MS2 bacteriophage.

In order to mimic groundwater in the laboratory studies, 2 mM NaCl pH 7 solution was used in each experiment. This solution reflects the low ionic strength and neutral pH typical of the groundwater of Christchurch, New Zealand. For the degradation, adsorption and transport studies natural aquifer media (collected in Canterbury, New Zealand) were used, which are commonly found in local aquifers. These experiments were setup under saturated conditions, however, due to regular sampling, the air could not be eliminated from the samples of the degradation studies. Due to health and safety concerns the experiments on the enteric viruses were undertaken in a biosafety cabinet present in a physical containment 2 (PC2) laboratory. As the temperature could not be controlled in these experiments, all studies were performed at room temperature (20 – 23°C), which was higher than the temperature of the groundwater in New Zealand (11 – 18°C, based on the data from the New Zealand Ministry for the Environment, 2013).

New methods were developed for the purification of the rotavirus and the MS2 bacteriophage. The methods were based on size exclusion chromatography using a fast liquid chromatography system with a poly-methacrylate column. With this setup large quantities (1 mL) of viruses could be purified in each run with high recovery. Further examinations showed that purified virus stocks contained high concentration of infectious virus particles, while the amount of impurities and free nucleic acids were reduced to a level which had no effect on the further characterisation of the viruses. The size exclusion chromatography introduced during this work is a fast and affordable way to purify viruses for various purposes, and a good alternative if limited time is available or if equipment for traditional purification methods (e.g. ultracentrifugation) is not accessible.

The adenovirus stocks were purified using a commercially available purification kit, which has been shown to produce highly pure virus stocks with high infectivity. The characterisation of the purified adenovirus performed in this study verified the presence of high number of intact adenovirus particles in the purified stocks, while non-encapsidated virus DNA was not present.

For quantification of all the viruses used in this study, new qPCR and qRT-PCR protocols were designed and used. These allow for rapid and accurate quantification of the viruses. The

runs are performed in 75 min and are more sensitive (detection limit: 1 – 3 genome copies/μL) than the traditionally used culturing. As the qPCR-based methods are not sensitive to aggregation of the virus particles, they may provide more accurate representation of the actual virus number than the quantification via culturing. For the quantification of the RNA viruses, rotavirus and MS2 bacteriophage, a single-step qRT-PCR was used, which incorporated the reverse transcription of the virus RNA and the DNA amplification in one step, reducing the time required for performing the run and the risk of cross-contamination.

The PCR-based methods detect any target RNA/DNA in the samples, even if the nucleic acids are non-encapsidated. Therefore, the PCR may overestimate the number of intact and infectious virus particles. In this study, the virus stocks used were purified, and therefore the free viral nucleic acids were eliminated. The purified virus stocks were stored at –80°C, where they were all stable for 6 – 9 months. Hence all experiments were carried out in six months after purification. Individual size and surface charge determinations and the adsorption and transport studies required only seven hours, thus the virus inactivation was considered insignificant. In the virus degradation studies (discussed in Chapter 4) the emergence and increase of the non-encapsidated viral nucleic acids through the experiments were considered. Therefore, DNase treatment for adenovirus and filtration for rotavirus samples were used prior to qPCR/qRT-PCR. The DNase treatment eliminated all free viral DNA from the samples, while the intact virus particles were left unaffected. The filtration was also suitable for eliminating the nucleic acids, however, some loss (approximately 20%) of the intact virus particles was observed. Thus, the current method is only suitable for determining relative concentrations. The infectivity of these intact particles may be questionable, however, previous findings suggest that the results of DNase treatment combined with qPCR reflect the number of infectious virus particles (Fongaro *et al.*, 2013). Overall, these techniques give a good interpretation on virus concentration, and, considering the poor sensitivity of culturing, are valuable tools to quantify viruses.

For construction of the surrogates, silica nanoparticles were labelled with a 302 bp dsDNA marker for particle detection by agarose gel electrophoresis and accurate quantification by qPCR. The DNA-labelling and protein-coating of the nanoparticles were accomplished by a simplified two-step EDC method which allowed covalent bond between the amine-groups of molecules and carboxylated surfaces. The EDC method is commonly used for protein-coating of carboxylated particles, and has been used to label microspheres (0.15 μm and 0.55 μm in

diameter) with short, single stranded oligonucleotides (Yang *et al.*, 1996). However, this is the first study where a long (302 bp), dsDNA sequence was used for labelling nanoparticles. According to the results of various methods used for validation (e.g. gel electrophoresis, qPCR and surface charge measurements), the DNA-labelling was successful and resulted in approximately one DNA tag/nanoparticle. Thus the nanoparticles could be quantified by qPCR, and the results represented the concentration of the particles. Further validation showed that even though the size and charge of the nanoparticles coated with different proteins were similar, their hydrophobicity, adsorption and transport behaviour differed, confirming that the protein-coating was successful.

This study is the first measuring the size and surface charge of the human rotavirus A and the adenovirus type 41. The size of all viruses and nanoparticles used in this study was measured using TEM and Zetasizer. The size of the adenovirus and the rotavirus was measured by both methods yielding similar results. The size of the rotavirus was 78 nm in diameter, whereas the adenovirus was slightly smaller, 74 nm in diameter, which both correlate with previous findings regarding porcine rotavirus and adenovirus type 2 (Gutierrez *et al.*, 2009; Wong *et al.*, 2012). The size of the MS2 was 26 nm, determined by TEM, also correlating with previous studies (Gutierrez *et al.*, 2009). Overall findings based on numerous Zetasizer measurements suggest that the size of the 70-nm silica nanoparticles was not affected by DNA-labelling and protein-coating, therefore, the particles mimic the size and shape of the two enteric viruses.

Furthermore, this is the first study where time-dependent virus aggregation was monitored using a Zetasizer. The results showed that the aggregation of the rotavirus and adenovirus differed. While rotavirus was stable in size over two months at room temperature, adenovirus aggregated after two weeks at room temperature, and in one day at 4°C, suggesting that low temperature promoted the aggregation of adenovirus. On the contrary, the DNA-labelled and the protein-coated silica nanoparticles were stable in size for at least one year at 4°C, indicating that the nanoparticles are more stable over time than the enteric viruses.

The zeta potential of all the viruses was between –20 and –25 mV, measured by Zetasizer, consistent with previous findings (Gutierrez *et al.*, 2009; Wong *et al.*, 2012). The carboxylated silica nanoparticles were slightly more negatively charged (approximately –38 mV) than the viruses, and the DNA-labelling and protein-coating hardly affected the overall surface charge. According to these findings, the nanoparticles mimic the negative surface

charge of the enteric viruses, thus have similar electrostatic interactions with aquifer media as those viruses. However, the elevated charge of the surrogates may result in slightly stronger electrostatic interactions to oppositely charged surfaces.

It was also noted that the zeta potential of the DNA-labelled nanoparticles decreased in seven months, which was probably due to degradation of the DNA. The results of the agarose gel electrophoresis performed on the DNA-labelled nanoparticles 19 weeks and one year after preparation also supported that. On the other hand, the surface charge of the protein-coated, DNA-labelled nanoparticles was stable for at least one year, and the results of the agarose gel electrophoresis showed no DNA degradation over one year. These findings suggest that the protein-coating may protect the DNA from degradation.

The hydrophobicity of the viruses and nanoparticles was determined using a modified MATH assay, and the order of hydrophobicity was determined. The MS2 bacteriophage was extremely hydrophobic (98%), followed by the adenovirus (89%), the glycoprotein-coated (76%) and the streptavidin-coated nanoparticles (54%). The rotavirus was rather hydrophilic (42%), along with the rest of the nanoparticles (0 – 34%). Therefore, the modified nanoparticles, which are less hydrophobic than the enteric viruses may be better surrogates than the MS2 when hydrophobic matter is present in groundwater.

The preliminary validation and characterisation results showed that the surrogates developed in this study successfully mimic the size, shape and surface charge of the adenovirus and rotavirus. The nanoparticles were less hydrophobic, hence less reactive than the viruses. In contrast, the MS2 bacteriophage is smaller in size, and more hydrophobic than the two enteric viruses, thus its behaviour in aquifer media may differ as well. For studying the enteric viruses, they need to be cultured and purified in large quantities, which takes weeks to achieve, whereas the surface modifications of the nanoparticles can be performed in two days and results in a concentration two orders of magnitude higher than the purified virus stocks. Furthermore, while the viruses are stored and handled with extreme care in specialised environment, the surrogates can be stored in a fridge; they are easy to use and environmentally safe. Considering these advantages, the surface-modified silica nanoparticles will be useful new tools for studying the fate and transport of viruses in the environment.

In order to study the usefulness of the modified nanoparticles as surrogates for the adenovirus and rotavirus, their degradation, adsorption, and transport in aquifer media was investigated.

This is the first study where the rotavirus degradation was examined for prolonged time (one year). The degradation results showed that the DNA-labelled silica nanoparticles were more stable over time than the rotavirus, the adenovirus, even the plasmid DNA. Less than one order of magnitude DNA degradation was observed in the 1.5-year experiment in samples stored in 2 mM pH 7 NaCl solution, and day light did not promote degradation. On the contrary, the results of other long-term experiments, where the DNA-labelled nanoparticles were examined by agarose gel electrophoresis and by Zetasizer, the results suggested some DNA degradation. However, those methods are not as sensitive and accurate as the qPCR used in the degradation study, and the sample concentration used may have been close to their detection limit. Thus even small loss in DNA concentration could result in unreliable results. Both rotavirus and adenovirus were demonstrated to be extremely stable in simulated groundwater. Interestingly, the rotavirus was more stable over time than the adenovirus, however, adenovirus has been more persistent than rotavirus and other enteric viruses in groundwater (Charles *et al.*, 2009; Sidhu *et al.*, 2010). Nonetheless, the degradation of the rotavirus was enhanced by day light, which had little effect on the degradation of the adenovirus.

The findings of the degradation studies suggest that both enteric viruses may be more stable in the environment than previously presumed. This study also showed that DNA-labelled silica nanoparticles may be useful surrogates for the most persistent enteric viruses.

Results of the adsorption studies showed that the two aquifer media commonly found in Canterbury, New Zealand, the fine beach sand and the fine gravel, both remove adenovirus and rotavirus at high rate. The MS2 bacteriophage was found to be more strongly adsorbed to the gravel than the two enteric viruses, however, it was barely adsorbed to the beach sand, thus MS2 over- and underestimated the adsorption of the enteric viruses. All the surface-modified silica nanoparticles, regardless of the type of coating, successfully mimicked the adsorption of the adenovirus to gravel confirming the usefulness of these particles as virus surrogates in similar aquifer media. The adsorption of the nanoparticles to the beach sand showed some variation. Most particles weakly adsorbed to the sand, only the casein-coated nanoparticles adsorbed strongly, reflecting the adsorption of the rotavirus. All nanoparticles along with the rotavirus and MS2 weakly adsorbed to the Ottawa sand as well, whereas the adenovirus showed strong interactions with that sand. The adenovirus and the MS2 bacteriophage strongly adsorbed to the hydrophobic sand, whereas the rotavirus and the

nanoparticles showed weak adsorption. These finding verified the findings of the hydrophobicity assay for the viruses and nanoparticles.

Overall findings of the adsorption of the viruses and nanoparticles to the four types of porous media suggest that the interactions between the nanoparticles and the media are similar but weaker than between the viruses and the media, implying that the surface-modified nanoparticles may be useful surrogates for the enteric viruses. The only nanoparticles that showed strong adsorption to the beach sand was the casein-coated particles overestimating the adsorption of the adenovirus. Thus, these particles may be more useful if hydrophobic materials are present.

The fine gravel and fine beach sand were used for investigating the transport of the viruses and surrogates under saturated condition. Even though the same aquifer media was used in the adsorption and in the transport studies, the results of the experiments differed considerably. The results showed that, regardless of the adsorption capacity of the gravel in batch tests, all viruses and surrogates travelled through the gravel columns with little retention due to insufficient reaction time, suggesting that the gravel aquifers may be vulnerable to contamination with viruses.

The transport of the viruses and nanoparticles showed great variation in the beach sand columns. Results showed that the adenovirus and the DNA-labelled nanoparticles were recovered at a similar degree (35 – 60%) although their transport pattern was different. The rotavirus recovery was lower (3 – 5%), similarly to the glycoprotein-, protein A- and AMBP-coated nanoparticles, suggesting that these nanoparticles are promising surrogates for rotavirus. The streptavidin- and casein-coated nanoparticles were hardly recovered, thus they are not useful for studying the transport of either of the enteric viruses. The observed differences in the transport of the nanoparticles coated with different proteins suggested that the surface structure has a major role in particle transport. Contrary to the transport of enteric viruses and the nanoparticles, the MS2 bacteriophage was not retained in the beach sand, thus overestimating the recovery of the two enteric viruses by 1 – 2 orders of magnitude.

7.2 Implications

The methods developed and used in this study can be utilised in a board range of environmental studies. The size exclusion-based virus purification methods can be used with no or minor modification for the purification of other viruses found in the environment. The purified viruses are suitable for accurate characterisation and other experiments, and give more reliable results than the studies on unpurified virus stocks, where the impurities derived from culturing affect the outcomes.

The qPCR and qRT-PCR methods have been used in many environmental studies for detection and quantification of viruses with success (Pang *et al.*, 2004b; Rodríguez *et al.*, 2009). However, the organic matter can inhibit the polymerase enzymes, and the purification or dilution of the samples is needed prior to the PCR reactions (Tebbe & Vahjen, 1993). Furthermore, PCR-based methods detect not only the viruses, but the viral nucleic acids derived from degraded virus particles, which may be helpful for tracking viral contamination. On the other hand, when focusing on the number of intact and infectious virus particles, PCR can be combined with culturing (as in integrated cell culturing PCR), or the free nucleic acids of the samples can be eliminated by nuclease treatment or filtration. The later methods reduce the time required for virus quantification, and are suitable for viruses that cannot or are hard to be maintained *in vitro*.

For identifying the possible interactions between aquifer media and viruses, the virus characteristics influencing the interactions need to be evaluated. The size and the surface charge can easily be determined by Zetasizer, however, highly concentrated and pure virus stocks are needed for accurate measurements. The hydrophobicity of the viruses can also be determined using the modified MATH assay combined with q(RT-)PCR developed in this study. The test can be performed in 15 min, and by using q(RT-)PCR for quantification the initial virus concentration can be reduced. These methods can be applied for any pathogen found in the environment.

In this study, the investigation of time-dependent virus aggregation using a Zetasizer was carried out. Many long-term studies on virus inactivation/degradation showed signs of aggregation when culturing was used for virus quantification (Charles *et al.*, 2009; Espinosa *et al.*, 2008; Ogorzaly *et al.*, 2010), however, the aggregation under similar experimental conditions was not investigated. For a better understanding on the fate of viruses in the

environment the determination of the aggregation behaviour of viruses using Zetasizer may also be useful.

In this work, the DNA-labelling and protein-coating of the silica nanoparticles was shown to be successful. The particles with different protein-coating had different surface characteristics and it was observed that their behaviour in aquifer media was different as well. Using the two-step EDC method described here, surrogates for other important pathogens can be constructed. Particles of various sizes are available on the market, thus surrogates for other pathogens (bacteria and protozoa) can be designed. For instance, surface-modified nanoparticles with sizes of 20 – 30 nm in diameter may be useful to study the filtration and transport of enteroviruses and hepatitis A and E viruses in groundwater. By using particles of various material and different proteins, the fundamental characteristics of the surrogates (e.g. charge and hydrophobicity) can be altered. Therefore, polystyrene particles coated with highly hydrophobic proteins which tend to aggregate may be able to mimic the hydrophobic pathogens, e.g. adenovirus which adsorption and transport pattern differed from the behaviour of the fairly hydrophilic surrogates use in this study.

These particles are expected to be safe to humans, animals and the environment, hence they can be used in field studies. Furthermore, the surrogates can be used for industrial applications as well. As some pathogens, especially viruses are difficult to filter from water, the efficacy of filtration systems and the adsorption capacity of the filtration media used in drinking water treatment can be tested with the surrogates.

7.3 Future research

My work has focused on determining the physico-chemical characteristics of two enteric viruses, a bacteriophage and several potential surrogates. Laboratory experiments were carried out to study the fate and transport of these viruses and nanoparticles in two natural aquifer media and their adsorption to hydrophobic matter. For further validation of the surrogates, similar experiments should be carried out using other media, such as pumice sand, sewage or soils, under saturated and unsaturated conditions. In order to understand the interactions between the aquifer media, the viruses and the nanoparticles, bivalent cation solution (e.g. $CaCl_2$) instead of NaCl solutions may also be introduced. The experiments described here were all performed at room temperature, which is higher than the temperature

of groundwater. Therefore, the effect of lower temperatures typical in groundwater should be studied as well.

All experiments have been performed in laboratory environment using sterilised solutions and media. The effect of microbes on the persistence and transport of the viruses and the nanoparticles should also be investigated in the future.

7.4 Concluding remarks

The work carried out in this study demonstrated that the silica nanoparticles can be labelled with double stranded DNA and different proteins. These particles successfully mimic the size and surface characteristics of the enteric viruses studied. The various experiments on the validation showed that the surface-modified nanoparticles are able to mimic the behaviour of viruses under different conditions, however, due to the weak interactions applied, may overestimate the recovery of viruses. Overall the DNA-labelled and protein-coated nanoparticles have potential to mimic the behaviour of similar-sized pathogenic viruses.

References

Adams, M. H. (1959). *Bacteriophages*. New York: Interscience publisher.

Adlhoch, C., Kaiser, M., Hoehne, M., Mas Marques, A., Stefas, I., Veas, F. & Ellerbrok, H. (2011). Highly sensitive detection of the group A Rotavirus using Apolipoprotein H-coated ELISA plates compared to quantitative real-time PCR. *Virology Journal* **8**.

Agarwal, A., Sankaran, S., Vajpayee, M., Sreenivas, V., Seth, P. & Dandekar, S. (2007). Correlation of immune activation with HIV-1 RNA levels assayed by real-time RT-PCR in HIV-1 subtype C infected patients in Northern India. *Journal of Clinical Virology* **40**, 301-306.

Ahmad, F., Tourlousse, D. M., Stedtfeld, R. D., Seyrig, G., Herzog, A. B., Bhaduri, P. & Hashsham, S. A. (2009). Detection and occurence of indicator organisms and pathogens. *Water Environment Research* **81**, 959-980.

Alvarez, A. J., Yumet, G. M., Santiago, C. L. & Toranzos, G. A. (1996). Stability of manipulated plasmid DNA in aquatic environments. *Environmental Toxicology and Water Quality* **11**, 129-135.

Alvarez, M. E., Aguilar, M., Fountain, A., Gonzalez, N., Rascon, O. & Saenz, D. (2000). Inactivation of MS-2 phage and poliovirus in groundwater. *Canadian Journal of Microbiology* **46**, 159-165.

Anders, R. & Chrysikopoulos, C. (2009). Transport of Viruses Through Saturated and Unsaturated Columns Packed with Sand. *Transp Porous Med* **76**, 121-138.

Anders, R. & Chrysikopoulos, C. V. (2005). Virus fate and transport during artificial recharge with recycled water. *Water Resources Research* **41**, W10415-10411-W10415-10414.

APHA, AWWA & WPCF (1998). *Standard methods for the examination of water and wastewater, 19th ed.* Washington, D.C.: APHA, AWWA, WPCF.

Arnold, M., Patton, J. T. & McDonald, S. M. (2009). Culturing, storage, and quantification of rotaviruses. *Current Protocols in Microbiology*, 15C.13.11-15C.13.24.

Aronino, R., Dlugy, C., Arkhangelsky, E., Shandalov, S., Oron, G., Brenner, A. & Gitis, V. (2009). Removal of viruses from surface water and secondary effluents by sand filtration. *Water Research* **43**, 87-96.

Atkinson, W., Wolfe, C. & Hamborsky, J., (eds) (2011). *Epidemiology and Prevention of Vaccine-Preventable Diseases*. Washigton, D.C.: Public Health Foundation.

Attinti, R., Wei, J., Kniel, K., Thomas Sims, J. & Jin, Y. (2010). Virus' (MS2, PdblX174, and Aichi) attachment on sand measured by atomic force microscopy and their transport through sand columns. *Environmental Science and Technology* **44**, 2426-2432.

Bae, J. & Schwab, K. J. (2008). Evaluation of murine norovirus, feline calicivirus, poliovirus, and MS2 as surrogates for human norovirus in a model of viral persistence in surface water and groundwater. *Applied and Environmental Microbiology* **74**, 477-484.

Bales, R. C., Hinkle, S. R., Kroeger, T. W., Stocking, K. & Gerba, C. P. (1991). Bacteriophage adsorption during transport through porous media: Chemical perturbations and reversibility. *Environmental Science and Technology* **25**, 2088-2095.

Bales, R. C., Li, S., Maguire, K. M., Yahya, M. T. & Gerba, C. P. (1993). MS-2 and poliovirus transport in porous media: Hydrophobic effects and chemical perturbations. *Water Resources Research* **29**, 957-963.

Bales, R. C., Li, S., Yeh, T. C. J., Lenczewski, M. E. & Gerba, C. P. (1997). Bacteriophage and microsphere transport in saturated porous media: Forced-gradient experiment at Borden, Ontario. *Water Resources Research* **33**, 639-648.

Bangs Laboratories, I. (2002). TechNote 205. Covalent coupling. *KT/MM- 03/2002* **Bangs Lab., Fishers, IN.**

Barth, G. R. & Hill, M. C. (2005). Parameter and observation importance in modelling virus transport in saturated porous media - Investigations in a homogenous system. *Journal of Contaminant Hydrology* **80**, 107-129.

Becker, M. W., Collins, S. A., Metge, D. W., Harvey, R. W. & Shapiro, A. M. (2004). Effect of cell physicochemical characteristics and motility on bacterial transport in groundwater. *Journal of Contaminant Hydrology* **69**, 195-213.

Becker, M. W., Metge, D. W., Collins, S. A., Shapiro, A. M. & Harvey, R. W. (2003). Bacterial Transport Experiments in Fractured Crystalline Bedrock. *Ground Water* **41**, 682-689.

Becker, M. W., Reimus, P. W. & Vilks, P. (1999). Transport and attenuation of carboxylate-modified latex microspheres in fractured rock laboratory and field tracer tests. *Ground Water* **37**, 387-395.

Berk, A. J. (2013). Adenoviridae. In *Fields Virology*, 6. edn, pp. 2 v. p. 1704-1731. Edited by D. M. K. Bernard N. Fields, Peter M. Howley Philadelphia: Wolters Kluwer Health/Lippincott Williams & Wilkins.

Bian, D., Mahanivong, C., Yu, J., Frisch, S. M., Pan, Z. K., Ye, R. D. & Huang, S. (2005). The G12//13-RhoA signaling pathway contributes to efficient lysophosphatidic acid-stimulated cell migration. *Oncogene* **25**, 2234-2244.

Blanc, R. & Nasser, A. (1996). Effect of effluent quality and temperature on the persistence of viruses in soil. *Water Science and Technology* **33**, 237-242.

Blanford, W. J., Brusseau, M. L., Yeh, T. C. J., Gerba, C. P. & Harvey, R. (2005). Influence of water chemistry and travel distance on bacteriophage PRD-1 transport in a sandy aquifer. *Water Research* **39**, 2345-2357.

Borchardt, M. A., Bradbury, K. R., Alexander, E. C., Kolberg, R. J., Alexander, S. C., Archer, J. R., Braatz, L. A., Forest, B. M., Green, J. A. & Spencer, S. K. (2011). Norovirus Outbreak Caused by a New Septic System in a Dolomite Aquifer. *Ground Water* **49**, 85-97.

Borchardt, M. A., Bradbury, K. R., Gotkowitz, M. B., Cherry, J. A. & Parker, B. L. (2007). Human enteric viruses in groundwater from a confined bedrock aquifer. *Environmental Science and Technology* **41**, 6606-6612.

Bosch, A., Pintó, R. M., Villena, C. & Abad, F. X. (1997). Persistence of human astrovirus in fresh and marine water. *Water Science and Technology* **35**, 243-247.

Bosshard, F., Armand, F., Hamelin, R. & Kohn, T. (2013). Mechanisms of human adenovirus inactivation by sunlight and UVC light as examined by quantitative PCR and quantitative proteomics. *Applied and Environmental Microbiology* **79**, 1325-1332.

Bradbury, K. R., Borchardt, M. A., Gotkowitz, M., Spencer, S. K., Zhu, J. & Hunt, R. J. (2013). Source and transport of human enteric viruses in deep municipal water supply wells. *Environmental Science and Technology* **47**, 4096-4103.

Bradford, S. A., Tadassa, Y. F. & Jin, Y. (2006). Transport of coliphage in the presence and absence of manure suspension. *Journal of Environmental Quality* **35**, 1692-1701.

Bruggemann, U. K., H. D.; Doerfler, W. (1985). Increased Infectivity of Extracellular Adenovirus Type 12. *Journal of Virology* **55**, 117-125.

Butler, M., Medlen, A. R. & Taylor, G. R. (1985). Electrofocusing of viruses and sensitivity to disinfection. *Water Science and Technology* **17**, 201-210.

Butot, S., Putallaz, T., Croquet, C., Lamothe, G., Meyer, R., Joosten, H. & Sánchez, G. (2007). Attachment of enteric viruses to bottles. *Applied and Environmental Microbiology* **73**, 5104-5110.

Callahan, K. M., Taylor, D. J. & Sobsey, M. D. (1995). Comparative survival of hepatitis a virus, poliovirus and indicator viruses in geographically diverse seawaters. *Water Science and Technology* **31**, 189-193.

Cao, H., Tsai, F. T. C. & Rusch, K. A. (2007). Virus sorption and transport in saturated sediments as influenced by salinity and soluble organic matter. In *World Environmental and Water Resources Congress: Restoring Our Natural Habitat*. Tampa, FL.

Cao, H., Tsai, F. T. C. & Rusch, K. A. (2010). Salinity and soluble organic matter on virus sorption in sand and soil columns. *Ground Water* **48**, 42-52.

Castello, A. A., Arguelles, M. H., Villegas, G. A., Olthoff, A. & Glikmann, G. (2002). Incidence and prevalence of human group C rotavirus infections in Argentina. *Journal of Medical Virology* **67**, 106-112.

Ceccherini, M. T., Ascher, J., Pietramellara, G., Vogel, T. M. & Nannipieri, P. (2007). Vertical advection of extracellular DNA by water capillarity in soil columns. *Soil Biology and Biochemistry* **39**, 158-163.

Chae, G. T., Stimson, J., Emelko, M. B., Blowes, D. W., Ptacek, C. J. & Mesquita, M. M. (2008). Statistical assessment of the accuracy and precision of bacteria- and virus-sized microsphere enumerations by epifluorescence microscopy. *Water Research* **42**, 1431-1440.

Champ, D. R. & Schroeter, J. (1988). Bacterial transport in fractured rock. A field-scale tracer test at the Chalk River nuclear laboratories. *Water Science and Technology* **20**, 81-87.

Charles, K. J., Schijven, J. F., Baker, D., Roser, D. J., Deere, D. A. & Ashbolt, N. J. (2004). Transport and fate of nutrients and pathogens during sewage treatment in a mound system. In *Source of the Document Proceedings of the 10th National Symposium on Individual and Small Community Sewage Systems - On-Site Wastewater Treatment X* pp. 460-469. Sacramento; United States.

Charles, K. J., Shore, J., Sellwood, J., Laverick, M., Hart, A. & Pedley, S. (2009). Assessment of the stability of human viruses and coliphage in groundwater by PCR and infectivity methods. *Journal of Applied Microbiology* **106**, 1827-1837.

Charles, K. J., Souter, F. C., Baker, D. L., Davies, C. M., Schijven, J. F., Roser, D. J., Deere, D. A., Priscott, P. K. & Ashbolt, N. J. (2008). Fate and transport of viruses during sewage treatment in a mound system. *Water Research* **42**, 3047-3056.

Chatterjee, P. K., Vayda, M. E. & Flint, S. J. (1986). Identification of proteins and protein domains that contact DNA within adenovirus nucleoprotein cores by ultraviolet light crosslinking of oligonucleotides 32P-labelled in vivo. *Journal of Molecular Biology* **188**, 23-37.

Chattopadhyay, D., Chattopadhyay, S., Lyon, W. G. & Wilson, J. T. (2002). Effect of surfactants on the survival and sorption of viruses. *Environmental Science and Technology* **36**, 4017-4024.

Chattopadhyay, S. & Puls, R. W. (1999). Adsorption of bacteriophages on clay minerals. *Environmental Science and Technology* **33**, 3609-3614.

Chen, F., Zhu, Y., Tang, X., Sun, Y., Jia, W., Sun, Y. & Han, X. (2011). Dynamic Regulation of PDX-1 and FoxO1 Expression by FoxA2 in Dexamethasone-Induced Pancreatic β-cells Dysfunction. *Endocrinology* **152**, 1779-1788.

Chen, J. Z. S., Ethan C; Aoki, Scott T; Zhang, Xing; Bellamy, A Richard; Dormitzer, Philip R; Harrison Stephen C; Grigorieff Nikolaus (2009). Molecular interactions in rotavirus assembly and uncoating seen by high-resolution cryo-EM. *Proc Natl Acad Sci U S A* **106**, 10644 - 10648.

Chendorain, M., Yates, M. & Villegas, F. (1998). The fate and transport of viruses through surface water constructed wetlands. *Journal of Environmental Quality* **27**, 1451-1458.

Cheung, E. Y., Hnatko, S. I., Gunning, H. & Wilson, J. (1982). Comparison of Rotazyme and direct electron microscopy for detection of rotavirus in human stools. *Journal of Clinical Microbiology* **16**, 562-563.

Chrysikopoulos, C. V. & Aravantinou, A. F. (2012). Virus inactivation in the presence of quartz sand under static and dynamic batch conditions at different temperatures. *Journal of Hazardous Materials* **233-234**, 148-157.

Chu, Y., Jin, Y., Baumann, T. & Yates, M. V. (2003). Ground Water Quality: Effect of Soil Properties on Saturated and Unsaturated Virus Transport through Columns. *Journal of Environmental Quality* **32**, 2017-2025.

Chu, Y., Jin, Y. & Yates, M. V. (2000). Virus transport through saturated sand columns as affected by different buffer solutions. *Journal of Environmental Quality* **29**, 1103-1110.

Clark, K. J., Sarr, A. B., Grant, P. G., Phillips, T. D. & Woode, G. N. (1998). In vitro studies on the use of clay, clay minerals and charcoal to adsorb bovine rotavirus and bovine coronavirus. *Veterinary Microbiology* **63**, 137-146.

Claverie, J. M. & Abergel, C. (2010). Mimivirus: The emerging paradox of quasi-autonomous viruses. *Trends in Genetics* **26**, 431-437.

Cleaves, H. J., Crapster-Pregont, E., Jonsson, C. M., Jonsson, C. L., Sverjensky, D. A. & Hazen, R. A. (2011). The adsorption of short single-stranded DNA oligomers to mineral surfaces. *Chemosphere* **83**, 1560-1567.

Close, M. E., Pang, L., Flintoft, M. J. & Sinton, L. W. (2006). Distance and flow effects on microsphere transport in a large gravel column. *Journal of Environmental Quality* **35**, 1204-1212.

Collins, K. E., Cronin, A. A., Rueedi, J., Pedley, S., Joyce, E., Humble, P. J. & Tellam, J. H. (2006). Fate and transport of bacteriophage in UK aquifers as surrogates for pathogenic viruses. *Engineering Geology* **85**, 33-38.

Corapcioglu, M. Y., Vogel, J. R., Munster, C. L., Pillai, S. D., Dowd, S. & Wang, S. (2006). Virus transport experiments in a sandy aquifer. *Water, Air, and Soil Pollution* **169**, 47-65.

Craun, G. F. (1984). Health aspects of groundwater pollution. In *Groundwater pollution microbiology*, pp. 135-179. Edited by G. Bitton & C. P. Gerba. New York: John Wiley&Sons.

Craun, G. F., Nwachuku, N., Calderon, R. L. & Craun, M. F. (2002). Outbreaks in drinking-water systems, 1991-1998. *Journal of Environmental Health* **65**, 16-23.

Crecchio, C. & Stotzky, G. (1998). Binding of DNA on humic acids: Effect on transformation of Bacillus subtilis and resistance to DNase. *Soil Biology and Biochemistry* **30**, 1061-1067.

Daughney, C. J. & Reeves, R. R. (2006). Analysis of temporal trends in New Zealand's groundwater quality based on data from the National Groundwater Monitoring Programme. *Journal of Hydrology New Zealand* **45**, 41-62.

Davis, J. A., Farrah, S. R. & Wilkie, A. C. (2006). Adsorption of viruses to soil: Impact of anaerobic treatment. *Water Science and Technology* **54**, 161-167.

de Abreu Corrêa, A., Carratala, A., Barardi, C. R. M., Calvo, M., Girones, R. & Bofill-Mas, S. (2012). Comparative inactivation of murine norovirus, human adenovirus, and human jc polyomavirus by chlorine in seawater. *Applied and Environmental Microbiology* **78**, 6450-6457.

De Roda Husman, A. M., Lodder, W. J., Rutjes, S. A., Schijven, J. F. & Teunis, P. F. M. (2009). Long-term inactivation study of three enteroviruses in artificial surface and groundwaters, using PCR and cell culture. *Applied and Environmental Microbiology* **75**, 1050-1057.

Debartolomeis, J. & Cabelli, V. J. (1991). Evaluation of an Escherichia coli host strain for enumeration of F male-specific bacteriophages. *Applied and Environmental Microbiology* **57**, 1301-1305.

DeBorde, D. C., Woessner, W. W., Kiley, Q. T. & Ball, P. (1999). Rapid transport of viruses in a floodplain aquifer. *Water Research* **33**, 2229-2238.

DeBorde, D. C., Woessner, W. W., Lauerman, B. & Ball, P. N. (1998). Virus occurrence and transport in a school septic system and unconfined aquifer. *Ground Water* **36**, 825-834.

Deng, M. Y. & Cliver, D. O. (1995). Antiviral effects of bacteria isolated from manure. *Microbial Ecology* **30**, 43-54.

Desselberger, U. (2000). Rotaviruses: Basic Facts. In *Rotaviruses: Methods and protocols*, pp. 1-8. Edited by J. Gray & U. Desselberger. New Jersey: Humana Press Inc.

Desselberger, U. & Gray, J. (2009). Viral gastroenteritis. *Medicine* **37**, 594-598.

Dika, C., Gantzer, C., Perrin, A. & Duval, J. F. L. (2013). Impact of the virus purification protocol on aggregation and electrokinetics of MS2 phages and corresponding virus-like particles. *Physical Chemistry Chemical Physics* **15**, 5691-5700.

DiMarzio, E. A. & Guttman, C. M. (1970). Separation by flow. *Macromolecules* **3**, 131-146.

Dizer, H., Nasser, A. & Lopez, J. M. (1984). Penetration of different human pathogenic viruses into sand columns percolated with distilled water, groundwater, or wastewater. *Applied and Environmental Microbiology* **47**, 409-415.

Dormond, E., Chahal, P., Bernier, A., Tran, R., Perrier, M. & Kamen, A. (2010). An efficient process for the purification of helper-dependent adenoviral vector and removal of helper virus by iodixanol ultracentrifugation. *Journal of Virological Methods* **165**, 83-89.

Doultree, J. C., Druce, J. D., Birch, C. J., Bowden, D. S. & Marshall, J. A. (1999). Inactivation of feline calicivirus, a Norwalk virus surrogate. *Journal of Hospital Infection* **41**, 51-57.

Dowd, S. E., Pillai, S. D., Wang, S. & Corapcioglu, M. Y. (1998). Delineating the specific influence of virus isoelectric point and size on virus adsorption and transport through sandy soils. *Applied and Environmental Microbiology* **64**, 405-410.

Dulbecco, R. (1952). Production of Plaques in Monolayer Tissue Cultures by Single Particles of an Animal Virus. *Proceedings of the National Academy of Sciences* **38**, 747-752.

Enriquez, C., Alum, A., Suarez-Rey, E. M., Choi, C. Y., Oron, G. & Gerba, C. P. (2003). Bacteriophages MS2 and PRD1 in turfgrass by subsurface drip irrigation. *Journal of Environmental Engineering* **129**, 852-857.

Espinosa, A. C., Mazari-Hiriart, M., Espinosa, R., Maruri-Avidal, L., Méndez, E. & Arias, C. F. (2008). Infectivity and genome persistence of rotavirus and astrovirus in groundwater and surface water. *Water Research* **42**, 2618-2628.

Estes, M. K. & Greenberg, H. B. (2013). Rotaviruses. In *Fields Virology*, 6. edn, pp. 2 v. p. 1347-1401. Edited by D. M. K. Bernard N. Fields, Peter M. Howley Philadelphia: Wolters Kluwer Health/Lippincott Williams & Wilkins.

Farrah, S. R., Goyal, S. M., Gerba, C. P., Conklin, R. H. & Smith, E. M. (1978). Comparison between adsorption of poliovirus and rotavirus by aluminum hydroxide and activated sludge flocs. *Applied and Environmental Microbiology* **35**, 360-363.

Floyd, R. & Sharp, D. G. (1977). Aggregation of poliovirus and reovirus by dilution in water. *Applied and Environmental Microbiology* **33**, 159-167.

Flynn, R., Taylor, R., Kulabako, R. & Miret-Gaspa, M. (2012). Haematite in lateritic soils aids groundwater disinfection. *Water, Air, and Soil Pollution* **223**, 2405-2416.

Flynn, R. M., Rossi, P. & Hunkeler, D. (2004). Investigation of virus attenuation mechanisms in a fluvioglacial sand using column experiments. *FEMS Microbiology Ecology* **49**, 83-95.

Flynn, R. M. & Sinreich, M. (2010). Characterisation of virus transport and attenuation in epikarst using short pulse and prolonged injection multi-tracer testing. *Water Research* **44**, 1138-1149.

Fong, T. T., Mansfield, L. S., Wilson, D. L., Schwab, D. J., Molloy, S. L. & Rose, J. B. (2007). Massive microbiological groundwater contamination associated with a waterborne outbreak in Lake Erie, South Bass Island, Ohio. *Environmental Health Perspectives* **115**, 856-864.

Fongaro, G., Nascimento, M. A. D., Rigotto, C., Ritterbusch, G., Da Silva, A. D. A., Esteves, P. A. & Barardi, C. R. M. (2013). Evaluation and molecular characterization of human adenovirus in drinking water supplies: Viral integrity and viability assays. *Virology Journal* **10**.

Foppen, J. W., Orup, C., Adell, R., Poulalion, V. & Uhlenbrook, S. (2011). Using multiple artificial DNA tracers in hydrology. *Hydrological Processes* **25**, 3101-3106.

Fragneto, G., Su, T. J., Lu, J. R., Thomas, R. K. & Rennie, A. R. (2000). Adsorption of proteins from aqueous solutions on hydrophobic surfaces studied by neutron reflection. *Physical Chemistry Chemical Physics* **2**, 5214-5221.

Frazier, C. S., Graham, R. C., Shouse, P. J., Yates, M. V. & Anderson, M. A. (2002). A field study of water flow and virus transport in weathered granitic bedrock. *Vadose Zone Journal* **1**, 113-124.

Frost, F. J., Kunde, T. R. & Craun, G. F. (2002). Is contaminated groundwater an important cause of viral gastroenteritis in the United States? *Journal of Environmental Health* **65**, 9-14.

Fu, Z. F., Hampson, D. J. & Blackmore, D. K. (1989). Detection and survival of group A rotavirus in a piggery. *Veterinary Record* **125**, 576-578.

Funderburg, S. W., Moore, B. E., Sagik, B. P. & Sorber, C. A. (1981). Viral transport through soil columns under conditions of saturated flow. *Water Research* **15**, 703-711.

Futch, J. C., Griffin, D. W. & Lipp, E. K. (2010). Human enteric viruses in groundwater indicate offshore transport of human sewage to coral reefs of the Upper Florida Keys. *Environmental Microbiology* **12**, 964-974.

Gallay, A., De Valk, H., Cournot, M., Ladeuil, B., Hemery, C., Castor, C., Bon, F., Mégraud, F., Le Cann, P. & Desenclos, J. C. (2006). A large multi-pathogen waterborne community outbreak linked to faecal contamination of a groundwater system, France, 2000. *Clinical Microbiology and Infection* **12**, 561-570.

Gassilloud, B. & Gantzer, C. (2005). Adhesion-aggregation and inactivation of Poliovirus 1 in groundwater stored in a hydrophobic container. *Applied and Environmental Microbiology* **71**, 912-920.

Gentilomi, G. A., Cricca, M., De Luca, G., Sacchetti, R. & Zanetti, F. (2008). Rapid and sensitive detection of MS2 coliphages in wastewater samples by quantitative reverse transcriptase PCR. *New Microbiologica* **31**, 273-280.

Gerba, C. P. (1984). Applied and theoretical aspects of virus adsorption to surfaces. *Advances in Applied Microbiology* **30**, 133-168.

Gerba, C. P. & Bitton, G. (1984). Microbial pollutants: their survival and transport pattern to groundwater. *Groundwater pollution microbiology*, 65-88.

Gerba, C. P., Gramos, D. M. & Nwachuku, N. (2002). Comparative inactivation of enteroviruses and adenovirus 2 by UV light. *Applied and Environmental Microbiology* **68**, 5167-5169.

Gerba, C. P., Wallis, C. & Melnick, J. L. (1975). Fate of wastewater bacteria and viruses in soil. *JIRRIGATDRAINAGE DIVASCE* **101**, 157-174.

Gitis, V., Adin, A., Nasser, A., Gun, J. & Lev, O. (2002). Fluorescent dye labeled bacteriophages - A new tracer for the investigation of viral transport in porous media: 1. Introduction and characterization. *Water Research* **36**, 4227-4234.

Gitis, V., Dlugy, C., Gun, J. & Lev, O. (2011). Studies of inactivation, retardation and accumulation of viruses in porous media by a combination of dye labeled and native bacteriophage probes. *Journal of Contaminant Hydrology* **124**, 43-49.

Goodridge, L., Goodridge, C., Wu, J., Griffiths, M. & Pawliszyn, J. (2004). Isoelectric Point Determination of Norovirus Virus-like Particles by Capillary Isoelectric Focusing with Whole Column Imaging Detection. *Analytical Chemistry* **76**, 48-52.

Gordon, C. & Toze, S. (2003). Influence of groundwater characteristics on the survival of enteric viruses. *Journal of Applied Microbiology* **95**, 536-544.

Goyal, S. M. & Gerba, C. P. (1979). Comparative adsorption of human enteroviruses, simian rotavirus, and selected bacteriophages to soils. *Applied and Environmental Microbiology* **38**, 241-247.

Greening, G. E., Hewitt, J. & Lewis, G. D. (2002). Evaluation of integrated cell culture-PCR (C-PCR) for virological analysis of environmental samples. *Journal of Applied Microbiology* **93**, 745-750.

Grove, S. F., Forsyth, S., Wan, J., Coventry, J., Cole, M., Stewart, C. M., Lewis, T., Ross, T. & Lee, A. (2008). Inactivation of hepatitis A virus, poliovirus and a norovirus surrogate by high pressure processing. *Innovative Food Science and Emerging Technologies* **9**, 206-210.

Guan, H., Schulze-Makuch, D., Schaffer, S. & Pillai, S. D. (2003). The Effect of Critical pH on Virus Fate and Transport in Saturated Porous Medium. *Ground Water* **41**, 701-708.

Gutierrez, L., Li, X., Wang, J., Nangmenyi, G., Economy, J., Kuhlenschmidt, T. B., Kuhlenschmidt, M. S. & Nguyen, T. H. (2009). Adsorption of rotavirus and bacteriophage MS2 using glass fiber coated with hematite nanoparticles. *Water Research* **43**, 5198-5208.

Gutierrez, L., Mylon, S. E., Nash, B. & Nguyen, T. H. (2010). Deposition and aggregation kinetics of rotavirus in divalent cation solutions. *Environmental Science and Technology* **44**, 4552-4557.

Gutierrez, L. & Nguyen, T. H. (2012). Interactions between rotavirus and Suwannee River organic matter: Aggregation, deposition, and adhesion force measurement. *Environmental Science and Technology* **46**, 8705-8713.

Gülser, C., Yilmaz, N. K. & Candemir, F. (2008). Accumulation of Tobacco mosaic virus (TMV) at different depths clay and loamy sand textural soils due to tobacco waste application. *Environmental Monitoring and Assessment* **146**, 235-242.

Han, J., Jin, Y. & Willson, C. S. (2006). Virus retention and transport in chemically heterogeneous porous media under saturated and unsaturated flow conditions. *Environmental Science and Technology* **40**, 1547-1555.

Hansen, J. J., Warden, P. S. & Margolin, A. B. (2007). Inactivation of adenovirus type 5, rotavirus WA and male specific coliphage (MS2) in biosolids by lime stabilization. *International Journal of Environmental Research and Public Health* **4**, 61-67.

Hari Prasad, K. S., Ratha, D. N. & Ojha, C. S. P. (2012). Identification of virus transport parameters in groundwater: Data errors and bias. *Journal of Hydro-Environment Research* **6**, 41-50.

Harvey, R. W., George, L. H., Smith, R. L. & Leblanc, D. R. (1989). Transport of microspheres and indigenous bacteria through a sandy aquifer: Results of natural- and forced-gradient tracer experiments. *Environmental Science and Technology* **23**, 51-56.

Harvey, R. W., Kinner, N. E., Bunn, A., MacDonald, D. & Metge, D. (1995). Transport behavior of groundwater protozoa and protozoan-sized microspheres in sandy aquifer sediments. *Applied and Environmental Microbiology* **61**, 209-217.

Harvey, R. W., Metge, D. W., Mohanram, A., Gao, X. & Chorover, J. (2011). Differential effects of dissolved organic carbon upon re-entrainment and surface properties of groundwater bacteria and bacteria-sized microspheres during transport through a contaminated, sandy aquifer. *Environmental Science and Technology* **45**, 3252-3259.

Harvey, R. W., Metge, D. W., Shapiro, A. M., Renken, R. A., Osborn, C. L., Ryan, J. N., Cunningham, K. J. & Landkamer, L. (2008). Pathogen and chemical transport in the karst limestone of the Biscayne aquifer: 3. Use of microspheres to estimate the transport potential of Cryptosporidium parvum oocysts. *Water Resources Research* **44**.

Harvey, R. W. & Ryan, J. N. (2004). Use of PRD1 bacteriophage in groundwater viral transport, inactivation, and attachment studies. *FEMS Microbiology Ecology* **49**, 3-16.

He, X. Q., Cheng, L., Li, W., Xie, X. M., Ma, M. & Wang, Z. J. (2008). Detection and distribution of rotavirus in municipal sewage treatment plants (STPs) and surface water in Beijing. *Journal of Environmental Science and Health - Part A Toxic/Hazardous Substances and Environmental Engineering* **43**, 424-429.

Heller, M. J. (2002). DNA microarray technology: Devices, systems, and applications. *Annual Review of Biomedical Engineering* **4**, 129-153.

Hendrix, R. W. (2013). Batceriophages. In *Fields Virology*, 6. edn, pp. 2 v. p. 2384-2417. Edited by D. M. K. Bernard N. Fields, Peter M. Howley Philadelphia: Wolters Kluwer Health/Lippincott Williams & Wilkins.

Herbold-Paschke, K., Straub, U., Hahn, T., Teutsch, G. & Botzenhart, K. (1991). Behaviour of pathogenic bacteria, phages and viruses in groundwater during transport and adsorption. *Water Science and Technology* **24**, 301-304.

Hijnen, W. A. M., Beerendonk, E. F. & Medema, G. J. (2006). Inactivation credit of UV radiation for viruses, bacteria and protozoan (oo)cysts in water: A review. *Water Research* **40**, 3-22.

Hijnen, W. A. M., Schijven, J. F., Bonné, P., Visser, A. & Medema, G. J. (2004). Elimination of viruses, bacteria and protozoan oocysts by slow sand filtration. *Water Science and Technology* **50**, 147-154.

Hopkins, R. S., Gaspard, G. B., Williams Jr, F. P., Karlin, R. J., Cukor, G. & Blacklow, N. R. (1984). A community waterborne gastroenteritis outbreak: Evidence for rotavirus as the agent. *American Journal of Public Health* **74**, 263-265.

Horká, M., Kubíček, O., Růžička, F., Holá, V., Malinovská, I. & Šlais, K. (2007). Capillary isoelectric focusing of native and inactivated microorganisms. *Journal of Chromatography A* **1155**, 164-171.

Horswell, J., Hewitt, J., Prosser, J., Van Schaik, A., Croucher, D., MacDonald, C., Burford, P., Susarla, P., Bickers, P. & Speir, T. (2010). Mobility and survival of Salmonella Typhimurium and human adenovirus from spiked sewage sludge applied to soil columns. *Journal of Applied Microbiology* **108**, 104-114.

Hoshino, Y. & Kapikian, A. Z. (2000). Rotavirus Serotypes: Classification and Importance in Epidemiology, Immunity, and Vaccine Development. *Journal of Health Population and Nutrition* **18**, 5-14.

Howard, G., Bartram, J., Pedley, S., Schmoll, O., Chorus, I. & Berger, P. (2006). Groundwater and public health. *Protecting groundwater for health: managing the quality of drinking-water sources London, International Water Association Publishing*, 3-19.

Hunt, R. J., Borchardt, M. A., Richards, K. D. & Spencer, S. K. (2010). Assessment of sewer source contamination of drinking water wells using tracers and human enteric viruses. *Environmental Science and Technology* **44**, 7956-7963.

Jansons, J., Edmonds, L. W., Speight, B. & Bucens, M. R. (1989). Survival of viruses in groundwater. *Water Research* **23**, 301-306.

Jean, J. S., Guo, H. R., Chen, S. H., Liu, C. C., Chang, W. T., Yang, Y. J. & Huang, M. C. (2006). The association between rainfall rate and occurrence of an enterovirus epidemic due to a contaminated well. *Journal of Applied Microbiology* **101**, 1224-1231.

Jiang, S., Ji, S., Tang, Q., Cui, X., Yang, H., Kan, B. & Gao, S. (2008). Molecular characterization of a novel adult diarrhoea rotavirus strain J19 isolated in China and its significance for the evolution and origin of group B rotaviruses. *Journal of General Virology* **89**, 2622-2629.

Jin, Y., Chu, Y. & Li, Y. (2000a). Virus removal and transport in saturated and unsaturated sand columns. *Journal of Contaminant Hydrology* **43**, 111-128.

Jin, Y. & Flury, M. (2001). Fate and transport of viruses in porous media. *Advances in Agronomy* **77**, 39-102.

Jin, Y., Pratt, E. & Yates, M. V. (2000b). Effect of mineral colloids on virus transport through saturated sand columns. *Journal of Environmental Quality* **29**, 532-539.

Jofre, J., Bosch, A., Lucena, F., Girones, R. & Tartera, C. (1986). Evaluation of bacteroides fragilis bacteriophages as indicators of the virological quality of water. *Water Science and Technology* **18**, 167-173.

John, D. E. & Rose, J. B. (2005). Review of factors affecting microbial survival in groundwater. *Environmental Science and Technology* **39**, 7345-7356.

Kalbfuss, B., Wolff, M., Morenweiser, R. & Reichl, U. (2007). Purification of cell culture-derived human influenza A virus by size-exclusion and anion-exchange chromatography. *Biotechnology and Bioengineering* **96**, 932-944.

Kallioniemi, O. P., Kallioniemi, A., Piper, J., Isola, J., Waldman, F. M., Gray, J. W. & Pinkel, D. (1994). Optimizing comparative genomic hybridization for analysis of DNA sequence copy number changes in solid tumors. *Genes Chromosomes and Cancer* **10**, 231-243.

Karen, K. A. & Hearing, P. (2011). Adenovirus Core Protein VII Protects the Viral Genome from a DNA Damage Response at Early Times after Infection. *Journal of Virology* **85**, 4135-4142.

Kelkar, S. D., Bhide, V. S., Ranshing, S. S. & Bedekar, S. S. (2004). Rapid ELISA for the diagnosis of rotavirus. *Indian Journal of Medical Research* **119**, 60-65.

Keller, A. A. & Sirivithayapakorn, S. (2004). Transport of colloids in unsaturated porous media: Explaining large-scale behavior based on pore-scale mechanisms. *Water Resources Research* **40**, 1-8.

Keller, A. A., Sirivithayapakorn, S. & Chrysikopoulos, C. V. (2004). Early breakthrough of colloids and bacteriophage MS2 in a water-saturated sand column. *Water Resources Research* **40**, W083041-W0830411.

Kidd, A. H., Chroboczek, J., Cusack, S. & Ruigrok, R. W. H. (1993). Adenovirus type 40 virions contain two distinct fibers. *Virology* **192**, 73-84.

Kinoshita, T., Bales, R. C., Maguire, K. M. & Gerba, C. P. (1993). Effect of pH on bacteriophage transport through sandy soils. *Journal of Contaminant Hydrology* **14**, 55-70.

Ko, G., Jothikumar, N., Hill, V. R. & Sobsey, M. D. (2005). Rapid detection of infectious adenoviruses by mRNA real-time RT-PCR. *Journal of Virological Methods* **127**, 148-153.

Kokoris, M., Dix, K., Moynihan, K., Mathis, J., Erwin, B., Grass, P., Hines, B. & Duesterhoeft, A. (2000). High-throughput SNP genotyping with the masscode system. *Molecular Diagnosis* **5**, 329-340.

Koroglu, M., Yakupogullari, Y., Otlu, B., Ozturk, S., Ozden, M., Ozer, A., Sener, K. & Durmaz, R. (2011). A waterborne outbreak of epidemic diarrhea due to group a rotavirus in malatya, Turkey. *New Microbiologica* **34**, 17-24.

Kovač, K., Bouwknegt, M., Diez-Valcarce, M., Raspor, P., Hernández, M. & Rodríguez-Lázaro, D. (2012). Evaluation of high hydrostatic pressure effect on human adenovirus using molecular methods and cell culture. *International Journal of Food Microbiology* **157**, 368-374.

Kukkula, M., Arstila, P., Klossner, M. L., Maunula, L., Bonsdorff, C. H. V. & Jaatinen, P. (1997). Waterborne outbreak of viral gastroenteritis. *Scandinavian Journal of Infectious Diseases* **29**, 415-418.

LaBelle, R. L. & Gerba, C. P. (1979). Influence of pH, salinity, and organic matter on the adsorption of enteric viruses to estuarine sediment. *Applied and Environmental Microbiology* **38**, 93-101.

Ladrière, L., Charron, M. J. & Malaisse, W. J. (1999). Metabolism of d-Glucose and Its Pentaacetate Ester in Muscles and Pancreatic Islets of GLUT4 Null Mice. *Biochemical and Biophysical Research Communications* **264**, 855-859.

Lance, J. C. & Gerba, C. P. (1984). Virus movement in soil during saturated and unsaturated flow. *Applied and Environmental Microbiology* **47**, 335-337.

Langlet, J., Gaboriaud, F., Gantzer, C. & Duval, J. F. L. (2008). Impact of chemical and structural anisotropy on the electrophoretic mobility of spherical soft multilayer particles: The case of bacteriophage MS2. *Biophysical Journal* **94**, 3293-3312.

Larson, A. M., Hsu, B. B., Rautaray, D., Haldar, J., Chen, J. & Klibanov, A. M. (2011). Hydrophobic polycationic coatings disinfect poliovirus and rotavirus solutions. *Biotechnology and Bioengineering* **108**, 720-723.

Lazouskaya, V. & Jin, Y. (2008). Colloid retention at air-water interface in a capillary channel. *Colloids and Surfaces A: Physicochemical and Engineering Aspects* **325**, 141-151.

Leclerc, H., Edberg, S., Pierzo, V. & Delattre, J. M. (2000). Bacteriophages as indicators of enteric viruses and public health risk in groundwaters. *Journal of Applied Microbiology* **88**, 5-21.

Lee, M. J., Kim, W. H., Cho, H. G. & Lee, S. S. (2012). Epidemiological study of ground-waterborne norovirus GI.3-associated gastroenteritis outbreaks in Gyeonggi province of South Korea in May 2011. *Journal of Bacteriology and Virology* **42**, 232-241.

Lepault, J. P., I; Erk, I; Navaza, J; Bigot, D; Dona, M ...(more)Lepault, J; Petitpas, I; Erk, I; Navaza, J; Bigot, D; Dona, M; Vachette, P; Cohen, J; Rey, F A (2001). Structural polymorphism of the major capsid protein of rotavirus *The EMBO journal* **20**, 1498 - 1507

Li, D., Gu, A. Z., Yang, W., He, M., Hu, X. H. & Shi, H. C. (2010). An integrated cell culture and reverse transcription quantitative PCR assay for detection of infectious rotaviruses in environmental waters. *Journal of Microbiological Methods* **82**, 59-63.

Li, L., Phan, T. G., Nguyen, T. A., Kim, K. S., Seo, J. K., Shimizu, H., Suzuki, E., Okitsu, S. & Ushijima, H. (2005). Molecular epidemiology of adenovirus infection among pediatric population with diarrhea in asia. *Microbiology and Immunology* **49**, 121-128.

Loveland, J. P., Ryan, J. N., Amy, G. L. & Harvey, R. W. (1996). The reversibility of virus attachment to mineral surfaces. *Colloids and Surfaces A: Physicochemical and Engineering Aspects* **107**, 205-221.

Lytle, C. D. & Routson, L. B. (1995). Minimized virus binding for tests of barrier materials. *Applied and Environmental Microbiology* **61**, 643-649.

Mandel, B. (1971). Characterization of type 1 poliovirus by electrophoretic analysis. *Virology* **44**, 554-568.

Matsui, K., Honjo, M. & Kawabata, Z. (2001). Estimation of the fate of dissolved DNA in thermally stratified lake water from the stability of exogenous plasmid DNA. *Aquatic Microbial Ecology* **26**, 95-102.

Matthess, G. & Pehdeger, A. (1981). Concepts of a survival and transport model of pathogenic bacteria and viruses in groundwater. *Studies in Environmental Science* **17**, 427-437.

Maurer, A. M. & Stürchler, D. (2000). A waterborne outbreak of small round structured virus, campylobacter and shigella co-infections in La Neuveville, Switzerland, 1998. *Epidemiology and Infection* **125**, 325-332.

McCarthy, J., Inkielewicz-Stepniak, I., Corbalan, J. J. & Radomski, M. W. (2012). Mechanisms of toxicity of amorphous silica nanoparticleson human lung submucosal cells in vitro: Protective effects of fisetin. *Chemical Research in Toxicology* **25**, 2227-2235.

McCarthy, J. F., McKay, L. D. & Bruner, D. D. (2002). Influence of ionic strength and cation charge on transport of colloidal particles in fractured shale saprolite. *Environmental Science and Technology* **36**, 3735-3743.

McCaulou, D. R., Bales, R. C. & Arnold, R. G. (1995). Effect of temperature controlled motillity on transport of bacteria and microspheres through saturated sediment. *Water Resources Research* **31**, 271-280.

Mei, Y.-F., Harrach, B. & Wadell, G. (2011). Mastadenovirus. In *The Springer Index of Viruses*, pp. 33-48. Edited by C. Tidona & G. Darai: Springer New York.

Melnick, J. L. (1997). Poliovirus and other enteroviruses in viral infections of humans. In *Viral infections in humans*, 4th edn, pp. 583-657. Edited by A. S. Enabs & R. A. Kaslow. London: Plenum Medical Book Company.

Mena, K. D. & Gerba, C. P. (2009). Waterborne adenovirus. *Source of the Document Reviews of Environmental Contamination and Toxicology* **198**, 133-167.

Meschke, J. S. & Sobsey, M. D. (1998). Comparative adsorption of Norwalk virus, poliovirus 1 and F+ RNA coliphage MS2 to soils suspended in treated wastewater. *Water Science and Technology* **38**, 187-189.

Metge, D. W., Harvey, R. W., Anders, R., Rosenberry, D. O., Seymour, D. & Jasperse, J. (2007). Use of carboxylated microspheres to assess transport potential of Cryptosporidium parvum oocysts at the Russian River water supply facility, Sonoma County, California. *Geomicrobiology Journal* **24**, 231-245.

Miyajima, Y., Satoh, K., Uchida, T., Yamada, T., Abe, M., Watanabe, S.-i., Makimura, M. & Makimura, K. (2013). Rapid real-time diagnostic PCR for Trichophyton rubrum and Trichophyton mentagrophytes in patients with tinea unguium and tinea pedis using specific fluorescent probes. *Journal of Dermatological Science* **69**, 229-235.

Mocé-Llivina, L., Lucena, F. & Jofre, J. (2004). Double-layer plaque assay for quantification of enteroviruses. *Applied and Environmental Microbiology* **70**, 2801-2805.

Mohanram, A., Ray, C., Harvey, R. W., Metge, D. W., Ryan, J. N., Chorover, J. & Eberl, D. D. (2010). Comparison of transport and attachment behaviors of Cryptosporidium parvum oocysts and oocyst-sized microspheres being advected through three minerologically different granular porous media. *Water Research* **44**, 5334-5344.

Mondal, P. K. & Sleep, B. E. (2013). Virus and virus-sized microsphere transport in a dolomite rock fracture. *Water Resources Research* **49**, 808-824.

Moore, R. S., Taylor, D. H., Sturman, L. S., Reddy, M. M. & Fuhs, G. W. (1981). Poliovirus adsorption by 34 minerals and soils. *Applied and Environmental Microbiology* **42**, 963-975.

Muehllehner, G. & Karp, J. S. (2006). Positron emission tomography. *Physics in Medicine and Biology* **51**, R117-R137.

Mylon, S. E., Rinciog, C. I., Schmidt, N., Gutierrez, L., Wong, G. C. L. & Nguyen, T. H. (2010). Influence of salts and natural organic matter on the stability of bacteriophage MS2. *Langmuir* **26**, 1035-1042.

Nasser, A. M., Battagelli, D. & Sobsey, M. D. (1992). Isoelectric focusing of hepatitis A virus in sucrose gradients. *Israel Journal of Medical Sciences* **28**, 73.

Nasser, A. M., Glozman, R. & Nitzan, Y. (2002). Contribution of microbial activity to virus reduction in saturated soil. *Water Research* **36**, 2589-2595.

Nasser, A. M. & Oman, S. D. (1999). Quantitative assessment of the inactivation of pathogenic and indicator viruses in natural water sources. *Water Research* **33**, 1748-1752.

Nasser, A. M., Tchorch, Y. & Fattal, B. (1993). Comparative survival of E. coli, F+bacteriophages, HAV and poliovirus 1 in wastewater and groundwater. *Water Science and Technology* **27**, 401-407.

Nasser, A. M., Tchorch, Y. & Fattal, B. (1995). Validity of serological methods (ELISA) for detecting infectious viruses in water. *Water Science and Technology* **31**, 307-310.

Nguyen, T. H. & Chen, K. L. (2007). Role of divalent cations in plasmid DNA adsorption to natural organic matter-coated silica surface. *Environmental Science and Technology* **41**, 5370-5375.

Nguyen, T. H. & Elimelech, M. (2007). Adsorption of plasmid DNA to a natural organic matter-coated silica surface: Kinetics, conformation, and reversibility. *Langmuir* **23**, 3273-3279.

Nilsson, M., Svenungsson, B., Hedlund, K. O., Uhnoo, I., Lagergren, A., Akre, T. & Svensson, L. (2000). Incidence and genetic diversity of group C rotavirus among adults. *Journal of Infectious Diseases* **182**, 678-684.

Ogorzaly, L., Bertrand, I., Paris, M., Maul, A. & Gantzer, C. (2010). Occurrence, survival, and persistence of human adenoviruses and F-specific RNA phages in raw groundwater. *Applied and Environmental Microbiology* **76**, 8019-8025.

Ogorzaly, L., Cauchie, H. M., Penny, C., Perrin, A., Gantzer, C. & Bertrand, I. (2013). Two-day detection of infectious enteric and non-enteric adenoviruses by improved ICC-qPCR. *Applied Microbiology and Biotechnology* **97**, 4159-4166.

Oishi, I., Yamazaki, K. & Minekawa, Y. (1993). An occurrence of diarrheal cases associated with group C rotavirus in adults. *Microbiology and Immunology* **37**, 505-510.

Okitsu-Negishi, S., Nguyen, T. A., Phan, T. G. & Ushijima, H. (2004). Molecular epidemiology of viral gastroenteritis in Asia. *Pediatrics International* **46**, 245-252.

Olsthoorn, R. & Duin, J. (2011). Levivirus. In *The Springer Index of Viruses*, pp. 799-804. Edited by C. Tidona & G. Darai: Springer New York.

Pang, L., Close, M. & Flintoft, M. (2004a). Attenuation and transport characteristics of cadmium, zinc and lead in selected New Zealand aquifer systems. *Journal of Hydrology (NZ)* **43**, 95-110.

Pang, L., Close, M., Goltz, M., Noonan, M. & Sinton, L. (2005). Filtration and transport of Bacillus subtilis spores and the F-RNA phage MS2 in a coarse alluvial gravel aquifer: Implications in the estimation of setback distances. *Journal of Contaminant Hydrology* **77**, 165-194.

Pang, L., Nowostawska, U., Ryan, J. N., Williamson, W. M., Walshe, G. & Hunter, K. A. (2009). Modifying the surface charge of pathogen-sized microspheres for studying pathogen transport in groundwater. *Journal of Environmental Quality* **38**, 2210-2217.

Pang, L., Nowostawska, U., Weaver, L., Hoffman, G., Karmacharya, A., Skinner, A. & Karki, N. (2012). Biotin- and glycoprotein-coated microspheres: Potential surrogates for studying filtration of cryptosporidium parvum in porous media. *Environmental Science and Technology* **46**, 11779-11787.

Pang, X. L., Lee, B., Boroumand, N., Leblanc, B., Preiksaitis, J. K. & Ip, C. C. Y. (2004b). Increased Detection of Rotavirus Using a Real Time Reverse Transcription-Polymerase Chain Reaction (RT-PCR) Assay in Stool Specimens from Children with Diarrhea. *Journal of Medical Virology* **72**, 496-501.

Parashar, U. D., Burton, A., Lanata, C., Boschi-Pinto, C., Shibuya, K., Steele, D., Birmingham, M. & Glass, R. I. (2009). Global Mortality Associated with Rotavirus Disease among Children in 2004. *Journal of Infectious Diseases* **200**, S9-S15.

Park, S. H., Kim, E. J., Yun, T. H., Lee, J. H., Kim, C. K., Seo, Y. H., Oh, S. A., Choi, S. S., Cho, S. J., Kim, M. S., Han, G. Y., Kim, M. Y., Jeong, H. S., Cheon, D. S. & Kim, H. S. (2010). Human enteric viruses in groundwater. *Food and Environmental Virology* **2**, 69-73.

Payne, A. F., Binduga-Gajewska, I., Kauffman, E. B. & Kramer, L. D. (2006). Quantitation of flaviviruses by fluorescent focus assay. *Journal of Virological Methods* **134**, 183-189.

Pecson, B. M., Decrey, L. & Kohn, T. (2012). Photoinactivation of virus on iron-oxide coated sand: Enhancing inactivation in sunlit waters. *Water Research* **46**, 1763-1770.

Peng, H. H., Wu, S., Davis, J. J., Wang, L., Roth, J. A., Marini Iii, F. C. & Fang, B. (2006). A rapid and efficient method for purification of recombinant adenovirus with arginine–glycine–aspartic acid-modified fibers. *Analytical Biochemistry* **354**, 140-147.

Penrod, S. L., Olson, T. M. & Grant, S. B. (1995). Whole Particle Microelectrophoresis for Small Viruses. *Journal of Colloid And Interface Science* **173**, 521-523.

Pesavento, J. B. C., S. E.; Estes, M. K.; Venkataram Prasad, B. V. (2006). Rotavirus proteins: Structure and Assembly. In *Reoviruses: Entry, Assembly, Morphogenesis*, pp. 190-219. Edited by P. Roy: Springer Berlin Heidelberg.

Pham, M., Mintz, E. A. & Nguyen, T. H. (2009). Deposition kinetics of bacteriophage MS2 to natural organic matter: Role of divalent cations. *Journal of Colloid and Interface Science* **338**, 1-9.

Philippe, N., Legendre, M., Doutre, G., Couté, Y., Poirot, O., Lescot, M., Arslan, D., Seltzer, V., Bertaux, L., Bruley, C., Garin, J., Claverie, J.-M. & Abergel, C. (2013). Pandoraviruses: Amoeba Viruses with Genomes Up to 2.5 Mb Reaching That of Parasitic Eukaryotes. *Science* **341**, 281-286.

Phillips, G., Lopman, B., Tam, C. C., Iturriza-Gomara, M., Brown, D. & Gray, J. (2009). Diagnosing rotavirus A associated IID: Using ELISA to identify a cut-off for real time RT-PCR. *Journal of Clinical Virology* **44**, 242-245.

Pieper, A. P., Ryan, J. N., Harvey, R. W., Amy, G. L., Illangasekare, T. H. & Metge, D. W. (1997). Transport and recovery of bacteriophage PRD1 in a sand and gravel aquifer: Effect of sewage-derived organic matter. *Environmental Science and Technology* **31**, 1163-1170.

Player, V. & Westmoreland, D. (1989). Rapid diagnosis of adenovirus pharyngoconjunctival fever: Use of a monoclonal antibody-based ELISA test during an outbreak. *Journal of Virological Methods* **24**, 307-312.

Poté, J., Ceccherini, M. T., Van, V. T., Rosselli, W., Wildi, W., Simonet, P. & Vogel, T. M. (2003). Fate and transport of antibiotic resistance genes in saturated soil columns. *European Journal of Soil Biology* **39**, 65-71.

Poté, J., Mavingui, P., Navarro, E., Rosselli, W., Wildi, W., Simonet, P. & Vogel, T. M. (2009). Extracellular plant DNA in Geneva groundwater and traditional artesian drinking water fountains. *Chemosphere* **75**, 498-504.

Poté, J., Rosselli, W., Wigger, A. & Wildi, W. (2007). Release and leaching of plant DNA in unsaturated soil column. *Ecotoxicology and Environmental Safety* **68**, 293-298.

Powelson, D. K. & Gerba, C. P. (1994). Virus removal from sewage effluents during saturated and unsaturated flow through soil columns. *Water Research* **28**, 2175-2181.

Powelson, D. K., Simpson, J. R. & Gerba, C. P. (1990). Virus transport and survival in saturated and unsaturated flow through soil columns. *Journal of Environmental Quality* **19**, 396-401.

Purcell, R. H. (1996). Hepatitis E virus. In *Fields Virology*, 3. edn, pp. 2 v. (2831-2843). Edited by D. M. K. Bernard N. Fields, Peter M. Howley Philadelphia: Lippincott-Raven Publishers.

Quanrud, D. M., Carroll, S. M., Gerba, C. P. & Arnold, R. G. (2003). Virus removal during simulated soil-aquifer treatment. *Water Research* **37**, 753-762.

Rao, V. C. & Melnick, J. L. (1986). Introduction. In *Environmental virology*, pp. 1-9. Edited by V. C. Rao & J. L. Melnick. U.K.: Van Nostrand Reinhold.

Raphael, R. A., Sattar, S. A. & Springthorpe, V. S. (1985). Long-term survival of human rotavirus in raw and treated river water. *Canadian Journal of Microbiology* **31**, 124-128.

Redman, J. A., Grant, S. B., Olson, T. M., Hardy, M. E. & Estes, M. K. (1997). Filtration of recombinant norwalk virus particles and bacteriophage MS2 in quartz sand: Importance of electrostatic interactions. *Environmental Science and Technology* **31**, 3378-3383.

Regli, S., Rose, J. B., Haas, C. N. & Gerba, C. P. (1991). Modeling the risk from Giardia and viruses in drinking water. *Journal / American Water Works Association* **83**, 76-84.

Rigotto, C., Hanley, K., Rochelle, P. A., De Leon, R., Barardi, C. R. M. & Yates, M. V. (2011). Survival of adenovirus types 2 and 41 in surface and ground waters measured by a plaque assay. *Environmental Science and Technology* **45**, 4145-4150.

Rodgers, F. G., Hufton, P., Kurzawska, E., Molloy, C. & Morgan, S. (1985). Morphological response of human rotavirus to ultra-violet radiation, heat and disinfectants. *Journal of Medical Microbiology* **20**, 123-130.

Rodríguez, R. A., Pepper, I. L. & Gerba, C. P. (2009). Application of PCR-based methods to assess the infectivity of enteric viruses in environmental samples. *Applied and Environmental Microbiology* **75**, 297-307.

Roingeard, P. (2008). Viral detection by electron microscopy: Past, present and future. *Biology of the Cell* **100**, 491-501.

Romanowski, G., Lorenz, M. G., Sayler, G. & Wackernagel, W. (1992). Persistence of free plasmid DNA in soil monitored by various methods, including a transformation assay. *Applied and Environmental Microbiology* **58**, 3012-3019.

Romero, O. C., Straub, A. P., Kohn, T. & Nguyen, T. H. (2011). Role of temperature and suwannee river natural organic matter on inactivation kinetics of rotavirus and bacteriophage MS2 by solar irradiation. *Environmental Science and Technology* **45**, 10385-10393.

Rosen, M. R. (2001). Hydrochemistry of New Zealand's Aquifers. In *Groundwaters of New Zealand*, pp. 77-110. Edited by M. R. Rosen & P. A. White. New Zealand: New Zealand Hydrological Society Inc.

Rosenberg, M. (2006). Microbial adhesion to hydrocarbons: Twenty-five years of doing MATH. *FEMS Microbiology Letters* **262**, 129-134.

Rossi, P., De Carvalho-Dill, A., Müller, I. & Aragno, M. (1994). Comparative tracing experiments in a porous aquifer using bacteriophages and fluorescent dye on a test field located at Wilerwald (Switzerland) and simultaneously surveyed in detail on a local scale by radio-magneto-tellury (12-240 kHz). *Environmental Geology* **23**, 192-200.

Ryan, J. N., Elimelech, M., Ard, R. A., Harvey, R. W. & Johnson, P. R. (1999). Bacteriophage PRD1 and silica colloid transport and recovery in an iron oxide-coated sand aquifer. *Environmental Science and Technology* **33**, 63-73.

Ryan, J. N., Harvey, R. W., Metge, D., Elimelech, M., Navigato, T. & Pieper, A. P. (2002). Field and laboratory investigations of inactivation of viruses (PRD1 and MS2) attached to iron oxide-coated quartz sand. *Environmental Science and Technology* **36**, 2403-2413.

Rysz, M. & Alvarez, P. J. J. (2006). Transport of antibiotic-resistant bacteria and resistance-carrying plasmids through porous media. *Water Science and Technology* **54**, 363-370.

Rzeżutka, A. & Cook, N. (2004). Survival of human enteric viruses in the environment and food. *FEMS Microbiology Reviews* **28**, 441-453.

Sabbatini, M. E., Bi, Y., Ji, B., Ernst, S. A. & Williams, J. A. (2010). CCK activates RhoA and Rac1 differentially through Gα13 and Gαq in mouse pancreatic acini. *American Journal of Physiology - Cell Physiology* **298**, 592-601.

Sabir, I. H., Haldorsen, S., Torgersen, J. & Aleström, P. (1999). DNA tracers with information capacity and high detection sensitivity tested in groundwater studies. *Hydrogeology Journal* **7**, 264-272.

Sabir, I. H., Haldorsen, S., Torgersen, J., Aleström, P., Gaut, S., Colleuille, H., Pedersen, T. S. & Kitterød, N. O. (2000). Synthetic DNA tracers: Examples of their application in water related studies. *IAHS-AISH Publication*, 159-165.

Sadeghi, G., Behrends, T., Schijven, J. F. & Hassanizadeh, S. M. (2013). Effect of dissolved calcium on the removal of bacteriophage PRD1 during soil passage: The role of double-layer interactions. *Journal of Contaminant Hydrology* **144**, 78-87.

Sadeghi, G., Schijven, J. F., Behrends, T., Hassanizadeh, S. M., Gerritse, J. & Kleingeld, P. J. (2011). Systematic Study of Effects of pH and Ionic Strength on Attachment of Phage PRD1. *Ground Water* **49**, 12-19.

Saiers, J. E. & Lenhart, J. J. (2003). Ionic-strength effects on colloid transport and interfacial reactions in partially saturated porous media. *Water Resources Research* **39**, SBH81-SBH813.

Saini, G., Nasholm, N., Dolan, M. E. & Wood, B. D. (2011). Application of salting-out agent to enhance the hydrophobicity of weakly hydrophobic bacterial strains. *Journal of Adhesion Science and Technology* **25**, 2169-2182.

Samad, M. A., Okuwaki, M., Haruki, H. & Nagata, K. (2007). Physical and functional interaction between a nucleolar protein nucleophosmin/B23 and adenovirus basic core proteins. *FEBS Letters* **581**, 3283-3288.

San Martin, C. (2012). Latest insights on adenovirus structure and assembly. *Viruses* **4**, 847-877.

Scandura, J. E. & Sobsey, M. D. (1997). Viral and bacterial contamination of groundwater from on-site sewage treatment systems. *Water Science and Technology* **35**, 141-146.

Schaldach, C. M., Bourcier, W. L., Shaw, H. F., Viani, B. E. & Wilson, W. D. (2006). The influence of ionic strength on the interaction of viruses with charged surfaces under environmental conditions. *Journal of Colloid and Interface Science* **294**, 1-10.

Schaub, S. A. & Sorber, C. A. (1977). Virus and bacteria removal from wastewater by rapid infiltration through soil. *Applied and Environmental Microbiology* **33**, 609-619.

Scheibe, T. D. & Wood, B. D. (2003). A particle-based model of size or anion exclusion with application to microbial transport in porous media. *Water Resources Research* **39**, 1080.

Schijven, J. F., De Bruin, H. A. M., Hassanizadeh, S. M. & De Roda Husman, A. M. (2003). Bacteriophages and clostridium spores as indicator organisms for removal of pathogens by passage through saturated dune sand. *Water Research* **37**, 2186-2194.

Schijven, J. F. & Hassanizadeh, S. M. (2000). Removal of viruses by soil passage: Overview of modeling, processes, and parameters. *Critical Reviews in Environmental Science and Technology* **30**, 49-127.

Schijven, J. F., Mülschlegel, J. H. C., Hassanizadeh, S. M., Teunis, P. F. M. & de Roda Husman, A. M. (2006). Determination of protection zones for Dutch groundwater wells against virus contamination - Uncertainty and sensitivity analysis. *Journal of Water and Health* **4**, 297-312.

Sen, T. K. (2011). Processes in pathogenic biocolloidal contaminants transport in saturated and unsaturated porous media: A review. *Water, Air, and Soil Pollution* **216**, 239-256.

Sen, T. K. & Khilar, K. C. (2006). Review on subsurface colloids and colloid-associated contaminant transport in saturated porous media. *Advances in Colloid and Interface Science* **119**, 71-96.

Shimizu, Y., Sogabe, H. & Terashima, Y. (1998). The effects of colloidal humic substances on the movement of non-ionic hydrophobic organic contaminants in groundwater. *Water Science and Technology* **38**, 159-167.

Sidhu, J. P. S. & Toze, S. (2012). Assessment of pathogen survival potential during managed aquifer recharge with diffusion chambers. *Journal of Applied Microbiology* **113**, 693-700.

Sidhu, J. P. S., Toze, S., Hodgers, L., Shackelton, M., Barry, K., Page, D. & Dillon, P. (2010). Pathogen inactivation during passage of stormwater through a constructed reedbed and aquifer transfer, storage and recovery. *Water Science and Technology* **62**, 1190-1197.

Silverman, A. I., Peterson, B. M., Boehm, A. B., McNeill, K. & Nelson, K. L. (2013). Sunlight inactivation of human viruses and bacteriophages in coastal waters containing natural photosensitizers. *Environmental Science and Technology* **47**, 1870-1878.

Sinclair, R. G., Rose, J. B., Hashsham, S. A., Gerba, C. P. & Haase, C. N. (2012). Criteria for selection of surrogates used to study the fate and control of pathogens in the environment. *Applied and Environmental Microbiology* **78**, 1969-1977.

Sinreich, M., Flynn, R. & Zopfi, J. (2009). Use of particulate surrogates for assessing microbial mobility in subsurface ecosystems. *Hydrogeology Journal* **17**, 49-59.

Sinton, L. (2001). Microbial contamination of New Zealand's aquifers. In *Groundwaters of New Zealand*, pp. 221-251. Edited by M. R. Rosen & P. A. White. New Zealand: New Zealand Hydrological Society Inc.

Sinton, L. W., Finlay, R. K., Pang, L. & Scott, D. M. (1997). Transport of bacteria and bacteriophages in irrigated effluent into and through an alluvial gravel aquifer. *Water, Air, and Soil Pollution* **98**, 17-42.

Sinton, L. W., MacKenzie, M. L., Karki, N., Dann, R. L., Pang, L. & Close, M. E. (2012). Transport of Escherichia coli and F-RNA bacteriophages in a 5-M column of saturated, heterogeneous gravel. *Water, Air, and Soil Pollution* **223**, 2347-2360.

Sinton, L. W., Noonan, M. J., Finlay, R. K., Pang, L. & Close, M. E. (2000). Transport and attenuation of bacteria and bacteriophages in an alluvial gravel aquifer. *New Zealand Journal of Marine and Freshwater Research* **34**, 175-186.

Smirnov, Y. A., Kapitulets, S. P., Amitina, N. N., Ginevskaya, V. A. & Kaverin, N. V. (1991). Effect of UV-irradiation on rotavirus. *Acta Virologica* **35**, 1-6.

Sobsey, M. D., Shields, P. A., Hauchman, F. H., Hazard, R. L. & Caton Iii, L. W. (1986). Survival and transport of hepatitis A virus in soils, groundwater and wastewater. *Water Science and Technology* **18**, 97-106.

Sprinzl, M. F., Oberwinkler, H., Schaller, H. & Protzer, U. (2001). Transfer of hepatitis B virus genome by adenovirus vectors into cultured cells and mice: Crossing the species barrier. *Journal of Virology* **75**, 5108-5118.

Stockley, P. G., Stonehouse, N. J. & Valegard, K. (1994). Molecular mechanism of RNA phage morphogenesis. *International Journal of Biochemistry* **26**, 1249-1260.

Storch, G. A. (2000). Diagnostic Virology. *Clinical Infectious Diseases* **31**, 739-751.

Straub, T. M., Pepper, I. L. & Gerba, C. P. (1993). Virus survival in sewage sludge amended desert soil. *Water Science and Technology* **27**, 421-424.

Straube, J., Albert, T., Manteufel, J., Heinze, J., Fehlhaber, K. & Truyen, U. (2011). In vitro influence of d/l-lactic acid, sodium chloride and sodium nitrite on the infectivity of feline calicivirus and of ECHO virus as potential surrogates for foodborne viruses. *International Journal of Food Microbiology* **151**, 93-97.

Syngouna, V. I. & Chrysikopoulos, C. V. (2010). Interaction between viruses and clays in static and dynamic batch systems. *Environmental Science and Technology* **44**, 4539-4544.

Syngouna, V. I. & Chrysikopoulos, C. V. (2012). Transport of biocolloids in water saturated columns packed with sand: Effect of grain size and pore water velocity. *Journal of Contaminant Hydrology* **129-130**, 11-24.

Tallon, L. A., Love, D. C., Moore, Z. S. & Sobsey, M. D. (2008). Recovery and sequence analysis of hepatitis A virus from springwater implicated in an outbreak of acute viral hepatitis. *Applied and Environmental Microbiology* **74**, 6158-6160.

Tang, Y. N., Wu, P. X., Hou, Y. K., Zhu, N. W. & Dang, Z. (2012). Adsorption properties of salmon sperm DNA on organic and inorganic modified montmorillonite. *Gongneng Cailiao/Journal of Functional Materials* **43**, 1712-1717.

Tanneru, C. T., Rimer, J. D. & Chellam, S. (2013). Sweep flocculation and adsorption of viruses on aluminum flocs during electrochemical treatment prior to surface water microfiltration. *Environmental Science and Technology* **47**, 4612-4618.

Tartera, C., Bosch, A. & Jofre, J. (1988). The inactivation of bacteriophages infecting Bacteroides fragilis by chlorine treatment and UV-irradiation. *FEMS Microbiology Letters* **56**, 313-316.

Taylor, R., Cronin, A., Pedley, S., Barker, J. & Atkinson, T. (2004). The implications of groundwater velocity variations on microbial transport and wellhead protection - Review of field evidence. *FEMS Microbiology Ecology* **49**, 17-26.

Tebbe, C. C. & Vahjen, W. (1993). Interference of humic acids and DNA extracted directly from soil in detection and transformation of recombinant DNA from bacteria and a yeast. *Applied and Environmental Microbiology* **59**, 2657-2665.

Teunis, P. F. M., Moe, C. L., Liu, P., Miller, S. E., Lindesmith, L., Baric, R. S., Le Pendu, J. & Calderon, R. L. (2008). Norwalk virus: How infectious is it? *Journal of Medical Virology* **80**, 1468-1476.

Thompson, S. S. & Yates, M. V. (1999). Bacteriophage inactivation at the air-water-solid interface in dynamic batch systems. *Applied and Environmental Microbiology* **65**, 1186-1190.

Thurston-Enriquez, J. A., Haas, C. N., Jacangelo, J., Riley, K. & Gerba, C. P. (2003). Inactivation of feline calicivirus and adenovirus type 40 by UV radiation. *Applied and Environmental Microbiology* **69**, 577-582.

Tidona, C. & Darai, G. (2011). *The Springer Index of Viruses*. New York: Springer Science+Business Media.

Tolmachev, V. & Stone-Elander, S. (2010). Radiolabelled proteins for positron emission tomography: Pros and cons of labelling methods. *Biochimica et Biophysica Acta (BBA) - General Subjects* **1800**, 487-510.

Tong, M., Shen, Y., Yang, H. & Kim, H. (2012). Deposition kinetics of MS2 bacteriophages on clay mineral surfaces. *Colloids and Surfaces B: Biointerfaces* **92**, 340-347.

Torkzaban, S., Hassanizadeh, S. M., Schijven, J. F., De Bruin, H. A. M. & De Roda Husman, A. M. (2006). Virus transport in saturated and unsaturated sand columns. *Vadose Zone Journal* **5**, 877-885.

Trilisky, E. I. & Lenhoff, A. M. (2007). Sorption processes in ion-exchange chromatography of viruses. *Journal of Chromatography A* **1142**, 2-12.

van der Wielen, P. W. J. J., Blokker, M. & Medema, G. J. (2006). Modelling the length of microbiological protection zones around phreatic sandy aquifers in The Netherlands. *Water Science and Technology* **54**, 63-69.

Van Voorthuizen, E. M., Ashbolt, N. J. & Schäfer, A. I. (2001). Role of hydrophobic and electrostatic interactions for initial enteric virus retention by MF membranes. *Journal of Membrane Science* **194**, 69-79.

Vellinga, J. V. d. H., S.; Hoeben, R. C. (2005). The adenovirus capsid: major progress in minor proteins. *Journal of General Virology* **86**, 1581-1588.

Venkataram Prasad, B. V. & Estes, M. K. (1997). Molecular basis of rotavirus replication. In *Structural biology of viruses*, pp. 239-268. Edited by W. Chiu, R. M. Burnett & R. Garcea. New York: Oxford University Press.

Viancelli, A., Garcia, L. A. T., Kunz, A., Steinmetz, R., Esteves, P. A. & Barardi, C. R. M. (2012). Detection of circoviruses and porcine adenoviruses in water samples collected from swine manure treatment systems. *Research in Veterinary Science* **93**, 538-543.

Villegas, G. A., Argüelles, M. H., Castello, A. A., Mas, N. J. & Glikmann, G. (2002). A rapid method to produce high yields of purified rotavirus particles. *Journal of Virological Methods* **104**, 9-19.

Vonderfecht, S. L., Huber, A. C., Eiden, J., Mader, L. C. & Yolken, R. H. (1984). Infectious diarrhea of infant rats produced by a rotavirus-like agent. *Journal of Virology* **52**, 94-98.

Wadell, G. (1984). Molecular Epidemiology of Human Adenoviruses. In *The Molecular Biology of Adenoviruses 2*, pp. 191-220. Edited by W. Doerfler: Springer Berlin Heidelberg.

Wait, D. A. & Sobsey, M. D. (1983). Method for recovery of enteric viruses from estuarine sediments with chaotropic agents. *Applied and Environmental Microbiology* **46**, 379-385.

Wall, K., Pang, L., Sinton, L. & Close, M. (2008). Transport and attenuation of microbial tracers and effluent microorganisms in saturated pumice sand aquifer material. *Water, Air, and Soil Pollution* **188**, 213-224.

Wallender, E. K., Ailes, E. C., Yoder, J. S., Roberts, V. A. & Brunkard, J. M. (2013). Contributing Factors to Disease Outbreaks Associated with Untreated Groundwater. *Groundwater*, Article in Press.

Walsh, M. K., Wang, X. & Weimer, B. C. (2001). Optimizing the immobilization of single-stranded DNA onto glass beads. *Journal of Biochemical and Biophysical Methods* **47**, 221-231.

Walshe, G. E., Pang, L., Flury, M., Close, M. E. & Flintoft, M. (2010). Effects of pH, ionic strength, dissolved organic matter, and flow rate on the co-transport of MS2 bacteriophages with kaolinite in gravel aquifer media. *Water Research* **44**, 1255-1269.

Wang, D. Z., Wang, S. Y., Jiang, X., Heng, L. S., Tan, J. F., Liu, S. L. & Cao, Y. X. (2009). Characteristics of DNA adsorption and desorption in variable and constant charge soil colloids. *Huanjing Kexue/Environmental Science* **30**, 2761-2766.

Wang, R., Guan, S., Sato, A., Wang, X., Wang, Z., Yang, R., Hsiao, B. S. & Chu, B. (2013). Nanofibrous microfiltration membranes capable of removing bacteria, viruses and heavy metal ions. *Journal of Membrane Science* **446**, 376-382.

Ward, R. L., Bernstein, D. I., Young, E. C., Sherwood, J. R., Knowlton, D. R. & Schiff, G. M. (1986). Human rotavirus studies in volunteers: Determination of infectious dose and serological response to infection. *Journal of Infectious Diseases* **154**, 871-880.

Weaver, L., Sinton, L. W., Pang, L., Dann, R. & Close, M. (2013). Transport of microbial tracers in clean and organically contaminated silica sand in laboratory columns compared with their transport in the field. *Science of the Total Environment* **443**, 55-64.

Weisbrod, N., Meron, H., Walker, S. & Gitis, V. (2013). Virus transport in a discrete fracture. *Water Research* **47**, 1888-1898.

Woessner, W. W., Ball, P. N., DeBorde, D. C. & Troy, T. L. (2001). Viral transport in a sand and gravel aquifer under field pumping conditions. *Ground Water* **39**, 886-894.

Wold, W. S. M. & Ison, M. G. (2013). Adenoviruses. In *Fields Virology*, 6. edn, pp. 2 v. p. 1732-1767. Edited by D. M. K. Bernard N. Fields, Peter M. Howley Philadelphia: Wolters Kluwer Health/Lippincott Williams & Wilkins.

Wong, K., Mukherjee, B., Kahler, A. M., Zepp, R. & Molina, M. (2012). Influence of inorganic ions on aggregation and adsorption behaviors of human adenovirus. *Environmental Science and Technology* **46**, 11145-11153.

Wong, K., Voice, T. C. & Xagoraraki, I. (2013). Effect of organic carbon on sorption of human adenovirus to soil particles and laboratory containers. *Water Research* **47**, 3339-3346.

Xu, H., Zhang, S., Liu, L. & Liang, C. C. (2001). End-labeling of long DNA fragments with biotin and detection of DNA immobilized on magnetic beads. *Applied Biochemistry and Biotechnology - Part B Molecular Biotechnology* **17**, 183-185.

Yahya, M. T., Galsomies, L., Gerba, C. P. & Bales, R. C. (1993). Survival of bacteriophages MS-2 and PRD-1 in ground water. *Water Science and Technology* **27**, 409-412.

Yang, X., Wu, J. Y., Yi, S., Li, H. J., Zhang, G. M., Gao, Y., Jia, Q. M., Zhao, X. N. & Sun, M. S. (2012). Purification of rotavirus by two chromatographic methods. *Chinese Journal of Biologicals* **25**, 754-758.

Yang, Z., Burlage, R. S., Sanford, W. E. & Moline, G. R. (1996). DNA-labeled silica microspheres for groundwater tracing and colloid transport studies. *ACS Division of Environmental Chemistry, Preprints* **36**, 156-158.

Yeh, H. Y., Pieniazek, N., Pieniazek, D., Gelderblom, H. & Luftig, R. B. (1994). Human adenovirus type 41 contains two fibers. *Virus Research* **33**, 179-198.

Zaitlin, M. (2011). Tobamovirus‡. In *The Springer Index of Viruses*, pp. 2065-2069. Edited by C. Tidona & G. Darai: Springer New York.

Zerda, K. S. & Gerba, C. P. (1984). Agarose isoelectrofocusing of intact virions. *Journal of Virological Methods* **9**, 1-6.

Zhang, H., Zhang, J., Zhao, B. & Zhang, C. (2010). Removal of bacteriophages MS2 and phiX174 from aqueous solutions using a red soil. *Journal of Hazardous Materials* **180**, 640-647.

Zhang, H., Zhao, B. Z., Zhang, J. B., Zhang, C. Z., Wang, Q. Y. & Chen, J. (2007). Virus adsorption from batch experiments as influenced by air-water interface. *Huanjing Kexue/Environmental Science* **28**, 2800-2805.

Zhu, B. (2006). Degradation of plasmid and plant DNA in water microcosms monitored by natural transformation and real-time polymerase chain reaction (PCR). *Water Research* **40**, 3231-3238.

Zhuang, J. & Jin, Y. (2003). Virus retention and transport through Al-oxide coated sand columns: Effects of ionic strength and composition. *Journal of Contaminant Hydrology* **60**, 193-209.

Zhuang, J. & Jin, Y. (2008). Interactions between viruses and goethite during saturated flow: Effects of solution pH, carbonate, and phosphate. *Journal of Contaminant Hydrology* **98**, 15-21.

Appendix I.

Hydrophobicity of amino acids for protein hydrophobicity value calculations

Table I.1 Hydrophobicity of the amino acids at pH 6.8. Adapted from: http://oligoweb.com/ePeP_LifeTein/References/pHScores.pdf.

Amino Acid	Hydrophobicity at pH 6.8
Alanine	41
Cysteine	49
Aspartic Acid	-55
Glutamic Acid	-31
Phenylalanine	97
Glycine	0
Histidine	8
Isoleucine	99
Lysine	-23
Leucine	100
Methionine	74
Asparagine	-41
Proline	-46
Glutamine	-10
Arginine	-14
Serine	-5
Threonine	13
Valine	76
Tryptophan	97
Tyrosine	63

Appendix II.
Transmission electron microscope (TEM) images

II. 1 Rotavirus

TEM images show rotavirus particles from the unpurified stock and fraction derived from SEC. Images were taken by negative stain using Leo 912 TEM (operating at 120 kV) at University of Cape Town, South Africa.

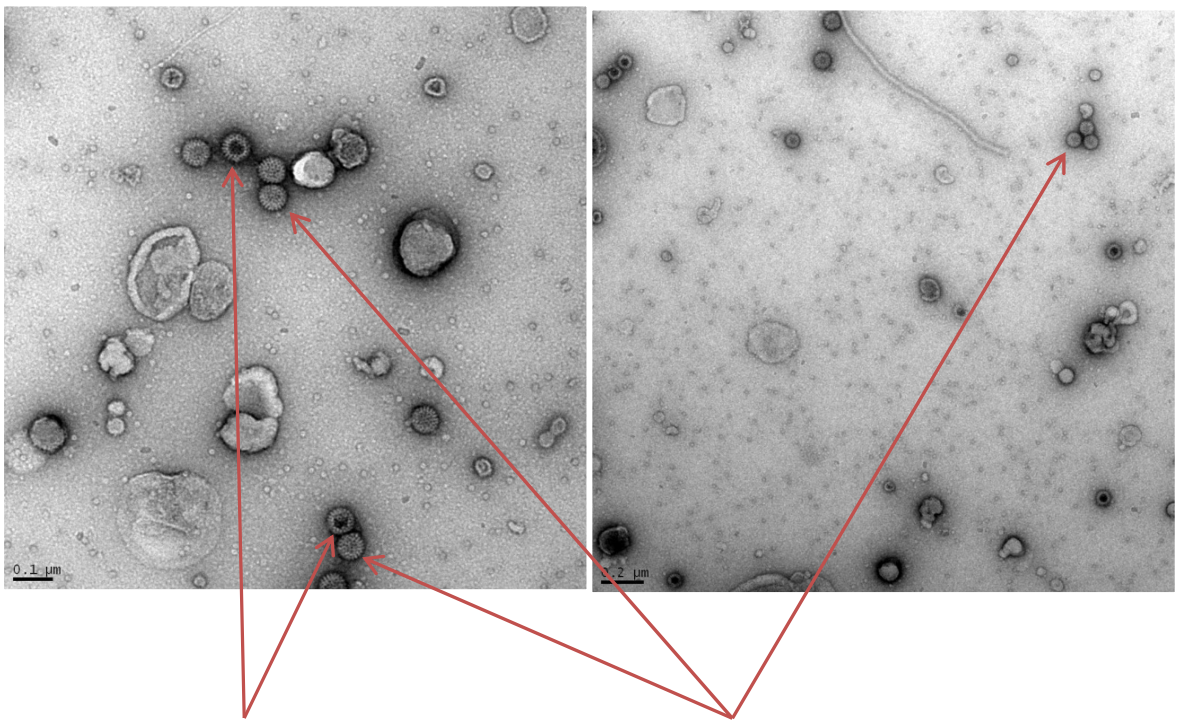

Figure II.1 Rotavirus - unpurified stock. Samples contained impurities and some intact virus particles and dark-centred particles (empty capsids).

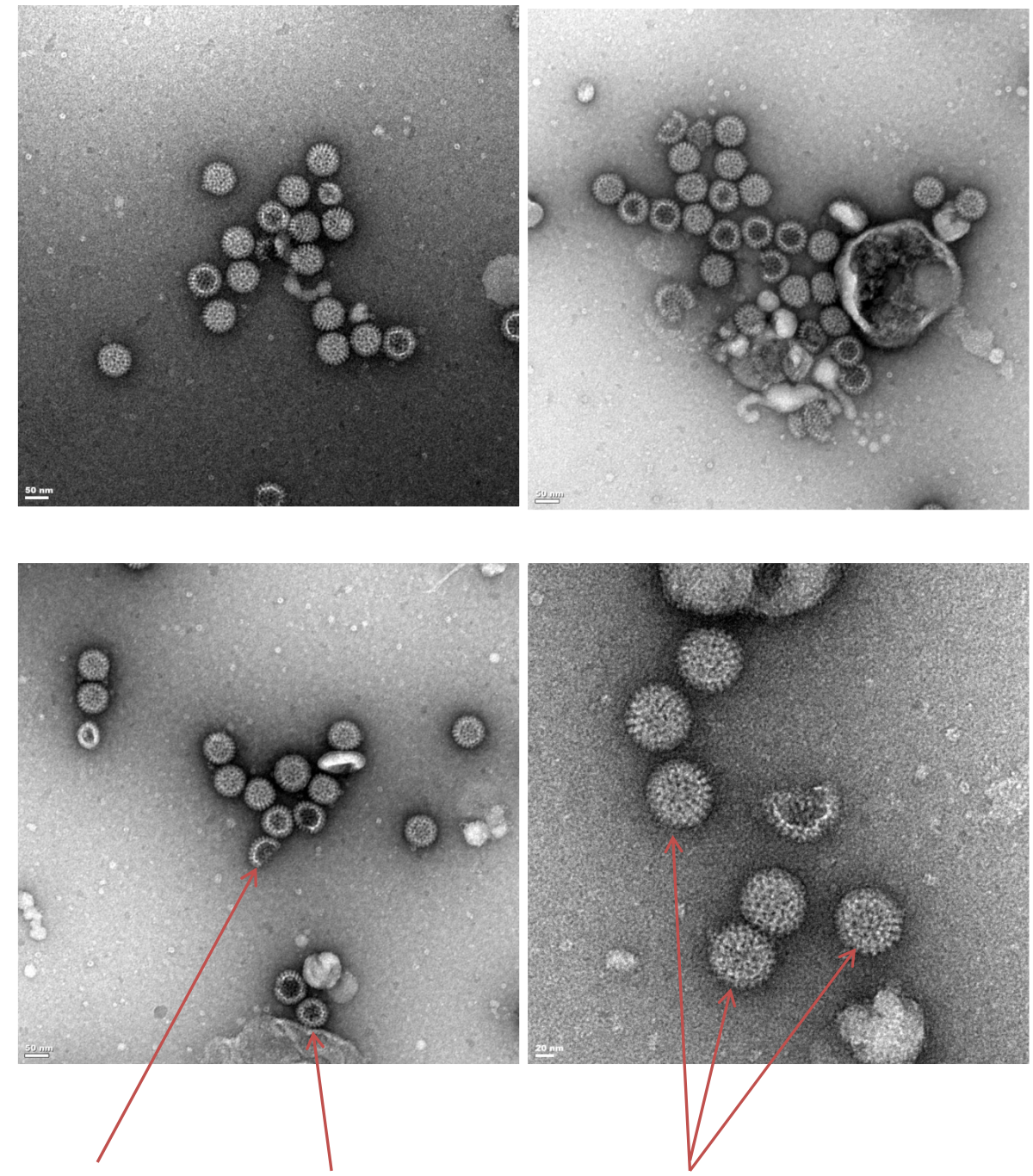

Figure II.2 Rotavirus – Fraction 1. Sample contained high number of intact virus particles with the VP4 protein present on the surface. The presence of empty/degraded capsids may have been a result of virus decay due to sample transport.

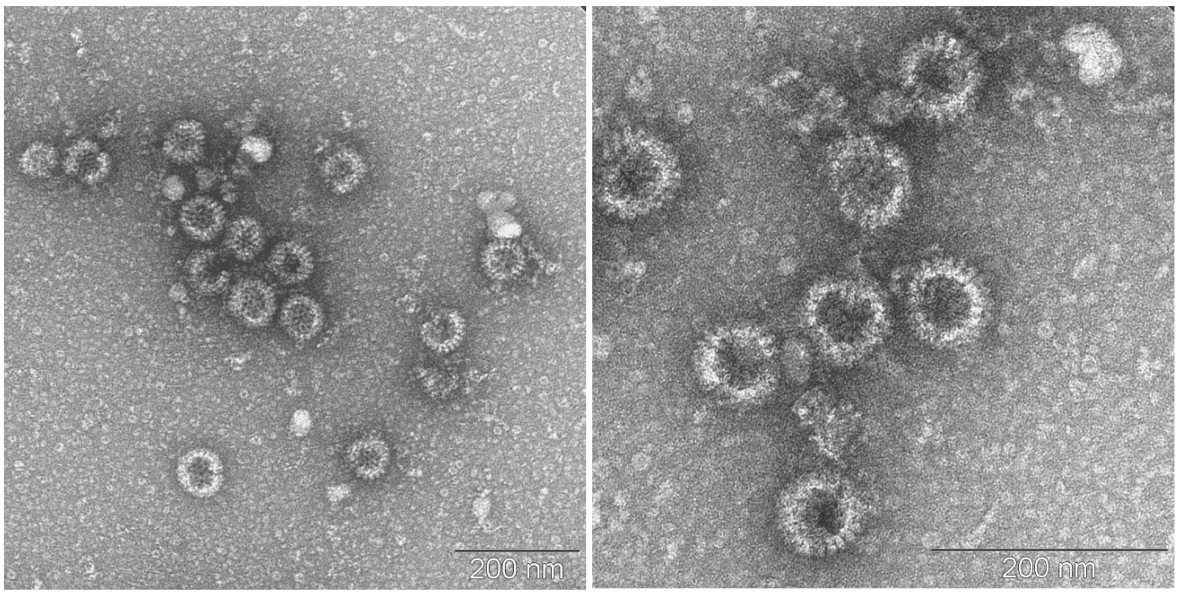

Figure II.3 Rotavirus – Fraction 2. The majority of the particles in this sample were empty capsids. Hardly any intact virus particles were detected.

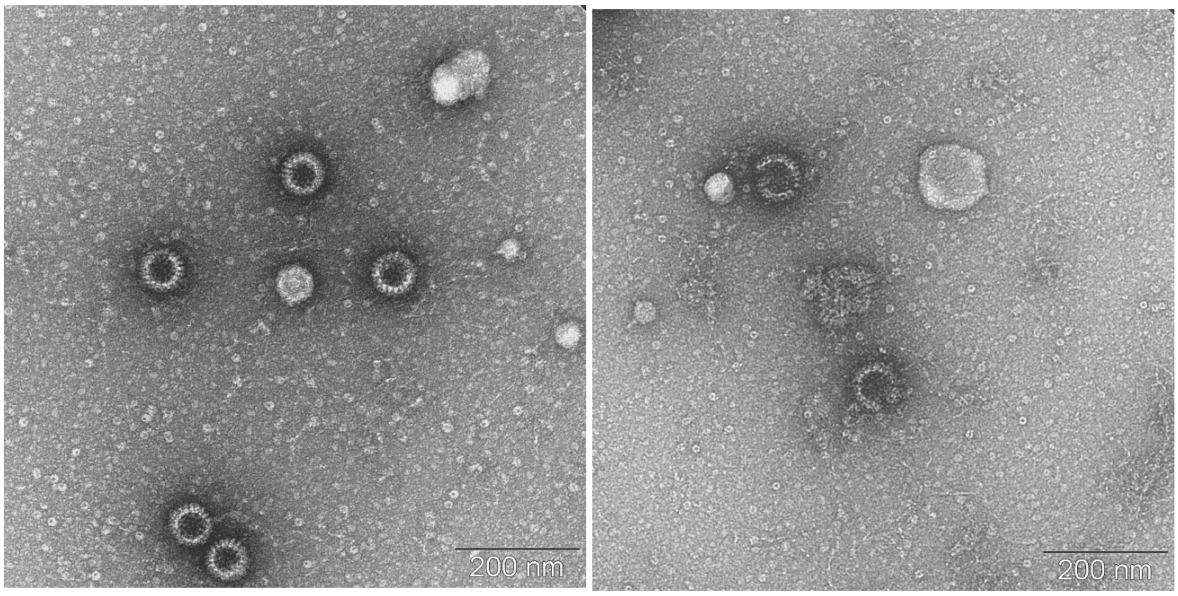

Figure II.4 Rotavirus – Fraction 3. The majority of the particles in this sample were empty capsids. Hardly any intact virus particles were detected.

II.2 Adenovirus

TEM images show the adenovirus particles of the purified stock. Images were taken by negative stain using Philips CM100 BioTWIN TEM at University of Otago, New Zealand.

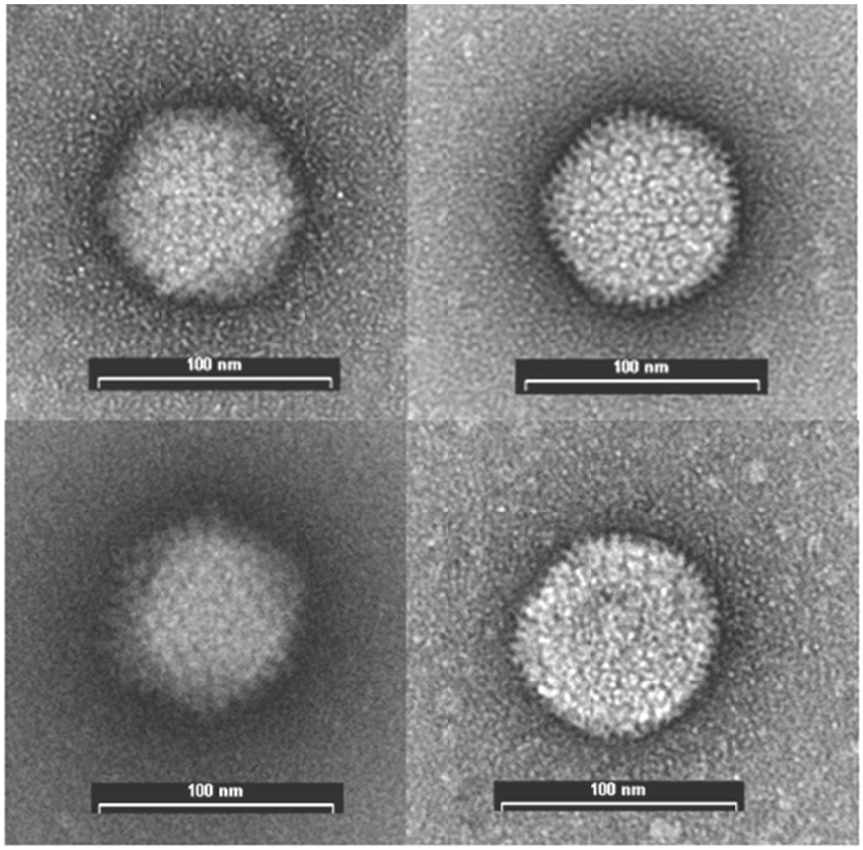

Figure II.5 Adenovirus particles of the purified stock. High number of intact virus particles was present in the sample.

II. 3 MS2 bacteriophage

TEM images show MS2 particles of the purified stock. Images were taken by negative stain using Philips CM100 BioTWIN TEM at University of Otago, New Zealand.

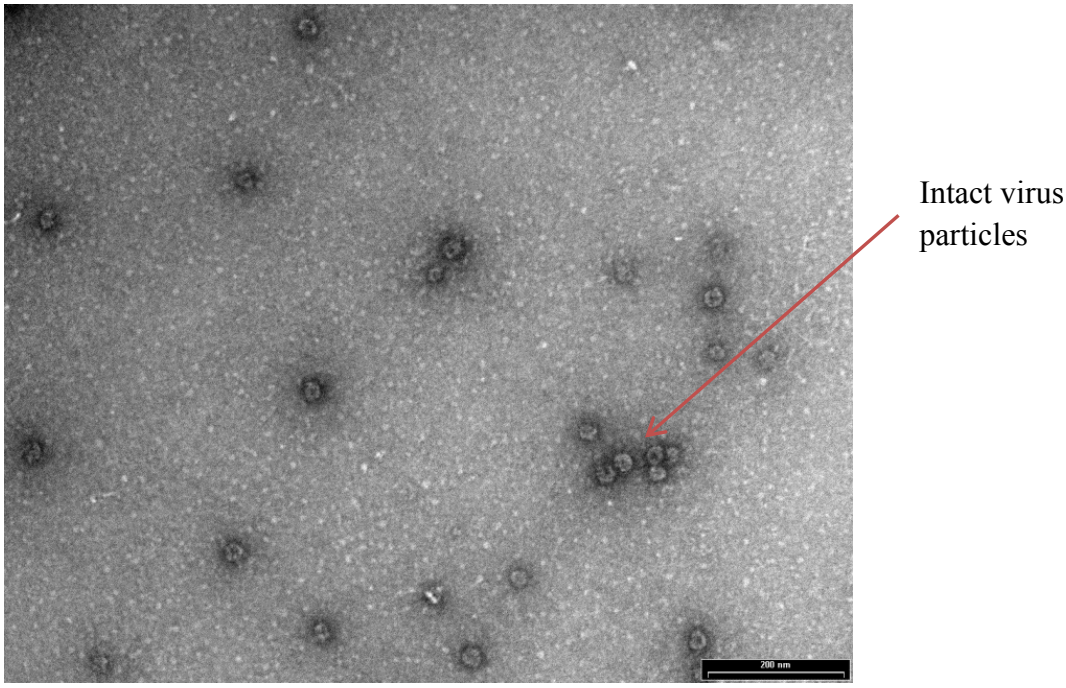

Figure II.6 MS2 particles of the purified stock. High number of intact virus particles was present in the sample.

Appendix III.
Porous media

III. 1 Porous media from New Zealand

The gravel and beach sand used in this study were chosen to represent the natural aquifers common in New Zealand. The properties of the aquifer media are summarised in Table III.1. Beach sand was collected from New Brighton Beach, Christchurch, New Zealand, and gravel was from an alluvial gravel aquifer in the Canterbury Plains, New Zealand. The gravel particles were predominantly composed of silicon dioxide (70%) and aluminium oxide (14%) (Pang *et al.*, 2005). The main component of the beach sand was also silicon dioxide (82%) and aluminium oxide (9%) (Pang *et al.*, 2004a).

Table III.1 Characteristics of the porous media. Zeta potential was measured at Otago University, New Zealand using Zetasizer Nano ZS. Data derived from triplicate measurements on four samples of each media.

	Beach sand	**Gravel**	**Ottawa sand**
Source	New Brighton Beach, New Zealand	Canterbury Plains, New Zealand	Fisher Scientific, UK
Particle size	< 2 mm d_{50} = 0.19 mm	2 – 4 mm d_{50} = 3 mm	0.595 – 0.841 mm
Classification	Fine sand	Fine gravel	Coarse sand
Zeta potential	–42.26 ± 1.01 mV	–35.86 ± 1.02 mV	Not determined
Porosity in column	0.44	0.40	Not determined
Bulk density in column	1.46 g/cm^3	1.57 g/cm^3	Not determined

In order to eliminate debris and particles other than sand, the collected beach sand was sieved using a 2 mm sieve. The particle sizes of the sand material smaller than 2 mm was determined by manual sieving method. The average size of the sand particles was 0.19 mm, thus the sand was classified as fine sand.

As the gravel collected was heterogeneous in size, thus the 2 – 4 mm fraction was separated by manual sieving for further work. The average size of the gravel particles was 3 mm, and the material was classified as fine gravel.

Both media were thoroughly washed first with chlorine-free tap water (sourced from groundwater extracted from alluvial gravel aquifers beneath Christchurch, New Zealand), then rinsed with sterile 2 mM NaCl pH 7 solution. The media were oven dried at 104°C overnight, and autoclaved at 121°C for 30 min.

In order to simulate groundwater for the degradation studies (Chapter 4), the beach sand and the gravel were mixed with 2 mM NaCl pH 7 solution and agitated overnight. The solutions were separated from the solid material and filtered through 0.22 μm filters. Some proportion of the solutions was sent for a chemical analysis and the results were compared with the chemistry of the local groundwater and tap water (Table III.2). The gravel and beach sand solution mimicked the pH and hardness of the local groundwater, however, they contained higher concentrations of chloride, potassium and sodium.

Table III.2. Water chemistry of ESR tap water, Burnham groundwater, beach sand and gravel solutions. Analytical results of the tap water and Burnham groundwater were sourced from ESR internal unpublished data. The analysis of the gravel and beach sand solutions was performed at Hill Laboratories, New Zealand.

Solution	**pH**	**Conduc-tivity**	**CO_3**	**Cl**	**NO_2-N**	**NO_3-N**	**Na**	**K**	**Ca**	**Mg**	**SO_4**	**Fe**
		mS/m	ppm	g/m^3	g/m^3	g/m^3	g/m^3	g/m^3	g/m^3	g/m^3	g/m^3	g/m^3
Tap water (Christchurch, New Zealand)	7.2	12.0	64.3	5	0.001	0.91	7	0.7	13.7	1.9	5.6	0.038
Groundwater (Burnham, New Zealand)	6.9	10.4	37.4	6	0.001	1.67	8	0.8	11.0	3.7	54	0.1
Gravel solution	6.3	33.4	49.0	85	<0.002	0.21	38	2.7	12.8	4.2	8.4	<0.02
Beach sand solution	7.5	43.9	18.8	95	<0.002	1.26	69	7.5	3.1	2.7	18.1	0.06

For the column experiments, where glass columns were packed with the gravel and the beach sand under saturated conditions, the porosity and the bulk density of the columns were calculated according to the following formulas:

$$Porosity = \frac{Volume\ of\ the\ solution\ used\ for\ packing\ the\ column\ (\mathrm{cm}^3)}{Volume\ of\ the\ column\ (\mathrm{cm}^3)}$$

$$Bulk\ density = \frac{Weight\ of\ the\ dry\ media\ used\ for\ packing\ the\ column\ (g)}{Volume\ of\ the\ column\ (\mathrm{cm}^3)}$$

III.2 Ottawa sand

Ottawa sand mesh 20 – 30 (particle size: 0.595 – 0.841 mm; Table III.1) was purchased from Fisher Scientific (UK). The sand was washed using the method of Bales *et al.* (1991). In brief, 60 g of the sand was mixed with 200 mL 0.1 M NH_4OH for 5 min. The solution was discarded, and the process was repeated using 200 mL of 1 M and 0.5 M HCl. The acid was eliminated by washing the sand with 200 mL dH_2O (pH 7.0) seven times. The pH of the last wash was 7.2. The sand was oven dried at 104°C overnight.

Some proportion of the sand was coated with organosilane to give the particles hydrophobic surface. For this 100 g of the washed sand was mixed with 150 mL dH_2O (pH 7.0) and 0.13 mL octadecyltrichlorosilane (Acros Organics, USA) and stirred for 3 hr at room temperature. The mixture was oven dried at 104°C overnight. Then 50 g of the coated sand was washed twice with 150 mL pentane, twice with 150 mL methanol, twice with 150 mL 1 M HCl and seven times with 150 mL dH_2O (pH 7.0). The pH of the last wash was 7.0.

III. 3 Effect of the porous media on q(RT)-PCR

In order to determine whether the porous media interfere with the enzymes of qPCR and qRT-PCR reactions, all four types of media was mixed with 2 mM NaCl pH 7 solution, and then the mixtures were rotated overnight at 2 rpm, at room temperature. This solution was added to qPCR and qRT-PCR reactions where plasmid DNA and rotavirus RNA were amplified. Results suggested that the solutions incubated in porous media had no effect on the qPCR/qRT-PCR reactions.